Sov. Sci. Rev. A. Phys. Vol. 15, 1990, pp. 1–250
Photocopying permitted by license only

Printed in the United Kingdom

SPIN GLASSES AND RELATED PROBLEMS

V.S. DOTSENKO, M.V. FEIGEL'MAN and L.B. IOFFE

Landau Institute for Theoretical Physics, Moscow

ABSTRACT

Recent developments in the theory of spin glasses and related strongly disordered systems (including granular superconductors and neural networks) are reviewed. In particular, the problems of irreversibility and nonergodicity in the framework of the mean field theory, a phase transition in three-dimensional spin glasses and glass-like systems with hidden correlations are discussed.

A su modo este libro es muchos libros, pero sobre todo es dos libros.
Julio Cortázar "Rayuela"

1. INTRODUCTION

1.1 Scope and Structure of the Review

After more than a decade of active research that started with pioneering experimental [1] and theoretical [2] work, the spin-glass problem has far outgrown the confines of its initial formulation in the context of magnetic order in specific magnetic materials. Excellent reviews of the advances made so far in the solution of the problem can be found in refs. [3–5]. However, despite numerous efforts, the theory of spin glasses is still far from complete. The volume of results obtained up to now is an indication of the scope and importance of the problem — but a full solution is yet to be achieved.

In the present review, which should be considered as a supplement to the fundamental works [3–5], we discuss mainly unresolved problems in the theory, promising approaches to their solutions, and new areas connected with spin glasses: superconducting glasses, neural networks, etc. Needless to say, our choice has been biased by our own particular interests. In the rest of this introductory section we discuss the physical basis of these problems, some useful experimental data and the models considered. In the bulk of the review we study these models theoretically and discuss the implications for experiment that can be drawn from this study.

Since the problems discussed are diverse, we propose, following Cortázar (in the epigraph), a few possible schemes of reading this review.

(a) Sections 2–5, where genuine (i.e. without any correlations) spin glasses are considered; *or*

(b) Sections 6–8, where we discuss spin glasses and their analogues with some degree of correlation.

(c) Sections 1, 6.1, 7.1, 7.2 and 8, which contain only rigorous (from a physicist's viewpoint) results on spin glasses or their analogues with infinite-range interaction; *or*

(d) Sections 2, 3, 4 and 7.3, where more physically realistic problems of

spin glasses with finite-range interaction are considered, with special emphasis placed on their differences from a spin glass with an infinite-range interaction.

The following subsections of this introduction are in one-to-one correspondence with the remaining sections of the review (i.e. 1.2 corresponds to 2, 1.3 to 3, etc.).

Note that references are given at the end of each section.

1.2 Sherrington-Kirkpatrick Model: Nonergodicity and History Dependence

Spin glasses can be defined as magnetic systems in which interactions between the magnetic moments are frustrated owing to a quenched disorder. The canonical example is provided by diluted alloys of transition metals (Fe, Mn) with noble ones (Cu, Ag, Au). For all these systems, which have been known ever since the pioneering work of Canella and Mydosh in 1972 [1], it has gradually come to be understood that something very unusual happens at low temperatures. And it has turned out that the unusual properties of spin glasses are in fact fairly universal: they can be observed in such different materials as diluted alloys, concentrated insulators (e.g. $Eu_xSr_{1-x}S$ [6]) and noncrystalline solids (e.g. $CrSnTe_4$); moreover, analogous phenomena have been observed in disordered ferroelectrics (e.g. $K_{1-x}Li_xTaO_3$ [7]). A number of characteristic properties of spin glasses are now known, but the first to be observed [1] was the cusp in the low-frequency a.c. susceptibility $\chi_{ac}(T)$. In a simplified picture, the magnetic moments of a spin glass become frozen below a transition temperature T_c in some random configuration determined by the realization of random interactions in a given sample. This freezing of spins results in the cusp in the susceptibility at T_c. Since the configuration of the frozen spins is random, no magnetic order is observed in neutron-scattering experiments. Furthermore, since the configuration is determined by the unsteady balance between frustrated interactions, it can be easily changed irreversibly by the external magnetic field, which leads to large hysteresis and remanence effects in spin glasses. Of all these irreversibility effects, the most instructive is the difference between the susceptibilities measured in different ways. Usually two methods are employed: the field-cooling technique, in which the sample is cooled down in the applied field and the magnetization then measured; and the zero-field-cooling technique, in which the

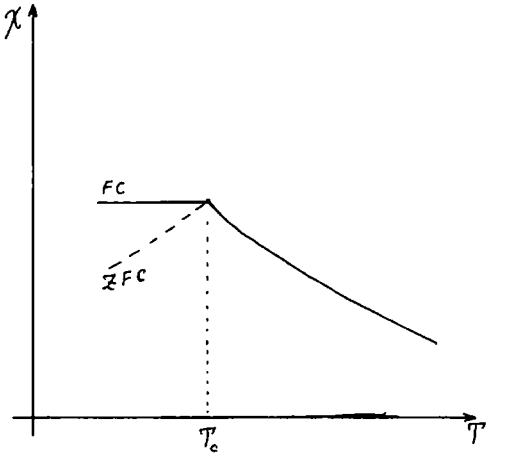

Figure 1 Field-cooling (full line) and zero-field-cooling (dashed line) susceptibilities in a real spin glass.

magnetization is measured on applying the field to a sample at constant temperature. The difference between these susceptibilities appears only below T_c (see Figure 1) and indicates unambiguously the history dependence of the state and the spin-glass nature of the observed transition. The vast number of possible frozen spin configurations at low temperatures leads to the existence of a great many metastable states with macroscopically long lifetimes. Long as they are, however, these lifetimes are finite — leading to a number of very slow effects such as the slow relaxation of the remanent magnetization [8] or various ageing effects [9]. The relaxation in the vicinity of each metastable state is rapid, thus determining the high-frequency properties of spin glasses. However, some of the "fast" modes in the vicinity of each metastable state are soft, so that the frequency spectrum of real spin glasses extends continuously from microscopic (10^{-12} s) to macroscopic (weeks) times.

In spite of a great deal of effort, the theoretical description of spin glasses is still far from complete. The only developed microscopic theory is based entirely on the mean-field approximation, and so can be applied directly only to the Sherrington–Kirkpatrick model [10] with infinite-range interaction between spins. Despite the unphysical infinite-range interaction, the properties of the SK model resemble

many of the phenomena observed in real spin glasses, and its solution is at the least very instructive. Like real spin glasses, it undergoes a transition: below the transition temperature, the field cooled and zero-field cooled susceptibilities differ, many metastable states appear and all properties become history-dependent; the relaxation in the vicinity of each metastable state is also slowed down to a power law. The most important qualitative difference of the SK-model properties from the properties of real spin glasses is the absence of finite energy barriers in the former, so that all effects of ageing and slow relaxation of magnetization are missing.

As we should expect, the MFT cannot describe the singularity of physical quantities at the transition temperature. Indeed, the differences between the values of the critical exponents in the SK model and those observed experimentally are large. For instance, the SK value for the exponent γ of the nonlinear susceptibility, $\chi_3 \equiv -\partial^2\chi/\partial h^2 \propto \tau^{-\gamma}$, is $\gamma = 1$, whereas the experimental value of γ varies from 3.3 ± 0.2 in refs. [11, 12] to 2.2 ± 0.2 in refs. [13, 14].

The presence of a small magnetic field smears out the cusp in the susceptibility, but the temperature $T_f(h)$ at which irreversibility appears remains a well-defined quantity. Below this temperature, a large number of metastable states still appear. Surprisingly, the MFT result $T_f(h) - T_f(0) \propto h^{2/3}$ [15] coincides with the experimental observations [16, 17].

Below the transition temperature in the SK model, the state with the lowest energy is separated from the next state by the energy gap $\approx T_c$, so that it has a statistical weight of order unity. Small variations of the external parameters of the model (temperature, magnetic field, etc.) cause an exchange of the ground state with some other state, so that the full thermodynamic average implies transitions across the infinite barriers separating different metastable states. The qualitative correspondence between the SK model and real spin glasses means that some of the barriers in the real spin glass become finite, but there are a large number of barriers that are effectively impenetrable at a given timescale. Thus it is possible that equilibrium properties of real spin glasses resemble more closely the properties of the SK model, but their observation must take an infinite time and so — alas — is impossible. The correspondence between the short-time properties of real spin glasses and the properties of a single metastable state seems more encouraging, but here we meet another difficulty: the spectrum of the

"fast" relaxation and the spectrum of "slow" transitions over the barriers overlap in real spin glasses, so we do not know what these short times are — if indeed there are any. So, comparing the results of the MFT with experiment, we can expect only that the experimental results resemble something in between the thermodynamic average and the properties of a single state in the SK model.

Two different techniques have been developed to obtain analytical results in the SK model. The first is based on the replica trick, and describes thermodynamic properties of the system and the structure of the space of metastable states, which was proved to have an ultrametric topology (the states are organized in a form of a hierarchical tree) [18]. The second is based on the dynamic approach, and was originally developed to describe thermodynamic properties and to check the replica scheme. In order to obtain the properties of a single metastable state, we must somehow specify it. The most physically appealing way to do this is to specify the history of cooling the system from the paramagnetic state. The dynamic approach can be slightly modified to handle this problem and provide the valuable information on the properties of a spin glass with impenetrable barriers. We state the general results and formulate the SK model in Section 2.1, review its thermodynamic properties in Section 2.2, and then discuss the dynamical approach and the properties of a single metastable state in Section 3.3.

This scheme is based on the hierarchical nature of the space of metastable states in the SK model, but presumably it can also be applied to other systems with a similar organization of metastable states.

1.3 Slow Relaxation and Ageing

Just as ordinary glasses creep slowly under strain, the magnetic properties of spin glasses vary slowly over the time of an experiment. This phenomenon reveals the nature of the spin-glass state, proving that it is always a non-equilibrium state in any real experiment. Numerous experimental papers are devoted to the study of this phenomenon (see [19, 20] and references therein). Several experimental techniques are usually employed to cover the time interval 10^{-2}–10^{5} s where the phenomena occur.

In the simplest and most straightforward approach, the relaxation of magnetization $\delta M(t)$ is measured as a reaction to a small stepwise

variation of the magnetic field $\delta h(t) = \Delta h\,\theta(t-t')$. The response function $p(t, t') = \delta M(t)/\delta h$ is related to the usual response function $G(t, t') = \delta M(t)/\delta h(t')$ by

$$p(t, t') = \int_{t'}^{t} G(t, t'')\,\mathrm{d}t''. \tag{1.3.1}$$

At equilibrium the functions $p(t, t')$ and $G(t, t')$ would depend only on $t-t'$, and the fluctuation-dissipation theorem (FDT) would hold:

$$T[p(t) - p(\infty)] = C(t), \tag{1.3.2}$$

where $C(t)$ is the irreducible correlation function

$$C(t) = \overline{\langle S(t)S(0)\rangle} - \overline{\langle S(0)\rangle^2}.$$

In the alternative approaches the frequency-dependent susceptibility $\chi(\omega)$ or the magnetic noise spectrum $\langle M^2(\omega)\rangle$ [21] are measured directly. The latter technique is unique because it allows one to study the system behaviour in zero magnetic field and to check the FDT, which would imply

$$\mathrm{Im}\,\chi(\omega) = \frac{\omega}{2T}\langle M^2(\omega)\rangle. \tag{1.3.3}$$

The correlation function $C(t)$ measured by all of these techniques decreases slowly with time; it has been approximated by various analytical forms: logarithmic, power-law, stretched exponential and others. The relaxation processes in spin glasses are sometimes described by a continuum spectrum of relaxation times $g(t)$, which is usually defined by the integral representation of $C(t)$:

$$C(t) = \int_{0}^{\infty} \mathrm{e}^{-t/\tau} g(t)\,\frac{\mathrm{d}\tau}{\tau}. \tag{1.3.4}$$

Experimental results* show that the function $g(\tau)$ decreases slowly with time over all achievable times of measurements. Therefore a spin glass can never reach equilibrium in a real experiment, which is performed after a finite time $\tilde{t}$ has passed since cooling the sample to the

* A review of experiments and further references can be found in [19, 20].

given temperature. The nonequilibrium reveals itself even in the short-time ($t < \tilde{t}$) properties because the interaction of nonequilibrium slow modes with fast ones can lead to nonequilibrium deviations in the dynamics of the latter. Indeed, experiments confirm that the observed relaxation spectrum $g(\tau)$ depends on the waiting time t_w during which the glass stays at a constant temperature before the measurement begins. The first observation of this dependence was made by the Uppsala group [22], who measured magnetic relaxation in CuMn spin glass and examined the spectrum $g(\tau)$ derived from their results. They found that the spectrum $g(\tau)$ has a maximum at $\tau \approx t_w$; only at $\tau \ll t_w$ is it independent of the waiting time t_w, so that the equilibrium properties can be deduced from the experimental data. The time $\tilde{t} = t_w + t$ that a sample stayed at a constant temperature is often called the "age" of a spin glass, and all these phenomena are called "ageing". Ageing occurs in all spin glasses, and its influence on relaxation processes should always be taken into consideration.

A phenomenological but quantitative description of ageing was proposed by the Saclay group [23, 9], who measured the time decay of the thermoremanent magnetization $M_{TRM}(t)$ in the following experiment: the sample was first cooled in a small field H down to a desired temperature $T < T_g$; then, after some waiting time t_w at a temperature T, the magnetic field was switched off and the time decay of $M_{TRM}(t)$ was recorded as a function of the observation time t. Their description was based on the approach employed in the study of the strain creep in glassy polymers [24]. They assumed that the slow dynamics at age $\tilde{t}_a$ is $(\tilde{t}_a/\tilde{t}_b)^\mu$ times slower than the dynamics at age $\tilde{t}_b$. Then introducing the effective time variable $\xi(t)$ by

$$\frac{d\xi}{t_0} = \left(\frac{t_0}{t_w + t}\right)^\mu dt,$$

$$\xi = \frac{t_0^{\mu-1}}{1-\mu}\left[(t_w + t)^{1-\mu} - t_w^{1-\mu}\right] \tag{1.3.5}$$

(here t_0 is an arbitrary timescale), they found that all of the experimental decay curves $M_{TRM}(t)$ collapsed to a single curve $M(\xi)$ when expressed in terms of the variable $\xi(t)$. The experimental study of diverse spin glasses ($Ag_{1-x}Mn_x$, $CsNiFeF_6$ and $CdIn_{0.3}Cr_{1.7}S_4$) shows that the ansatz (1.3.5) describes the relaxation equally well in all of them. The obtained values of μ usually lie in the interval 0.7–0.9 and

depend on T/T_g. The master curve $M(\xi)$ can be fitted by the product of a power law and a stretched exponential:

$$M(t) = M_\tau(t_w)\xi^{-\alpha} \exp\left[- \left(\frac{\xi}{\tau_p}\right)^{\beta} \right]. \qquad (1.3.6)$$

In the cases of $Ag_{1-x}Mn_x$ and $CdIn_{0.3}Cr_{1.7}S_4$ the dependence of $M_\tau(t_w)$ on the waiting time can be fitted by a power-law form $M_\tau \propto t_w^{\alpha\mu}$, so that (1.3.6) is simplified to

$$M(t) = M_0 t^{-\alpha} \exp\left[- \left(\frac{\xi}{\tau_p}\right)^{\beta} \right], \quad \beta = 0.5\text{–}0.8, \qquad (1.3.7)$$

where M_0 does not depend on t_w. The difference between these spin glasses and $CsNiFeF_6$, which cannot be described by (1.3.7), is probably due to the large value of the ferromagnetic-type interaction in the latter compound. Certainly, neither (1.3.7) nor (1.3.6) can describe the rapid relaxation of the magnetization that happens immediately after the switching off the field, and so neither of them can be applied to a region t, $\xi \to 0$. In quasiequilibrium, which is attained only as $t_w \to \infty$, the relaxation (1.3.7) acquires a simple power-law form with the exponent α which is approximately 0.15 near T_g and decreases rapidly with temperature.

This phenomenological theory of ageing in spin glasses is further substantiated by experimental study of magnetic noise under the same conditions [21, 20]. Moreover, the values of the magnetic noise and the susceptibility obey the FDT if they are measured at the same spin-glass age.

A quantitative theoretical explanation of ageing is still lacking. The results obtained in the infinite-range SK model are absolutely useless here because slow relaxation processes, which could, in principle, explain ageing, imply transition over the barriers separating the metastable states, which become infinite in the thermodynamic limit in the SK model. The SK model gives an adequate explanation only of the dependence of the system state on its magnetic history (i.e. the dependence on the path in the (H, t) plane), since this dependence does not imply a transition over the barriers (see Section 2.3). The semiphenomenological scaling theory of the low-temperature spin-glass state does not explain all ageing phenomena, either, but at least it helps in understanding why the equilibrium is difficult to attain in spin glasses. This theory [25] is based on the results of Monte-Carlo simulations of short-

range spin glasses, which show that at low temperatures the energy of the excitation scales with its size L as L^y, $y \approx 0.25$ [26, 27]. The excitations at low temperatures consist of inversion of some system of spins. In ferromagnets the spins would occupy a compact domain, but in spin glasses the dimension of the domain occupied by this spin system can be fractal and less than the dimension of space ($d = 3$). The influence of the external perturbation (a small change in temperature, magnetic field, etc.) on the energy of excitation also scales with its size as $L^{d_s/2}$, where d_s is the fractal dimension of the excitation itself or its border. In any case, $d_s \geqslant 1$, so that on large scales the energy of the excitation becomes less than the influence of a small variation in the external parameters. Therefore any small variation in the external parameter modifies the ground state of the spin glass [28]. Clearly in order to regain equilibrium after such a modification of the ground state, the spin system must be completely reorganized on large scales, which takes an infinite time.

Interestingly, the simple model of one-particle motion displays the same time scaling (1.3.5) as real spin glasses. In this simple model, considered in Section 3.1, the particle drifts in a random potential $U(x)$ due to external thermal noise. The random potential is generated by a random Gaussian force $F(x) = U'(x)$ with $\overline{F(x)} = F$, $\overline{F^2} - \overline{F}^2 = \gamma\delta(x-x')$. As we show in Section 3.1, for $\kappa = 2FT/\gamma < 1$, the motion of a particle is described by the time scaling (1.3.5) with $\mu = 1 - \kappa$.

In spite of being unable to predict the finite energy barriers between metastable states, the SK model can, in principle, give the qualitative structure of the space of metastable states. Indeed, some details of this structure have been experimentally corroborated: the SK model predicts an increase in the ramification of the hierarchical structure of the metastable-states space with decreasing temperature. Experimental study [29] of a modified ageing — occurring when the normal process of ageing is interrupted by a rapid cooling and then a reheating after a period of time — shows that at a lower temperature transitions occur only between metastable states that have a common ancestor at a higher temperature, so that reheating the system deletes all memory of its dynamics at a lower temperature. The same process of cooling–heating applied to the SK model can be studied theoretically and leads to qualitatively similar results (Section 2.3). This similarity compels us to think that the tree-like hierarchical organization of metastable states in the SK model resembles the space of metastable states in real spin

glasses. At present no microscopic theory describing the space of metastable states in real spin glasses is available (although the hierarchy of paramagnetic clusters appearing at a critical point T_g (Section 4) may represent a precursor of the low-temperature hierarchy). In the absence of *any* microscopic theory of metastable states in a real spin glass, the study of the one-dimensional spin-glass model with long-range interaction appears to be very instructive (Section 3.2), because, despite its one-dimensionality, it has a ramified structure of metastable states and exposes various phenomena of slow relaxation and ageing.

1.4 Critical Behaviour in Three Dimensions

The existence of a genuine thermodynamic transition in a real three-dimensional spin glass was the subject of long-standing controversy. Before 1983 it was generally believed that the spin-glass transition is a dynamic phenomenon and does not result in thermodynamic singularities. After 1983 this belief was rocked by several very accurate measurements of nonlinear magnetic susceptibility $\chi_3 = \partial^3 M/\partial h^3$ (see e.g. [11, 33]). The results of these measurements pointed almost unambiguously to the singular behaviour of the susceptibility $\chi_3(T) \propto (T-T_f)^{-\gamma}$, with γ varying from one spin glass to another, but generally being within the range (2.5–3.5). The singular behaviour of the susceptibility χ_3, if proved, implies the thermodynamic nature of the spin-glass transition; moreover, it is precisely χ_3 that plays the role of a generalized susceptibility associated with the spin-glass order parameter. These results were later confirmed by a set of analogous measurements on various spin glasses: transition-metal alloys, rare-earth alloys, semiconducting and insulating spin glasses. (For exhaustive reviews see [3, 4].) Other evidence also appeared favouring the phase transition: it was shown that the characteristic relaxation time diverges for $T \to T_f$ as $\tau \sim (T-T_f)^{-z\nu}$, with $z\nu = 7$–9 [3, 4, 30, 31]. It has now been generally accepted that real spin glasses undergo a thermodynamic transition. (One possible exception that should be mentioned is the class of magnetically diluted insulating compounds [32–34].)

This belief is further supported by large-scale numerical simulations of Ising spin glasses with nearest-neighbour interaction [35–37]; the values of the critical exponents γ, ν and z provided by these simulations are close to the values observed in experiments on real spin glasses,

which are usually Heisenberg magnets with weak anisotropy. This coincidence of critical exponents in numerical simulations and experiments performed on systems of different symmetries can be explained by other results of numerical simulations, which indicate the absence of a transition in XY [38, 39] and Heisenberg [40] spin glasses with nearest-neighbour interaction. If this is the case then the observed phase transition in real spin glasses arises from the weak anisotropy and belongs to the same universality class as the transition in the Ising spin glass.

Unfortunately, there is still no theory of the spin-glass transition. Early attempts to use the renormalization-group approach, which has proved so useful for ordinary phase transitions ($(6-\epsilon)$-expansion) [41], failed because, as was shown later [42–44], the results of the $(6-\epsilon)$-expansion cannot be applied to dimensions $D \leqslant 4$ owing to the essential singularity at $D = 4$. In fact, this essential singularity at $D = 4$ was at first interpreted as evidence against any spin-glass transition below $D_c = 4$, whereas at present it is believed that this singularity indicates a change in the nature of the transition at $D_c = 4$. One way or the other, one thing is certain: the ϵ-expansion cannot be employed for the description of the spin-glass transition in three dimensions.

Another, phenomenological, approach was developed in [45–47]. It is based on the concept of critical fractal clusters and combines the old Néel idea of independent paramagnetic clusters with the idea of critical growth of these clusters in the vicinity of the phase transition. Although quite successful as a phenomenological approach, it makes one somewhat uneasy, with its principal concepts — critical clusters and their growth — left unexplained.

In Section 4 we discuss an analytic theory of the spin-glass transition, proposed by us in a series of papers [48–50], that yields a semiquantitative description of three-dimensional spin-glass phase transitions. Roughly speaking, this theory explains the origin of the critical clusters and their growth. Below in this section we outline the main ideas of our approach.

We start from a slightly modified Edwards–Anderson model Hamiltonian with random spin–spin interaction J_{ij} that is finite-range so that the number of spins interacting with a given one is $Z_0 \gg 1$ (in the usual Edwards–Anderson model $Z_0 = 2D$). Our goal is to construct some renormalization procedure. For this purpose, we employ neither real-space nor momentum-space representations, which are now common,

but rather a representation based on the eigenfunctions of J_{ij} matrix, which is more appropriate for this problem. The spectrum of the J_{ij} matrix consists of the delocalized eigenfunctions with eigenvalues $|E_\lambda| < E_c$ and the localized ones with $|E_\lambda| > E_c$.

This representation based on the eigenfunctions of the J_{ij} matrix helps to pick out the slow modes and average over fluctuations of the fast ones, which is the usual procedure in any renormalization-group scheme. However, whereas in the momentum-space renormalization scheme the fast modes are separated from the slow ones by their momentum, in the spin-glass problem the only characteristic of the eigenfunction is its energy E_λ.

In the vicinity of the transition temperature T_0 determined from mean-field equations (which become exact in the limit $z \to \infty$) the slowly relaxing part of the magnetization m_i can be easily determined in terms of the representation $m_i = \Sigma_\lambda a_\lambda \psi_\lambda(i)$ through the eigenfunctions ψ_λ of the J_{ij} matrix: the slow part corresponds to the localized eigenfunctions ψ_λ with E_λ near the localization mobility edge E_c: $E_\lambda - E_c \ll E_c$. These amplitudes a_λ constitute the desired set of slow modes that are similar to the original spins σ_i; thus we have constructed the first step of the renormalization scheme — we have passed from the variables σ_i to variables a_λ that govern the slow relaxation of σ_i. The interaction between the new variables ("pseudospins") a_λ increases rapidly with decreasing temperature, so at some temperature T_1,

$$\frac{T_0 - T_1}{T_0} \approx Z_0^{-p}, \quad 0 < p < 1 \tag{1.4.1}$$

we get the same model that we started with: the system of "pseudospins" $a_\lambda/|a_\lambda|$ near its transition temperature (determined again from the mean-field equations). The only parameter that characterizes the new effective spin-glass Hamiltonian $\bar{H}\{\sigma\}$ is the mean number of interacting "neighbours" Z_1. All the calculations outlined are possible under the condition $Z_0 \gg 1$. Therefore two rather different scenarios of RG transformation can be imagined: (I) $Z_1 \geqslant Z_0$, so that the accuracy of the employed $1/Z$ expansion is retained or improved; and (II) $Z_1 < Z_0$, i.e. Z decreases under the action of the RG, thus leading to a spin-glass problem with $Z \approx 1$, which is beyond any present analytic approach. To discriminate between these two possibilities, we need to know some power-law exponents associated with the localization transition (we adopt the ideas of the scaling theory of the localization

transition [51–52]). A specially designed numerical study points at (I) as the most probable, so we shall bear it in mind below. Therefore the sequence of crossover points T_n corresponding to the appearance of the nth hierarchy level (cf. (1.4.1)) converges rapidly to an accumulation point T_f. As $T \to T_f$ from above, the number of hierarchy levels tends to infinity, along with the nonlinear susceptibility χ_3 and the average relaxation time. Thus at the critical point the spin glass can be viewed as an infinite hierarchy of fractal "clusters". (Note, however, that the term "cluster" must be used with some care here, since these clusters overlap and intersect each other.)

The above picture is by no means the only one that is possible in the framework of the approach used. Another plausible scenario is macroscopic condensation into the maximum-eigenvalue ($E_\lambda = E_c$) extended mode. Indeed, precisely that picture (which is similar to the usual Bose condensation) was proposed in earlier treatments of the eigenfunction approach to the spin-glass transition [53–55]. In fact, this macroscopic-condensation picture is valid for high space dimensions (probably for $D > 4$) whereas in three-dimensional cases the hierarchy of localized modes appears.

Moreover, there is also a third possibility, namely that there is no phase transition at all, which is certainly realized in two-dimensional models. In the three-dimensional Ising case our calculations show that the transition undoubtedly does exist — in agreement with Monte-Carlo results [35–37]. The situation with three-dimensional vector models is less clear. Our results point at the existence of a phase transition (though with less certainty than for the Ising case) — in contrast with the Monte-Carlo results [38–40]. Among possible origins for this discrepancy, it should be noted that Monte-Carlo simulations refer to the nearest-neighbour model, whereas our theory is developed for the case of large coordination number $Z_0 \gg 1$, which can belong to another universality class.

Unfortunately, at present we are unable to calculate the critical exponents γ, ν and z of the above phase transitions, since these exponents are expressed in terms of two localization-problem exponents, which are still only known with poor accuracy. Nevertheless, the new phase-transition picture obtained seems interesting as it unifies in a natural way the concept of critical fractal clusters [45–47] and the concept of hierarchy known to be relevant [5, 18, 29] for the low-temperature spin-glass state.

Additionally, a very interesting class of spin-glass models is represented by the XY model with a complex (Hermitian) random matrix J_{ij}. This "gauge-glass" model describes granular superconductors in the intermediate magnetic-field range (see Sections 1.7 and 7); therefore its critical behaviour can be explored experimentally. Corresponding critical exponents are related (Section 4) to localization exponents for the unitary ensemble.

1.5 Nonexponential Relaxation in the Griffiths Phase

The onset of spin-glass ordering reveals itself in the critical slowing down of order-parameter relaxation. This means that the relevant time-scale t_r entering the relaxation function $q(t) = \langle S_i(t)S_i(0)\rangle$ diverges as $T \to T_f + 0$, as has been demonstrated in numerous experiments (see [30–34]); other references can be found in [3, 4]) and Monte-Carlo simulations [37, 3, 4]. This phenomenon is common for continuous phase transitions, but usually (in regular systems) all the nonanalytic behaviour is associated only with the transition point, so that at $T > T_f$ the $q(t)$ asymptotic is exponential,

$$-\ln q(t) \underset{t\to\infty}{\to} t/t_r, \tag{1.5.1}$$

and t_r has the meaning of maximum relaxation time. The relation (1.5.1) also holds for the infinite-range spin-glass model. However, the situation is very different in short-range spin glasses, as was demonstrated in large-scale Monte-Carlo simulations of the three-dimensional nearest-neighbours $\pm J$ Edwards–Anderson model [37]. It was shown unambiguously that

$$-\ln q(t) \underset{t\to\infty}{\sim} (t/t_r)^{\beta}. \tag{1.5.2}$$

Here β is some temperature-dependent exponent that increases monotonically with temperature from $\beta(T_f) \approx \frac{1}{3}$ up to $\beta(T_0) = 1$, where T_0 is the temperature of the ferromagnetic phase transition on the same lattice ($T_0 = 4.5J \approx 4T_f$). Thus it turns out that the relaxation at $T > T_f$ is of the "stretched-exponential" type and the spectrum of relaxation times is unbounded, in a broad temperature interval extended up to T_0, i.e. far above T_f. The usual exponential relaxation (1.5.1) is recovered only at $T > T_0$. Therefore three different phases can be distinguished in spin glasses according to different dynamic behaviour: the usual

paramagnetic phase at $T > T_0$; an intermediate paramagnetic phase with an unbounded spectrum of relaxation times at $T_f < T < T_0$; and a low-temperature condensed phase at $T < T_f$. The temperature T_0, which does not appear in the usual thermodynamic quantities of the system, can nevertheless be defined in terms of them: it was recognized sometime ago by Griffiths [56] that at $T < T_0$ the free energy of any random system is nonanalytic as a function of temperature, magnetic field, etc. Here T_0 is the highest transition temperature allowed by a given distribution of random variables; for example, in the case of a dilute ferromagnet [56] with transition temperature $T_c(p)$ (p is the degree of dilution) the loss of free-energy analyticity occurs at $T < T_c(0) = T_0$. The intermediate paramagnetic phase at $T_c < T < T_0$ with nonanalytic behaviour of thermodynamic quantities is known as the Griffiths phase; its existence is the result of disorder fluctuations, which make it possible to find local regions with any "local T_c" values up to T_0. The relevance of these fluctuations for dynamics was first recognized by Randeria, Setha and Palmer [57], who considered the probability of finding a cluster of ferromagnet bonds, and obtained a "lower bound" on the Ising-spin-glass relaxation function $q(t)$ in the form

$$-\ln q(t) \underset{t\to\infty}{\sim} (\ln t)^{\alpha}, \tag{1.5.3}$$

where $\alpha = d/(d-1)$ and d is the space dimension (see [58] for more details).

The apparent contradiction between the simulation result (1.5.2) and the "lower bound" (1.5.3) can possibly be resolved by the following argument. Generally, one can distinguish between two types of "long-time" behaviour. The first refers to the form of scaling function $g(t/t_r)$ entering the critical relaxation function $q(t) \sim t^{-x} g(t/t_r)$, which was found in [37]:

$$q(t) \sim \frac{1}{t^x} \exp\left[-\left(\frac{t}{t_r}\right)^{\beta}\right]. \tag{1.5.4}$$

The second is the true limiting behaviour as $t \to \infty$, which probably reveals itself at times much larger than t_r and obeys the inequality (1.5.3). Usually relaxation of the type (1.5.3) is given by considerations in terms of compact "clusters" for Ising-like systems.

The relaxation time t of a "cluster" is determined by the rate of thermal activation over a high free-energy barrier $E \gg T$; thus

$t \propto e^{E/T}$. For a cluster of size L, the barrier E as well as the logarithm of the probability of finding such a cluster are power-law functions of L; thus leading to (1.5.3) with some value of α. The physical nature of such "clusters" depends on the model and timescale considered. In Section 5 we discuss several models possessing nonexponential relaxation, which appear to be solvable analytically.

Disordered ferromagnets obeying the Ginzburg criterion for the weakness of thermal fluctuations are considered in Section 5.1. For the Ising case it is shown that the long-time tail of $q(t)$ is of the form (1.5.3) with $\alpha = 1$, i.e. a power law (with nonuniversal exponent decreasing with increasing disorder). Three-dimensional spin glasses with long-range (but finite) interactions are explored in Section 5.2.1. For the Ising case the intermediate asymptotic behaviour (5.3) with $\alpha = 1$ is obtained. At very long times this asymptote is probably replaced by that of Randeria *et al.* [57, 58] with $\alpha = \frac{3}{2}$.

Vector spin counterparts of the above models are also considered in Section 5. Although compact clusters are also important for vector-spin glasses, the activation barriers are absent and a cluster's relaxation time is proportional to its volume. This results in the stretched-exponential behaviour (1.5.2) with $\beta = \frac{1}{2}$. The same result is obtained in Section 5.2 for the RKKY vector spin glass in the broad temperature range $T_f < T < T_0$ (here $T_0 \sim X^{-1}T_f$ and $x \ll 1$ is the atomic concentration of magnetic ions). Neutron spin-echo experiments [59] showed nonexponential relaxation far above T_f in dilute metallic spin glasses, although a quantitative analysis was not carried out.

Turning back to Ogielski's result [37] (1.5.4) for the Ising spin glass in the intermediate region $t \geqslant t_r$, we recognize that the picture of isolated compact clusters of any kind is inappropriate here. In this region an adequate approach should take simultaneously into account both the interactions between critical fluctuations and the effects of disorder. Such a theory does not yet exist.

A simple model that probably captures some features of real spin glasses was introduced by Campbell [60]. He suggested that Ising-spin-glass relaxation at $T_c < T < T_0$ be mimicked by free diffusion over a randomly diluted set of vertices of a 2^N-dimensional hypercube representing the phase space of the model. It was assumed that the decrease in the spin-glass temperature corresponds to the increase in the dilution degree p, so that the critical temperature T_c corresponds to the percolation threshold $p = p_c$ in phase space. Rather surprisingly, this sug-

gestion was confirmed by computer simulation [61], where stretched-exponential relaxation with p-dependent exponent β was observed; it was also shown that $\beta(p_c) \approx \frac{1}{3}$ is in agreement with Ogielski's result $\beta(T_c) \approx \frac{1}{3}$. Moreover, experimental data obtained for different types of glassy systems seem to point to the universal nature of the relaxation law (1.5.4) with $\beta \approx \frac{1}{3}$ (see [62] for a discussion).

A somewhat more general approach based on the concept of the fractal structure of the free-energy surface is discussed in Section 5.3. This allows consideration of the relaxation process in terms of diffusion in a fractal-like potential, which could give both stretched-exponential, (1.5.2.), and quasi-power-law, (1.5.3), relaxation.

1.6 Spin Glasses with Helical Correlations

Canonical diluted metallic spin glasses such as $Cu_{1-x}Mn_x$ and $Au_{1-x}Fe_x$ are characterized by a spin–spin interaction that is an oscillating function $J(r_{ij})$ of the distance between spins, which is usually approximated by the RKKY form

$$J_{\mathrm{RKKY}}(r) = J_0 \frac{\cos p_0 r}{r^3}. \tag{1.6.1}$$

Thus the random nature of spin glasses is the consequence of the randomness in the spin positions combined with rapid oscillations of $J(r)$ (it is assumed that $p_0 \bar{r}_{ij} \gg 1$, where $\bar{r}_{ij} \approx C^{-\frac{1}{3}}$ is the mean value of the distance between spins situated at random with concentration C). In a pioneering paper [2] Edwards and Anderson suggested a simplification of the problem by mimicking the true interaction $J(r_{ij})$ by random uncorrelated quantities J_{ij} with a given variance $\overline{J_{ij}^2} = K(r_{ij})$. The Edwards–Anderson (EA) model captures the main properties of spin glasses and is the starting point for most spin-glass studies.

Nevertheless, one can worry about some situations when correlations between J_{ij} values are relevant and thus the EA model is too oversimplified. Indeed, it has been shown in neutron-scattering experiments that in the RKKY alloys $Cu_{1-x}Mn_x$ and $Ag_{1-x}Mn_x$ with moderate concentrations of magnetic ions ($x = 0.05$–0.2) there are short-range helical correlations [63–65]. The wavelength of the helix appears to be concentration-dependent, and the correlation length of the helical order is definitely larger than $\bar{r}_{ij}$ for $x \geqslant 0.1$. Thus the properties of these alloys cannot be described correctly by the EA model, and J_{ij} correlations

should be taken into account. We shall name such systems correlated spin glasses.

An even more remarkable example of this kind is provided by rare-earth spin glasses $Y_{1-x}R_x$ with R = Gd, Dy, Tb, Er. Neutron-scattering study [66, 67] of the $Y_{1-x}Gd_x$ alloy with $x \geqslant 0.015$ shows the helical correlation length $R_c > 600$ Å in the low-temperature state, so that this system was identified as a long-range helical antiferromagnet (whereas magnetic measurements on other $Y_{1-x}R_x$ alloys in this concentration range reveal spin-glass properties [16, 68, 69]). The appearance of such a structure at a rather low concentration was attributed to the Overhauser picture [70] of spin-density-wave (SDW) stabilization by localized magnetic moments of Gd (see [71] for an extensive discussion). The proximity of the yttrium host to the SDW formation should be accompanied by the existence of very soft virtual excitations — paramagnons — which contribute substantially to the indirect interaction between the guest's magnetic moments. The simplest form of that interaction in the Fourier representation is

$$w(p) = w_0 \left[\left(\frac{p - p_0}{\kappa} \right)^2 + 1 \right]^{-1}, \tag{1.6.2}$$

where κ^{-1} is the interaction length, $\kappa \ll p_0$. In real space, (1.6.2) gives

$$J_0(r) = w_0 \frac{\kappa p_0}{2\pi r} \sin p_0 r \, \mathrm{e}^{-\kappa r}. \tag{1.6.3}$$

Less-singular behaviour of $J_0(r)$ (with respect to $J_{\mathrm{RKKY}}(r)$ at small r leads to qualitative differences between these interactions: the effective number of interacting neighbours is $Z \approx c\kappa^{-3}$, and can be large in the former case while it is of the order of unity in the latter case. In Section 6 we investigate the properties of the model with the interaction (1.6.3) under the condition $Z \approx c\kappa^{-3} \gg 1$. It will be shown that the correlations between J_{ij} can be neglected and the EA model can be used under the condition $\gamma \equiv \kappa p_0^2/\pi c \gg 1$ only. In the opposite limit $\gamma \leqslant 1$ these correlations are relevant despite the inequality $p_0 c^{-1/3} \gg 1$ being fulfilled. Therefore a new lower-temperature state of a helical spin glass emerges — which differs qualitatively from the low-temperature state in the EA model.

The above formulae (1.6.2) and (1.6.3) refer to the case of exact spherical symmetry of the paramagnon spectrum. All of the parameters w_0, κ and p_0 can be dependent on the unit vector $\boldsymbol{l} = \boldsymbol{p}/p$. In fact, only

the $w(l)$ dependence is substantial, since it removes the degeneracy with respect to the direction of the helix wave-vector $\boldsymbol{Q}$. There always exists a $\boldsymbol{Q}$-direction that is preferred with respect to the crystalline-lattice axis; for example, in the $Y_{1-x}R_x$ alloys $\boldsymbol{Q}$ is colinear with the hexagonal C-axis, while there are twelve possible $\boldsymbol{Q}$-directions in CuMn and AgMn alloys [63–65]. It seems probable that the $w_0(l)$ dependence is rather smooth near (each) optimal direction l_c, so that the generic form of the interaction that we shall use below is

$$w(p) = w_0(1+\omega(l))\left[\left(\frac{p-p_0}{\kappa}\right)^2 + 1\right]^{-1}, \quad \frac{\partial^2\omega}{\partial l^2} \ll 1. \tag{1.6.4}$$

Clearly the indirect spin–spin interaction depends mainly on the host-lattice properties; thus the form (1.6.4) is equally applicable to YGd as well as to other $Y_{1-x}R_x$ alloys [72, 73] (the differences in their behaviour are probably connected with the role of single-ion anisotropy, which is very weak for Gd but rather strong in other cases). It has also been shown [72] that the RKKY interaction in the concentration region $c \geqslant p_0^3$ is virtually equivalent (with respect to large-scale properties) to the interaction (1.6.3). Thus we believe that helical correlations in Cu(Ag)Mn alloys with moderate Mn concentrations can also be described by the interaction (1.6.4).

In Section 6.1 we discuss the mean-field ($Z \to \infty$) phase diagram of a system consisting of randomly situated Ising as well as vector spins with the interaction (1.6.4). An equation for the transition temperature is derived for the whole range of the parameter $\gamma = \kappa p_0^3/4\pi c$ determining the degree of correlations in the system. Note that similar equations are obtained in formally similar problems of spin-glass superconductivity (Section 7.1) and neural networks (Section 8.1): all three problems refer to the general class of "correlated spin glasses" as well as the problem of concentrated magnetic alloys with strong random anisotropy [74].

The subsequent subsections of Section 6 are devoted to the renormalization-group (RG) study of the low-temperature state with helical correlations at $\gamma \ll 1$. We consider here equilibrium thermodynamic properties and thus confine ourselves to the vector-spin case ($n = 2, 3$) inasmuch as in the Ising case the equilibrium is unattainable definitely. We identify slow (in the RG sense) variables and derive their effective Hamiltonian in Section 6.2. In Section 6.3 we undertake the RG study of that Hamiltonian, show that helical long-range order is unstable with

respect to fluctuations and obtain the results for the correlation lengths of helical short-range order. In Section 6.4 we discuss the magnetic-response properties of the helical structure, i.e. the linear susceptibility $\chi(T)$, the nonlinear susceptibility $\tilde{\chi}(T) = -\partial^3 M/\partial h^3$ and the differential susceptibility with finite fields $\chi(T, h)$.

In Section 6.5 we compare our results with experimental data on the YGd system, and propose additional experiments that can elucidate the nature of the magnetic state in other YR alloys [73].

1.7 Superconducting Analogue of Spin Glasses

One of the main achievements of spin-glass studies is the widespread realization that spin-glass concepts can be successfully applied in various fields of physics and other sciences (an extensive review of different applications is given in the book [75]). The examples extend from structural and polar glasses to optimization problems, models of associative memory and even the origin of life.

Section 7 below is concerned with one of the physical applications — we consider the properties of granular superconductors in a strong magnetic field, i.e. Josephson networks.

These systems are notable for the existence of a new superconducting state that is the superconducting analogue of the low-temperature state in spin glasses. Hereinafter we shall call this state the superconducting-glass (SCG) state. The SCG was theoretically predicted in [76–80] and some of its properties have been observed in a growing number of experiments (e.g. [81–85]).

Granular superconductors have two-level organization: intragranular, where an ordinary superconducting order parameter is generated; and intergranular, which can be described as the interaction between the phases of the order parameters in different granules. The macroscopic properties of the systems are governed mainly by the latter. The energy of the interaction between the phases across the junctions between the granules is given by

$$H = \sum_{i,j} J_{ij}^{(0)} \cos(\phi_i - \phi_j - \phi_{ij}) \tag{1.7.1}$$

where ϕ_i is the phase of the ith granule, ϕ_{ij} is the phase difference originating from the magnetic field H, and $J_{ij}^{(0)}$ is the energy of the junction, which can be expressed in terms of the critical current I_{ij}^c: $J_{ij}^{(0)} = \hbar I_{ij}/2e$.

There are two different junction types: the Josephson junction through a dielectric layer, and the proximity junction through the normal metal. In the former case the interaction $J_{ij}^{(0)}$ couples the nearest-neighbouring granules only, while in the latter case the interaction length is equal to the coherence length in the normal metal $\xi_n(T)$.

Superconducting ceramics are very likely candidates for Josephson networks giving SCG behaviour in rather weak magnetic fields, as has been suggested by experiment [85–86].

A network of proximity junctions between superconducting granules is generated in a compound system of Pb granules (approx. 1 μm size) immersed in a Zn matrix [87]. Generally the proximity network can exhibit two regimes of different kinds: if $\xi_n(T) \gg r_{ij}$ (the mean intergranular distance) then the fluctuations of the interaction $J_{ij}^{(0)}$ are negligible and the network as a whole at $H = 0$ is described by a weakly disordered XY model, whereas in the opposite limit $\xi_n(T) \ll r_{ij}$ the system resembles a percolation network (see e.g. [87, 88]). Below, we shall be concerned only with the latter case. Percolation networks can also be created artificially (the system of Josephson-coupled superconducting granules in a dielectric is a very good example), and have been extensively studied over the last few years (see e.g. [89–92]).

In the absence of a magnetic field ($\phi_{ij} \equiv 0$ in (1.7.1)) the system undergoes a phase transition into an ordered low-temperature state. The magnetic field changes the situation drastically: phases ϕ_{ij} in the energy (1.7.1) are no longer zero, and this leads to the frustration of the interaction (1.7.1). The values of ϕ_{ij} are given by:

$$\phi_{ij} = \frac{1}{\phi_0} \int_{x_i}^{-x_j} \boldsymbol{A}\, \mathrm{d}\boldsymbol{x}\,. \tag{1.7.2}$$

ϕ_0 is the flux quantum, $\boldsymbol{A}$ is the vector potential, and the integral is taken over the straight line connecting the centres of the ith and jth granules. The effect of frustration is large if the plaquette sums of ϕ_{ij} over the relevant contours are large ($\Sigma_{i,j}\phi_{ij} \gtrsim 2\pi$). In the case of the proximity networks the relevant contours contain only neighbouring granules; thus the characteristic value of the magnetic field that induces strong frustration is

$$H_0 = \frac{\phi_0}{(l_{ij})^2}, \quad l_{ij} = |\boldsymbol{x}_i - \boldsymbol{x}_j|\,. \tag{1.7.3}$$

If the mean granular radius a_0 is small ($\ll l_{ij}$) then H_c is too small to suppress the intragranular SC. In the case of the Josephson-coupled percolation network the relevant contours have the large size of the percolation correlation length $\xi_p \approx (p-p_c)^{-\nu_p}$; thus $H_0 = \phi_0/\xi_p^2$.

Since the granules are situated at random, the frustration is also random in nature, and is thus the main ingredient of the spin-glass-type behaviour. At $H \gg H_0$ the Hamiltonian (1.7.1) closely resembles that of the XY spin glass; the only difference is the complex nature of the effective couplings $J_{ij} = J_{ij}^{(0)} \exp(i\phi_{ij})$. The exact isotropy within the order-parameter space (which is due to global gauge invariance) is the unique property of the SCG system. It would therefore be very interesting to experimentally compare these systems and vector spin glasses, which inevitably possess a small amount of anisotropy.

We have mentioned several types of physical systems that can possess an SCG low-temperature state in a broad range of magnetic fields. All of these superconductivity networks can probably be characterized as systems with short-range interaction. Unfortunately, the only tractable model of spin glasses is still the Sherrington–Kirkpatrick model [10] with infinite-range interaction. We therefore begin our theoretical investigation of the SCG state in Section 7 with the formulation of the superconducting analogue of the Sherrington–Kirkpatrick model. Then in Section 7.1 we show that the infinite-range model undergoes a thermodynamic phase transition at $T = T_c(H)$ to the low-temperature SCG state. The function $T_c(H)$ tends to a finite constant at $H \gg H_0$, where H_0 is the characteristic scale of the magnetic field that induces strong frustration. In this field range the model considered is equivalent to the XY infinite-range spin glass. Furthermore, there exists a wide field interval $H \ll H_0$ where the low-temperature state is of the "correlated-spin-glass" type (cf. Sections 6.1 and 8.1) and $T_c(H)$ decreases with increasing H. If the temperature approaches $T_c(H)$ from above then there develops a critical slowing down. Specifically, we study the diamagnetic response $M(\omega)$ of the network to variation of the magnetic field. Far above T_c the response is due to the normal currents through the junctions. Near the transition temperature superconducting fluctuations appear and the response to $H(t)$ increases logarithmically with decreasing reduced temperature $\tau = T/T_c - 1$ or frequency ω; moreover, a critical growth of the inductive part of response sets in.

In Section 7.2 the properties of the low-temperature SCG state are

studied within the infinite-range model. It is shown that the SCG state is nonergodic and history-dependent. History-dependent "equations of state" (of the type proposed in Section 2.3 for spin glasses) are derived and some of their properties are discussed. In particular, the diamagnetic response to *variation* of the magnetic field at $T < T_c$ is predicted.

Section 7.3 is devoted to finite-range systems. We discuss previously considered models [76, 78] with short-range interactions. We then suggest several models with large but finite coordination number Z; these studies can help to fill the gap between the above short-range systems and the mean-field theory developed in Sections 7.1 and 7.2. The following discussion of critical dynamics in finite-range SCG systems is based on the theory of phase transitions in large-Z vector spin glasses (Section 4). Scaling expressions for the diamagnetic response are derived. Experimental investigations of this can clarify the problem of phase transitions in spin-glass-like systems with a continuous order parameter. We then discuss qualitatively the low-temperature history-dependent behaviour and predict the nonzero (but possibly metastable) value of the superconducting density ρ_s. In concluding, we discuss a number of experimental results concerning magnetic properties of high-T_c superconducting ceramics and propose experiments that can unambiguously corroborate (or contradict) the existence of a superconducting glass in these exciting materials.

1.8 Statistical Models of Neural Networks

Amazingly the simple spin-glass theory based for the most part on the SK model — and therefore inapplicable to real spin glasses — has recently acquired a new significance in that it is able to provide a description and explanation of memory.

The problem of thought is a very long-standing one — it was probably born with thought itself. Prodigious progress has occurred in this area over the last few years. We still lack a full description of real human thought, but we have learned to construct models that imitate well some of the most general features of associative memory, and we hope that these models do resemble a part of the real brain or at least that the experience gained with them will help in understanding the real brain. In addition, the process of pattern recognition in these models is

related to that in parallel computing and so they are of great interest from a practical point of view.

All the models are based on a few biological facts (or rather what a physicist calls "biological facts"!), including both experimental discoveries and hypotheses, as well as our own experience as a "thinking machine".

(i) The minimal structure element is a "neuron", whose state can be described by one real variable S corresponding to the firing rate of a real neuron. In experiments two neuron states — quiescent and firing — with smooth transitions between them, are usually observed. This can be modelled by introducing an appropriate energy function $H_0(\phi)$ with two minima at S_1 and S_2, which ensures that for most of the time the neuron is in the vicinity of S_1 or S_2, and only rarely do transitions occur between the two states. A simpler Ising ($S_{1,2} = \pm 1$, with instantaneous transitions) representation is often used. It is generally believed — and for some models it has been shown explicitly — that the simplified Ising representation of the S-variable and the more realistic model employing $H_0(S)$ are essentially equivalent.

Sometimes an alternative representation of the Ising variables S is used, with $S = 2V - 1$ ($V = 0, 1$); this is more in accord with the tradition in neurobiology of ascribing the $V = 0$ state to a quiescent neuron and $V = 1$ to a firing neuron. Certainly the S and V representations are equivalent, but the "natural" form of interneuron interaction in the two representations is different, and so the models based on these representations differ also.

(ii) The process of pattern recognition occurs through the parallel dynamics of neurons, with the initial neuron configuration corresponding to the current visual image, whereas the stable final neuron configuration corresponds to the ideal memorized pattern. The condition of parallel dynamics is very important: with each neuron working very slowly (the fastest have relaxation times $\tau_0 \approx 2 \times 10^{-3}$ s), the system of neurons can beat a modern supercomputer (with $\tau_0 \approx 10^{-10}$ s) in recognizing visual images only if all neurons work in parallel.

(iii) The memory of the ideal memorized patterns is stored via the properties of interneuron interaction [93, 94]. In the real brain the interneuron interaction results from neuron–neuron connections whose properties are governed mainly by the properties of the synaptic

junction between the dendrite of one neuron and the axon of another (the Hebb hypothesis [93]). There are at least two types of synaptic junction (exciting and inhibitory), and there are very many of them (about 10^{14} in the mammalian brain), so that the amount of information that can be stored in them is certainly sufficient (10^{14} bits). Probably the type of synaptic junction is modified in the learning process in order to store the required information. However, a correlation of synaptic modification and learning has never been observed experimentally, and other possibilities do exist: for example, instead of modification, there may be destruction of some junctions. With the occurrence of modification unclear, the number of possible types of synaptic junction is certainly not known. From general considerations, it seems unlikely that this number is very large, because the type of a given synaptic junction should be very stable with respect to external influences (note that no chemical poison can destroy long-term memory without destroying the cells themselves). In most of the models considered the junction type is described by a real variable J (so that the number of types is infinite), but numerical study of analogous models with this variable replaced by its sign (corresponding to only two (excitatory and inhibitory) types of junction) shows only slight differences between them.

(iv) The memory is content-addressable, i.e. the whole pattern can be reconstructed from any small part of it.

(v) The destruction (death) of a small proportion of neurons does not affect the stored information. With each neuron receiving a large number of input signals (about 10^4), its output can be a very complicated function of the input. Hypothesis (iii) means that only a small fraction of all possible realizations of output/input functions are employed, which are constructed in the following way: first, the input signals are transformed when they pass through the synaptic junction according to the junction type (in most models this transformation is assumed to be linear: the input signal is multiplied by the junction factor, with a positive factor corresponding to an excitatory junction and a negative factor to an inhibitory junction); then all input signals from different dendrites are added to the total input signal; finally, the neuron reaction — nonlinearly delayed and contaminated with noise — occurs. In the simplest model the neuron output S_i is the sign of the total input h_i and occurs with a time delay τ_0, which sets the timescale. In a

slightly more general model $S_i = \text{sign}\,(h_i - t_i)$, where t_i is a constant threshold for each neuron.

The first such model of neural dynamics was formulated in 1974 by Little [95]. It had almost no impact on the physical community: it was too early, and the analysis of spin glasses that would prove so fruitful later had not yet appeared. A few years later (in 1982) Hopfield [96] noticed that the Little model can be further simplified if symmetric interconnections between neurons are assumed; this modification allows a statistical-mechanical formulation. More importantly, the Hopfield model appeared just when the time was ripe: the necessary physical theories had been developed but could hardly be applied to real objects. As a result, there was a boom in activity. The success of the Hopfield model is also due to a combination of two facts: it allows an analytic solution, and various modifications of it can be used as a starting point in a study of more complicated systems.

Before discussing the details of the Hopfield model and the properties of its solution, we note that its main assumption of symmetric interconnections is entirely unrealistic for real neural systems, in which the reverse assumption (if neuron A acts on B then B does not act on A) is more likely. The difference between the properties of the Hopfield model and the properties of analogous asymmetric models is not very great; we discuss the physical reasons for it below and consider the solution of the asymmetric analogue of the Hopfield model in Section 8.3.

In the Hopfield model each Ising spin variable S_i describing neuron i is aligned along the field h_i produced by the other variables: $S_i = \text{sign}\, h_i$, $h_i = \Sigma_j J_{ij} S_j$; the constants J_{ij} are chosen by the Hebb rule (see below) to ensure the correct retrieval of the stored patterns

$$J_{ij} = \sum_{\alpha} \xi_i^{\alpha} \xi_j^{\alpha} \tag{1.8.1}$$

where index α numbers different patterns ($\alpha = 1, \ldots, p$). In the alternative formulation the stable configurations of S_i ensure minimization of the Hamiltonian

$$H = -\frac{1}{2} \sum_{i,j} J_{ij} S_i S_j. \tag{1.8.2}$$

The interaction (1.8.1) implies that the system is infinite-range: each spin can interact with any other. As mentioned before, this assumption

is far more realistic for neural systems than for real spin glasses. In the analogous V model the interaction has the same form (1.8.2) (with the obvious replacement $S_i \to V_i$), but the Hebb rule is modified:

$$\tilde{J}_{ij} = \frac{1}{2} \sum_{\alpha} (2\tilde{\xi}_i^{\alpha} - 1)(2\tilde{\xi}_j^{\alpha} - 1),$$

where ξ_i^{α} are ideal patterns in the V representation, $\tilde{\xi}_i^{\alpha} = (0, 1)$. Note that in both models thresholds are absent, and so they are not equivalent but only alike.

In the discrete-time version of the dynamics of the model the spin at the next time step is aligned along the field h_i:

$$S_i(t_{n+1}) = \text{sign } [h_i(t_n)] = \text{sign } \left[\sum_j J_{ij} S_j(t_n) \right]. \qquad (1.8.3)$$

Strictly speaking, there are two possibilities: either all fields h_i are computed at a time step n and then all spins are overturned simultaneously; or the fields h_i are computed and the corresponding spins are overturned subsequently — which is more realistic. Numerical simulation [97] and analytical calculations [98] show that these different dynamics lead to essentially the same results.

In a modified version of the model noise is included. The dynamics is then no longer deterministic but probabilistic:

$$S_i(t_{n+1}) = \begin{cases} \text{sign } [h_i(t_n)] & \text{with probability } p_i = e^{\beta h_i} \text{ sech } \beta h_i, \\ -\text{sign } [h_i(t_n)] & \text{with probability } 1 - p_i. \end{cases} \qquad (1.8.4)$$

The parameter $\beta = 1/T$ determines the noise intensity. The form of the probabilistic dynamics (1.8.4) is natural only if the noise has a thermal origin. Real neuron systems are far from equilibrium (as are all living systems), and the noise in them can hardly be described by the dynamics (1.8.4). Nevertheless, until some more realistic model of neural dynamics appears, (1.8.4) provides a useful starting point for the study of the influence of noise.

The relaxation process (1.8.3) leads to a minimum of the energy (1.8.2), whereas at low noise levels the probabilistic relaxation (1.8.4) leads to a solution that fluctuates slightly in the vicinity of the minimum. With increasing noise level, the fluctuations become stronger, and at large values of the noise different minima are

undistinguishable — at least levels the system can no longer function as a memory.

The interactions J_{ij} must be chosen so as to ensure that the minimum of the energy (1.8.2) corresponds to the stored ideal patterns ξ_i^α. The Hebb rule (1.8.1) is the simplest choice that ensures this. Indeed, let us consider for a moment the model with only one stored pattern ξ_i. Then the Hamiltonian H is the sum of independent negative-definite forms,

$$H = -\frac{1}{2}\left(\sum_i \xi_i S_i\right)^2, \tag{1.8.5}$$

so its minimum is unique $S_i = \xi_i$. (Henceforth we consider states related by a global change of sign $S_i \to S_i$ as essentially equivalent.) The dynamics (1.8.3) always leads to the minimum $S_i = \xi_i$, and so the pattern ξ_i is always retrieved correctly.

So far, the model does not resemble the real memory, but the situation changes when the number of stored patterns is more than one. Each pattern is a minimum of H as before and a stable solution of the dynamical equations (1.8.3) because the field h_i produced by other spins of the same pattern (say $\xi_i^{(1)}$) is parallel to the spin $S_i = \xi_i^{(1)}$. Indeed, it can be divided into two parts:

$$\left.\begin{aligned} h_i = h_i^{(1)} + h_i^{(r)}, \quad h_i^{(1)} &= \sum_j \xi_i^{(1)}\xi_j^{(1)}\xi_j^{(1)} = N\xi_i^{(1)} \\ h_i^{(r)} &= \sum_{\alpha\neq 1} \xi_i^{(\alpha)} \sum_j \xi_j^{(\alpha)}\xi_j^{(1)} \end{aligned}\right\}. \tag{1.8.6}$$

If the patterns are uncorrelated then $h_i^{(r)} \simeq O[(Np)^{1/2}] \ll h_i^{(1)}$ (p is the total number of patterns, $p \ll N$), and $h_i \approx N\xi_i^{(1)}$ is parallel to $\xi_i^{(1)}$. Not only is each stored pattern a stable point of the dynamics (1.8.3), but also if the initial configuration of S_i resembles one of the patterns more than all the others then the solution $S_i(t)$ is attracted to this pattern and a retrieval occurs. Indeed, introducing the overlaps $q^\alpha(t)$ of a spin-$S_i(t)$ configuration with the pattern $\xi_i^{(\alpha)}$, the dynamics (1.8.3) can be rewritten in the form

$$S_i(t_{n+1}) = \operatorname{sign}\left[\xi_i^{(\alpha_0)} q^{\alpha_0}(t_n) + \sum_{\alpha\neq\alpha_0} \xi_i^{(\alpha)} q^\alpha(t_n)\right], \tag{1.8.7}$$

where index α_0 labels the pattern that most resembles the initial configuration. From (1.8.7), we can see that if the first term in brackets is

larger than the second for a large majority of "neurons" then the transformation (1.8.7) applied a few times results in the ideal pattern $\xi_i^{(\alpha_0)}$. The stored patterns $\xi_i^{(\alpha)}$ are not the only stationary solutions of the dynamical equations (1.8.3); many spurious states (such as $S_i = \text{sign}\,(\xi_i^{(\alpha_1)} + \xi_i^{(\alpha_2)} + \xi_i^{(\alpha_3)})$) also appear [99]. The number of spurious states increases rapidly with the number of the stored patterns, and when the latter becomes of the order of $N/\ln N$ the ideal patterns $\xi_i^{(\alpha)}$ cease to be stationary solutions of (1.8.3) — the system is overloaded. Indeed, if $1 \ll p \ll N$ the field $h_i^{(\mathrm{r})}$ is a random Gaussian variable with zero mean and variance pN then the probability P of finding the large $h_i^{(\mathrm{r})}$ that overturns the spin S_i ($|h_i^{(\mathrm{r})}| \geqslant N$) is exponentially small:

$$P = \int_N^\infty \frac{\mathrm{d}h}{(\pi pN)^{1/2}} \exp\left(-\frac{h^2}{2pN}\right) \approx \left(\frac{N}{\pi p}\right)^{1/2} \exp\left(-\frac{N}{2p}\right).$$

Multiplying this probability by the number of neurons N, we conclude that the probability of retrieving the stored pattern without any errors is of order unity at $p \approx N/(2 \ln N)$. At larger p the retrieved pattern differs from the stored one in a small number of points; moreover, a large number of different stable patterns appear in the vicinity of a stored one. Regarding the energy surface, one can say that a number of small energy minima appear against the background of a large minimum, and the system is always trapped in one of them. A small amount of thermal noise cures this "disease": it smooths the small minima, leaving the large minimum intact, but it cannot help to restore the exact stored pattern. At still larger p the stable patterns resembling the stored pattern disappear completely; the system can no longer function as a memory (even with errors). For the Hopfield model (1.8.1), (1.8.2), this happens at $p/N = \alpha_c \approx 0.138$ [100], whereas for the analogous model with V representation of neurons (without thresholds) it occurs at $p/N = \tilde{\alpha}_c \approx 0.059$ [97]. The detailed derivation of these results and further discussion of the phase diagram on the plane of noise intensity versus number of stored patterns is presented in Section 8.1.

The condition that the patterns stored by the algorithm (1.8.1) must be uncorrelated is very worrying. We want to retrieve correlated patterns; in particular, we want to store and retrieve hierarchically organized sets of them, since our own experience tells us that our memory is very well suited for this purpose. The attempt to employ the

algorithm (1.8.1) fails since it appears that the number of correlated patterns that can be stored without overloading decreases rapidly with increasing pattern correlation, and is negligible for a hierarchically organized set. The form of the J_{ij} matrix that ensures correct retrieval of any set of p patterns ($p \leqslant n$) was proposed in reference [101]:

$$J_{ij} = \sum_{\alpha,\mu} \xi_i^{(\alpha)} \xi_j^{(\mu)} B_{\alpha\mu}^{-1}, \tag{1.8.8}$$

where $B_{\alpha\mu}^{-1}$ is the matrix inverse of $B_{\alpha\mu} = \Sigma_i \xi_i^{(\alpha)} \xi_j^{(\mu)}$. Unfortunately, the algorithm (1.8.8) is very nonlocal, and it is unlikely to be employed in a real neural system. A far simpler algorithm that allows the storage of a large number of highly correlated patterns (or a hierarchy of them) is proposed and discussed in Section 8.2.

We have mentioned above that the assumption of symmetry of neural interconnections in neural systems can hardly be justified. In a more realistic model the neurons are interconnected by asymmetric (one-way) synapses that can be modified arbitrarily as before. Generalization of the Hebb rule (1.8.1) leads to the matrix J_{ij} that governs the dynamics (1.8.3) (or (1.8.4)) in that case:

$$J_{ij} = \left(\sum_{\alpha} \xi_i^{(\alpha)} \xi_j^{(\alpha)} \right) \frac{1 + p_{ij}}{2}, \tag{1.8.9}$$

where p_{ij} are random variables that control the direction of the (ij)-bond.

Like the algorithm (1.8.1), the algorithm (1.8.9) allows storage and correct retrieval of a large number of patterns. Surprisingly, it even works slightly better: it does not need external noise in order to store $O(N)$ patterns (Section 8.3).

So far we have discussed only the retrieval dynamics, assuming that the matrix J_{ij} has somewhat already been formed. In more advanced models both learning and retrieval dynamics should occur, so that the model should recognize the new pattern, i.e. find the stored pattern that it resembles, determine its place in the hierarchical structure and store it if this pattern was displayed often. At present there are no such models. So far, only a very useful "unlearning" dynamics has been discovered [102], which allows levelling of the depths of different minima and a decrease in the number of spurious states so that correlated patterns can be stored using the Hebb rule (1.8.1) as a starting point. Numerical simulations (Section 8.4) show that the "unlearning" increases the

region of attraction around each stored pattern, and so improves efficiency of the system substantially. There is an interesting speculation [103] that some analogous effects occur during the rapid eye movement part of mammalian sleep. An analytical theory of this phenomenon is presently lacking.

A more important (from our point of view) and still unresolved problem is the inclusion in the retrieval dynamics of the notion of equivalent patterns that are related to each other by some specified transformations such as rotations, dilatations and translations.

In conclusion, we hope that the study of memory models using the methods of spin-glass theory (and more generally of theoretical physics) is only at the beginning of a long and fruitful path.

REFERENCES

[1] Canella, V. and Mydosh, J.A. (1972) *Phys. Rev.* **B6**, 4220.
[2] Edwards, S.F. and Anderson, P.W. (1975) *J. Phys.* **F5**, 965.
[3] Binder, K. and Young, A.P. (1986) *Rev. Mod. Phys.* **58**, 801.
[4] *Proceedings of Heidelberg Colloquium on Glassy Dynamics*. Lecture Notes in Physics, Vol. 275. Berlin: Springer-Verlag (1987), Eds. J.L. van Hemmen and I. Morgenstern.
[5] Mezard, M., Parisi, G. and Virasoro, M.A. (1987) *Spin Glass Theory and Beyond*. Singapore: World Scientific.
[6] Maletta, H. and Felsch, W. (1979) *Phys. Rev.* **B20**, 1245.
[7] Höchli, U.T. (1982) *Phys. Rev. Lett.* **48**, 1494.
[8] Chamberlin, R.V., Mazurkevich, G. and Orbach, R. (1984) *Phys. Rev. Lett.* **52**, 867.
[9] Alba, M., Ocio, M. and Hamman, J. (1986) *Europhys. Lett.* **2**, 45.
[10] Sherrington, D. and Kirkpatrick, S. (1975) *Phys. Rev. Lett.* **35**, 1792. Kirkpatrick, S. and Sherrington, D. (1978) *Phys. Rev.* **B17**, 4384.
[11] Omari, R., Prejean, J.J. and Soultie, J. (1983) *J. Phys. (Paris)* **44**, 1069.
[12] Barbara, B., Malozemoff, A.P. and Ymry, Y. (1981) *Phys. Rev. Lett.* **47**, 1852; (1982) *J. Appl. Phys.* **53**, 7672.
[13] Taniguchi, T., Hiyako, Y. and Tholence, J.L. (1985) *J. Phys. Soc. Jpn* **54**, 220.
[14] Bouchiat, H. (1986). *J. Phys. (Paris)* **47**, 71.
[15] D'Almeida, J.R.L. and Thouless, D.J. (1978) *J. Phys.* **A11**, 983.
[16] Wendler, R. and Baberschke, K. (1983) *Solid State Commun.* **48**, 91.
[17] Salamon, M.B. and Tholence, J.L. (1982) *J. Appl. Phys.* **53**, 7684; (1983) *J. Magn. Magn. Mater.* **31–34**, 1375.
[18] Mezard, M., Parisi, G., Sourlas, N., Toulouse, G. and Virasoro, M. (1984) *Phys. Rev. Lett.* **52**, 1156; (1984) *J. Phys. (Paris)* **45**, 843.
[19] Granberg, P., Svedlindh, P., Nordblad, P. and Lundgren, L., in [4], p. 40.
[20] Alba, M., Bouchiat, H., Hammann, J., Ocio, M. and Refregier, P. (1987) *J. Appl. Phys.* **61**, 3683.
[21] Refregier, P., Ocio, M. and Bouchiat, H. (1987) *Europhys. Lett.* **3**, 503.

[22] Lundgren, L., Svedlindh, P., Nordblad, P. and Beckman, O. (1983) *Phys. Rev. Lett.* **51**, 911.
[23] Ocio, M., Alba, M. and Hammann, J. (1985) *J. Phys. (Paris) Lett.* **46**, L1101.
[24] Struik, L.C.E. (1978) in *Physical Ageing in Amorphous Polymers and Other Materials*. Houston: Elsevier.
[25] Fisher, D.S. and Huse, D.A. (1986) *Phys. Rev. Lett.* **56**, 1601; Bray, A.J. and Moore, M.A. in [4], p. 121.
[26] Bray, A.J. and Moore, M.A. (1984) *J. Phys.* **C17**, L463.
[27] McMillan, W.L. (1985) *Phys. Rev.* **B32**, 3032.
[28] Bray, A.J. and Moore, M.A. (1987) *Phys. Rev. Lett.* **58**, 57.
[29] Refregier, P., Vincent, E., Hammann, J. and Ocio, M. (1987) *J. Phys. (Paris)* **48**, 1533.
[30] Svedlindh, P., Lundgren, L., Nordbland, P. and Chen, H.S. (1987) *Europhys. Lett.* **3**, 243.
[31] Vincent, E., Hammann, J. and Alba, M. (1986) *Solid State Commun.* **58**, 57.
[32] Souletie, J. and Tholence, J.L. (1985) *Phys. Rev.* **B32**, 516.
[33] Souletie, J. (1985) *Ann. Phys. (France)* **10**, 69.
[34] Tholence, J.L. (1984) *Physica* **126B**, 157.
[35] Bhatt, R.N. and Young, A.P. (1985) *Phys. Rev. Lett.* **54**, 924.
[36] Ogielski, A.T. and Morgenstern, I. (1985) *Phys. Rev. Lett.* **54**, 928.
[37] Ogielski, A.T. (1985) *Phys. Rev.* **B32**, 7384.
[38] Morris, B.W., Colborne, S.G., Moore, M.A., Bray, A.J. and Canisius, J. (1986) *J. Phys.* **C19**, 1157.
[39] Jain, S. and Young, A.P. (1986) *J. Phys.* **C19**, 3913.
[40] Olive, J.A., Young, A.P. and Sherrington, D. (1986) *Phys. Rev.* **B34**, 6341.
[41] Harris, A.B., Lubensky, T.C. and Chen, J.H. (1976) *Phys. Rev. Lett.* **36**, 415.
[42] Bray, A.J. and Moore, M.A. (1979) *J. Phys.* **C12**, 79.
[43] Pytte, E. and Rudnick, J. (1979) *Phys. Rev.* **B19**, 3603.
[44] Feigel'man, M.V. and Tsvelick, A.M. (1979) *ZhETF* **77**, 2524; (1979) *Sov. Phys. JETP* **50**, 1222.
[45] Malozemoff, A.P. and Barbara, B. (1985) *J. Appl. Phys.* **57**, 3410.
[46] Confinentino, M. and Malozemoff, A.P. (1986) *Phys. Rev.* **B34**, 471.
[47] Lundgren, L., Nordblad, P. and Svedlindh, P. (1986) *Phys. Rev.* **B34**, 8164.
[48] Ioffe, L.B. and Feigel'man, M.V. (1985) *Sov. Phys. ZhETF* **89**, 654; (1985) *JETP* **62**, 376.
[49] Feigel'man, M.V. and Ioffe, L.B. (1984) *J. Phys. (Paris) Lett.* **45**, L475.
[50] Feigel'man, M.V. and Ioffe, L.B. (1985) *J. Phys. (Paris) Lett.* **46**, L695.
[51] Abrahams, E., Anderson, P.W., Licciardello, D.C. and Ramakrishnan, T.V. (1979) *Phys. Rev. Lett.* **42**, 673.
[52] Wegner, F. (1976) *Z. Phys.* **25**, 327; (1980) *ibid.* **36**, 209.
[53] Anderson, P.W. (1970) *Mater. Res. Bull.* **5**, 549.
[54] Hertz, J.A., Fleishman, L. and Anderson, P.W. (1979) *Phys. Rev. Lett.* **43**, 942.
[55] Hertz, J.A. (1983) *Phys. Rev. Lett.* **51**, 1880; NORDITA Preprint 1983/12.
[56] Griffiths, R. (1969) *Phys. Rev. Lett.* **23**, 17.
[57] Randeria, M., Setha, J.R. and Palmer, R.G. (1985) *Phys. Rev. Lett.* **54**, 1321.
[58] Dhar, D., Randevia, M. and Setha, J.-P. (1988) *Europhys. Lett.* **5**, 485.
[59] Mezei, F. (1982) *J. Appl. Phys.* **53**, 7654; (1983) *J. Magn. Magn. Mater.* **31–34**, 1327.
[60] Campbell, I.A. (1985) *J. Phys. (Paris) Lett.* **46**, L1159; (1986) *Phys. Rev.* **B33**, 3587.
[61] Campbell, I.A., Flesselles, J.-M., Jullien, R. and Botet, R. (1987) *J. Phys.* **C20**, L47.

[62] Campbell, I.A., Flesselles, J.-M., Jullien, R. and Botet, R. (1988) *Phys. Rev.* **B37**, 3825.
[63] Cable, J.W., Werner, S.A., Felcher, G.P. and Wakabayashi, N. (1982) *Phys. Rev. Lett.* **49**, 829; (1984) *Phys. Rev.* **B29**, 1268.
[64] Werner, S.A., Rhyne, J.J. and Gotaas, J.A. (1985) *Solid State Commun.* **56**, 457; (1985) *J. Appl. Phys.* **57**, 3404.
[65] Ishibashi, K., Tsunoda, Y., Kunitomi, N. and Cable, J.W. (1985) *Solid State Commun.* **56**, 585.
[66] Gotaas, J.A., Rhyne, J.J., Wenger, L.E. and Hydosh, J.A. (1986) *J. Magn. Magn. Mater.* **54–57**, 93.
[67] Wenger, L.E., Hunter, G.W., Mydosh, J.A., Gotaas, J.A. and Rhyne, J.J. (1986) *Phys. Rev. Lett.* **56**, 1090.
[68] Ketelsen, J.P. and Salamon, M.B. (1985) *Phys. Rev.* **B32**, 7425.
[69] Baberschke, R., Pureur, P., Fert, A., Wendler, R. and Senoussi, S. (1984) *Phys. Rev.* **B29**, 4999.
[70] Overhauser, A.W. (1959) *Phys. Rev. Lett.* **3**, 414; (1960) *J. Phys. Chem. Solids* **13**, 71.
[71] Mydosh, J.A. (1988) *J. Appl. Phys.* **63**, 4357.
[72] Ioffe, L.B. and Feigel'man, M.V. (1985) *ZhETF* **88**, 604; (1985) *Sov. Phys. JETP* **61**, 354.
[73] Feigel'man, M.V. and Ioffe, L.B. (1987) *Phys. Rev. Lett.* **58**, 1157.
[74] Feigel'man, M.V. and Tsodyks, M.V. (1986) *ZhETF* **91**, 955; (1986) *Sov. Phys. JETP* **64**, 562.
[75] Chowdhury, D. (1986) *Spin Glasses and Other Frustrated Systems*. Singapore: World Scientific.
[76] Shih, W.Y., Ebner, C. and Stroud, D. (1984) *Phys. Rev.* **B30**, 134.
[77] Ebuer, C. and Stroud, D. (1985) *Phys. Rev.* **B31**, 165.
[78] John, S. and Lubensky, T. (1985) *Phys. Rev. Lett.* **55**, 1014; (1986) *Phys. Rev.* **B34**, 4815.
[79] Vinokur, V.M., Ioffe, L.B., Larkin, A.I. and Feigel'man, M.V. (1987) *ZhETF* **93**, 342.
[80] Feigel'man, M.V., Ioffe, L.B., Larkin, A.I. and Vinokur, V.M. (1988) in *Progress in High-T_c Superconductors*, Vol. 4 (ed A. Barone and A. Larkin), p. 340. Singapore: World Scientific.
[81] Müller, K.A., Takashige, M. and Bednorz, J.G. (1987) *Phys. Rev. Lett.* **58**, 1143.
[82] Klimenko, A.G., Blinov, A.G., Vesnin, Yu.I. and Starikov, M.A. (1987) *Pis'ma ZhETF Suppl.* **46**, 196.
[83] Mota, A.C., Pollini, A., Visani, P., Müller, K.A. and Bednorz, J.G. (1987) *Phys. Rev.* **B36**, 4011.
[84] Tuominen, T., Gordon, A.M. and Macartney, M.L. (1988) *Phys. Rev.* **B37**, 548.
[85] Giovannella, C., Chappert, C. and Beauvillain, P. (1988) *Europhys. Lett.* **5**, 535.
[86] Rabotou, A., Peyral, P., Rosenblatt, J., Lebeau, C., Pena, O., Perrin, A., Perrin, C. and Sergent, M. (1987) *Europhys. Lett.* **4**, 1321.
[87] Boysel, R.M., Caplin, A.D., Dalimin, M.N.B. and Guy, C.N. (1983) *Phys. Rev.* **B27**, 554.
[88] Ioffe, L.B. and Larkin, A.I. (1981) *ZhETF* **81**, 707.
[89] Raboutou, A., Rosenblatt, J. and Peyral, P. (1980) *Phys. Rev. Lett.* **45**, 1035.
[90] Rosenblatt, J., Peyral, P. and Raboutou, A. (1983) *Phys. Lett.* **98A**, 463.
[91] Ioffe, L.B. (1981) *ZhETF* **80**, 1199.
[92] Ebner, C. and Stroud, D. (1983) *Phys. Rev.* **B28**, 5053.
[93] McCulloch, W.A. and Pitts, W. (1943) *Bull. Math. Biophys.* **5**, 115.
[94] Hebb, D.O. (1949) *The Organization of Behaviour*. New York: Wiley.

[95] Little, W.A. (1974) *Math. Biosci.* **19**, 101.
[96] Hopfield, J.J. (1982) *Proc. Natl. Acad. Sci. USA* **79**, 2554; (1984) *ibid.* **81**, 3088.
[97] Bruce, A.O., Gardner, E. and Wallace, D.J. (1987) *J. Phys.* **A20**, 2909.
[98] Perretto, P. (1984) *Biol. Cybern.* **50**, 51.
[99] Gutfreund, H., Sompolinsky, H. and Amit, D.J. (1985) *Phys. Rev.* **A32**, 1007.
[100] Amit, D.J., Gutfreund, H. and Sompolinsky, H. (1985) *Phys. Rev. Lett.* **55**, 1530; (1987) *Ann. Phys. (NY)* **173**, 30.
[101] Personaz, L., Gyuon, I. and Dreyfus, G. (1985) *J. Phys. (Paris) Lett.* **46**, L359.
[102] Hopfield, J.J., Feinstein, D.I. and Palmer, R.B. (1983) *Nature* **304**, 158.
[103] Crick, F.C. and Mitchison, G. (1983) *Nature* **304**, 111.

2. THE SHERRINGTON–KIRKPATRICK MODEL: NONERGODICITY AND HISTORY DEPENDENCE

2.1 Formulation of the SK Model and its General Properties

In 1975 Sherrington and Kirkpatrick proposed an "exactly solvable" model of spin glasses [1], which is now called the SK model. The exact solution of this model took the next ten years and was very instructive. In close analogy with ferromagnets, where mean-field theory becomes exact for infinite-range interaction, the interaction between Ising spins in the SK model is random, but its strength does not depend on the distance between spins. The SK model is defined by the Hamiltonian

$$H = \frac{1}{2} \sum_{i,j} J_{ij} \sigma_i \sigma_j + h \sum_i \sigma_i, \tag{2.1.1}$$

where the quenched random interactions J_{ij} are independent for any pair (i, j) of sites and have a Gaussian distribution

$$P[J_{ij}] = \exp\left[- \frac{(J_{ij} - J_0)^2 N}{2J^2} \right] \left(\frac{N}{2\pi J^2} \right)^{1/2}. \tag{2.1.2}$$

The spins σ_i can be either Ising variables $\sigma = \pm 1$ or vectors of unit length $|\sigma_i| = 1$. We shall discuss in detail only the Ising case, and in this Section we consider for the most part only the model (2.1.2) with $J_0 = 0$ (i.e. zero ferromagnetic exchange) unless otherwise specified.

All physical quantities (e.g. the free energy F) must be averaged over random interactions:

$$F = \int \prod_{i,j} \mathrm{d}J_{ij} \, P[J_{ij}] \, F\{J_{ij}\}, \tag{2.1.3}$$

where $F\{J_{ij}\}$ is the free energy for a given realization of J_{ij} interactions:

$$F\{J_{ij}\} = -T \ln Z\{J_{ij}\}, \quad Z\{J_{ij}\} = \sum_{\{\sigma_i\}} e^{-H/T}. \tag{2.1.4}$$

There are two approaches to calculating the averages of physical quantities over randomness in the SK model. The first uses the replica trick, while the second employs the dynamic equations. In total, both approaches provide an insight into the nature of the SK spin glass. The replica-trick approach gives an understanding of the structure of the space of metastable states that appear at low temperatures as well as the thermodynamic properties of the system, whereas the dynamic approach permits investigation of complex history-dependent physical properties of the system due to the existence of a vast number of metastable states at low temperatures. We discuss both approaches in detail in Sections 2.2 and 2.3, but for now we state some resulting properties of the model. In Section 2.4 we discuss briefly a third approach, which was originally developed by Thouless, Anderson and Palmer (TAP) [2] for analytical calculation of thermodynamic properties of the SK model without using the replica trick, but which subsequently proved to be useful for numerical investigations of the metastable states.

A modification of the TAP approach will be used in subsequent sections when we discuss qualitative properties of short-range spin glasses near and above the transition temperature.

Below the transition temperature T_c the magnetizations $m_i = \langle \sigma_i \rangle$ become frozen into some configuration $\{m_i\}$, which depends on the way in which the system is prepared. In of all these states the Edwards–Anderson order parameter is nonzero and increases continuously with decreasing temperature as in an ordinary second-order transition:

$$q_{EA} = \overline{\langle \sigma_i \rangle^2} \approx \tau + O(\tau^2), \quad \tau = \frac{T_c - T}{T_c}. \tag{2.1.5}$$

Here and below $\langle \ldots \rangle$ stands for the thermal average while an overbar denotes the average over the quenched disorder.

The Edwards–Anderson order parameter does not distinguish between different metastable states, and so cannot describe any novel properties that appear below the transition; furthermore, in nonzero magnetic fields the singularity of $q_{EA}(T)$ is smeared out, while the

critical point at which the metastable states appear still exists. This critical temperature $T_{AT}(h)$ decreases with increasing magnetic field, this dependence being called the de Almeida–Thouless line [3]; below it the state of the system must be described by a functional order parameter. The physical meaning of this function is different in replica and dynamical approaches: in the former it determines the distribution of overlaps between metastable states with each state weighted with the Boltzmann factor, while in the latter it determines the system "memory" of its magnetic history.

The susceptibility $\chi(T)$ depends on the measurement technique; its form for two standard techniques (field cooling and zero-field cooling techniques) is depicted in Figure 2.

So far, we have discussed the properties of the model with $J_0 = 0$. No changes result from nonzero J_0 at $h = 0$ as long as there is no average magnetization. The large ferromagnetic exchange leads to an ordinary transition at high temperature into the ferromagnetic state. However, even large values of J_0 cannot prevent a second transition at low temperature into the mixed ferromagnetic–spin-glass state — because at any J_0 there are finite densities of "soft" spins (so that the molecular field acting upon them is small), these spins can freeze at low temperature in a spin-glass fashion. The "pure" spin-glass state is separated

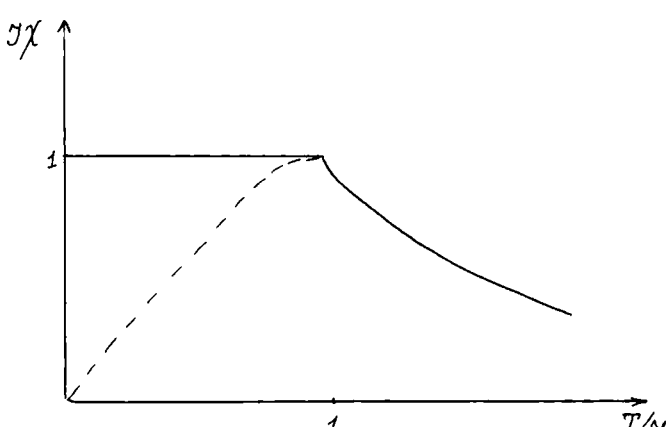

Figure 2 Field-cooling (full line) and zero-field-cooling (dashed line) susceptibilities of the SK model.

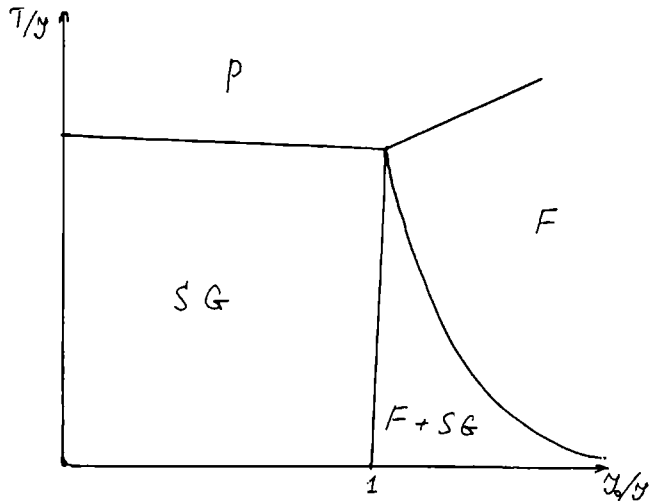

Figure 3 Phase diagram of the SK model: P, paramagnetic; SG, spin-glass; F, ferromagnetic.

from the state of coexistence of ferromagnetic and spin-glass order parameters by another transition line. All transitions are second- (or higher-) order transitions (Figure 3).

2.2 Replica Solution of the SK Model

The free energy averaged over random interactions J_{ij} can be represented in the form

$$F = \langle F\{J_{ij}\}\rangle = -T \lim_{n\to 0} \left\langle \frac{1}{n} [Z^n - 1] \right\rangle$$

$$= -T \lim_{n\to 0} \frac{\langle Z^n\rangle - 1}{n}. \tag{2.2.1}$$

The nth power of the partition function in (1.2.1) can be obtained as a partition function of the replica Hamiltonian

$$Z^n = \sum_{\{\sigma_i^{(\alpha)}\}} \exp\left(-\frac{H\{\sigma_i^\alpha\}}{T}\right),$$

$$H = \frac{1}{2} \sum_{i,j,\alpha} J_{ij} \sigma_i^\alpha \sigma_j^\alpha + h \sum_{i,\alpha} \sigma_i^\alpha, \tag{2.2.2}$$

where $\alpha = 1, 2, \ldots, n$ labels the replicas. We can now carry out the averaging in (2.2.1) and get

$$\langle Z^n \rangle = \sum_{\{\sigma_i^\alpha\}} \exp \left[\frac{J^2}{4NT^2} \sum_{i,j,\alpha,\beta} \sigma_i^\alpha \sigma_j^\alpha \sigma_i^\beta \sigma_j^\beta + \frac{h}{T} \sum_{i,\alpha} \sigma_i^\alpha \right] \times \exp \left(\frac{nJ^2 N}{4T^2} \right). \tag{2.2.3}$$

Introducing new variables $Q^{\alpha\beta}$ that are analogues of the mean field for the infinite-range ferromagnet, and using a Gaussian transformation, we get

$$\langle Z^n \rangle = \exp \left(\frac{nJ^2 N}{4NT^2} \right) \int \prod_{\alpha \neq \beta} \mathrm{d}Q_{\alpha\beta} \sum_{\{\sigma\}} \exp \left[- \left(\frac{NQ_{\alpha\beta}^2}{4T^2} + \frac{1}{2T^2} Q_{\alpha\beta} \sum_i \sigma_i^\alpha \sigma_i^\beta \right) J^2 + \frac{h}{T} \sum_{\alpha,i} \sigma_i^\alpha \right] \left(\frac{N}{4\pi T^2} \right)^{1/2}. \tag{2.2.4}$$

The thermodynamic condition $N \gg 1$ allows us to carry out the integration over $Q_{\alpha\beta}$ by the steepest-descent method:

$$\left.\begin{aligned} \langle Z^n \rangle &= \exp \left(\frac{nJ^2 N}{4T^2} \right) \exp \left(- \frac{NJ^2}{4T^2} \sum_{\alpha \neq \beta} Q_{\alpha\beta}^2 - \frac{1}{T} f_s\{Q_{\alpha\beta}\} \right), \\ f_s\{Q_{\alpha\beta}\} &= -T \ln \sum_{\{\sigma_i^\alpha\}} \exp \left[\frac{J^2}{2T^2} \sum_{\alpha \neq \beta} Q_{\alpha\beta} \sigma_i^\alpha \sigma_i^\beta \right], \end{aligned}\right\} \tag{2.2.5}$$

where $Q_{\alpha\beta}$ is the saddle-point solution, which is determined by the equation:

$$Q_{\alpha\beta} = \langle \sigma^\alpha \sigma^\beta \rangle \equiv \sum_{\{\sigma^\alpha\}} \sigma^\alpha \sigma^\beta \exp \left(\frac{J^2}{2T^2} \sum_{\alpha \neq \beta} Q_{\alpha\beta} \sigma^\alpha \sigma^\beta + \frac{h}{T} \sum_\alpha \sigma^\alpha \right). \tag{2.2.6}$$

The most difficult part of the replica approach is the solution of (2.2.6). Generally, we must find all the solutions of (2.2.6) for arbitrary n, continue them to $n = 0$ and seek a stable one. This rigorous procedure has never been implemented, but the common belief now is that

the unique correct stable solution was guessed by Parisi [4–7]. Historically, the first solution was the SK one [1], which supposed the simple form of $Q_{\alpha\beta}$ matrix $Q_{\alpha\beta} = q$ ($\alpha \neq \beta$). Inserting this form into (2.2.6) and introducing an auxiliary variable z, we get

$$q = \int \frac{dz}{(2\pi)^{1/2}} \sum_{\{\sigma\}}' \sigma^\alpha \sigma^\beta \exp\left[\sum_\alpha \sigma^\alpha \left(\frac{h + Jzq^{1/2}}{T}\right)\right] \exp\left(-\frac{z^2}{2}\right) \times \exp\left(-\frac{n}{2T^2}\right). \tag{2.2.7}$$

The summation over spin variables of different replicas can be carried out independently, and yields

$$q = \int \frac{dz}{(2\pi)^{1/2}} e^{-z^2/2} \tanh^2 \frac{Jzq^{1/2} + h}{T}. \tag{2.2.8}$$

For $h = 0$, (2.2.8) has only one trivial solution $q = 0$ at high temperatures ($T \geqslant T_c = J$) and two solutions at low temperatures ($T \leqslant T_c = J$). It is tempting to associate the bifurcation point T_c with the spin-glass transition and suppose that the trivial solution becomes unstable at $T < T_c$ (which is correct) while the other is stable (which is wrong). In this scenario the value of q has a break at $T = T_c$: $q = 0$ at $T \geqslant T_c$ and

$$q = \tau + \frac{1}{3}\tau^2, \quad \tau = \frac{T_c - T}{T_c} \ll 1. \tag{2.2.9}$$

The expressions (2.2.1), (2.2.5) for the free energy F are also simplified for the SK solution:

$$F = -\frac{(1-q)^2}{4T^2} J^2 - T \int \frac{dz}{(2\pi)^{1/2}} e^{-z^2/2} \ln\left(2 \cosh \frac{Jzq^{1/2} + h}{T}\right). \tag{2.2.10}$$

Keeping only the leading terms in τ and h and using (2.2.9), we get an expression for the free energy per spin f in the vicinity of the transition point T_c:

$$f = -\frac{J^2}{4T} + \theta(\tau)\frac{\tau^3}{6} - \frac{1}{2}h^2 \frac{1}{T}[1 - \theta(\tau)\tau] \quad (h, \tau \ll 1). \tag{2.2.11}$$

The singularity (at $T = T_c$) occurs only in the third derivative of the free energy with respect to τ, so that the transition can be called a

"third-order" transition. Note a strange aspect of this transition: the free energy below the transition is larger than the value of the free energy obtained by analytic continuation of the value of the free energy above the transition. The magnetic susceptibility $\chi = -\partial^2 f/\partial h^2$ follows from (2.2.10) and (2.2.11); it has a cusp at the transition point.

So far so good. However, calculations of the low-temperature properties reveal a disaster! As $T \to 0$ the solution of (2.2.8) can be obtained analytically: $q = 1 - (2/\pi)^{1/2} T/J + O(T^2)$. Inserting this expression into (2.2.10) we get the leading contribution to the free energy as $T \to 0$: $f = (2\pi)^{-1} JT$, from which we can see that the solution (2.2.8) leads to a negative value $(-1/2\pi)$ of the entropy as $T \to 0$; this means that something is wrong with the SK solution. However, as we shall see later, it does give the right value for the leading term in τ at $T \approx T_c$.

To understand the situation, let us study the stability of the SK solution [1]. We consider small deviations of $Q_{\alpha\beta}$ from the SK solution, $Q_{\alpha\beta} = q + q_{\alpha\beta}$, and calculate the leading terms in the free energy. Inserting this expression into (2.2.5) and keeping only the necessary terms, we get

$$F(Q_{\alpha\beta}) = f(q) - \frac{J^2}{8T^4} \sum_{\alpha,\beta,\gamma,\delta} q_{\alpha\beta} q_{\alpha\delta} (\langle \sigma^\alpha \sigma^\beta \sigma^\gamma \sigma^\delta \rangle - \langle \sigma^\alpha \sigma^\beta \rangle \langle \sigma^\gamma \sigma^\delta \rangle), \tag{2.2.12}$$

where the angular brackets $\langle \ldots \rangle$ mean the average over spin variables σ^α with Hamiltonian

$$H = \sum_{\alpha \neq \beta} \sigma^\alpha \sigma^\beta \frac{J^2}{2T^2} q + \Sigma h \sigma^\alpha.$$

To sum over spin variables, we again introduce an auxiliary variable z and obtain, after some algebra,

$$f(Q_{\alpha\beta}) = f(q) + \frac{J^2}{8nT^4} \left[(2T^2 - c_0) \sum_{\alpha \neq \beta} (q^{\alpha\beta})^2 - 4c_1 \sum_{\alpha,\beta,\gamma} q^{\alpha\beta} q^{\beta\gamma} - c_2 \left(\sum_{\alpha \neq \beta} q^{\alpha\beta} \right)^2 \right], \tag{2.2.13}$$

$$c_0 = 2 \int \frac{dz}{(2\pi)^{1/2}} e^{-z^2/2} \operatorname{sech}^4 \left(\frac{Jzq^{1/2} + h}{T} \right),$$

$$c_1 = \int \frac{dz}{(2\pi)^{1/2}} e^{-z^2/2} \tanh^2\left(\frac{Jzq^{1/2} + h}{T}\right) \operatorname{sech}^2\left(\frac{Jzq^{1/2} + h}{T}\right),$$

$$c_2 = \int \frac{dz}{(2\pi)^{1/2}} e^{-z^2/2} \tanh^4\left(\frac{Jzq^{1/2} + h}{T}\right) - q^2.$$

The quadratic forms in $q^{\alpha\beta}$ in (2.2.13) are positive-definite at $n > 0$ and are generally (at $n \neq 1$) independent, so that the stability is governed by the signs of the coefficients $2T^2 - c_0$, c_1 and c_2. The signs of these coefficients that correspond to the stable solutions are not evident *a priori*, because analytic continuation to $n = 0$ could, in principle, change them. To determine them rigorously, the dynamics of the model must be considered. We avoid this by using the physical argument that the SK solution is certainly stable at high temperatures; hence at high temperatures all coefficients in (2.2.13) have the right sign. The coefficients c_1 and c_2 do not change their signs with decreasing temperature, whereas the coefficient $2T^2 - c_0$ changes its sign at some temperature $T_{AT}(h)$. Below this temperature the replica-symmetric SK solution becomes unstable and the replica symmetry is broken. The transition that occurs at $T_{AT}(h)$ is usually associated with the appearance of hysteresis in real spin glasses (see below). The line $T_{AT}(h)$ separating the low-temperature spin-glass phase from the high-temperature phase (the de Ameida–Thouless line) is determined by the equation

$$T^2 = \int \frac{dz}{(2\pi)^{1/2}} e^{-z^2/2} \operatorname{sech}^4\left(\frac{Jzq^{1/2} + h}{T}\right). \qquad (2.2.14)$$

In the cases of small and large magnetic fields the stability condition (2.2.14) can be simplified:

$$T_{AT} = \begin{cases} \left(\frac{3}{4}\right)^{2/3}\left(\frac{h}{J}\right)^{2/3} & (h \ll J), \qquad (2.2.15a) \\ \frac{4}{3}\frac{J}{(2\pi)^{1/2}} \exp\left(-\frac{h^2}{2J^2}\right) & (h \gg J). \qquad (2.2.15b) \end{cases}$$

The condition (2.2.15b) means that even in the limit of large magnetic fields the replica-symmetric solution becomes unstable at low enough temperatures.

Although it is strange at first sight, this statement can be understood from physical arguments. The effective field acting on each spin σ_i consists of the large external field $h \gg J$, T and the field $\tilde{h}_i = \Sigma_j J_{ij}\sigma_j$

produced by interaction with other spins. Almost all spins are aligned along the large field h and frozen; $\tilde{h}_i$ is therefore a random Gaussian variable with $\overline{\tilde{h}^2} = J^2$. However, there are a small number (ρN) of spins that are not aligned and frozen because for them the field $\tilde{h}_i$ almost compensates the field h: $|h - \tilde{h}_i| \approx T$. The density of these spins is $\rho \approx T \exp(-h^2/2J^2)$. The effective strength of interaction of the unfrozen spins with one another is also small: $J_{\text{eff}} = \rho^{1/2} J$, but it decreases slowly with temperature so that at some temperature T_g, $J_{\text{eff}} = T_g$; at lower temperatures we expect a gradual freezing of these spins in some glass configuration, i.e. we expect the spin-glass transition at $T_g \sim \exp(-h^2/2J^2)$, which coincides with (2.2.15b).

A successful scheme for breaking the replica symmetry was proposed by Parisi [4–7], but before expanding it, we discuss the physical meaning of this symmetry breaking. The Edwards–Anderson order parameter $q_{\text{EA}} = \overline{\langle \sigma_i \rangle^2}$ can be expressed in the replica approach by the replica correlation function $Q_{\alpha\beta}$:

$$q_{\text{EA}} = \frac{\left[\sum_{\{\sigma\}} \sigma_i \exp\left(-H\{\sigma_i\}/T\right)\right]^2}{\left[\sum_{\{\sigma\}} \exp\left(-H\{\sigma\}/T\right)\right]^2} = \lim_{n \to 0} \sum_{\{\sigma_i\}} \sigma_i^1 \sigma_i^2 \exp\left(-\frac{H\{\sigma_j^\alpha\}}{T}\right) = Q_{12}. \tag{2.2.16}$$

Therefore the replica-symmetric solution q_{EA} coincides with q, whereas for the solution with the broken replica symmetry, (2.2.16) must be modified. For each such solution, any solution that can be obtained from it by a replica permutation is also a solution of the mean-field equations; a physical quantity (such as q_{EA}) must be averaged over all solutions, which is equivalent to taking the average over all possible pairs of replicas in $Q_{\alpha\beta}$:

$$q_{\text{EA}} = -\frac{1}{n} \sum_{\alpha \neq \beta} Q_{\alpha\beta}. \tag{2.2.17}$$

However, different solutions are separated from each other by infinite barriers (in the limit $N \to \infty$), so that the transitions between them take an infinite time. For a physical system, this means that there are many metastable states that are separated from each other by infinite

barriers. A given value of $Q_{\alpha\beta}$ then corresponds to the average $\overline{\langle\sigma_i\rangle_\alpha\langle\sigma_i\rangle_\beta}$, where the thermodynamic average $\langle\ldots\rangle_\alpha$ (or $\langle\ldots\rangle_\beta$) includes only the vicinity of the metastable state α (or β). Different values of $Q_{\alpha\beta}$ mean that overlaps between different metastable states are different (and, certainly, that there are many different metastable states). We therefore arrive at a very important conclusion: the replica-symmetry breaking is a manifestation of the appearance of metastable states in the system. The replica approach can yield instructive information on the distribution of overlaps between different metastable states. To express this distribution in terms of quantities that can be calculated in the replica approach, we consider distribution moments

$$p_k = \sum_{a,b} \left[\sum_i \langle\sigma_i\rangle_a\langle\sigma_i\rangle_b \right]^k p_a p_b \tag{2.2.18}$$

where p_a is the probability of the ath metastable state: $p_a \sim \exp(-E_a/T)$. The independence of thermodynamic fluctuations of different spins in one metastable state (i.e. $\langle S_i\rangle_a\langle S_j\rangle_b = \langle S_i S_j\rangle_a$) allows us to express the moments (2.2.18) through full thermodynamic averages, which can be calculated within the framework of the replica approach:

$$p_k = \sum_{i_1,\ldots,i_k} \overline{\langle\sigma_{i_1}\ldots\sigma_{i_k}\rangle\langle\sigma_{i_1}\ldots\sigma_{i_k}\rangle} = \lim_{n\to 0} \frac{1}{n(n-1)} \sum_{a\neq b} (Q_{ab})^k. \tag{2.2.19}$$

We now turn to a discussion of the concrete scheme of replica-symmetry breaking. We do not know how to break the symmetry in the limit $n \to 0$ in the general case. Some help comes from the physical condition that all physical quantities (like (2.2.19)) are finite in the $n \to 0$ limit. The only known way to fulfil this condition is to impose the condition that every quantity that contains only one replica index is replica-independent (i.e. $\Sigma_\beta Q_{\alpha\beta}^k = q_k$). Using this weak condition, Parisi [4] proposed a replica-symmetry-breaking scheme that was later proved [8, 9] to be a stable solution of (2.2.6). In his scheme the matrix $Q_{\alpha\beta}$ is built as follows. First, the full $n \times n$ matrix is divided into $m_1 \times m_1$ blocks situated along its diagonal, and the value $q(n)$ is given to the elements of the full matrix outside the $m_1 \times m_1$ blocks; then smaller matrices $m_2 \times m_2$ are separated from the $m_1 \times m_1$ blocks and the value $q(m_1)$ is given to the elements

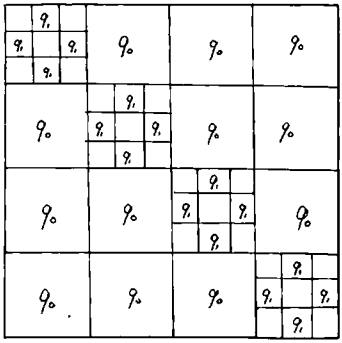

Figure 4 Parisi ansatz for the matrix $Q_{\alpha\beta}$.

inside the $m_1 \times m_1$ block, but outside the $m_2 \times m_2$ the matrices, and so on (Figure 4). If this procedure is repeated k times then a sequence of order parameters is generated that corresponds to the sequence of m_i:

$$n \equiv m_0 > m_1 > \ldots > m_k \geqslant 1. \tag{2.2.20}$$

We then assume, following Parisi [4], that in the limit $n \to 0$ the discrete finite sequence (2.2.20) becomes a continuous interval (0, 1), whereas the sequence $q(m_i)$ becomes a continuous function $q(x)$ on this interval.

The $n = 0$ limit of physical quantities that do not contain external replica indices can be expressed as integrals over $q(x)$. For instance, to express the moments p_k of the overlap distribution (2.2.19), we note that the number of elements of the $Q_{\alpha\beta}$ matrix that have the value q_i is $n(m_{i+1} - m_i)$, so that we get

$$p_k = \lim_{n\to 0}\left(-\frac{1}{n}\sum_{\alpha,\beta} Q_{\alpha\beta}^k\right) = \lim_{n\to 0}\left(-\frac{1}{n}\sum_{i=0}^{k}(m_i - m_{i+1})q_i^k\right) = \int_0^1 q^k(x)\,\mathrm{d}x. \tag{2.2.21}$$

This means that the parameter x is the probability measure for finding a given overlap q. The function $q(x)$ cannot be determined explicitly; only a partial differential equation can be obtained for all tempera-

tures. A closed form of $q(x)$ can be obtained only in the vicinity of the transition temperature T_c. In that region the free energy (2.2.1), (2.2.5) can be expanded in powers of $Q_{\alpha\beta}$:

$$f = f_0 - T\frac{1}{n}\left[\frac{1}{2}\tau\sum_{\alpha\neq\beta}Q_{\alpha\beta}^2 + \frac{1}{6}\operatorname{Tr}\hat{Q}^3 + \frac{1}{8}\operatorname{Tr}\hat{Q}^4 - \frac{1}{4}\sum_{\alpha,\beta,\gamma}Q_{\alpha\beta}^2 Q_{\beta\gamma}^2 + \frac{1}{12}\sum_{\alpha,\beta}Q_{\alpha\beta}^4\right], \tag{2.2.22}$$

where we preserve the fourth-order terms in $Q_{\alpha\beta}$, which are the lowest-order terms responsible for the symmetry breaking. Moreover, expanding (2.2.22) near the SK solution, we see that of all fourth-order terms only the term $\frac{1}{12}\Sigma_{\alpha,\beta}Q_{\alpha\beta}^4$ is responsible for the symmetry breaking, so all other fourth-order terms can be neglected in the lowest order in τ. Using the continuous limit of $\operatorname{Tr} Q_{\alpha\beta}^3$ (which is obtained by direct computation in the Parisi scheme analogously to (2.2.21)), we get the $n = 0$ limit of the free energy (2.2.22):

$$f = f_0 + \frac{1}{2}T\int_0^1 \mathrm{d}x\left[|\tau|q^2(x) + \frac{1}{6}q^4(x) - \frac{1}{3}q^3(x) - q(x)\int_0^x \mathrm{d}y\, q^2(y)\right]. \tag{2.2.23}$$

Variation of (2.2.23) with respect to $q(x)$ yields an integral equation for $q(x)$:

$$2|\tau|q(x) - xq^2 - \int_0^x \mathrm{d}y\, q^2(y) - 2q(x)\int_0^1 \mathrm{d}y\, q(y) + \frac{2}{3}q^3(x) = 0. \tag{2.2.24}$$

This integral equation can be solved explicitly: differentiating it with respect to x, we get

$$|\tau| - xq(x) - \int_x^1 \mathrm{d}y\, q(y) + q^2(x) = 0 \tag{2.2.25a}$$

or

$$q'(x) = 0. \tag{2.2.25b}$$

Differentiating (2.2.25a) with respect to x again, we obtain

$$q(x) = \tfrac{1}{2}x \quad \text{or} \quad q'(x) = 0. \tag{2.2.26}$$

Therefore the general solution of (2.2.25a, b) has the form (Figure 5)

$$q(x) = \begin{cases} \tfrac{1}{2}x & (x \leqslant x_1), \\ q(1) & (x \geqslant x_1). \end{cases} \tag{2.2.27}$$

Insertion of the form (2.2.27) into (2.2.24) yields the values of x_1 and $q(1)$. There are two possible solutions of (2.2.24): one with $q(x) =$ const, i.e. the SK solution, and the other with $q(1) \approx \tau + O(\tau^2)$, $x_1 = 2|\tau|$. The value of $\int dx\, q(x)$ can be obtained from (2.2.25a) in the leading- and next-order terms in τ: $\int dx\, q(x) = \tau + O(\tau^3)$. Therefore the equilibrium susceptibility

$$\chi_{eq} = T^{-1}[1 - \int dx\, q(x)] = T_c^{-1}, \tag{2.2.28}$$

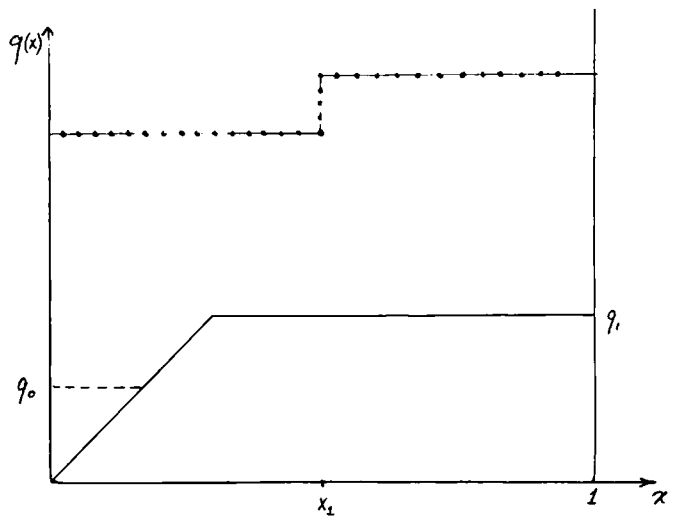

Figure 5 Solution $q(x)$ in the vicinity of T_c for zero (full line), small (dashed line) and large (dotted line) magnetic fields.

to order τ^3. Sommers [10] showed that (2.2.28) follows from the condition $q(0) = 0$, which seems to be true for all temperatures. He also calculated the next orders in τ for $q(x)$ [10]:

$$q(1) = \tau + \tau^2 - \tau^3 + \frac{5}{2}\tau^4 - \frac{39}{2}\tau^5 + O(\tau^6),$$

$$x_1 = 2\tau - 4\tau^2 + 12\tau^3 - 69\tau^4 + O(\tau^5),$$

$$q(x) = \begin{cases} \frac{1}{2}(1+3\tau+12\tau^3)x - \frac{1}{8}(1-\tau)x^3 + O(\tau^5) & (x \leqslant x_1), \\ q(1) & (x \geqslant x_1). \end{cases}$$

The solution $q(x)$ is not known explicitly at low temperatures $T \leqslant T_c$. Parisi [4] supposed that it can be approximated by steplike functions, which correspond to only finite k in the procedure of replica symmetry breaking. The results obtained with the simplest approximation [4] ($k = 1$) are quite satisfactory: the zero-temperature entropy ($h = 0$) increases from the SK value $S_0 \approx -0.17$ to $S_1 \approx -0.01$ (the correct answer is $S_\infty = 0$); the zero-temperature internal energy is in good agreement with numerical data — near T_c the maximum value of the negative eigenvalue is approximately ten times smaller than the same quantity for the SK solution.

We considered above only the case of zero magnetic field. The effect of a small magnetic field can be calculated in the same way [5]. The solution for $q(x)$ consists in this case of two plateau regions — the old one at $q(1)$ (for $x \geqslant x_1$) and the new one at $q(0)$ (for $x \leqslant x_0$) — which are connected by the same $q(x) = \frac{1}{2}x$ line (Figure 5). The values of $q(0)$ and $x_0 = 2q(0)$ increase slowly with magnetic field h:

$$q(0) = \frac{3}{4}\left(\frac{h^2}{J^2}\right)^{2/3}. \tag{2.2.29}$$

In large magnetic fields the temperature T_{AT} of the replica instability decreases rapidly (see (2.2.15b)). Slightly below this temperature the Parisi solution can also be obtained explicitly. In this temperature region the deviation of the Parisi solution from the SK solution q is small, $Q_{\alpha\beta} = q + q_{\alpha\beta}$, so the free energy f can be expanded about the SK solution in terms of $\tilde{Q}_{\alpha\beta}$. A tedious but straightforward calculation yields:

$$f(-Q_{\alpha\beta}) = f_{SK}(q) - \frac{J^2}{4T} Q_0^2 \left(1 - \frac{J}{T} c_4\right) - \frac{J^3}{2T^2} (c_2 - c_4) Q_1^2$$

$$- \frac{J^5}{6T^4} [(2c_2 - 7c_4 + 5c_6) Q_1^3 - 6(c_4 - c_6) Q_0^2 Q_1$$

$$- 2(c_4 - c_6) Q_3^3 - 2c_6 Q_2^3], \tag{2.2.30}$$

where we denote

$$Q_0^2 = -\frac{1}{n} \sum_{\alpha,\beta} \tilde{Q}_{\alpha\beta}^2, \quad Q_1 = -\frac{1}{n} \sum_{\alpha,\beta} \tilde{Q}_{\alpha\beta},$$

$$Q_2^3 = \frac{1}{2n} \sum_{\alpha,\beta,\gamma} \tilde{Q}_{\alpha\beta}^3 \tilde{Q}_{\beta\gamma} \tilde{Q}_{\gamma\alpha},$$

$$Q_3^3 = -\frac{1}{n} \sum_{\alpha,\beta} \tilde{Q}_{\alpha\beta}^3;$$

$$c_k = \int \frac{dz}{(2\pi)^{1/2}} e^{-z^2/2} \operatorname{sech}^k \left(\frac{Jzq^{1/2} + h}{T}\right) \frac{J}{T}.$$

In (2.2.30) we have kept only terms up to third order in $\tilde{Q}_{\alpha\beta}$ because in this case the instability is revealed even at second order in $\tilde{Q}_{\alpha\beta}$. From (2.2.30) we can see that in the saddle-point solution Q_1 has the next order in $\tilde{\tau} = -1 + (J/T)^2 c_4$ compared with Q_0, so that all terms containing Q_1 can be neglected if the additional condition $Q_1 = 0$ is imposed. As before, the Parisi ansatz allows us to express all forms Q_i as continuous integrals over x in the limit $n \to 0$. Inserting these expressions into (2.2.30), we get

$$f(Q) = f_{SK}(q) + \frac{J^2 \tilde{\tau}}{4T} \int dx\, q^2(x) + \frac{J^5}{3T^4} \left\{ (c_4 - c_6) \int dx\, q^3(x) \right.$$

$$\left. - \frac{1}{2} c_6 \int dx \left[x q^3(x) + 3q(x) \int_0^x dy\, q^2(y) \right] \right\}. \tag{2.2.31}$$

To impose the additional condition $Q_1 = \int dx\, q(x) = 0$, we add to the free energy (2.2.31) the Lagrange term $\lambda \int dx\, q(x)$. Variation of the resulting free energy over $q(x)$ yields the saddle-point equation

$$
\begin{aligned}
&-\theta q(x)+\left[\frac{1}{2}\,c_6 x-(c_4-c_6)\right]q^2(x)-\\
&c_6 q(x)\int_0^x \mathrm{d}y\; q(y)+\frac{1}{2}\,c_6\int_0^x \mathrm{d}y\; q^2(y)+\lambda=0,\\
&\theta=\frac{T^3}{2J^3}\left(\frac{J}{T}\,c_4-1\right).
\end{aligned}
\tag{2.2.32}
$$

Differentiating this equation twice with respect to x, we find that, apart from the trivial solution $q'(x) = 0$ (with the condition $Q_1 = 0$ it means that $q(x) \equiv 0$), it has a solution that obeys

$$
\left(x-2\,\frac{c_4-c_6}{c_6}\right)q'(x)=0. \tag{2.2.33}
$$

The only nontrivial solution of (2.2.32) is the discontinuous steplike function with a step at x_1:

$$
q(x)=q_0+(q_1-q_0)\theta(x-x_1),\quad x_1=\frac{2(c_4-c_6)}{c_6}. \tag{2.2.34}
$$

Inserting the solution (2.2.34) into (2.2.32) and using the condition $Q_1 = 0$, we find that (2.2.32) is satisfied only if

$$
q_0=-\frac{\theta}{2(c_4-c_6)},\quad q_1=\frac{\theta}{3c_6-2c_4}. \tag{2.2.35}
$$

The solution (2.2.34) corresponds to a single step of the replica-breaking scheme. In large magnetic fields the parameters c_4 and c_6 in (2.2.35) are both of order $I_{AT}(h)$, so that q_0 and q_1 are of order $(T/J)^2$ T/T_{AT}, which is small at any $T < T_{AT}$. So we see that for a large magnetic field the solution (2.2.34) is a good approximation to $q(x)$ at all temperatures. Higher-order corrections in τ are important only for the region near x_1, where they lead to smearing of the steplike singularity in the solution (2.2.34). Thus we suspect that the simplest approximation of the replica-breaking scheme with only one replica-breaking step ($k = 1$) is a numerically good approximation in the whole (I, h) plane.

To study the stability of the Parisi solution, one must find the

eigenvalues of the $K_{\alpha\beta\gamma\delta}$ term in (2.2.12), where $\langle \ldots \rangle$ now means the average over spin variables σ^α with Hamiltonian

$$H = \frac{J^2}{2T^2} \sum_{\alpha \neq \beta} Q_{\alpha\beta} \sigma^\alpha \sigma^\beta + h \sum_\alpha \sigma^\alpha.$$

Since the matrix $Q_{\alpha\beta}$ is not known explicitly and has a complicated structure, nobody has succeeded in rigorously proving the stability of the Parisi solution in general. However, it can be proved (in the leading-order approximation in τ) near the transition point T_c, where the matrix $K_{\alpha\beta\gamma\delta}$ can be expressed explicitly. The simplest way to obtain $K_{\alpha\beta\gamma\delta}$ is to expand the free energy (2.2.22) near the saddle-point solution $Q_{\alpha\beta}$ and keep only those terms of fourth order that are responsible for the replica-symmetry breaking:

$$\begin{aligned} K_{\alpha\beta\gamma\delta} = & -2(\tau + Q_{\alpha\beta}^2)\delta_{\alpha\beta,\gamma\delta} - Q_{\alpha\gamma}\delta_{\beta\delta} - Q_{\alpha\delta}\delta_{\beta\gamma} \\ & - Q_{\beta\gamma}\delta_{\alpha\delta} - Q_{\beta\delta}\delta_{\alpha\gamma}. \end{aligned} \tag{2.2.36}$$

Straightforward but cumbersome calculations show that all eigenvalues of the $K_{\alpha\beta\gamma\delta}$ matrix are negative or zero, i.e. they have the same sign as the eigenvalues at high temperature; therefore the Parisi solution is stable. We restrict ourselves to a simpler problem of stability in the subspace that can be described by the Parisi ansatz. To study stability in this subspace, we can use the continuous description of the $n \to 0$ limit of the free energy (2.2.23) and expand it around the saddle point (2.2.27) to second order in small deviations $\tilde{q}(x)$ ($q = q^c + \tilde{q}$):

$$\begin{aligned} f = f_0\{q^c(x)\} + \frac{1}{2} T \int \mathrm{d}x \Bigg[& (\tau + q^2(x) - xq(x))\tilde{q}^2(x) \\ & - 2\tilde{q}(x) \int_0^x \mathrm{d}y\, \tilde{q}(y) q^c(y) - q(x) \int_0^x \mathrm{d}y\, q^2(y) \Bigg]. \end{aligned} \tag{2.2.37}$$

The spectrum of the $K_{\alpha\beta\gamma\delta}$ matrix then follows from the equation $\delta f/\delta q(x) = \lambda q(x)$. Inserting in this equation the value of (2.2.37) using (2.2.25) and then differentiating with respect to x, we get

$$\lambda \tilde{q}'(x) = -2q'(x) \int_x^1 \mathrm{d}y\, \tilde{q}(y). \tag{2.2.38}$$

From (2.2.38) we conclude that every $\tilde{q}(x)$ that is supported only by the

interval $(x_1, 1)$ has eigenvalue 0, and vice versa, whereas for functions supported by the interval $(0, x_1)$ we have

$$\lambda\tilde{q}''(x) = \tilde{q}(x). \tag{2.2.39}$$

Together with the boundary conditions $\tilde{q}(0) = 0$ (which follows from the equation $\delta f/\delta q(x) = \lambda q(x)$) and $\tilde{q}'(x_1) = 0$ (which follows from (2.2.38)), (2.2.39) means that $\lambda < 0$. Thus we have shown that in the considered subspace of all matrices the eigenvalues of the quadratic form of the energy deviations are all less than or equal to zero, i.e. the Parisi solution is stable in that subspace. It is only marginally stable, since there is a large family of q-functions that have a zero eigenvalue. There are many reasons for the existence of a large number of zero eigenvalues: first, the free energy is invariant under any reparametrization of x in the interval $(x_1, 1)$; a second (physical) reason is that a small (even infinitesimal in the thermodynamic limit $N \to \infty$) change of the external parameter can mix the metastable states of the system completely (see below), so that there must be some soft directions in the corresponding field theory.

The probability $P(q_{12})$ of overlap q_{12} of the metastable states 1 and 2 can be expressed through the Parisi function $q(x)$. Comparing the expression for different moments of q_{12}: $p_k = \int \mathrm{d}q_{1,2} q_{12}^k P(q_{12})$ with (2.2.21), we conclude that

$$P(q) = \mathrm{d}x/\mathrm{d}g. \tag{2.2.40}$$

The quantity $P(q)$ measures the probability of overlap of metastable states, with each metastable state being taken with the Boltzmann probability $\exp(-E_\alpha/T)$, $E_\alpha = Nf$. Small changes in f_α (the free energy per spin) can change the relative weights of metastable states and thus the value of $P(q)$. These changes can result from the thermodynamically small changes in J_{ij} or external parameters, so we cannot expect $P(q)$ to be a self-averaging quantity. Even for a short-range system, where we expect all physical quantities to be self-averaging, the weights of the metastable states are not. The usual arguments do not apply to the weights because they imply that the system can be divided into many subsystems so that the influence of the interaction of the subsystems on the weight of each of them is small (which is wrong) and the weight for the whole system is some average of the subsystem weights. In fact, it can be shown [11] that the average of its square does not coincide with the square of its average:

$$\overline{P_J(q_1)P_J(q_2)} - \overline{P_J(q_1)}\,\overline{P_J(q_2)} = \frac{1}{3}\,[P(q_1)\delta(q_1 - q_2) - P(q_1)\,P(q_2)]. \tag{2.2.41}$$

The distribution function of $P_J(q)$ can be partially reconstructed from its moments [11].

The average number of states with a weight in the interval $(P, P + \mathrm{d}P)$ (which we denote by $f(P)\,\mathrm{d}P$) can be calculated explicitly [11]. The result shows that there are an infinite number of states with infinitesimally small weights, but there are also a small number of states with finite weights, for example, the plateau in $q(x)$ (or the δ-function in $P(q)$: see (2.2.40)) comes from a single state with a minimum value of free energy. These results obtained from replica theory agree with the results from the simple physical hypothesis that the energies of metastable states are independent random variables with the exponential distribution $\rho(f) \propto \exp\,[x_1 N(f - f_c)/T]$, where f_c is the minimum free energy [12]. The number of metastable states increases exponentially with f, but their contribution to thermodynamic quantities falls rapidly owing to the Boltzmann factor $\exp\,(-Nf/T)$ $(x_1 < 1)$ [13, 14, 15].

The overlaps between three metastable states are not independent. To investigate their correlations, the joint probability $P(q_{12}, q_{23}, q_{31})$ must be studied. A calculation analogous to the derivation of (2.2.19) yields

$$P(q_{12}, q_{23}, q_{31}) = \lim_{n\to 0} \frac{1}{n(n-1)(n-2)} \sum_{\alpha,\beta,\gamma} \delta(Q_{\alpha\beta} - q_{12}) \times \delta(Q_{\beta\gamma} - q_{23})\delta(Q_{\alpha\gamma} - q_{31}). \tag{2.2.42}$$

An interesting property follows directly from the Parisi ansatz: the probability $P(q_{12}, q_{23}, q_{31}) \neq 0$ only if $q_{ab} = q_{bc} \geqslant q_{ac}$, where (a, b, c) is some permutation of $(1, 2, 3)$. The value of the overlap determines the "distance" $d_{ab} = q(1) - q_{ab}$ between metastable states. Such a space of metastable states with this distance between them is known as an "ultrametric" space. It can be imagined as a hierarchical tree (Figure 4) with the distance between two states determined by the position of the first common ancestor.

The ultrametric space cannot include all metastable states of the spin glass because, on the one hand, the number of states that form an ultrametric space cannot exceed N in the system of N elements, and, on the other hand, the number of all metastable states in a spin glass can be

obtained by counting the number of solutions of the TAP equations and is of order $e^{\alpha N}$ [13, 14, 15]. It is difficult to observe ultrametricity in numerical experiments because finite-size effects smear the distributions so that the ultrametricity condition $q_{ab} = q_{bc}$ (we suppose $q_{ac} \geqslant q_{ab}, q_{bc}$) can easily be confused with the triangular inequality $q_{ab} - q_{bc} \leqslant q(1) - q_{ca}$. However, the finite-size scaling analysis carried out in [16] shows that $|q_{ab} - q_{bc}|$ decreases as $N^{-1/3}$ as $N \to \infty$ (the values of N up to 512 were studied).

2.3 Dynamics of the SK Model and its History Dependence

The most interesting properties of spin glasses are their dynamical properties, which include very slow relaxation and various effects of history dependence at low temperatures. The SK model possesses, at least qualitatively, these properties. Below the transition temperature, where a vast number of metastable states appear, we must differentiate between the dynamics that takes place on a finite timescale in the vicinity of one metastable state and the dynamics that includes transitions over the barriers — the processes that take an infinite time in the thermodynamic limit. Taking the SK model seriously, we may think that the physical properties are governed only by the finite-time dynamics, so that we can restrict our study to the vicinity of the metastable state. However, the following problem then arises: what is the metastable state that we are studying? There are two possible ways to overcome this difficulty: (i) we can average all physical quantities over all metastable states with Boltzmann weight, either with the help of the replica trick (Section 1) (but if we want to check the results of the replica theory then this is unacceptable) or by considering the dynamics on an infinite timescale that leads to equilibrium (this approach was developed mainly by Sompolinsky [17–20]); (ii) the other possibility is to consider the slow variation of the external parameter that brings the system from the high-temperature paramagnetic state, where all relaxational processes take a finite time, to the low-temperature state [21, 22]. The approach (i) may help in checking the results of the replica approach and understanding better the meaning of the Parisi ansatz. In principle, it can also yield some valuable information on the barriers separating different metastable states; however, this goal has not yet been achieved. The second approach (ii) allows us to obtain the history-dependent physical properties. The lack of self-averaging that

plagues quantities in the Parisi scheme or in the Sompolinsky approach is absent in the dynamic approach, where the history dependence is explicitly taken into account, because small (in the thermodynamic sense) changes of the external parameters or interactions J_{ij} cannot change the energy of a given metastable state or its other physical quantities, but can change the relative weights of different metastable states (cf. the discussion preceding (2.2.41)).

All dynamic approaches to the spin-glass problem are based on the functional-integral representation of the Langevin equations. Usually the simplest form of the Langevin equations that are compatible with the Hamiltonian (2.1.1) is considered. It is generally accepted that the results for the dynamics at a large timescale do not depend on the concrete form of the one-spin dynamics. To construct the Ising spin dynamics, the soft-spin version of the SK model is considered, which is defined by

$$H = H_0 + H_1, \quad H_0 = T \sum_i \left(\tfrac{1}{4}u\sigma_i^4 + \tfrac{1}{2}r\sigma_i^2 + \beta h\sigma_i\right), \tag{2.3.1}$$

where H_1 is the interaction energy between spins ($H_1 = H\{\sigma\}$, (2.1.1)), which ensures that each spin is almost always of a fixed length $|\sigma| = -u/r$ (the Ising model is recovered in the limit $u \to \infty$ $r \to -\infty$). The simplest form of the dynamics compatible with the energy (2.3.1) is purely relaxational:

$$\Gamma_0^{-1} \frac{\partial \sigma_i(t)}{\partial t} - \beta \frac{\delta H}{\delta \sigma_i(t)} + \xi_i(t), \tag{2.3.2}$$

where $\xi_i(t)$ is a Gaussian random variable with variance $\langle \xi_i(t)\, \xi_j(t')\rangle = 2\Gamma_0^{-1}\delta_{ij}\delta(t-t')$, which ensures the proper equilibrium distribution. The physical quantities must be averaged over noise $\xi_i(t)$ and over random J_{ij} interactions. We shall mainly be concerned with the two-spin correlation function $C(t)$ and the response function $G(t, t')$:

$$\left.\begin{aligned} C(t, t') &= \overline{\langle \sigma_i(t)\sigma_i(t')\rangle}, \\ G(t, t') &= \frac{\partial \langle \sigma_i(t)\rangle}{\partial [\beta h(t')]}. \end{aligned}\right\} \tag{2.3.3}$$

The averages over the thermal noise in (2.3.3) (denoted by $\langle \ldots \rangle$) can be represented as functional integrals over $\sigma_i(t)$ and the auxiliary field $\hat{\sigma}_i(t)$:

$$\left.\begin{aligned} C(t, t') &= \overline{\langle \sigma_i(t)\sigma_i(t')\rangle}, \\ G(t, t') &= i\overline{\langle \sigma_i(t)\hat{\sigma}_i(t')\rangle}_A \end{aligned}\right\} \tag{2.3.4}$$

where $\langle \ldots \rangle_A$ denotes the functional average with weight A:

$$\left.\begin{aligned} \langle x\rangle_A &= \int \mathscr{D}\sigma\, \mathscr{D}\hat{\sigma}\, x(\sigma, \hat{\sigma}) \exp\,[A(\sigma, \hat{\sigma})], \quad A = A_0 + A_1 + W, \\ A_0 &= i\int \mathrm{d}t \sum_i \hat{\sigma}_i(t)\Big[-\Gamma_0^{-1}\frac{\partial \sigma_i}{\partial t} \\ &\quad - r\sigma_i(t) - u\sigma_i^3(t) + \beta h_i(t) + \Gamma_0^{-1}\mathrm{i}\hat{\sigma}(t)\Big], \\ A_1 &= i\int \mathrm{d}t \sum_{i,j} \hat{\sigma}_i(t)\beta J_{ij}\sigma_j(t), \\ W &= -\frac{1}{2}\int \mathrm{d}t \sum_i \frac{\delta^2 \beta H}{\delta \sigma_i^2} = -\frac{1}{2}\int \mathrm{d}t \sum_i [r_0 + 3u\sigma_i^2(t)]. \end{aligned}\right\} \tag{2.3.5}$$

The last term (W) in the action A stems from the functional Jacobian that ensures the proper normalization of the action: $\langle 1\rangle_A = 1$. Differentiating this normalization condition with respect to $h(t)$, we conclude that all averages of the auxiliary fields $\hat{\sigma}_i(t)$ (without $\sigma(t)$) are identically zero. Since the function (2.3.5) is normalized, the quenched averaging over J_{ij} can be performed straightforwardly; it leads to a new effective interaction part A_{eff} in the action A instead of A_1:

$$\left.\begin{aligned} A &= A_0 + A_{\text{eff}} + W, \\ A_{\text{eff}} &= -\frac{1}{2N}\int \mathrm{d}t\, \mathrm{d}t' \sum_{i,j} [\hat{\sigma}_i(t)\hat{\sigma}_i(t')\sigma_j(t)\sigma_j(t') \\ &\quad + \hat{\sigma}_i(t)\sigma_i(t')\hat{\sigma}_j(t')\sigma_j(t)](\beta J)_t(\beta J)_{t'}, \end{aligned}\right\} \tag{2.3.6}$$

where we take into account that any of the quantities β, J can be an external parameter and very slowly in time.

So far the transformations have been exact. We now use the MFA to cope with the fourth-order terms in (2.3.6). To make the MFA rigorous in the SK model, we decouple the fourth-order terms by auxiliary fields $Q_i(t, t')$ and then seek the saddle-point solution. Using the identity $\langle \hat{\sigma}_i(t)\hat{\sigma}_i(t')\rangle_A \equiv 0$ and the causality condition $G(t < t') = 0$, we get

$$\begin{aligned} A_{\text{eff}} = \frac{1}{2}\int \mathrm{d}t\, \mathrm{d}t' \sum_i [&C(t, t')\mathrm{i}\hat{\sigma}_i\mathrm{i}\hat{\sigma}_i\mathrm{i}\hat{\sigma}_i(t') + 2G(t, t')\mathrm{i}\hat{\sigma}_i(t)\sigma_i(t)] \\ &\times (\beta J)_t(\beta J)_{t'}. \end{aligned} \tag{2.3.7}$$

The resulting action A describes the dynamics of the independent spin variables σ_i. This dynamics can be described by Langevin equations that are nonlocal in time:

$$\Gamma_0^{-1}\sigma_i^0 = -\frac{\delta H_0}{\partial \sigma_i} + (\beta J)_t \int \mathrm{d}t'\, G(t, t')\sigma(t')(\beta J)_{t'} + \zeta_i(t), \tag{2.3.8}$$

where the effective noise $\zeta_i(t)$ is a Gaussian random variable of width

$$\langle \zeta_i(t)\zeta_i(t')\rangle = [2\Gamma_0^{-1}\delta(t-t') + (\beta J)_t(\beta J)_{t'} C(t, t')].$$

The response and correlation functions $G(t, t')$ and $C(t, t')$ can each be divided into two parts:

$$\left.\begin{aligned} G(t, t') &= \Delta(t, t') + \tilde{G}_t(t-t'), \\ C(t, t') &= q(t, t') + \tilde{C}_t(t-t'), \end{aligned}\right\} \tag{2.3.9}$$

where $\Delta(t, t')$ and $q(t, t')$ vary only on a very long timescale $t_1 \gg \Gamma^{-1}$ determined by the timescale of the external parameter variation or by transitions through the barriers between metastable states in the finite system, whereas $\tilde{G}_t(t-t')$ and $\tilde{C}_t(t-t')$ vary on a small timescale of order Γ_0^{-1}; they depend on the time difference $t-t'$ and on the absolute value of time as a parameter (if we take into account the variation of the external parameters).

Above the transition point the time-persistent parts of the correlators are absent and the fluctuation–dissipation theorem (FDT) holds:

$$\tilde{G}_t(t-t') = \tilde{C}_t(t-t'). \tag{2.3.10}$$

Near the transition point a critical slowing down occurs. Its form can be obtained from perturbation theory in u applied to (2.3.8) [18]. Using the definition of the renormalized damping function

$$\Gamma^{-1}(\omega) = \mathrm{i}\,\frac{\partial \tilde{G}^{-1}(\omega)}{\partial \omega}$$

and the Dyson equation

$$\tilde{G}^{-1}(\omega) = \tilde{G}_0^{-1}(\omega) + \Sigma(\omega),$$

where $\tilde{G}_0(\omega)$ is the response function of (2.3.8) with $u = 0$, $\tilde{G}_0^{-1}(\omega) = \tau - \mathrm{i}\omega\Gamma_0^{-1} - (\beta J)^2\tilde{G}^2(\omega)$, and $\Sigma(\omega)$ is the self-energy, we get

$$\Gamma^{-1}(\omega) = \frac{\Gamma_0^{-1} + \mathrm{i}\partial\Sigma/\partial\omega}{1-(\beta J)^2\tilde{G}^2(\omega)}. \tag{2.3.11}$$

Direct calculation shows that $\partial\Sigma/\partial\omega$ has no singularity in perturbation theory at $T = T_c$, so that the qualitative form of the critical slowing down is determined only by the denominator in (2.3.11). The FDT implies that $\tilde{G}(\omega=0) = \tilde{D}\hat{t}=0) = \overline{|\sigma^2|}$. In the Ising limit $\overline{|\sigma^2|} = 1$; therefore the zero of the denominator in (2.3.10) and hence the transition occur at $\beta J = 1$, which coincides with the thermodynamic result of the previous section. The form of the critical slowing down does not depend on the bare values of r and u:

$$\left.\begin{aligned} &\Gamma(\omega) \sim \tau \qquad (\omega \ll \tau^2), \\ &\Gamma(\omega) \sim \omega^{1/2} \qquad (1 \gg \omega \gg \tau^2). \end{aligned}\right\} \tag{2.3.12}$$

The universality of (2.3.12) allows us to suppose that they hold even in the opposite limit of hard Ising spins. A separate study of the Glauber relaxation of the Ising spins showed [23] that this is indeed the case.

Below the transition point the time-persistent parts of the correlators appear. As we discussed above, in order to define the state of the system below the transition temperature, we must either specify its history (i.e. how it was cooled to this temperature) or consider the relaxation, which takes infinite time. Here we describe only the former possibility. A detailed discussion of the latter can be found in the reviews [24–26].

To handle the time-persistent part of $C(t, t')$, it is convenient to introduce an auxiliary slowly varying Gaussian variable $Z(t)$ with variance

$$\langle Z(t)Z(t')\rangle = (\beta J)_t q(t, t')(\beta J)_{t'} \tag{2.3.13}$$

and divide the noise $\xi(t)$ in (2.3.8) into two parts: slow $Z(t)$ and fast $\tilde{\xi}(t)$: $\xi(t) = Z(t) + \tilde{\xi}(t)$. Now the right-hand side of (2.3.8) can also be divided into two parts:

$$\left.\begin{aligned} \Gamma_0^{-1}\dot{\sigma}_i &= \left[-\frac{\delta H_0}{\delta\sigma_i} + \beta J \int \mathrm{d}t'\ \tilde{G}_t(t-t')\sigma(t') + \tilde{\xi}(t) \right] + H(t), \\ \langle \xi(t)\xi(t')\rangle &= 2\Gamma_0^{-1}\delta(t-t') + (\beta J)^2 \tilde{D}_t(t-t'), \end{aligned}\right\} \tag{2.3.14}$$

where the term in square brackets is purely local in time, whereas in the effective field all time-persistent terms are included:

$$H(t) = (\beta J)_t \int \mathrm{d}t'\ \Delta(t, t')\sigma(t')(\beta J)_{t'} + Z(t). \tag{2.3.15}$$

From now on, we suppose that the variation of the external parameters is very slow, so that local equilibrium is achieved long before the

external parameters vary sufficiently, and the equation (2.3.13) for the fast relaxation can be solved ignoring the variation of the effective field $H(t)$. The presence of a slow part $\Delta(t, t')$ of the response function means that the field produces nonzero magnetization long after it has been switched off ($t - t' \gg \Gamma_0^{-1}$), so we can say that the magnetic field can be frozen into the system.

The perturbation theory in u shows that the "fast" parts of correlators obey the FDT to all orders in u, so we suppose that even below T_c the FDT (2.3.10) holds for the "fast" parts of the correlators. The FDT (2.3.10) implies that at a given value of the effective field $H(t)$

$$\begin{aligned} \tilde{G}(\omega = 0) &= \langle \sigma^2 \rangle - \langle \sigma(t)\sigma(t') \rangle_{|t-t'| \gg \Gamma_0^{-1}} \\ &= 1 - m_t^2, \quad m_t = \langle \sigma_t \rangle . \end{aligned} \tag{2.3.16}$$

Here and below in this section we denote the average over the fast noise $\tilde{\xi}(t)$ by $\langle \ldots \rangle$ and that over the slow noise $Z(t)$ by $[\ldots]$, and we consider the Ising normalization of spin lengths: $\langle \sigma^2 \rangle = 1$. From (2.3.15), we conclude that the reaction to the slow effective field $H(t)$ is described by the usual formula for the static equilibrium magnetization:

$$m_{t_1} = \tanh \{H(t_1) + h(t_1)\}. \tag{2.3.17}$$

Equation (2.3.16) allows us to disregard the details of the fast dynamics and the specific form of H_0 when studying the quasistatic reaction to the slow variation of the external parameters, provided that the fast dynamics (2.3.13) is stable. The necessary condition for stability follows from the requirement $\mathrm{Re}\, \Gamma^{-1}(\omega) \geqslant 0$. Using perturbation theory in u to solve the fast equation of motion (2.3.13) at a given constant value of $H(t)$ and then averaging its solution over $Z(t)$, we arrive at a low-temperature generalization of (2.3.11):

$$\Gamma^{-1}(\omega) = \frac{\Gamma_0^{-1} + \mathrm{i}\, \tilde{G}^{-2}(\omega)\, \partial [\Sigma_H(\omega)\, \tilde{G}_H^2(\omega)]_Z / \partial \omega}{1 - (\beta J)^2 [\tilde{G}_H^2(\omega)]_Z} \tag{2.3.18}$$

where $\tilde{G}_H(\omega)$ and $\Sigma_H(\omega)$ denote the fast response function and the self-energy for a given effective field H. The perturbation theory shows that the numerator of (2.3.17) does not change its sign, so that the necessary condition for stability of the fast dynamics is $1 - (\beta J)_t^2 [\tilde{G}_H^2(0)]_Z \geqslant 0$, or, using the FDT,

$$1 - 2[m_t^2]_Z + [m_t^4]_Z \leqslant \frac{T^2}{J^2}. \tag{2.3.19}$$

For the SK static solution, the stability condition (2.3.18) agrees with the de Almeida–Thouless criterion. We shall prove below that quasistatics, which follows from (2.3.16), leads to the equality sign in (2.3.18), so that the fast dynamics is only marginally stable below T_c. Assuming that this marginal stability leads to a scaling form of the response function at $\omega \to 0$, the scaling index ν ($G(\omega) \sim \omega^{\nu}$) can be found from perturbation theory [18, 20]:

$$\frac{4\pi \coth \pi\nu}{B(\nu, \nu)} = \frac{[2m(1-m)^2]_z}{[(1-m^2)^3]_z}. \tag{2.3.20}$$

To obtain the quasistatic equation of state, we note that since the variation of $\Delta(t, t')$ occurs on a much longer timescale than the fast relaxation of σ, the "fast" function $\sigma(t')$ in the integral (2.3.14) for the effective field $H(t)$ can be replaced by its mean value $m(t')$:

$$H(t) = (\beta J)_t \int \mathrm{d}t'\, \Delta(t, t')(\beta J)_{t'} m(t') + Z(t). \tag{2.3.21}$$

Equation (2.3.20), together with (2.3.16), allows us to determine in principle the value $m(t)$ at a given configuration of the field $Z(t)$. We then insert (2.3.14) into (2.3.16) and differentiate the latter with respect to $\beta h(t_2)$ ($t_1 - t_2 \gg \Gamma_0^{-1}$) using the self-consistency equations $\Delta(t_1, t_2) = [\partial m(t_1)/\partial t_2]_z$, $t_1 - t_2 \gg \Gamma_0^{-1}$ and $\partial m_t/\partial(\beta h_t) = 1 - m^2$, (2.3.15), and finally get

$$\Delta(t_1, t_2) = \left[(1-m^2)_{t_1} (\beta J)_{t_1} \Delta(t_1, t_2)(\beta J)_{t_2} (1-m^2)_{t_2} + (\beta J)_{t_1} (1-m^2)_{t_1} \int \mathrm{d}t \Delta(t_1, t)(\beta J)_t \Delta(t, t_2) \right]_z. \tag{2.3.22}$$

In the limit $t_1 \to t_2$ (but $|t_1 - t_2| \gg \Gamma_0^{-1}$) the integral in the second term on the right-hand side of (2.3.20) is small compared with the first term, since the causality condition requires $\Delta(t, t_2) = 0$ at $t < t_2$; therefore, for any nonzero solution $\Delta(t_1, t_2)$, the condition $[(1-m^2)^2]_z = T^2/J^2$ must be fulfilled, which is exactly the condition for marginal stability (2.3.18). The other possible solution of (2.3.20), $\Delta(t_1, t_2) = 0$, leads to the SK static solution that becomes unstable below T_c.

The other equation of state follows directly from the self-consistency equation:

$$q(t, t') = [m(t)m(t')]_z. \tag{2.3.23}$$

Together, (2.3.21) and (2.3.22) form a closed system of equations that determines the quasistatic behaviour of the system at all temperatures.

In the vicinity of T_c the equations of state are substantially simplified. First, we note that the exact condition for marginal stability determines $q_t = [m_t^2]$ to second order in τ (we use $[m^4] \approx 3q^2 + O(\tau^3)$): $q = \tau + \tau^2 + O(\tau^3)$, which agrees with $q(1)$ for the Parisi solution (2.2.28). Inserting this equation into (2.3.20) and keeping only terms of leading order in τ, we get

$$\Delta(t_1, t_2)\{2q^2(t_1, t_2) - \tau^2(t_1) - \tau^2(t_2)\} + \int \mathrm{d}t\, \Delta(t_1, t)\Delta(t, t_2). \tag{2.3.24}$$

The equation for $q(t_1, t_2)$ follows from its definition, i.e. $q(t_1, t_2) = [m(t_1)m(t_2)]$ and (2.3.16). Keeping only the leading terms, we get

$$q(t_1, t_2)\left\{\frac{2}{3} q^2(t_1, t_2) - \tau^2(t_1) - \tau^2(t_2)\right\} + \int \mathrm{d}t\, [\Delta(t_1, t)q(t_2, t) + \Delta(t_2, t)q(t_1, t)] + h(t_1)h(t_2) = 0 \tag{2.3.25}$$

Together, (2.3.23) and (2.3.24) form a closed system of integral equations that determines the system behaviour below T_c. The solutions of (2.3.23) and (2.3.24) are adiabatic, i.e. no physical quantity depends on the rate of the variation of the external parameters, since any change of the timescale $\tilde{t} = f(t)$ can be compensated by a transformation $\Delta(t_1, t_2) \to \tilde{\Delta}(\tilde{t}_1, \tilde{t}_2) = \Delta(t_1, t_2)\, \mathrm{d}t_2/\mathrm{d}\tilde{t}_2$ leaving (2.3.23) and (2.3.24) invariant. In the simplest case of a monotonic decrease of temperature, $\tau(t) = t$ ($h = 0$), the solution of the system can be guessed:

$$\Delta(t, t') = 2\theta(t - t')t', \quad q(t, t') = \theta(t - t')t' + \theta(t' - t)t. \tag{2.3.26}$$

The explicit form of the solution of (2.3.23) allows us to calculate the value of the field-cooled susceptibility, which is expressed in terms of $\Delta(t, t')$ by

$$\chi_{FC} = \int \mathrm{d}t'\, T_{t'}^{-1} G(t, t') = T^{-1}(1 - q(t, t)) + \int \mathrm{d}t'\, \beta_{t'} \Delta(t, t'), \tag{2.3.27}$$

whereas the zero-field-cooled susceptibility is measured keeping the temperature fixed and so can be expressed through the "fast" response of the system:

$$\chi_{ZFC} = T^{-1} \int \mathrm{d}t' \, \tilde{G}(t, t') = T^{-1}\{1 - q(t, t)\}. \qquad (2.3.28)$$

Inserting the solution (2.3.25) into (2.3.26) and using the expression for $q(t, t)$ to second order in τ, we get

$$\chi_{FC} = \chi_{ZFC} + T_c^{-1}\tau^2 + O(\tau^3) = \{1 + O(\tau^3)\} T_c^{-1} \qquad (2.3.29)$$

From (2.3.28) we see that in the considered second order in τ the equilibrium susceptibility does not depend on the temperature, which agrees with the result of the replica theory for the equilibrium susceptibility (2.2.8). However, we are not aware of any proof of this result for the low-temperature range. The difference between the dynamic approach considered here and the replica scheme can originate, in principle, from the following physical reasons: the slow cooling of the system does not lead to the lowest metastable state, but to some state close to the lowest — this state depending on the process of cooling (e.g. the values of the magnetic field) — whereas averaging over all metastable states with

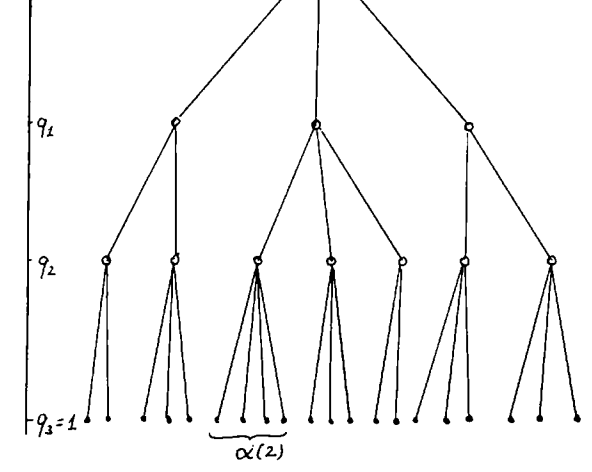

Figure 6 Hierarchical tree with three levels.

Boltzmann weights is implied in the replica scheme. The correspondence between the dynamic quantity $q(t, t)$ and $q(1) = \langle m_i \rangle^2$ in the replica scheme means that this physical quantity calculated in one metastable state differs only slightly from the same quantity in the other, and so its Boltzmann average coincides with its value in some metastable state that the system is in after slow cooling. The hierarchical structure of the space of metastable states is not explicit in this dynamic approach, because slow cooling of the system always leads to some definite metastable state. Only variation of the external parameters in the course of cooling can lead to different metastable states. However, the energies of these states differ from one another by a macroscopic value, so that these states are not the same as those described by the hierarchical structure; moreover, it is unclear whether all physically relevant metastable states can be described by the hierarchical structure.

As we concluded above, the state of the system does not depend on the rate of variation of the external parameters; moreover, it does not change if the temperature is varied nonmonotonically.

Here we show this for the temperature variation in the vicinity of T_c in the leading approximation in τ; however, this fact can be proved for all temperatures by considering higher-order terms in τ. In the leading approximation in τ it is sufficient to solve the system (2.3.23, 2.3.24); its solution for any form of the temperature variation can be found explicitly. By a change of timescale, any function $\tau(t)$ can be transformed, leaving the system (2.3.23), (2.3.24) invariant, to a piecewise continuous function $\tau_i(t) = \pm t + c_i$. Consider a typical function $\tau_i(t)$ depicted in Figure 7. For this function, the solution (2.3.23), (2.3.24) has the form

$$\left.\begin{aligned} \Delta(t, t') &= \begin{cases} 2t' & (t' \leqslant t_1,\ t' \geqslant t_2), \\ 0 & (t_1 \leqslant t' \leqslant t_2), \end{cases} \\ q(t, t') &= t', \end{aligned}\right\} \tag{2.3.30}$$

which can be verified by direct substitution. The absence of $\Delta(t, t')$ for $t_1 \leqslant t' \leqslant t_2$ means that the field cannot be frozen into the system if it is heated and that the field that has been frozen at time t ($t_1 \leqslant t \leqslant t_0$) is thawing out when the system is heated back to the same temperature $T = T(t)$ — both of these properties are very natural. We believe that in the general case, where few parameters are varied to achieve the given state, this state depends only on the path in the parameter space along

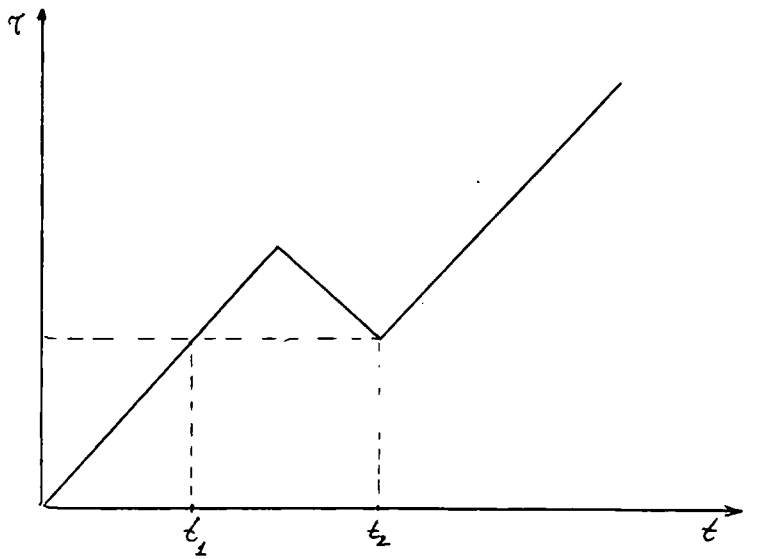

Figure 7 Thermal history of the SK model considered in the text ($\epsilon = (T_c - T)/T_c$).

which the system has been driven, but not on the way it has been driven along that path.

The solution (2.3.25) was obtained in the leading approximation in τ. Higher-order terms can also be computed in this approach:

$$\left.\begin{aligned} \Delta(t, t') &= 2t' + t'(t-t'), \\ q(t, t') &= t' + \tfrac{1}{2}t'(t+t'), \end{aligned}\right\} \quad t > t'. \tag{2.3.31}$$

Using the functions $\Delta(t, t')$ and $q(t, t')$ from (2.3.30), and the marginal stability condition (2.3.18), we get the Edwards–Anderson order parameter $q_{EA} = q(t, t)$ for a state resulting from a slow cooling process to high accuracy in τ:

$$q_{EA} = \tau + \tau^2 - \tau^3 + \frac{5}{2}\tau^4 - 17.2\tau^5 + O(\tau^6); \tag{2.3.32}$$

this differs from the result of the equilibrium theory (2.2.28); $q_{EA} - q_{eq} = 2.3\tau^5 + O(\tau^6)$.

The internal energy u of a quasi-equilibrium state can be expressed in

terms of the order parameters $q(t, t')$ and $\Delta(t, t')$. To do this, we average the expression for the internal energy

$$U = \frac{1}{2} \sum_{i,j} \langle J_{ij} S_i S_j \rangle \tag{2.3.33}$$

over random bonds J_{ij} using the dynamical functional (2.3.5) and get

$$U = -\frac{1}{2T}\left\{1 - q^2(t, t) + 2T \int \mathrm{d}t'\ \Delta(t, t')q(t, t')\beta(t')\right\}. \tag{2.3.34}$$

Again, the marginal-stability condition (2.3.18) helps in calculating the integral in (2.3.32) to a high degree of accuracy:

$$U = -\frac{1}{2T}\left(1 - \tau^2 + \frac{2}{3}\tau^2 + \tau^4 - \frac{13}{5}\tau^5\right).$$

This is slightly above the internal energy of the equilibrium state: $U - U_{\mathrm{eq}} = \frac{1}{5}\tau^5 + O(\tau^6)$, which means that the slow cooling process, even in zero magnetic field, results in a nonequilibrium state. In the SK model all barriers are infinite and the system will stay forever in this state, while in real glasses it relaxes slowly towards equilibrium — which explains qualitatively the abundance of ageing effects in spin glasses.

The zero-field-cooling and field-cooling susceptibilities can also be computed with a high degree of accuracy. The results for the zero-field-cooling susceptibility follow from $\chi_{\mathrm{ZFC}} = \beta(1-q)$ and (2.3.31), while the field-cooling susceptibility follows from (2.3.26) and (2.3.30):

$$\chi_{\mathrm{FC}} = T_{\mathrm{c}}^{-1} + O(\tau^4). \tag{2.3.35}$$

This coincides with the equilibrium susceptibility in Parisi's theory, which is T_{c}^{-1} at $T < T_{\mathrm{c}}$; however, we are not aware of any proof of (2.3.28) at higher order in τ.

2.4 The TAP-Equations Approach

The dynamic approach to the SK model discussed in the previous section was originally proposed in order to avoid the use of replicas. Earlier, Thouless, Anderson and Palmer [2] had suggested that replicas can be avoided if the mean-field equations are written down without

averaging for each site i and the averaging is postponed until the very end of the procedure.

The naive guess is that in the leading-order approximation the molecular field at site i is $\sum_j J_{ij} m_j$. (This would lead to equations of state $m_i = \tanh(\beta \sum_j J_{ij} m_j)$.) However, in contrast with the ordinary MFT for ferromagnets, the first correction term in the Kirkwood approximation must be taken into account for spin glasses (this term is also known as the Onsager reaction term). The reason for this is simple: in the first term different items in the sum $\sum_j J_{ij} m_j$ compensate each other, whereas in the reaction term they have the same sign so that the resulting order of magnitude of the first and the reaction terms is the same.

Instead of deriving the MF equations of state, we prefer to derive the free-energy functional of m_i that we shall use in subsequent Sections. The variation of this functional of m_i yields the equations of state (the TAP equations). To derive the effective functional of new variables m_i, we introduce a new term with Lagrange multiplier λ_i into the Hamiltonian (2.1.1), which ensures the condition $\langle \sigma_i \rangle = m_i$:

$$H_{\text{eff}} = H + H_{\text{L}}, \quad H_{\text{L}} = \sum_i (\sigma_i - m_i)\lambda_i. \tag{2.4.1}$$

We then expand the free-energy functional $F = -T \ln \{\Sigma_{\{\sigma\}} \exp(-H_{\text{eff}}/I)\}$ for the full interacting system as a series of cumulants in the interaction energy H:

$$\left.\begin{aligned} -\beta F &= -\beta F_0 + \sum_{n=1}^{\infty} \frac{1}{n!} (-\beta)^n c_n(H), \\ \beta F_0 &= \sum_i \lambda_i m_i - \ln \cosh \lambda_i. \end{aligned}\right\} \tag{2.4.2}$$

The first cumulants $c_n(H)$ are

$$\left.\begin{aligned} c_1(H) &= \langle H \rangle_{\text{L}}, \\ c_2(H) &= \langle H^2 \rangle_{\text{L}} - \langle H \rangle_{\text{L}}^2, \\ c_3(H) &= \langle (H - \langle H \rangle_{\text{L}})^3 \rangle_{\text{L}}, \end{aligned}\right\} \tag{2.4.3}$$

where $\langle \ldots \rangle_{\text{L}}$ denotes the average with respect to the reference Hamiltonian H_{L}. The expansion (2.4.2), (2.4.3) was introduced by Kirkwood [27] in 1938 as the expansion for the Ising model. The Lagrange parameter λ can be expressed through the condition:

$$\partial F/\partial \lambda_i = 0. \tag{2.4.4}$$

In the following we keep in F only terms of second order in H (or J_{ij}). Using (2.4.2) and (2.4.3), we get

$$\begin{aligned} \beta F = & \sum_i \lambda_i m_i - \ln \cosh \lambda_i - \frac{1}{2} \sum_{i,j} J_{ij} \mu_i \mu_j \\ & - \frac{1}{2} \sum_{i \neq k, j} J_{ij} J_{jk} (1 - \mu_j^2) \mu_i \mu_k \\ & - \frac{1}{4} \sum_{i,j} J_{ij}^2 (1 - \mu_i^2 \mu_j^2), \end{aligned} \tag{2.4.5}$$

where $\mu_i \equiv \tanh \lambda_i$. Inserting (2.4.5) into (2.4.4), we get

$$m_i = \mu_i - \sum_j (1 - \mu_i^2) J_{ij} \mu_j + O(J^2). \tag{2.4.6}$$

Finally excluding μ_i from (2.4.5) and (2.4.6), we obtain the TAP free-energy functional

$$\begin{aligned} F = & -\frac{1}{2} \sum_{i,j} J_{ij} m_i m_j - \frac{1}{4T} \sum_{i,j} J_{ij}^2 (1 - m_i^2)(1 - m_j^2) \\ & + \frac{T}{2} \sum_i \left[(1 + m_i) \ln \frac{1 + m_i}{2} + (1 - m_i) \ln \frac{1 - m_i}{2} \right] \\ & + \sum_i h_i m_i. \end{aligned} \tag{2.4.7}$$

The first term in (2.4.7) represents the part of the free energy originating from direct spin–spin interaction, the second is the entropy of a single spin in a field producing magnetization m_i, the third describes the influence of the external field h_i, and the last is the Onsager reaction term. Taking the variational derivative of (2.4.7) with respect to m_i, we obtain the TAP equations of state

$$m_i = \tanh \left\{ \beta \left[\sum_j J_{ij} m_j + h_i - \beta \sum_j J_{ij}^2 (1 - m_j^2) m_i \right] \right\}. \tag{2.4.8}$$

The solutions of (2.4.8) must also be checked for stability. In the TAP approach the stable solutions correspond to a minimum of the free energy (2.4.7), i.e. the Hessian matrix of the second derivatives of F_{TAP},

$$A_{ij} = \frac{\partial^2 F}{\partial m_i \, \partial m_j} = -J_{ij} - 2\beta J_{ij}^2 m_i m_j + \delta_{ij}\left[\frac{T}{1-m_i^2} + J^2\beta(1-m_i^2)\right] \tag{2.4.9}$$

must be positive-definite for the solution to be stable. Consideration [28, 29] of the eigenvalues of the A_{ij} matrix shows that it is positive-definite if

$$1 - \beta^2 J^2(1 - 2\overline{m_i^2} + \overline{m_i^4}) \leqslant 0. \tag{2.4.10}$$

The stability condition (2.4.10) coincides with the stability condition (2.3.18) derived in the dynamic approach. As we have proved in Section 2.3, the condition (2.4.10) is satisfied as an equality in the spin-glass state, so that the spin-glass state is always marginally stable.

The TAP solution can be further studied analytically in the vicinity of the transition point. Expanding the tanh in (2.4.8) and keeping only the terms linear in m_i, we have

$$m_i - \beta \sum_j J_{ij} m_j + J^2\beta^2 m_i = O(m_i^2), \tag{2.4.11}$$

where we have used the identity $\Sigma_j J_{ij}^2 = J^2$. The density of eigenvalues of the J_{ij} matrix is known (Section 4); it forms a semicircle, with the largest eigenvalue $2J$. Introducing the eigenfunctions $\psi_\lambda(i)$ of the J_{ij} matrix and representing m_i as a sum over these eigenfunctions, $m_i = \sum_\lambda m_\lambda \psi_\lambda(i)$, yields

$$m_\lambda[1 - \beta J_\lambda + (\beta J)^2] = O(m_i^2). \tag{2.4.12}$$

The transition occurs when the coefficient in square brackets in (2.4.12) vanishes for some eigenvalue J_λ. Hence it occurs at $T = J$, in agreement with the replica and dynamic calculations of the preceding sections. This transition can be described as a macroscopic condensation into the mode with the largest eigenvalue; however, at $T < T_c$ the interaction of modes with eigenvalues close to the largest is strong, so that the number of solutions increases rapidly and this description is not very helpful. Note that T_c would have been calculated incorrectly without the reaction term.

At low temperatures the notion of the effective molecular field $\tilde{h}_i$ (the expression in square brackets in (2.4.8)) is very convenient. The marginal-stability condition (2.4.10) implies that the probability of

finding the small molecular field is small (so that $1 - \overline{m}_i^2 \approx T^2$). Numerical simulation of the TAP equation at low temperatures [2, 30] shows that the molecular-field distribution is linear at small magnetic field $P(\tilde{h}) \approx \tilde{\alpha}h$. The coefficient $\tilde{\alpha}$ of the linear dependence can then be found analytically from the marginal-stability condition. The susceptibility χ of a single solution is related to q_{EA} by $\chi = \beta(1 - q_{EA})$, which can be calculated using the coefficient $\tilde{\alpha}$: $1 - q_{EA} = \tilde{\alpha}(T/J)^2$, $\tilde{\alpha} \approx 1.810$. This gives the susceptibility

$$\chi = \tilde{\alpha} T/J^2. \tag{2.4.13}$$

Numerical simulations carried out by Bray and Moore [31] show that the vast majority of the TAP solutions are unstable; moreover, for 90% of all samples (with $40 \leqslant N \leqslant 250$) no stable solutions exist in the vicinity of T_c. More recently, it has been found [32] that in many cases the instability results from only one eigenvalue, which is very small and negative so that in the thermodynamic limit the marginal-stable solution is recovered.

The number of solutions of the TAP equations below the transition temperature (or, more generally, below the AT line) is exponentially large [13–15]:

$$N_s \sim \exp\,[N\alpha(T, h)], \tag{2.4.14}$$

with the coefficient α being 0.20 at low temperatures and decreasing rapidly near the transition temperature:

$$\alpha \sim (T_c - T)^6.$$

2.5 *Towards a Renormalization-Group Theory of Spin Glasses*

The problem of any thermodynamic theory is to define and sum elementary excitations. In the renormalization-group theory of phase transitions in ordinary statistical systems one classifies all degrees of freedom according to their spatial scale and then sums step by step, starting from microscale ("fast" degrees of freedom) and going up to macroscale ("slow" degrees of freedom). Such a classification is justified since an equilibrium state of a system is expected to be homogeneous and therefore the microscale degrees of freedom are elementary excitations. The renormalized parameters of a Hamiltonian for slow degrees of freedom could then lead to effective trapping of a system near a certain macroscopic state.

Here it is proposed to follow a similar scheme. The main difference, however, is that the degrees of freedom of spin glass cannot be classified by their spatial scale, since the region of phase space where the system could be trapped is not expected to correspond to any homogeneous state.

The basic hypothesis of the present approach is that all thermodynamically relevant states of a spin-glass system can be classified in the form of a hierarchy (Figure 6). This was proved to be correct for the pure states of the Sherrington–Kirkpatrick model of a spin glass [1] at any finite temperature below T_c [11, 33]. Although an exact ultrametric

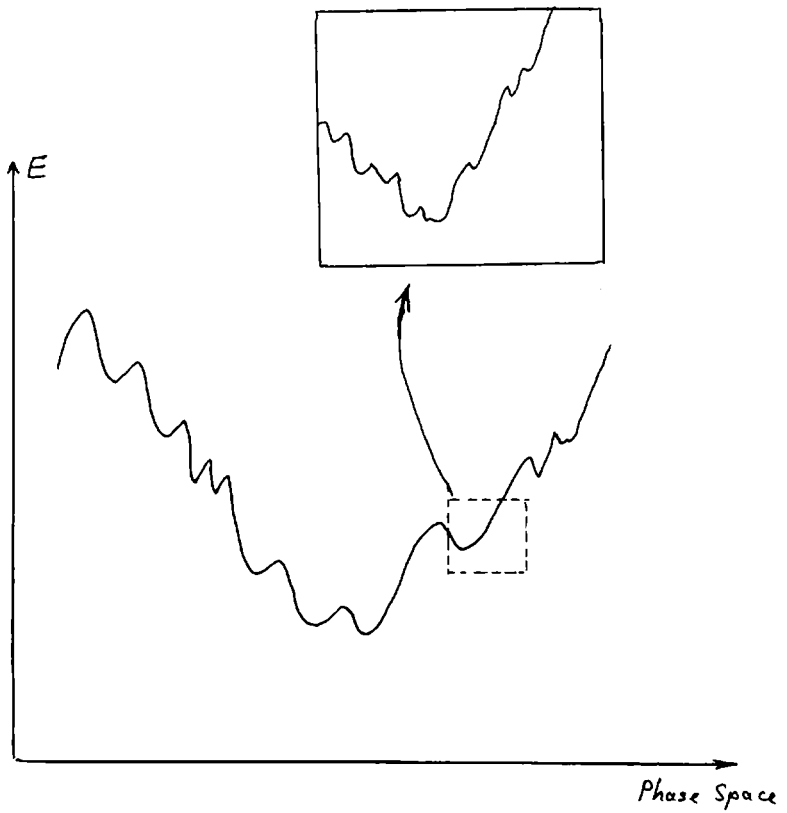

Figure 8 Fractal structure of the free-energy surface.

topology of the space of pure states is unlikely to exist in realistic spin-glass models, a fractal-like classification based on an approximate "ultrametricity" of some sort could be a rather general phenomenon for disordered systems. It can be considered as a sort of ramification of a general case when the free energy of the spin glass has a complicated fractal-like structure (Figure 8). Its form for finite T could then be considered as a result of the averaging over all relevant microscopic degrees of freedom up to a certain temperature-dependent scale $q(T)$ in phase space.

Actually a tree-like organization of the pure states of the SK model is known to exist, starting from the scale $q(T)$ up to the grand-ancestor state at the macroscopic scale. All of these states are separated by infinite (in the thermodynamic limit) barriers; therefore once the system has been left in a certain region of phase space corresponding to one of the pure states, it will remain there indefinitely. This is what is expected to happen in any spin glass below T_c, and it is the degrees of freedom at scales smaller than $q(T)$ that are responsible for the actual thermodynamic (and dynamic) properties of the system. Therefore what is going to be done in the present approach is to perform calculations starting from the microscopic level up to the scale $q(T)$. Although this approach definitely ignores the states beyond the tree-like organization, one can nevertheless hope that it takes into account all relevant degrees of freedom. Some justification for this hope is that the ultrametric structure of the pure states of the SK model remains true for all T down to zero. Of course, real justification could be found by obtaining reasonable results.

In the present renormalization-group (RG) approach all the metastable states of a spin-glass system are classified in classes or families so that each family can be represented by one "ancestor" state at a large scale of the phase space (the classification scheme presented here is slightly different from that of Virasoro and Mesard [33]). The point is to represent all states belonging to the family as some (small) deviations of variables from the inhomogeneous background that corresponds to the ancestor state at a slightly enlarged scale of the phase space. Summing these fast degrees of freedom of a family, one could obtain a new Hamiltonian with the renormalization parameters that correspond to the enlarged scale of the phase space. The ancestor states at this new scale are classified into families again, and so on. As a result of the RG process, the RG equations for the parameters of the effective Hamiltonian can be obtained. The solutions of these equations would

give characteristic values and correlations of the renormalized (effective) couplings and would eventually indicate what the macroscopic state of the system is. The observables should be calculated (for fixed microscopic spin–spin couplings) following the same RG scheme.

Although a general formulation of the RG scheme can be given rather clearly, the actual calculation of the RG equations is a nontrivial problem, and at present it is not clear how it can be done systematically. Therefore the derivation of the RG equations and their solutions is performed under some simplifying assumptions. Although under these assumptions, at least for the SK model, some important (TAP-like) interactions are missing, the solutions exhibit a spin-glass phase transition at finite T_c and show how the "trapping" of the system at some finite scale $q(T)$ (for $T < T_c$) occurs.

2.5.1 The renormalization-group scheme The procedure of classification of the metastable states is as follows. Let the system be described by the Hamiltonian

$$H = \frac{1}{2} \sum_{i,j} J_{ij} S_i S_j, \tag{2.5.1}$$

where the variables are Ising spins $S_i = \pm 1$. The ramdom matrix J_{ij} need not necessarily be of the SK type (it could be finite-range). But what is vital for the RG procedure (at least in its present form) is that all thermodynamically relevant metastable states produced by J_{ij} must form a hierarchical tree described below. These metastable states will be denoted by $\{S_i\}^{(\alpha)}$. The measure in phase space is defined by overlaps:

$$q^{\alpha\beta} = \frac{1}{N} \sum_{i=1}^{N} S_i^{(\alpha)} S_i^{(\beta)}, \tag{2.5.2}$$

where N is the number of spins.

The ultrametric topology in the space of these metastable states is defined by the property that for any three states α_1, α_2 and α_3 two out of three overlaps are necessarily equal and the third is not less than their value:

$$q^{\alpha_1\alpha_2} = q^{\alpha_1\alpha_2} \leqslant q^{\alpha_2\alpha_3}.$$

Assuming some regular discretization of the interval $0 \leqslant q \leqslant 1$ represented by $\{q_l\}$, $l = 1, 2, \ldots, L$; $q_0 = 1, q_1 = 1$; $q_{l+1} - q_l = \delta q \ll 1$, all metastable states will be classified into the form of a tree in terms of

spin states at every site. We take $q = q_{L-1}$ and divide all the metastable states into the families so that for any two states α_1 and α_2 belonging to one family $\{\alpha(L-1)\}$

$$q^{\alpha_1 \alpha_2} = q_{L-1}. \tag{2.5.3}$$

The ultrametric topology prevents these families from overlapping. Actually, it is the assumption of nonoverlapping of the families of states rather than the ultrametric topology itself that is crucial for the RG scheme.

For a given family $\{\alpha(L-1)\}$, we determine an average of every spin over the states of the family:

$$\langle S_i \rangle_{\{\alpha(L-1)\}} = m_i[\alpha(L-1)]. \tag{2.5.4}$$

Introducing a discretization of the interval $-1 \leqslant m \leqslant 1$, we get a partition of all the sites into disjoint clusters $\{\Omega^{\alpha}_{L-1}(m)\}$, where $\Omega^{\alpha}_{L-1}(m)$ is the set of sites for which $\langle S_i \rangle_{(\alpha)} = m$. Different families of states will be represented by different sets $\{\Omega_{L-1}(m)\}$. Such configurations of clusters will be called the ancestor states of the corresponding families of states. It can be assumed that the variables m are distributed over all the sites so that each site gets some number from the interval $-1 \leqslant m \leqslant 1$. Different configurations of $\{m_i\}$ would correspond to different ancestor states, although not every configuration is the ancestor state. According to the definitions (2.5.2)-(2.5.4), for any ancestor state at scale q_{L-1},

$$\frac{1}{N}\sum_{i=1}^{N} m_i^2 = q_{L-1} \quad \left(= \frac{1}{N}\sum_{m=-1}^{+1} m^2 \Omega_{L-1}(m) \right). \tag{2.5.5}$$

The next step is to take a new scale $q = q_{L-2}$. We again divide all the ancestor states at the scale q_{L-1} into families so that in terms of the redefined measure

$$q^{\alpha(L-1)\beta(L-1)} = \frac{1}{N}\sum_{i=1}^{N} m_i[\alpha(L-1)]\, m_i[\beta(L-1)], \tag{2.5.6}$$

for any two states $\alpha(L-1)$ and $\beta(L-1)$ belonging to one family,

$$q^{\alpha\beta} = q_{L-2}. \tag{2.5.7}$$

For a given family $\alpha(L-2)$, we determine

$$\langle m_i \rangle_{\alpha(L-2)} = m_i[\alpha(L-2)] \tag{2.5.8}$$

at each site. This results in a partition of all the sites into clusters $\{\Omega^{(\alpha)}_{L-2}(m)\}$ so that each cluster $\Omega^{(\alpha)}_{L-2}(m)$ contains the sites for which $\langle m_i \rangle_{\alpha(L-2)} = m$. Obviously,

$$\frac{1}{N}\sum_{i=1}^{N} m_i^2(L-2) = q_{L-2}. \tag{2.5.9}$$

This scheme can be continued up to $q_0 = 0$, where the "grand-ancestor" states can be defined.

Each metastable state with information on all its ancestors is therefore described by a set of functions $\{m_i(q)\}$ $(i = 1, 2, \ldots, N)$ $0 \leqslant q \leqslant 1$. Different states are given by different sets $\{m_i(q)\}$. According to this definition, the ancestor state $\alpha(q_0)$ at some intermediate scale q_0 is represented by a set of functions $\{m_i(q)\}^{(\alpha)}$, $0 \leqslant q \leqslant q_0$. All the states that are descendants of $\alpha(q_0)$ are represented by different sets of functions $\{m_i(q)\}$, $0 \leqslant q \leqslant 1$, that coincide with $\{m_i(q)\}^{(\alpha)}$ in the interval $0 \leqslant q \leqslant q_0$.

Note also that any ancestor state $\alpha(q_0)$ given by the set $\{m_i(q)\}^{(\alpha)}$ can be described by a hierarchy of spin clusters $\{\Omega^{(\alpha)}_{q_0}(m(q))\}$, where the cluster $\Omega_{q_0}(m(q)))$ is the set of sites at which the functions $m_i(q)$ coincide with $m(q)$. Obviously,

$$\frac{1}{N}\sum_{i=1}^{N} m_i^2(q_0) = q_0 \quad \left(= \frac{1}{N} \int\limits_{0 \leqslant q \leqslant q_0} \mathscr{D}\, m(q)\; \Omega_{q_0}[m(q)] \right) \tag{2.5.10}$$

and

$$\frac{1}{N} \int\limits_{0 \leqslant q \leqslant q_0} \mathscr{D}\, m(q)\; \Omega_{q_0}[m(q)] = 1 \tag{2.5.11}$$

for any ancestor state.

The idea of the present approach is to consider the functions $\{m_i(q)\}$ as the new relevant variables.

At some intermediate scale q the N-dimensional vector $\boldsymbol{m}$ in phase space belongs to the sphere

$$\boldsymbol{m}^2 = Nq. \tag{2.5.12}$$

By definition, it is also contained in the cube

$$|m_i| \leqslant 1. \tag{2.5.13}$$

The conditions (2.1.12) and (2.5.13) define a topology in the phase space by those sections of the sphere (2.5.12) that are contained inside the cube (2.5.13). For $q = 1$, this topology collapses into Ising points at the vertices of the cube: $m_i = \pm 1$. For $q < 1$, the m_i are continuous, but for large N they are mostly concentrated near the vertices of the cube — the only regions where the sphere of radius Nq can be inside the cube (2.5.13).

The idea of the RG approach is to represent the states of one family at scale q (the vectors $\boldsymbol{m}$ belong to the sphere of radius Nq) as deviations from the background corresponding to their common ancestor state at scale $q - \delta q$ (the sphere of radius $N(q-\delta q)$):

$$m_i(q) = m_i(q-\delta q) + \delta m_i(q), \tag{2.5.14}$$

where

$$\langle \delta m_i \rangle = 0. \tag{2.5.15}$$

Obviously the deviations $\{\delta m_i\}$ belong to the surface

$$\frac{1}{N}\sum_{i=1}^{N} (\delta m_i^2 + 2m_i(q-\delta q)\delta m_i) = \delta q. \tag{2.5.16}$$

The Hamiltonian at some intermediate scale q is expected to be described by some scale-dependent parameters $J_{ij}(q)$. Summing over all $\{\delta m_i\}$ (constrained by (2.5.15) and (2.5.16) and by the cube (2.5.13)), one could get a new Hamiltonian at the scale $q-\delta q$:

$$\exp\{-\beta H_{q-\delta q}[m_i(q-\delta q)]\}$$
$$= \langle \exp\{-\beta H_q[m_i(q-\delta q); \delta m_i]\}\rangle_{\{\delta m_i\}}. \tag{2.5.17}$$

This would give the RG equations for the parameters J_{ij}:

$$J_{ij}(q-\delta q) = J_{ij}(q) - \Gamma[J_{ij}; \beta]\,\delta q, \tag{2.5.18}$$

or

$$\frac{\mathrm{d}}{\mathrm{d}q} J_{ij}(q) = \Gamma[J_{ij}; \beta]. \tag{2.5.19}$$

The solutions of these equations,

$$J_{ij} = J_{ij}[q; \beta; J_{ij}^{(0)}], \tag{2.5.20}$$

where $J_{ij}^{(0)} = J_{ij}(q=1)$, would give the effective characteristic of the system when going from the microlevel ($q=1$) to larger and larger scales up to $q=0$.

It should be expected that below T_c there will be some intermediate scale $q(T)$ at which the characteristic values of $J_{ij}[q;\beta;J_{ij}^{(0)}]$, say $J_{ij}^2(q;\beta;J_{ij}^{(0)})$ (average over initial $J_{ij}^{(0)}$) will diverge indicating the appearance of infinite barriers and the freezing of the system in one of the states $m_i(q)$ with $q = q(T)$.

Following this scheme, the RG equations for observables could also be obtained.

We should mention briefly that the solutions of the RG equations for the couplings $J_{ij}(q)$ and for the spin clusters $\Omega_q(m)$ (which have not been discussed here) would immediately give the qualitative description of the relaxational dynamics. Keeping in mind the picture of Figure 8 for the free energy, the relaxation process could be described as a diffusion through such a fractal-like energy surface (Section 5.3) [34]. This process is characterized by the continuous spectrum of relaxation times: $\tau(q) \sim \tau_0 \exp\{J(q)/T\}$, which is described by the characteristic value $J(q)$ of the renormalized $J_{ij}(q)$. The weight function for each $\tau(q)$ could be obtained from $\Omega_q(m)$.

2.5.2 Calculations Since the topology of the variables is rather complicated, actual calculations become nontrivial and it is not clear so far how they can be performed rigorously.

However, as a first step, we can obtain some results with the following simplification. Let us ignore the restrictions $|m_i| \leqslant 1$. To some extent this seems reasonable, since even in this case for the variables on the sphere $\boldsymbol{m}^2 = Nq$ we have $\langle m_i^2 \rangle = q$. The statistics of the fluctuations $\{\delta m_i\}$ then becomes very simple. With the accuracy $O(N^{-1})$, (2.5.15) and (2.5.16) give

$$\langle \delta m_i \, \delta m_j \rangle = \delta_{ij} \, \delta q. \tag{2.5.21}$$

In the course of renormalization, the Hamiltonian remains of the form (2.4.1), where the couplings J_{ij} are scale-dependent parameters. Averaging over fluctuations $\{\delta m_i\}$ in (2.5.17) yields

$$J_{ij}(q-\delta q) = J_{ij}(q) - \beta \left(\sum_l J_{il} J_{lj} \right) \delta q, \tag{2.5.22}$$

or

$$\frac{\mathrm{d}}{\mathrm{d}q}\hat{J} = \beta J^2. \tag{2.5.23}$$

The solution of this equation is

$$\hat{J}(q) = \hat{J}^{(0)}[1 + \beta(1-q)\hat{J}^{(0)}]^{-1}, \tag{2.5.24}$$

which exhibits the growing long-range loop-like correlations of the couplings.

For the SK model characterized by an independent Gaussian distribution of the couplings J_{ij} (with $\overline{J_{ij}^2} = J_0^2$), (2.5.24) gives the phase-transition point at $T_c = 2J_0$. Below T_c there exists a critical scale $q(T) = 1 - T/T_c$ at which the characteristic values of the interactions $J_{ij}(q)$ diverge, indicating the appearance of infinite barriers. However, the value of the critical temperature is obviously wrong, and this indicates that the above simplification ignores essential (TAP-like) interactions of the variables.

Nevertheless, even in this oversimplified version, the proposed approach exhibits a nontrivial phase transition and probably gives a qualitatively correct description of spin-glass effects below T_c.

2.5.3 Conclusions Although even for the SK model the above scheme has not yet been completely elaborated, the most important problem is its relevance for realistic finite-range spin-glass systems. The great advantage (or maybe weak point ?) of the proposed approach is that basically the RG scheme itself is not sensitive to whether the actual distribution functional of the interaction matrix J_{ij} gives infinite-range or finite-range spin–spin interactions. It is certainly important in this respect whether or not it gives a tree-like (or more generally fractal-like) structure of metastable states. But, as far as it does, the RG procedure operates with arbitrary fixed J_{ij}, and the actual form of their distribution will be important only for analysis of the solutions.

REFERENCES

[1] Sherrington, D. and Kirpatrick, S. (1975) *Phys. Rev. Lett.* **35**, 1792. Kirkpatrick, S. and Sherrington, D. (1978) *Phys. Rev.* **B17**, 4384.
[2] Thouless, D.J., Anderson, P.W. and Palmer, R.G. (1977) *Phil. Mag.* **35**, 593.
[3] de Almeida, J.R.L. and Thouless, D.J. (1978) *J. Phys.* **A11**, 93.

[4] Parisi, G. (1979) *Phys. Rev. Lett.* **43**, 1754.
[5] Parisi, G. (1980). *J. Phys.* **A13**, 1101, 1887, L115.
[6] Parisi, G. (1980) *Phil. Mag.* **B41**, 677.
[7] Parisi, G. (1980). *Phys. Rep.* 67, 97.
[8] De Dominicis, C. and Kondor, I. (1983) *Phys. Rev.* **B27**, 606.
[9] De Dominicis, C. and Kondor, I. (1985) *J. Phys. (Paris) Lett.* **46**, L1037.
[10] Sommers, H.-J. (1985) *J. Phys. (Paris) Lett.* **46**, L779.
[11] Mezard, M., Parisi, G., Sourlas, N., Toulouse, G. and Virasoro, M. (1984) *Phys. Rev. Lett.* **52**, 1156; (1985) *J. Phys. (Paris)* **45**, 843.
[12] Derrida, B. and Toulouse, G. (1985) *J. Phys. (Paris) Lett.* **46**, L223.
[13] Bray, A.J. and Moore, M.A. (1980) *J. Phys.* **C13**, L469.
[14] De Dominicis, C., Gabay, M., Garel, T. and Orland, H. (1980) *J. Phys. (Paris)* **41**, 923.
[15] Tanaka, F. and Edwards, S.F. (1980) *J. Phys.* **F10**, 2471.
[16] Bhatt, R.N. and Young, A.P. (1986) *J. Magn. Magn. Mater.* **54–57**, 191.
[17] Sompolinsky, H. and Zippelius, A. (1981) *Phys. Rev. Lett.* **47**, 359.
[18] Sompolinsky, H. and Zippelius, A. (1982) *Phys. Rev.* **B25**, 6860.
[19] Sompolinsky, H. (1981) *Phys. Rev. Lett.* **47**, 935.
[20] Sompolinsky, H. (1981) *Phys. Rev.* **B23**, 1371.
[21] Ioffe, L.B. (1988) *Phys. Rev.* **B38**, 5181.
[22] Horner, H. (1987) *Z. Phys.* **B65**, 175; (1988) *Europhys. Lett.* **2**, 487.
[23] Sommers, H.-J. (1987) *Phys. Rev. Lett.* **58**, 1268.
[24] Binder, K. and Young, A.P. (1986) *Rev. Mod. Phys.* **58**, 801.
[25] *Proceedings of Heidelberg Colloquium on Glassy Dynamics*. Lecture Notes in Physics, Vol. 275. Berlin: Springer-Verlag (1989), Eds. J.L. van Hemmen and I. Morgenstern.
[26] Mezard, M., Parisi, G. and Virasova, M.A. (1987) *Spin Glass Theory and Beyond*. Singapore: World Scientific.
[27] Kirkwood, J.G. (1938) *J. Chem. Phys.* **6**, 70.
[28] Bray, A.J. and Moore, M.A. (1979) *J. Phys.* **C12**, L441.
[29] Owen, J.C. (1982) *J. Phys.* **C15**, L1071.
[30] Palmer, R.G. and Pond, C.M. (1979) *J. Phys.* **F9**, 1979.
[31] Bray, A.J. and Moore, M.A. (1979) *J. Phys.* **C12**, L441.
[32] Nemoto, K. and Takayama, H. (1985) *J. Phys.* **C18**, L529.
[33] Virasoro, M. and Mezard, M. (1985) *J. Phys. (Paris)* **46**, 1293.
[34] Dotsenko, V.S. (1985) *J. Phys.* **C18**, 6023.

3. SLOW RELAXATION AND AGEING

3.1 Simple Model of Ageing Phenomena

One can imagine two possible approaches to slow relaxation in random frustrated systems. The first is based on the notion of diffusion in a phase space with a complicated energy surface. In application to spin glasses this picture was proposed in, for example, references [1] and [2]; see also Section 5.3. In the second approach one deals with the notion of a free-energy surface obtained when irrelevant fast degrees of freedom

are integrated out [3]. This reasoning will be used for explicit calculations in Section 3.2 below. In the present section we accept the first approach and explore the simplest model of diffusion exhibiting some ageing properties.

We consider diffusion of particles in a one-dimensional relief characterized by a frozen random force field with nonzero mean. The equation of motion is

$$\frac{\mathrm{d}x}{\mathrm{d}t} = f(x) + F + \eta(x, t) = -\frac{\partial U(x)}{\partial x} + \eta(x, t). \tag{3.1.1}$$

Here $\overline{f(x)} = 0, \overline{f(x)f(x')} = \gamma\delta(x-x')$, and $\eta(x, t)$ is thermal noise with correlator $\langle \eta(x, t)\eta(x', t')\rangle = 2T\delta(x-x')\delta(t-t')$. Discrete versions of this model have been extensively studied [4–7]. Unusual behaviour of diffusion, namely

$$\langle x(t)\rangle \sim t^{\kappa}, \quad \kappa < 1, \tag{3.1.2}$$

occurs [4, 5, 7] at small values of F. A continuum model (3.1.1) was introduced in [8], and a simple way to obtain (3.1.2) was also suggested. The relaxation-time spectrum of this model was studied in [9] through reduction to the one-dimensional Schrödinger equation with a special kind of random potential.

Our main goal is to study the particle's response $\chi(\omega)$ with respect to infinitesimal harmonic force $\delta F(t) = f_\omega \mathrm{e}^{-\mathrm{i}\omega t}$. We show that in the low-F region ($F < \gamma/2T$) the response function $\chi(\omega)$ depends on the time t_w elapsed since the beginning of particle motion in a manner resembling ageing effects in spin glasses (see Section 1.3).

We begin with the derivation of (3.1.2) according to the lines of reference [8]. The energy relief $U(x)$ in (3.1.1) is represented by a Markovian process with diffusion coefficient $\frac{1}{2}\gamma$ and drift F (see Figure 9). The characteristic scale of the energy barriers E_0 and the corresponding distance x_0 are given by [8]

$$E_0 = \frac{\gamma}{2F}, \quad x_0 = \frac{\gamma}{4F^2}. \tag{3.1.3}$$

Rare strong fluctuations of the random field lead to energy barriers E higher than E_0 on the lengthscale $x_0 = E/E_0$. The density of these barriers is exponentially small (this can be shown by simple saddlepoint analysis),

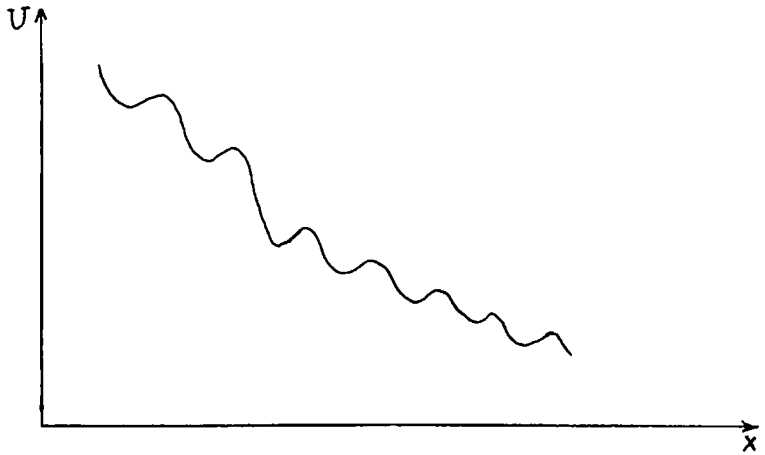

Figure 9 Typical energy relief $U(x)$.

$$\rho(E)\,\mathrm{d}E \approx x_0^{-1}\mathrm{e}^{-E/E_0}\,\mathrm{d}E/E, \tag{3.1.4}$$

but they are a serious obstacle for a moving particle and govern the slow relaxation processes in this system. Introducing the notion of the delay time $\tau \approx \tau_0 \mathrm{e}^{E/T}$ due to the presence of the barrier E, we get the density of these times:

$$w(\tau)\,\mathrm{d}\tau \approx x_0^{-1}\left(\frac{\tau}{\tau_0}\right)^{-\kappa-1}\frac{\mathrm{d}\tau}{\tau_0}, \tag{3.1.5}$$

which is valid in the range $\tau \gg \tau_1 (\tau_1 = \tau_0 \mathrm{e}^{1/\kappa}$ is the delay time of the typical barrier E_0). At $\kappa > 1$ the density (3.1.5) possesses a finite first moment, so the average delay time along the length L is given by

$$\tau_{\mathrm{tot}} = L\int \tau w(\tau)\,\mathrm{d}\tau \approx \frac{L}{x_0}\,\tau_0(\kappa-1)^{-1}. \tag{3.1.6}$$

Therefore the particle moves with the finite velocity

$$\langle v\rangle = \frac{x_0}{\tau_0}(\kappa-1). \tag{3.1.7}$$

At $\kappa < 1$ the integral (3.1.6) would diverge at large τ and should be cut off at $\tau \approx \tau_{\max}(L)$. Here $\tau_{\max}(L)$ is the largest delay time that can be

found with nonvanishing probability along the length L, i.e. $L \int_{\tau_{max}(L)} d\tau\, w(\tau) \approx 1$. Then, using (3.1.5), we get

$$\tau_{max}(L) \approx \tau_0 \left(\frac{L}{x_0}\right)^{1/\kappa}. \tag{3.1.8}$$

The total time that the particle needs to cover the segment of the length L is of order $\tau_{max}(L)$; inverting (3.1.8), we obtain (3.1.2) with $\kappa = 2FT/\gamma$. The appearance of an unusual sublinear drift at $\kappa < 1$ is obviously related to the lack of self-averaging in the distribution of delay times: the longer the distance covered, the higher the relevant barrier that determines the delay time.

We can describe this phenomenon somewhat more quantitatively using the notion of "renormalized" probability density $w_R(\tau)$, which determines the probability of finding a moving particle in the energy well with the delay time τ. $w_R(\tau)$ differs from the previously considered $w(\tau)$ mainly in the factor τ, which is due to the obvious fact that the more time the particle spends in the well, the more probable that this well is around the particle. Thus we obtain

$$w_R(\tau)\, d\tau \sim \frac{d\tau}{\tau^{\kappa}} \quad (\tau_1 \ll \tau \ll \tau_{max}(L)). \tag{3.1.9}$$

At $\kappa > 1$ the distribution density (3.1.9) is normalizable and stationary, i.e. it does not depend on the total time t_w of the particle motion in the limit $t_w \to \infty$. A typical energy relief in the reference frame moving with the particle is shown in Figure 10. The renormalized distribution density of barrier energies is

$$\rho_R(E)\, dE \sim \exp\left(\frac{1-\kappa}{T} E\right) dE, \quad E \gg E_0, \tag{3.1.10}$$

as follows from (3.1.9). Note that distributions in the moving reference frame were originally introduced in an earlier paper [10] dealing with the discrete version of the same problem. Our result (3.1.10) virtually coincides with that obtained in [10], although the methods employed are different.

For the mean values of the barrier energy E and size l (see Figure 10), we obtain

$$\langle E_R \rangle = \frac{T}{\kappa - 1}, \quad \langle l_R \rangle = \frac{\langle E_R \rangle}{F} = \frac{T}{F(\kappa - 1)}. \tag{3.1.11}$$

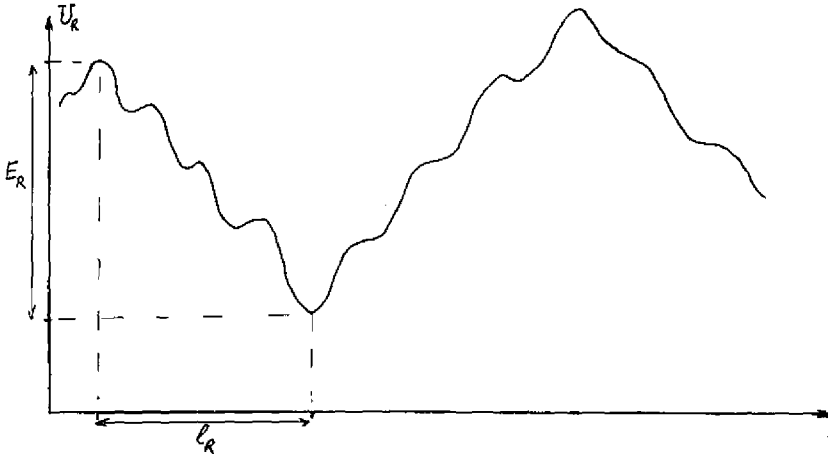

Figure 10 Typical energy relief $u_R(x)$ in the vicinity of a moving particle.

Equations (3.1.11) hold at $0 < \kappa - 1 \ll 1$, where average values are determined by the large-E region. The "waiting time" t_w needed to obtain the stationary distribution (3.1.10) can be estimated as

$$t_w \gg t_R \sim e^{1/(\kappa-1)}, \tag{3.1.12}$$

where t_R is the time associated with the average barrier $\langle E \rangle_R$. This estimate (which will be justified below) shows that at $\kappa \to 1 + 0$ the transient regime expands to infinity, whereas the stationary regime disappears.

We now consider the low-temperature region $\kappa < 1$ ($T < T_c = \gamma/2F$). The normalization integral of the density (3.1.9) now diverges at the upper limit and should be cut off at $\tau \approx \tau_{max}(L) \approx t_w$ ($L \sim t_w^\kappa$ is the full length spanned by the particle).* Thus the normalized probability density $w_R(\tau)$ is given by

$$w_R(\tau \mid t_w) \approx (1-\kappa) t_w^{\kappa-1} \tau^{-\kappa}, \quad \tau_1 \ll \tau \ll t_w. \tag{3.1.13}$$

*The condition (3.1.12) is justified now as that needed to neglect the contribution of the upper limit of integration.

The t_w dependence of $w_R(\tau)$ implies that the particle motion is non-stationary. The average depth and size of the energy well containing the particle grow with t_w:

$$\langle E\rangle_R = T \ln t_w, \quad \langle l\rangle_R = \frac{T}{F} \ln t_w. \tag{3.1.14}$$

In the infinite-t_w limit the particle appears to be localized in the symmetric energy relief with the "renormalized" potential energy

$$U_R(x) = \int_0^x dx' f(x') + F\cdot|x|. \tag{3.1.15}$$

We next proceed to the study of the finite-frequency particle dynamics in that potential well.

The probability density $\mathscr{P}(x, t)$ for the particle to be at point x at time t satisfies the Fokker–Planck equation

$$\frac{\partial \mathscr{P}}{\partial t} = \frac{\partial}{\partial x}\left[T\frac{\partial \mathscr{P}}{\partial x} + \left(\frac{\partial U_R(x)}{\partial x} - f_\omega e^{i\omega t}\right)\mathscr{P}\right], \tag{3.1.16}$$

where $U(x)$ is given by (3.1.15) and the term $f_\omega e^{i\omega t}$ represents the infinitesimal "measuring" force. We look for a solution of (3.1.16) in the form $\mathscr{P}(x, t) = \mathscr{P}_0(x) + \mathscr{P}_1(x) f_\omega e^{i\omega t}$, where $\mathscr{P}_0(x) = \text{const} \times e^{-U_R(x)/T}$ is the equilibrium solution of the unperturbed ($f_\omega = 0$) equation.* Then the "susceptibility" $\chi(\omega) = \partial\langle x_\omega\rangle/\partial f_\omega = \int dx\, \mathscr{P}_1 x$ can be represented in terms of the eigenfunctions $|\alpha\rangle$ and eigenvalues ϵ_α of the related Schrödinger equation

$$T\frac{\partial \psi}{\partial t} = T^2\frac{\partial^2\psi}{\partial x^2} - \left[\frac{1}{4}\left(\frac{\partial U_R}{\partial x}\right)^2 - \frac{T}{2}\frac{\partial^2 U_R}{\partial x^2}\right]\psi \tag{3.1.17}$$

(see e.g. [11, 12]) as follows:

$$\chi(\omega) = \sum_\alpha \langle 0|x|\alpha\rangle \left\langle \alpha \left| -\frac{\partial}{\partial x}\right| 0\right\rangle \frac{2}{\epsilon_\alpha/T - i\omega}$$

$$= \frac{1}{T}\sum_\alpha \frac{\epsilon_\alpha}{\epsilon_\alpha - i\omega T}\langle o|x|\alpha\rangle\langle\alpha|x|0\rangle. \tag{3.1.18}$$

*Note that the Fokker–Planck equation with "bare" potential $U(x)$ from (1.1) does not possess a solution of that kind as such a solution would not be normalizable.

Here $|0\rangle \equiv [\mathscr{P}_0(x)]^{1/2}$ is the ground-state eigenfunction with $\epsilon_0 \equiv 0$. It follows from (3.1.18) that the zero-frequency susceptibility $\chi(0) = T^{-1}\langle 0|\, x^2\, |0\rangle$, as it should. It is then reasonable to express $\chi(\omega)$ in terms of the spectral density:

$$\chi(\omega) = \frac{1}{T}\int \mathrm{d}\epsilon \sum_\alpha \delta(\epsilon - \epsilon_\alpha)|\langle 0|\, x\, |\alpha\rangle|^2 \frac{\epsilon}{\epsilon - \mathrm{i}\omega T}$$

$$= \frac{1}{T}\int \mathrm{d}\epsilon\, g(\epsilon) \frac{\epsilon}{\epsilon - \mathrm{i}\omega T}. \tag{3.1.19}$$

The spectral density $g(\epsilon)$ can be calculated by the methods developed in the theory of one-dimensional disordered systems [13, 14]. It appears [15] that the low-ϵ behaviour of $g(\epsilon)$ is virtually the same as that of the density of states $\rho(\epsilon)$, which was calculated in [9]:*

$$g(\epsilon) \sim \epsilon^{\kappa - 1}. \tag{3.1.20}$$

The asymptotic formula (3.1.20) holds at the energies $\epsilon \ll \mathrm{e}^{-1/\kappa}$ corresponding to the long-time limit $t \gg \tau_1$. Combining (3.1.19) and (3.1.20), we obtain

$$\mathrm{Im}\, \chi(\omega) \sim \omega^\kappa, \tag{3.1.21}$$

corresponding to a slowly decreasing relaxation function in the time domain:

$$\langle x(t)\rangle - \langle x(\infty)\rangle \sim t^{-\kappa}. \tag{3.1.22}$$

The above results refer to the limit $t_w \to \infty$ and thus give the stationary dynamic response in the sense discussed in Section 1.3.

We next consider the particle dynamics on timescale t for the case of finite "waiting time" $t_w \gg t$. Now the potential well $U_R(x \mid t_w)$, where the particle is located, is of the type depicted in Figure 10; the average parameters of that well are given by (3.1.14). Then the ground state $|0\rangle$ and low-lying ($\epsilon \ll \mathrm{e}^{-1/\kappa}$) states $|\alpha\rangle$ appear to be quasilocalized. The decay rates $\Gamma_0 \sim t_w^{-1}$ and γ_α for these states are of order $\tau^{-1} = \mathrm{e}^{-E/T}$, where the distribution density for the values of τ is given in (3.1.13). Then the states $|\alpha\rangle$ with $\epsilon_\alpha \gg \Gamma_\alpha$ are only slightly modified owing to the decay, and the spectral density $g(\epsilon)$ at $\epsilon \gg \langle \Gamma_\alpha\rangle_R$ can be calculated

* It should be emphasized that the spectral density $g(\epsilon)$, in contrast with the density of states $\rho(\epsilon)$, cannot be defined correctly when dealing with the "bare" potential $U(x)$ for the reasons mentioned in the preceding footnote.

within the framework of perturbation theory. The average value of the decay rate $\langle \Gamma_\alpha \rangle_R \equiv \Gamma$ is obtained from (3.1.13):

$$\Gamma = \int d\tau \frac{1}{\tau} w_R(\tau \mid t_w) \approx \frac{1-\kappa}{\kappa} t_w^{\kappa-1}. \tag{3.1.23}$$

It is assumed that t_w is the largest parameter involved, i.e. $\ln t_w \gg \max(\kappa^{-1}, (1-\kappa)^{-1})$. Thus the finite-$t_w$ generalization of (3.1.20) is

$$g(\epsilon) \sim \epsilon^{\kappa-1} f(\Gamma/\epsilon), \tag{3.1.24}$$

where $f(x)$ is some scaling function with $f(0) = 1$ and $f(\infty) = 0$ (the latter condition follows from the fact that $g(\epsilon < \epsilon_0) = 0$, where $\epsilon_0 \approx t_{max}^{-1} \approx t_w^{-1} \ll \Gamma$ is the ground-state eigenvalue). To find the explicit form of $f(x)$, a more thorough study is required.

Finally, we find from (3.1.19), (3.1.23) and (3.1.24) the finite-t_w response functions in the region $\omega^{-1}, t \ll t_w$:

$$\begin{aligned} \text{Im } \chi(\omega) &\sim \omega^\kappa f\left(\frac{\mu}{\omega t_w^\mu}\right), \\ \langle x(t) - \langle x(0) \rangle \rangle &\sim t^{-\kappa} f\left(\frac{t}{t_w^\mu}\right), \end{aligned} \tag{3.1.25}$$

where we take $1 - \kappa \equiv \mu$. Note the striking similarity between these results and the experimental data on ageing in spin glasses discussed in Section 1.3. Although the spin-glass relaxation is governed by two independent exponents: α (which stands for κ here) and μ, the measured values of both α and $1-\mu$ are rather small compared with unity; moreover, there are some experimental indications that the values of α and $1-\mu$ are correlated [16]. Evidently, spin glasses are much more complicated systems, but the similarity is suggestive.

Obviously, any power-law relaxation can be "explained" in terms of the multitude of modes with an exponential distribution of barriers, but the fact that this relaxation is accompanied by ageing (3.1.25) points at the strongly correlated (or hierarchical) nature of dynamics as in the simplest model considered.

Turning for a while to the "high-temperature" case $\kappa > 1$, we note that the relaxation-function behaviour (3.1.25) can also be obtained in that case, but with t_w^μ replaced by $t_R \sim e^{1/(\kappa-1)}$. Thus the purely dynamic transition occuring at $\kappa = 1$ is qualitatively reminiscent of the glass freezing transition.

A similar dynamic transition has recently been studied in the context of a nonrandom hierarchical diffusion model [17].

Note finally that, although the relation between our model and the spin-glass problem is rather speculative, it can probably be used more straightforwardly for the problem of domain-wall motion in disordered systems [18–20].

3.2 One-Dimensional Spin-Glass Model

We consider a chain of Ising spins, distributed randomly on a line, that interact with one another through a long-range oscillating potential:

$$\left.\begin{aligned} H &= \frac{1}{2}\sum_{i,j} J_{ij}\sigma_i\sigma_j - \sum_i h_i\sigma_i, \\ J_{ij} &= \gamma \exp(-\gamma|x_i - x_j|)\cos Q(x_i - x_j), \end{aligned}\right\} \tag{3.2.1}$$

where x_i is the coordinate of the ith spin, the interaction length is assumed to be large, while the wavelength of the oscillations is small ($2\pi Q^{-1} \ll 1$). (We choose the unit of length so that the average spin concentration $c \equiv 1$.)

We intend to study the space of metastable states and their influence on the dynamics in this model. For this purpose, we obtain below the effective free energy depending on only one continuous degree of freedom (φ_x). The metastable states correspond to the minima of the free energy and are organized hierarchically: each large valley appears on closer inspection to be a packed set of smaller valleys. The spin configurations corresponding to the different minima differ only within some interval of the line adjacent to the point x, with the length L of this interval decreasing with the energy E of the barrier separating them. The estimate $L(E)$ allows the estimation of the number of pairs of metastable states separated by a given energy barrier. The equilibrium susceptibility is governed by the transitions between metastable states with close energies ($|E_1 - E_2| \leqslant T$). In the temperature range $\gamma \ll T \leqslant 1$ the energies of the metastable states are distributed randomly, and the susceptibility is of order unity. At very low temperatures $T \ll \gamma$ the equilibrium distribution of state energies acquires a gap at $|E_1 - E_2| \leqslant \gamma$, and the susceptibility decreases rapidly with temperature. Since the susceptibility in this temperature range is very sensitive to the distribution function of the system between metastable states, the ageing effects

are enormous and the dependence of the equilibrium susceptibility on the waiting time can be estimated. We proceed with a brief sketch of the derivation of these results.

Using the well-known Hubbard-Stratonovich transformation and introducing a new complex field $\psi(x)$ (so that $\langle\sigma(x)\rangle = 2\,\mathrm{Re}\,\langle\psi(x)\rangle/T$) we get the effective Hamiltonian

$$H_{\mathrm{eff}}[\psi] = \int \left[\frac{1}{\gamma}\left|\left(\mathrm{i}\frac{\mathrm{d}}{\mathrm{d}x} + Q\right)\psi\right|^2 + |\psi|^2 - T\sum_i \delta(x-x_i)\ln\cosh\frac{\psi+\psi^*+h}{T}\right]\mathrm{d}x. \tag{3.2.2}$$

In the mean-field limit $\gamma \to 0$ in this model the phase transition occurs at $T = T_0 = 1$. The low-temperature state is characterized by the amplitude ρ and phase φ of the order parameter $\psi = \rho e^{-i\varphi + iQx}$. At finite x a true phase transition is absent because of the one-dimensional nature of the model, but the description in terms of the order parameter $\psi(x)$ is reasonable on timescales $t \ll t_{\max}$, where

$$t_{\max} \sim e^{f(\tau)/\gamma} \tag{3.2.3}$$

is the very long (for $\gamma \ll 1$) time of the order-parameter destruction.

Below we restrict our study of the configuration space to the low-temperature range $T \leqslant 1$ and consider only timescales $t \ll t_{\max}$. (A discussion of the system's properties in the vicinity of the transition point can be found in reference [21].) At these temperatures the fluctuations of the amplitude can be neglected $\rho(x) \equiv \rho_0 = 2/\pi$, as follows from the saddlepoint equation $\partial H_{\mathrm{eff}}[\psi]/\partial\rho = 0$ at $T \ll 1$. The configuration of spins $\langle\sigma_i\rangle$ are characterized by the slowly varying field $\varphi(x)$ with the Hamiltonian

$$H[\phi] = \int \mathrm{d}x\,\frac{\rho_0^2}{\gamma^2}\left(\frac{\mathrm{d}\phi}{\mathrm{d}x}\right)^2 + \sum_i V(\phi_i + Qx_i), \tag{3.2.4}$$

where

$$V(\Phi) = -T\ln\cosh\left(\frac{2\rho_0}{T}\cos\Phi + h\right).$$

The general approach to one-dimensional random problems described by local Hamiltonians such as (3.2.4) was developed in [22] in connection with charge-density-wave pinning, and has since been used for

several related problems [21, 23, 24]. In this approach we consider the free energy $\epsilon_n(\phi) = -T \ln Z_n(\phi)$ of a finite n-spin chain of Ising spins with the phase ϕ of the nth spin kept fixed (where $Z_n(\phi)$ is the corresponding partition function). Adding to the system an $(n+1)$th spin and integrating out the phase of the nth spin from the partition sum of an $(n+1)$-spin chain, we get a recursion relation for $\epsilon_n(\phi)$ [21, 22]:

$$\epsilon_{n+1}(\phi) - \epsilon_n(\phi) = -\frac{\gamma^2}{4\rho_0^2} \int \mathrm{d}\eta \left(\frac{\partial \epsilon_n}{\partial \phi}\right)^2 + \frac{T}{4} \frac{\gamma^2 l_n}{\rho_0^2} \frac{\partial^2 \epsilon_n}{\partial \phi^2} + V_0(\phi + Q x_n), \tag{3.2.5}$$

where $l_n = x_{n+1} - x_n$ and

$$V_0(\Phi) \equiv V(\Phi \mid h=0) = -T \ln \cosh \left(\frac{4}{\pi T} \cos \Phi\right).$$

Equation (3.2.5) contains two types of random variables: those originating from random distances l_n and those from random phase $\alpha_n = Qx_n$. Below we neglect the former and replace l_n by $\langle l_n \rangle = 1$ because l_n fluctuations lead to small corrections only. Moreover, it will be proved below that the term with $\partial^2 \epsilon / \partial \phi^2$ in (3.2.5) is irrelevant at $\gamma \ll T \ll 1$, and we neglect it for the time being. Thus the simplified version of (3.2.5) is

$$\frac{\partial \epsilon_n}{\partial x} = -\frac{\gamma^2}{4\rho_0^2} \left(\frac{\partial \epsilon_n}{\partial \phi}\right)^2 + V_0(\phi + \alpha_n), \tag{3.2.6}$$

where α_n is a random quantity distributed uniformly in the interval $(0, 2\pi)$ and independently at different points n.

To average the solution of (3.2.6) over random α_n, we pass on to its representation as a functional integral [21]. The generating functional $P\{j_n\}$ for the stationary probability distribution of the function $\epsilon_n(\phi)$ is

$$P\{j_n\} = \left\langle \int \mathscr{D}\mu_n(\phi)\, \mathscr{D}\epsilon_n(\phi) \exp \left\{ \mathrm{i} \sum_n \int \mathrm{d}\phi \left[\mu_n \left(\epsilon_{n+1} - \epsilon_n + \frac{\gamma^2}{4\rho_0^2} \left(\frac{\partial \epsilon_n}{\partial \phi}\right)^2 - V_0(\phi + \alpha_n) \right) \right] - \sum_n \int \mathrm{d}\phi\, j_n(\phi) \epsilon_n(\phi) \right\} \right\rangle_{\{\alpha_n\}}, \tag{3.2.7}$$

since the functional determinant

$$\mathrm{Det}\ \left\| \delta_{n,n+1} - \delta_{n,n} - \frac{\gamma^2}{4\rho_0^2}\frac{\partial\epsilon}{\partial\phi}\frac{\partial}{\partial\phi}\delta_{n,n} \right\| = 1.$$

The potential $V_0(\Phi)$ has a cusp singularity smoothed out on a scale $\Phi_0 \sim T \ll 1$. We can approximate $V_0''(\Phi)$ by a δ-function when we are interested in the behaviour of $\epsilon(\phi)$ on scales $\phi \gg \Phi_0(T)$. Using this fact, we can average over random α_n in (3.2.7) and obtain [21] generating function $P\{j_n\}$ in the form

$$P\{j_n\} = \int \mathscr{D}\epsilon(\phi, x) \exp\left\{ - \int \mathrm{d}x\, \mathrm{d}\phi\, [\mathscr{L}(\phi, x) + \epsilon(\phi, x) j(\phi, x)] \right\}, \tag{3.2.8}$$

where the Lagrangian $\mathscr{L} = \mathscr{L}_0 + \Delta\mathscr{L}$, with

$$\left.\begin{aligned} \mathscr{L}_0\{\epsilon\} &= \frac{1}{8\rho_0^2}\left\{ \frac{\partial^2}{\partial\phi^2}\left[\frac{\partial\epsilon}{\partial x} + \frac{\gamma^2}{4\rho_0^2}\left(\frac{\partial\epsilon}{\partial\phi}\right)^2 \right] \right\}^2, \\ \Delta\mathscr{L} &= \sum_{k=3}^{\infty} a_k [\mathscr{L}_0(\epsilon)]^{k/2}, \end{aligned}\right\} \tag{3.2.9}$$

where $\rho_0 = 2/\pi$ and a_k are numerical coefficients. Here we have replaced $\epsilon_{n+1}(\phi) - \epsilon_n(\phi)$ by $\partial\epsilon(\phi, x)/\partial x$, which is also valid at $\gamma \ll T$ [21]. We then assume that $\Delta\mathscr{L}_0 \ll \mathscr{L}_0$ and estimate the fluctuations of $\epsilon(\phi, x)$ that make the main contribution to the functional $P\{j_n\}$. The action $S_0 = \int \mathrm{d}x\, \mathrm{d}\phi\, \mathscr{L}_0$ for these fluctuations is of order unity, and both terms in the square brackets in $\mathscr{L}_0\{\epsilon\}$ should be of the same order. We consider fluctuations $\epsilon(\phi, x)$ of lengthscale X, phase scale Φ and magnitude E. Then we get two relationships

$$\left.\begin{aligned} EX^{-1} &\sim \gamma^2 E^2 \Phi^{-2} \\ E^2 X^{-1} \Phi^{-3} &\sim 1 \end{aligned}\right\} \tag{3.2.10}$$

which lead to the following estimates for X and E as functions of Φ:

$$X(\Phi) \sim \gamma^{-4/3}\Phi^{1/3}, \tag{3.2.11a}$$

$$E(\Phi) \sim \gamma^{-2/3}\Phi^{5/3}. \tag{3.2.11b}$$

The estimates (3.2.11) are valid at $\Phi_0(T) = T \leqslant \Phi \ll 1$; the inequality $\Delta Z \ll Z_0$ holds at $\Phi \gg \gamma$.

We now discuss the physical picture resulting from the above

estimates. Let us consider two metastable states characterized by the values of phases $\phi^{I,II}(x_n)$ at some arbitrary point x_n inside the system. Then both $\phi^I(x_0)$ and $\phi^{II}(x_0)$ are minima of the free energy $\tilde{\epsilon}(\phi(x_n)) = \epsilon^<(\phi(x_n)) + \epsilon^>(\phi(x_n))$. Here we denote by $\epsilon^{<,>}(\phi(x_n))$ the previously discussed free-energy functions $\epsilon(\phi(x_n))$ corresponding to the two parts ($x < x_n$ and $x > x_n$) of the whole system; obviously, the scaling estimates (3.2.11) remain unchanged when the function $\tilde{\epsilon}(\phi)$ is considered instead of $\epsilon(\phi)$. Then the difference in the free energies $\tilde{\epsilon}(\phi^I)$, $\tilde{\epsilon}(\phi^{II})$ is of order $E(\Phi)$ ($\Phi = \phi^I - \phi^{II}$) and also gives the characteristic scale of the free-energy barrier that must be overcome for transition between these metastable states. The highest barrier $E \sim \gamma^{-2/3}$ corresponds to the transition between the degenerate states that are related by spin inversion $\{\sigma_i\} \to \{-\sigma_i\}$, i.e. $\Phi = \pi$. The finiteness of E_1 shows once again the absence of a true low-temperature state in the thermodynamic sense; however, on timescales $t \ll t_1 \sim \exp(\gamma^{-2/3}/T)$ (note that $t \ll t_{\max}$ from (3.2.3)) the system can be considered as nonergodic. The lowest (at given T) barriers corresponding to $\Phi \sim T$ are of order $E_0(T) \sim T^{5/3}\gamma^{-2/3}$, i.e. much larger than T at $T \gg \gamma$. (The last circumstance justifies the neglect of the term $\partial^2\epsilon/\partial\phi^2$ in (3.2.5); the region $T \leqslant \gamma$ will be discussed later). The fact that $T \ll E_0 \ll E_1$ makes it sensible to consider three different types of statistical averaging corresponding to substantially different times of observation:

(i) equilibrium thermodynamics at $t \gg t_1$, when all the transitions between metastable states take place;
(ii) quasiequilibrium thermodynamics at $t \ll t_0 \sim \exp(E_0/T) \sim \exp[(T/\gamma)^{2/3}]$, when all transitions are absent (i.e. "absolute nonergodicity", cf. Section 1.3 and [3]);
(iii) slowly-time-dependent thermodynamics at $t_0 \ll t \ll t_1$ (i.e. "effective nonergodicity" [3]).

Cases (i) and (ii) were studied in detail in reference [21]. Here we discuss mainly the behaviour in case (iii), which resembles the behaviour of real spin glasses. We therefore consider [25] the structure of the free-energy surface as it follows from (3.2.11a, b). We begin with the estimation of the number M_0 of minima of the function $\tilde{\epsilon}(\phi)$. Let us consider the behaviour of the function $f(\phi) = \partial\epsilon/\partial\phi$ at $\phi = \phi^I + \Phi$, where ϕ^I is any zero of $f(\phi)$. The characteristic scale of $f(\phi^I + \Phi)$ is $F(\Phi) \sim E(\Phi)/\Phi \sim (\Phi/\gamma)^{2/3}$, whereas the scale β of $\partial f/\partial\phi$ is determined by the smallest-scale fluctuations with $\Phi \sim \Phi_0$: $\beta \sim \gamma^{-2/3}\Phi_0^{-1/3}$. Thus the

probability of finding a zero of $f(\phi^1 + \Phi)$ within an interval of width Φ_0 is

$$P(\Phi) \sim \frac{\Phi_0 \beta}{F(\Phi)} = \left(\frac{\Phi_0}{\Phi}\right)^{2/3}. \tag{3.2.12}$$

Therefore the total number of zeros (as well as the number of minima of $\epsilon(\phi)$) is given by

$$M_0 \sim \int_{\Phi_0}^{\pi} \frac{d\Phi}{\Phi_0} P(\Phi) \sim \left(\frac{\pi}{\Phi_0}\right)^{1/3} \sim T^{-1/3}. \tag{3.2.13}$$

The minima of $\epsilon(\phi)$ constitute a fractal set (situated on one-dimensional line) with fractal dimension $D_f = \frac{1}{3}$. As the temperature decreases, each metastable state (corresponding to $\epsilon(\phi)$ minima) splits up into to a closely packed set of metastable states in a hierarchical manner (see Figure 11). This structure of metastable states resembles the hierarchical organization of states in the SK model (Section 2.2). This fact, together with the experimental observation [26] of phenomena that can be interpreted as effects of the hierarchical organization of metastable states in real spin glasses, leads us to believe that hierarchical organization of metastable states really does occur in three-dimensional spin glasses.

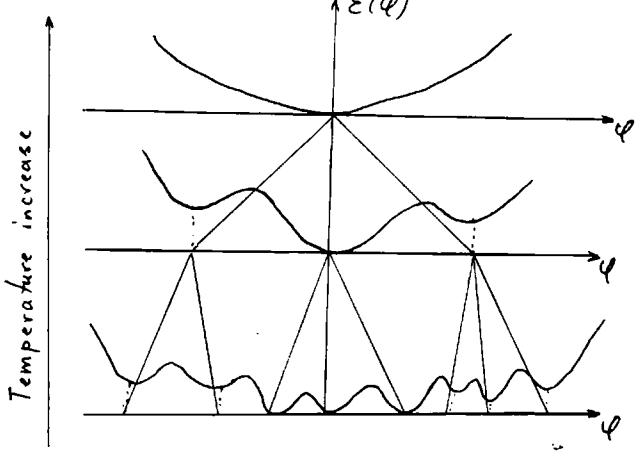

Figure 11 Hierarchical structure of metastable states.

To proceed further, we consider the equilibrium dynamics of the model on timescales in the region of effective nonergodicity ($t_0 \ll t \ll t_1$). Obviously, the relaxation is concurrent in distant parts of the system, so we require the linear density of the relaxation modes with given relaxation time t (or the corresponding barrier $E \sim T \ln t$). The number of minima of $\epsilon(\phi)$ separated by barriers higher than E is given by (3.2.13) with Φ_0 replaced by $\Phi \equiv \Phi(E)$ obtained from (3.2.11b):

$$M(E) \sim \frac{1}{\gamma^{2/15} E^{1/5}}. \tag{3.2.14}$$

The length of the part of the system that moves coherently when the barrier E is overcome can be obtained from (3.2.11a):

$$X(E) \equiv X(\Phi(E)) \sim \gamma^{-6/5} E^{1/5}. \tag{3.2.15}$$

Thus the linear density of relaxation modes with barriers in the interval $(E, E+\mathrm{d}E)$ is given by

$$W(E)\,\mathrm{d}E \sim \frac{\mathrm{d}}{\mathrm{d}E}\left(\frac{M(E)}{X(E)}\right)\mathrm{d}E \sim \gamma^{16/15}\frac{\mathrm{d}E}{E^{7/5}}. \tag{3.2.16}$$

The relaxation in a system with a complicated energy surface is governed mainly by "two-level" processes, so that the imaginary part of the susceptibility $\chi(\omega)$ is given by

$$\mathrm{Im}\,\chi(\omega) \sim \frac{1}{T}\int \mathrm{d}E\,\mathrm{d}\Delta\, R(E, \Delta)\frac{\omega\tau(E)}{1+[\omega\tau(E)]^2} N(E)\,\mathrm{sech}^2\frac{\Delta}{2T}. \tag{3.2.17}$$

Here $\tau(E) \sim \mathrm{e}^{E/T}$ is the free-energy difference between two metastable states, $R(E, \Delta)$ is the joint probability density, and $N(E) \sim \Phi(E)X(E) \sim (E/\gamma)^{4/5}$ is the number of spins that flip in the course of the transition between two metastable states (note that at $T \ll 1$, $\langle \sigma_i \rangle \approx \mathrm{sign}\,[(\cos(\phi_i + Qx_i)]$; therefore the relative part of all spins which differentiate between metastable states is of order $\phi_i^{\mathrm{I}} - \phi_i^{\mathrm{II}} = \Phi$). The characteristic scale of Δ is of order E, so that

$$\int \mathrm{d}\Delta\, R(E, \Delta)\,\mathrm{sech}^2\frac{\Delta}{2T} \sim W(E)\frac{T}{E} \tag{3.2.18}$$

Therefore, combining Eqs. (2.15–18) we obtain:

$$\operatorname{Im} \chi(\omega) \sim \int \frac{dE}{E} W(E)N(E) \frac{\omega\tau(E)}{1+[\omega\tau(E)]^2}$$

$$\sim \frac{\gamma^{4/15}}{(T \ln \omega^{-1})^{3/5}}, \tag{3.2.19}$$

which corresponds to the following asymptotics of the relaxation function $c(t)$ (which is the response to small stepwise variation of the magnetic field):

$$c(t) \sim \frac{\gamma^{4/5}}{(T \ln t)^{3/5}}. \tag{3.2.20}$$

The results ((3.2.19) and (3.2.20)) are valid for the dynamics at thermal equilibrium, i.e. in the limit of infinite waiting time ($t_w \to \infty$). At finite t_w the probability of finding the system in the given metastable state does not obey the Gibbs distribution; therefore the factor $\operatorname{sech}^2(\Delta/T)$ in (2.17) should be replaced by some more complicated τ- and ω-dependent expression.

All of the above discussion is valid for temperatures that are not too low: $\gamma \ll T \ll 1$. At $T \leqslant \gamma$ the smallest-scale structure of the function $\epsilon(\phi)$ (at $\Phi \leqslant \gamma$) does not obey the estimates (3.2.11a, b) since the conditions $\Delta\mathscr{L} \ll \mathscr{L}_0$ (see (3.2.9)) and $E(\Phi) \gg T$ no longer hold. Note, however, that the above results on scales $\Phi \geqslant \gamma$ are valid at $T \leqslant \gamma$ as well. The small-scale structure of $\epsilon(\phi)$ at $T \ll \gamma$ has been studied using a different method in [21]. It appears that the number of minima of $\epsilon(\phi)$ stops increasing at $T \geqslant \gamma$, and thus the maximum number of minima $M_0^{\max} \sim \gamma^{-1/3}$. At $T \ll \gamma$ the small-scale structure can be described by the approximate expression

$$\epsilon(\phi) \approx -T \ln \left(\sum_{k=i}^{M} a_k \exp \left(-\beta_k \frac{(\phi-\phi_k)^2}{2T} \right) \right] + \epsilon_b(\phi). \tag{3.2.21}$$

Here $a_k \sim 1$, $\beta_k \sim \gamma^{-1}$, $|\phi_k - \phi_{k+1}| \sim \gamma$, $M \sim \gamma^{-1/3}$, and $\epsilon_b(\phi)$ is the background relief with a characteristic scale larger than γ. Graphically, such a structure can be represented as a sum of pieces of parabolas (see Figure 12) with spikes between them. This form of the function $\epsilon(\phi)$ leads to the appearance of a gap of order γ in the distributions of internal fields $h_{\text{int}}(x_n) = 2\rho_0 \cos[\phi(x_n) + Qx_n]$. Thus the quasiequilibrium susceptibility (within the timescale $t \ll e^{\gamma/T}$) is exponentially small after zero-field cooling:

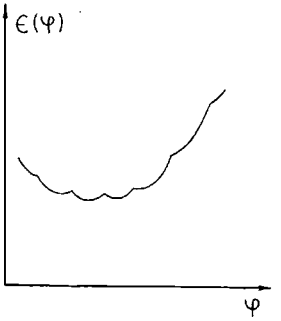

Figure 12 Small-scale structure of $\epsilon(\varphi)$ at $T \ll \gamma$.

$$\chi_{\mathrm{ZFC}} \sim \exp\left(-\text{const} \times \frac{\gamma}{T}\right), \tag{3.2.22}$$

whereas the "field-cooling" susceptibility χ_{FC} (as well as both susceptibilities at $T \gg \gamma$) is much larger [21]:

$$\chi_{\mathrm{FC}} = \chi(T \gg \gamma) = \frac{1}{2}. \tag{3.2.23}$$

Note finally that an interesting ageing phenomenon was obtained in reference [21]: at waiting times $t_{\mathrm{w}} \ll \mathrm{e}^{\gamma/T}$, χ_{ZFC} (at $t \ll t_{\mathrm{w}}$) appears to be t_{w}-dependent:

$$\chi_{\mathrm{ZFC}} \sim \exp\left[-\text{const} \times \left(\frac{\gamma}{T} \ln t_{\mathrm{w}}\right)^{1/2}\right]. \tag{3.2.24}$$

On timescales $t \gg \mathrm{e}^{\gamma/T}$ the nature of relaxation is the same as in the higher-temperature region $\gamma \ll T \ll 1$; in particular, the results (3.2.19) and (3.2.20) are valid at

$$\exp\left(\frac{\gamma}{T}\right) \ll t \ll \exp\left(\frac{\gamma^{-2/3}}{T}\right).$$

REFERENCES

[1] Dotsenko, V.S. (1985) *J. Phys.* **C18**, 6023.
[2] Teifel, S. and Domany, F. (1985) *Phys. Rev. Lett.* **55**, 2176.
[3] Palmer, R.G. (1987) in *Proceedings of Heidelberg Colloquium on Glassy*

Dynamics, p. 275. Lecture Notes in Physics, Vol. 275. Berlin: Springer-Verlag. Eds. J.L. van Hemmen and I. Morgenstern. (1982) *Adv. Phys.* **31**, 669.
[4] Kesten, H., Kozlov, M. and Spitzer, F. (1975) *Compos. Math.* **30**, 145.
[5] Solomon, F. (1975) *Ann. Probab.* **3**, 1.
[6] Sinai, Ya.G. (1982) *Theor. Probab. Applic.* **27**, 247.
[7] Derrida, B. and Pomeau, Y. (1982) *Phys. Rev. Lett.* **48**, 627.
[8] Vinokur, V.M. (1986) *J. Phys. (Paris)* **47**, 1425.
[9] Bouchaud, J.P., Comtet, A., Georges, A. and Le Doussal, P. (1987) *Europhys. Lett.* **3**, 653.
[10] Temkin, D.E. (1972) *Dokl. Akad. Nauk SSSR* **206**, 27.
[11] vam Kampen, N.G. (1981) *Stochastic Processes in Physics and Chemistry*. Amsterdam: North Holland.
[12] Feigel'man, M.V. and Tsvelick, A.M. (1982) *Sov. Phys. JETP* **56**, 823.
[13] Schmidt, H. (1957) *Phys. Rev.* **105**, 425. Halperin, B.I. (1965) *Phys. Rev.* **A139**, 104.
[14] Berezinsky, V.L. and Gor'kov, L.P. (1979) *ZhETF* **77**, 2498.
[15] Feigel'man, M.V., unpublished. "Spectral density of random-field Fokker-Planck equation".
[16] Ocio, M., private communication.
[17] Teitel, S., Kutasov, D. and Domany, E. (1987) *Phys. Rev.* **B36**, 684.
[18] Binder, K. Meermann, D.W., Milchev, A. and Sadiq, A. (1987) in *Proceedings of Heidelberg Colloquium on Glassy Dynamics*, p. 154. Lecture Notes in Physics, Vol. 275. Berlin: Springer-Verlag. Eds. J.L. van Hemmen and I. Morgenstern.
[19] Villain, J. (1985) in *Scaling Phenomena in Disordered Systems*, p. 423. New York: Plenum.
[20] Shapir, Y. (1987) *Phys. Rev.* **B35**, 62.
[21] Feigel'man, M.V. and Ioffe, L.B. (1983) *Z. Phys.* **B51**, 237.
[22] Feigel'man, M.V. (1980) *ZhETF* **79**, 1095; (1980) *Sov. Phys. JETP* **52**, 555.
[23] Vinokur, V.M., Mineev, M.B. and Feigel'man, M.V. (1981) *ZhETF* **81**, 2142; (1981) *Sov. Phys. JETP* **54**, 1138. Feigel'man, M.V. and Vinokur, V.M. (1989) in *Charge Density Waves in Solids*, to be published. Eds. G. Gruner and L.P. Gor'kov, North-Holland.
[24] Huse, D.A., Henley, C.L. and Fisher, D.S. (1985) *Phys. Rev. Lett.* **55**, 2924.
[25] Feigel'man, M.V. and Ioffe, L.B., to be published in *ZhETF*.
[26] Refregier, P., Vincent, E., Hammann, J. and Ocio, M. (1987) *J. Phys. (Paris)* **48**, 1533.

4. SPIN GLASSES WITH FINITE INTERACTION RANGE IN THE VICINITY OF THE CRITICAL TEMPERATURE

4.1 The Model and the Effective Hamiltonian of Slow Fluctuations

We consider the modification of the Edwards–Anderson model with large but finite-range interaction that is described by Hamiltonian

$$H = -\frac{1}{2}\sum_{i,j} J_{ij} S_i \cdot S_j, \tag{4.1.1}$$

where J_{ij} are random interaction constants that are characterized by the averages: $\overline{J_{ij}} = 0$, $\overline{J^2_{ij}} = cK(r_i - r_j)$, $\int K(r)\, d^3r = K$; S_i are classical n-component vector spins situated at random with concentration c. In this section we consider (unless stated otherwise) three-dimensional systems with a large average coordination number

$$Z = cK^{-3/2}[\int K(r) r^2\, d^3r]^{3/2} \gg 1. \tag{4.1.2}$$

To simplify notation, we choose units so that $c = K = 1$.

At $Z = N$ (N is the total number of spins) the model (4.1.1) becomes the Sherrington–Kirkpatrick model, whereas at $Z \approx 1$ it describes real spin glasses. We believe that the study of finite $Z \gg 1$ allows us to pick out the most important fluctuations, and so some qualitative results can be obtained for real spin glasses.

At intermediate temperatures these fluctuations can be described as independent fluctuations of "superspins" controlling the magnetization of a relatively large number of spins. At still lower temperatures superspin interaction must be taken into account.

To study these fluctuations we must find their effective action, which can be expanded over small $\boldsymbol{m}_i = \langle \boldsymbol{S}_i \rangle$ in the vicinity of the transition region just as the effective action of fluctuations near the ferromagnetic phase transition can be expanded over $\langle \boldsymbol{S} \rangle$. Continuing this analogy, we conclude that at large Z corrections to the effective Ginzburg–Landau functional are negligible, but the fluctuations of $\langle \boldsymbol{S} \rangle$ governed by this functional should be considered more carefully because they can contain divergences at low momenta. So the effective action of fluctuations in the spin-glass problem can be derived at $Z = N$; moreover, it is well known in the SK theory and called the Thouless–Anderson–Palmer [1] free energy $F\{\boldsymbol{m}_i\}$ (Section 2.4). The crucial difference from the SK theory is that now we should treat $F\{\boldsymbol{m}_i\}$ not as a free energy but rather as the effective action of the $\boldsymbol{m}_i$ field and should take its fluctuations into account. This functional has the form [2, 3]

$$F_{\mathrm{TAP}}\{\boldsymbol{m}_i\} = -\frac{1}{2}\sum_{i,j} J_{ij}\boldsymbol{m}_i\boldsymbol{m}_j - \frac{1}{4nT}\sum_{i,j} J_{ij}^2(1-\boldsymbol{m}_i^2)(1-\boldsymbol{m}_j^2)$$

$$+ Tn\sum_i \left[\frac{1}{2}\boldsymbol{m}_i^2 + \frac{n}{4(n+2)}(\boldsymbol{m}_i^2)^2 + \frac{1}{6}\frac{n^2(n+8)}{(n+4)(n+2)^2}(\boldsymbol{m}_i^2)^3\right], \tag{4.1.3}$$

where we keep only terms of the necessary order. We employ the expansion of the function m_i in eigenfunctions of the matrix J_{ij} that is customary in the study of ferromagnetic phase transitions when these eigenfunctions are plane waves and "expansion in eigenfunctions" means Fourier transformation:

$$m_i = \sum_\lambda a_\lambda \psi_\lambda(i), \quad \sum_j J_{ij}\psi_\lambda(i) = E_\lambda \psi_\lambda(i). \tag{4.1.4}$$

The properties of the spectrum and eigenfunctions $\psi_\lambda(i)$ of the matrix J_{ij} are discussed in detail in the Appendix to this section. In the infinite-range case $Z = N \to \infty$ the density of states of the matrix J_{ij} obeys the semicircular law,

$$\rho(E) = (2\pi)^{-1}(4-E^2)^{1/2}\theta(4-E^2), \tag{4.1.5}$$

and the $\psi_\lambda(i)$ are random Gaussian variables with the correlations between them being minimal compatible with the orthogonality condition (see Appendix).

If we continue the analogy with the magnetic phase transitions then we should suppose that at the critical temperature T_c there is a macroscopic condensation into the mode with the maximum eigenvalue $E = 2$. (In a ferromagnet this mode is a plane wave with $k = 0$; in an antiferromagnet it is a plane wave with $k = (\pi, \pi, \pi)$.) The modification of this approach to the SK-model was developed by Thouless, Anderson and Palmer [1]; however, its generalization for finite Z is by no means straightforward.

First of all we sketch the TAP approach [1] and show where it fails for finite Z. The local magnetization can be divided into two parts:

$$m_i = a_0\psi_0(i) + \delta m_i = a_0\psi_0(i) + \sum_{\alpha\neq 0} a_\alpha \psi_\alpha(i), \tag{4.1.6}$$

where ψ_0 corresponds to the largest $E_0 > E_\lambda$, and we restrict ourselves to Ising spins ($n = 1$). Substitution of (4.1.6) into (4.1.3) yields

$$F = \frac{1}{2}\tau^2 q + \frac{1}{2}\tau q^2 + \frac{1}{2}q^3 + \frac{1}{3}\sum_i a_0^3\psi_0^3(i)\left[\sum_{\alpha\neq 0} a_\alpha\psi_\alpha(i)\right]$$

$$+ \frac{1}{2}\sum_{\alpha\neq 0}(\tau^2 + 2 - E_\alpha)a_\alpha^2, \tag{4.1.7}$$

where $\tau = T - T_0 = T - 1$ and $q = a_0^2/N$. The last two terms in (4.1.7) are due to the mode coupling; they should be taken into account at

leading order in τ because at this order they result in a correction to the free energy (4.1.7) of order q^3, i.e. of the order of the free energy itself. (As was discovered by Thouless, Anderson and Palmer, the free energy without these terms has no nontrivial saddlepoints.) To take mode-coupling into account at leading order in τ, we should minimize (4.1.7) with respect to a_α, and insert the appropriate values of a_α into the free energy:

$$a_\alpha = -\frac{1}{3}\,\frac{1}{2+\tau^2-E_\alpha}\sum_j a_0^3\psi_0^3(j)\psi_\alpha(j), \tag{4.1.8}$$

$$F\{a_0\} = \frac{1}{2}\,\tau^2 q + \frac{1}{2}\,\tau q^2 + \frac{1}{2}\,q^3 - \frac{1}{18}\,T^2\sum_{i,j} a_0^3\psi_0^3(i)g(i,j)a_0^3\psi_0^3(j), \tag{4.1.9}$$

$$g(i,j) = \sum_{\alpha\neq 0}\frac{\psi_\alpha(i)\psi_\alpha(j)}{2+\tau^2-E_\alpha}. \tag{4.1.10}$$

As we stated above, the last term in (4.1.9) has the same order of magnitude as the free energy itself — in contrast with the usual mean-field theory of magnetism, where mode coupling results in small corrections. To calculate the last term in (4.1.9), we remember that $\psi_\alpha(i)$ are random Gaussian variables obeying the orthogonality condition, so that $g(i, j)$ can be replaced in the sum in (4.1.9) by

$$g_{ij} = \delta_{ij}\int\frac{\rho(E)\,\mathrm{d}E}{2-E+\tau^2} = \delta_{ij} + O(\tau). \tag{4.1.11}$$

Thus we get the TAP expression for the free energy:

$$F\{a_0\} = \frac{1}{6}\,(\tau+q)^3 - \frac{1}{6}\,\tau^3, \tag{4.1.12}$$

which has a nontrivial saddlepoint solution at $\tau < 0$:

$$q = \frac{a_0^2}{N} = |\tau|. \tag{4.1.13}$$

We note the unsual character of the solution (4.1.13) — it is neither a minimum nor a maximum of the free energy, but is rather a saddle-point. Moreover, the trivial solution $q = 0$ has a lower free energy than (4.1.13). This discrepancy was removed by Thouless, Anderson and

Palmer, who supposed the trivial solution to be unstable with respect to fast fluctuations that were integrated out in the course of the derivation of the free energy (4.1.12). Certainly, it would be better to derive the free energy that exhibits this instability explicitly — but no such derivation has yet been found.

The described picture of macroscopic condensation into one mode is correct at leading order in τ, but it is not preserved at the next orders [4, 5]. Generally the macroscopic number of modes (with eigenvalues $2-E_\lambda \leqslant \tau^4$) form the low-temperature state [5, 6], but this effect is negligible near the transition point. We neglect its influence on the phase transition in finite-range systems.

In finite-range systems the density of states of the matrix J_{ij} is non-zero at $E > 2$, but has a long tail for $\epsilon = E-2 \geqslant \epsilon_0 = Z^{-4/3}$ (see the Appendix):

$$\rho(\epsilon) \sim \exp\left[-c_1\left(\frac{\epsilon}{\epsilon_0}\right)^{3/4}\right]. \tag{4.1.14}$$

The corresponding eigenfunctions are localized with characteristic length

$$l(\epsilon) \sim Z^{1/3}\epsilon^{-1/4}. \tag{4.1.15}$$

The extended eigenfunctions constitute the main part of the spectrum $|E_\alpha| \leqslant 2$. The "mobility" edge ϵ_c lies somewhere in the region $\epsilon \sim \epsilon_0$. The density of states in this region is smooth and can be estimated as

$$\rho(\epsilon_0) \approx \epsilon_0^{1/2} = Z^{-2/3}. \tag{4.1.16}$$

It seems natural to suppose that all the eigenmodes a_α with eigenvalues near the mobility edge constitute a set of slow variables in the finite-range spin-glass transition problem just as the maximum-eigenvalue mode a_0 does in the infinite-range case. Thus we rewrite (4.1.6) in the form

$$m_i = \sum_\lambda a_\lambda \psi_\lambda(i) + \delta m_i = \sum_\lambda a_\lambda \psi_\lambda(i) + \sum_\lambda a_\alpha \psi_\alpha(i), \tag{4.1.17}$$

where we denote "slow" modes by a subscript λ and "fast" ones by α. Here $E_\lambda > 2 - \epsilon_d$ and $E_\alpha < 2 - \epsilon_d$, $\epsilon_d \sim \epsilon_0$; the choice of ϵ_d is somewhat ambiguous and we discuss this point later. Then we exclude "fast" modes just as was done above (cf. (4.1.7)–(4.1.10)) and obtain the effective Hamiltonian for the slow modes a_λ:

$$H\{a_\lambda\} = -\frac{1}{2}\sum_{i,j} J_{ij}\tilde{m}_i\tilde{m}_j - \frac{1}{4nT}\sum_{i,j} J_{ij}^2(1-\tilde{m}_i^2)(1-\tilde{m}_j^2)$$

$$+ Tn\sum_i \left[\frac{1}{2}\tilde{m}_i^2 + \frac{n}{4(n+2)}(\tilde{m}_i^2)^2 + \frac{n^2(n+8)}{6(n+4)(n+2)^2}(\tilde{m}_i^2)^3\right]$$

$$- \frac{1}{2}\left(\frac{Tn^2}{n+2}\right)^2 \sum_{i,j} [:\tilde{m}_i^2\tilde{m}_i^a:]g(i,j)[:\tilde{m}_j^2\tilde{m}_j^a:], \quad (4.1.18a)$$

$$\tilde{m}_i = \sum_\lambda a_\lambda \psi_\lambda(i), \quad (4.1.18b)$$

$$g(i,j) = \sum_{\epsilon_\alpha < -\epsilon_d} \frac{\psi_\alpha(i)\psi_\alpha(j)}{2 - E_\alpha + \tau^2}, \quad \tau = nT - 1 = n(T - T_0). \quad (4.1.18c)$$

The notation : $\tilde{m}_i^2\tilde{m}_i^a$: means the "normally ordered product", i.e. the irreducible part of $\tilde{m}_i^2\tilde{m}_i$,

$$:\tilde{m}_i^2\tilde{m}_i^a: = \tilde{m}_i^a\tilde{m}_i^2 - \tilde{m}_i^b\sum_\lambda [2\langle a_\lambda^a a_\lambda^b\rangle + \delta^{ab}\langle a_\lambda^2\rangle]\psi_\lambda^2(i), \quad (4.1.19)$$

which appears as a result of the orthogonality between $\psi_\lambda(i)$ and $g(i,j)$. In (4.1.18a) and (4.1.19) components of the spin vectors are labelled by indices a, b: these indices are summed over when repeated. Below we shall use the effective Hamiltonian (4.1.18a) in our discussion of spin-glass critical behaviour.

4.2 *Hierarchy of Interactions and Superparamagnetic Behaviour [3, 7]*

4.2.1 General discussion We start from the paramagnetic region $I \gg \tau \gg \tau_0 = Z^{-2/3}$ and consider the term in (4.1.18a) that is quadratic in a_λ:

$$H_2\{a_\lambda\} = \frac{1}{2}\sum_\lambda (\tau^2 - \epsilon_\lambda)a_\lambda^2 \quad (4.2.1)$$

where $\epsilon_\lambda = E_\lambda - 2$. It is evident from (4.1.14) that at any τ some modes with $\epsilon_\lambda > \tau^2$ are present that are unstable in the linear approximation. At $\tau \gg \tau_0$ the density of these modes is very small; moreover, they are well localized (cf. (4.1.15)) so that intermode interactions originating

from nonlinear terms in (4.1.18a) can be neglected, whereas intramode nonlinearity should be taken into account explicitly. Thus in this temperature range the free energy is the sum of the energies F_λ of non-interacting modes (λ):

$$F_\lambda(a_\lambda) = \frac{1}{2}(\tau^2 - \epsilon_\lambda)a_\lambda^2 + \frac{1}{6}a_\lambda^4 \sum_i \psi_\lambda^4(i) + \frac{1}{90}a_\lambda^6 \sum_i \psi_\lambda^6(i), \tag{4.2.2}$$

$$F_\lambda(a_\lambda) = \frac{1}{2}(\tau^2 - \epsilon_\lambda)a_\lambda^2 + \frac{n-1}{6(n+2)}(a_\lambda^2)^2 \sum_i \psi_\lambda^4(i), \tag{4.2.3}$$

where (4.2.2) applies to the Ising ($n = 1$) spins and (4.2.3) to the vector spins; in the latter case we omit the terms of 6th power in a_λ, which are irrelevant in this temperature range. To obtain the coefficients in these formulae we employ the condition $Z \gg 1$ since at leading order in Z^{-1}, $\psi_\lambda(i)$ are random Gaussian variables. The unstable ("condensed") modes (characterized by $\epsilon_\lambda > \tau^2$) acquire large values of $\langle a_\lambda^2 \rangle$, which can be found by minimization of $F_\lambda(a_\lambda)$. The corresponding eigenfunctions $\psi_\lambda(i)$ are localized so that the local symmetry (rotations of a_λ) is not broken. Thus we can say that the set of $a_\lambda \psi_\lambda(i)$ constitutes a set of independent clusters. The amplitudes a_λ that govern the magnetization m_λ of each cluster relax slowly, which results in the anomalous slow (nonexponential) relaxation that we discuss in Section 5.

At lower temperatures ($\tau \approx \tau_0$) the number of modes $\tilde{Z}$ interacting strongly with a given condensed mode increases and becomes of order unity ($\tilde{Z} \sim \rho(\epsilon_0)\epsilon_0 l^3(\epsilon_0) = O(1)$, cf. (4.1.15) and (4.1.16)).

The crucial feature of the large-Z spin-glass model is that the interaction terms can be divided into two types whose magnitudes are strongly different. The terms of the first type depend on the absolute values of all the amplitudes a_λ only; for example

$$a_\lambda^2 a_\mu^2 \sum_i \psi_\lambda^2(i)\psi_\mu^2(i). \tag{4.2.4}$$

Only these terms appear to be relevant at $\tau \sim \tau_0$. The terms of the second type depend on the relative signs of the amplitudes, for example

$$a_\lambda \cdot a_\mu a_\nu^2 \sum_i \psi_\lambda(i)\psi_\mu(i)\psi_\nu^2(i). \tag{4.2.5}$$

These terms are small in comparison with (4.2.4) owing to the random oscillating nature of the eigenfunctions $\psi_\lambda(i)$ (see Appendix and [8–10]). Indeed, the sum of oscillating terms in (4.2.5) is roughly $N^{1/2}_{\lambda,\mu,\nu}$ times smaller than the sum of positive terms in (4.2.4), where $N_{\lambda,\mu,\nu}$ is the mean number of sites where the eigenstates λ, μ, ν overlap. For the modes with $\epsilon_{\lambda,\mu,\nu} \approx \epsilon_0$, we get $N_{\lambda,\mu,\nu} \sim I^3(\epsilon_0) \sim Z^2 \gg 1$; therefore at $\tau \sim \tau_0$ interactions of the second type are Z times smaller and can be neglected. As the first type of interaction is independent of the signs of a_λ, it cannot lead to a phase transition, but only to a crossover from a simple paramagnet to a superparamagnet. On further decreasing the temperature, the second type of interaction can grow and lead to the freezing of that superparamagnet. This two-stage picture of the phase transition is in contrast with the behaviour of strongly disordered ferromagnets [11] or superconductors [12], where all the intermode interactions are of the same order of magnitude.

Below we consider the superparamagnetic behaviour of a three-dimensional spin glass governed by a Hamiltonian that includes only the first type of interaction. We show that in this case the superparamagnetic region exists over a relatively wide temperature interval $\tau_1 \geqslant -\tau \gg \tau_0$, with $\tau_1 \gg \tau_0$. It will be convenient to discuss the Ising and vector cases separately.

4.2.2 Ising spins As we discussed above, we neglect all terms that do not contain even powers of a_λ, and get

$$H_0 = \sum_\lambda \left\{ \frac{1}{2}(\tau^2 - \epsilon_\lambda)a_\lambda^2 + \frac{1}{2} a_\lambda^4 \sum_i \psi_\lambda^4(i) \left[\frac{1}{3}\tau + \sum_{\mu \neq \lambda} a_\mu^2 \psi_\mu^2(i) \right] \right\}$$

$$+ \frac{1}{2} \sum_{\lambda \neq \mu} a_\lambda^2 a_\mu^2 \sum_i \psi_\lambda^2(i)\psi_\mu^2(i) \qquad (4.2.6)$$

$$+ \frac{1}{6} \sum_{\lambda \neq \mu \neq \nu} a_\lambda^2 a_\mu^2 a_\nu^2 \sum_i \psi_\lambda^2(i)\psi_\mu^2(i)\psi_\nu^2(i).$$

In the derivation of (4.2.6) we have used (4.1.19) and the approximate equality

$$\sum_i \psi_\lambda^4(i) \approx 3 \sum_{i,j} \psi_\lambda^2(i)\psi_\nu^2(j) J_{ij}^2,$$

which is exact at leading order in Z^{-1} and we have omitted the term proportional to a_λ^6. Inspection of (4.2.6) shows immediately that the

intermode interaction terms change the coefficients of the terms quadratic and quartic in a_λ in the effective single-mode energy $F_\lambda(a_\lambda)$. To study the influence of mode–mode coupling, we introduce the molecular field B_i,

$$B_i = \sum_\lambda \langle a_\lambda^2 \rangle \psi_\lambda^2(i), \tag{4.2.7}$$

which describes the mean-square magnetization at site i. At $\tau \sim \tau_0$, B_i fluctuates strongly, with its average being of the same order of magnitude as its fluctuations (τ_0). At lower temperatures, modes with lower eigenvalues become condensed, so that ξ, which bounds the energy of the condensed modes, moves to the mobility edge ϵ_c that separates the localized and delocalized eigenfunctions of the matrix J_{ij}. The localized eigenfunctions that are close to the mobility edge overlap each other strongly; thus the effective coordination number for the interaction (4.2.6) becomes large, and therefore, at these temperatures, the interaction (4.2.6) can be studied by means of the mean-field approximation. In this approximation the fluctuations of B_i are neglected and it is replaced by its average

$$B = \frac{1}{N} \sum_i B_i = \frac{1}{N} \sum_\lambda \langle a_\lambda^2 \rangle. \tag{4.2.8}$$

Minimization of H_0 with respect to a_λ^2 then yields

$$\frac{\partial H_0}{\partial a_\lambda^2} = \frac{1}{2} [(\tau+\beta)^2 - \epsilon_\lambda] + \left(\frac{1}{3}\tau + B\right) a_\lambda^2 \sum_i \psi_\lambda^4(i) = 0. \tag{4.2.9}$$

If the scenario described above is valid then at low temperatures ($\tau < 0$, $|\tau| \gg \tau_0$) $\xi = (\tau+B)^2$ should tend to the mobility edge ϵ_c. Thus in this case $B \approx |\tau|$ and

$$a_\lambda^2 = \frac{3}{4|\tau|} (\epsilon_\lambda - \xi) V_\lambda \Theta(\epsilon_\lambda - \xi), \tag{4.2.10}$$

where $V_\lambda = [\sum_i \psi_\lambda^4(i)]^{-1}$, and $\Theta(x)$ is the unit-step function. Note that the equality $B \approx |\tau|$ is simply the generalization of the result (4.1.13) for the SK model. Inserting (4.2.10) into (4.2.8), we get the self-consistency condition:

$$\tau^2 = \frac{1}{N}\frac{3}{4}\sum_{\lambda}(\epsilon_\lambda - \xi)V_\lambda\Theta(\epsilon_\lambda - \xi)$$
$$\approx \frac{3}{4}\int \rho(\epsilon)(\epsilon - \xi)V(\epsilon)\,d\epsilon, \tag{4.2.11}$$

where $V(e)$ is the average of the inverse participation ratio V_λ over eigenfunctions with $\epsilon_\lambda \approx \epsilon$. The scaling concept applied to the localization problem results in the conclusion that $V(\epsilon)$ diverges as $\epsilon \to \epsilon_c$:

$$V(\epsilon) \sim Z^2\left(\frac{\epsilon - \epsilon_c}{\epsilon_0}\right)^{-\theta}. \tag{4.2.12}$$

(The prefactor in (4.2.12) was determined from the condition of matching in the crossover region the scaling formula (4.2.12) and the result (4.1.15) for the strongly localized region.) Unfortunately, the exact value of θ is still unknown, but computer simulations usually favour $\theta > 2$ for three-dimensional systems [13] (see also the Appendix). In that case the main contribution to the integral (4.2.11) comes from the region $\xi < \epsilon \leqslant \xi + (\xi - \epsilon_c)$, and we get

$$\left(\frac{\tau}{\tau_0}\right)^2 \sim \zeta^{2-\theta}, \quad \zeta = \frac{\xi - \epsilon_c}{\epsilon_0}. \tag{4.2.13}$$

The result (4.2.13) is very important for the theory of the spin-glass phase transition because it shows that the boundary ξ decreases with temperature toward the mobility edge but never reaches it at $\theta > 2$: $\zeta \sim (\tau_0/\tau)^{2/(\theta-2)}$. To check this, we also numerically compute the sum S over λ on the right-hand side of (4.2.11) as a function of ξ, using the exact eigenfunctions of the matrix J_{ij} obtained in numerical simulations (see the Appendix). It appears that S increases strongly as ξ approaches the mobility edge ϵ_c, qualitatively confirming the result (4.2.13). Thus we conclude that in the temperature range $\tau < 0$, $|\tau| \gg \tau_0$ the three-dimensional spin glass resembles a superparamagnet with each superspin being a "cluster", i.e. a nonlinear normal mode a_λ. The fluctuations of the absolute value of a_λ are small, but their signs fluctuate freely in this temperature range. Once again, we emphasize that these clusters overlap strongly, so that the local magnetization m_i is determined by a sum over a large number of normal modes λ. On short timescales (smaller than the long time of flipping of each cluster) the

system behaves as a frozen spin glass with Edwards–Anderson order parameter $q = |\tau|$. In Section 4.3 we discuss how the interaction between clusters results in a genuine phase transition at lower temperature, but for now a few remarks are in order.

First of all, we should justify the mean-field approximation that we have employed. To do that, we note that the main contribution to the sum (4.2.11) comes from the modes with $\epsilon_\lambda - \epsilon_c \sim \zeta\epsilon_0$. The number of these modes overlapping with a given one is roughly

$$\tilde{Z}(\zeta) \sim \rho(\epsilon_c)\zeta\epsilon_0 V(\epsilon_c + \zeta\epsilon_0) \sim \zeta^{1-\theta} \sim \left(\frac{|\tau|}{\tau_0}\right)^{2(\theta-1)/(\theta-2)} \gg 1. \tag{4.2.14}$$

Since $\tilde{Z}(\zeta)$ is the effective coordination number for the interaction (4.2.6), the estimate (4.2.14) means that corrections to the MFA are small. Moreover, the mean field B_i, (4.2.7), is given by a sum of a large number of positive terms so that the fluctuations of B_i are weak:

$$\overline{\delta B_i^2} = \overline{B_i^2} - B^2 = \frac{1}{N}\sum_\lambda a_\lambda^4 V_\lambda^{-1} \sim \frac{\tau_0^3}{|\tau|} \ll \tau_0^2. \tag{4.2.15}$$

Note that the main contribution to the sum in (4.2.15) comes from the modes in the crossover region $\epsilon_\lambda - \epsilon_c \sim \epsilon_0$, whose amplitudes are determined by thermal fluctuations, whereas the main contribution to B comes from the modes with $\epsilon_\lambda - \epsilon_c \sim \zeta\epsilon_0$. We now discuss the effect of small correction terms, $O(Z^{-1})$, that we have neglected in deriving the free energy (4.2.6) and the equation (4.2.10). Since the coefficient of a_λ^4 in the free energy (4.2.6) is large and increases at low temperatures, the corrections to this term are not important. The corrections to the first term in (4.2.6) (or (4.2.10)) are more dangerous, and deserve more careful consideration, because this term decreases at low temperatures. Generally, the corrections result in a constant term $\tilde{\epsilon} \sim \epsilon_0$, so that the first term in (4.2.9) becomes $[(\tau + B)^2 - \epsilon_\lambda - \tilde{\epsilon}]$. Inspection of the solution (4.2.10), (4.2.11) shows that it survives with a slight modification if $\tilde{\epsilon} > \epsilon_c$, whereas at $\tilde{\epsilon} < \epsilon_c$ such a solution becomes impossible. Moreover, it can be shown (using the numerical and analytical estimates of the ratio $\Sigma_i \psi_\lambda^6(i)/[\Sigma_i \psi_\lambda^4(i)]^2$ described in the Appendix) that any other nontrivial minima of the single-cluster free energy (4.2.2) also disappear at low temperatures, so that we conclude that the $\tilde{\epsilon} < \epsilon_c$ no nontrivial solution is possible — in obvious contradiction to the physical picture.

Finally, we note that the inequality $\theta < 2$ probably holds for higher

space dimensions. In that case the nature of the phase transition is changed completely: the right-hand side of (4.2.11) is finite at $\xi = \epsilon_c$, so that at finite τ microscopic condensation into one delocalized mode occurs [14]. In other words, we believe that there is a critical dimension of space d_c such that $\theta(d_c) = 2$ and the types of the the transition below and above d_c are different. Presumably $d_c = 4$.

4.2.3 Vector spins To clarify the origin of the difference between vector and Ising models, we again go back to the SK model. Proceeding analogously to the Ising case ((4.1.6)–(4.1.13)), we find that the mode $\boldsymbol{a}_0$ does not become unstable at $\tau = 0$; this is also reflected in the free energy (4.2.3), which has a positive coefficient of the $(\boldsymbol{a}_\lambda^2)^2$ term, whereas the corresponding coefficient in the Ising case is proportional to τ. The physical origin of this difference is simple: if condensation into one mode were also to occur in the vector case then the resulting low-temperature state would be anisotropic, with magnetization proportional to $\boldsymbol{a}_0\psi_0(i)$, whereas we expect the true low-temperature state to be isotropic. This suggests that the condensation occurs into a few modes with the highest eigenvalues, and the amplitudes of these modes form an orthonormal basis, $\boldsymbol{a}_\lambda = a\boldsymbol{e}_\lambda$, $\boldsymbol{e}_\lambda \boldsymbol{e}_\mu = \delta_{\lambda\mu}$, so that the magnetization

$$\boldsymbol{m}_i = \sum_{\lambda=1}^{\dot{n}} \boldsymbol{a}_\lambda \psi_\lambda(i) \tag{4.2.16}$$

is an isotropic random field. Indeed, the replacement of $\boldsymbol{a}_0\psi_0(i)$ in (4.1.6) by the sum (4.2.16) results in a free energy that has a saddlepoint with

$$q = \frac{1}{N}\sum_\lambda a_\lambda^2 = \frac{na^2}{N} = |\tau|, \tag{4.2.17}$$

which is a natural generalization of the Ising result (4.1.13).

We now consider a finite-range spin glass. Again we neglect all terms in the Hamiltonian (4.1.18) that are odd in $\boldsymbol{a}_\lambda$, and get

$$H_0 = \frac{1}{2}\sum_\lambda (\tau^2 - \epsilon_\lambda)\boldsymbol{a}_\lambda^2 - \frac{1}{4(1+\tau)}\sum_{\lambda,\mu} \boldsymbol{a}_\lambda^2 \boldsymbol{a}_\mu^2 \sum_{i,j} \psi_\lambda^2(i) J_{ij}^2 \psi_\mu^2(j)$$

$$+ (1+\tau)\frac{n}{4(n+2)}\sum_{\lambda,\mu}[2(\boldsymbol{a}_\lambda \cdot \boldsymbol{a}_\mu)^2 + \boldsymbol{a}_\lambda^2 \boldsymbol{a}_\mu^2] \sum_i \psi_\mu^2(i)\psi_\lambda^2(i)\left(1 - \frac{2}{3}\delta_{\lambda\mu}\right)$$

$$+\frac{n^2(n+8)}{6(n+4)(n+2)^2}\sum_{\lambda,\mu,\nu}[a_\lambda^2a_\mu^2a_\nu^2+6a_\nu^2(a_\lambda\cdot a_\mu)^2$$

$$+8(a_\lambda\cdot a_\mu)(a_\mu\cdot a_\nu)(a_\nu\cdot a_\lambda)]\sum_i\psi_\lambda^2(i)\psi_\mu^2(i)\psi_\nu^2(i)$$

$$-\frac{1}{2}\left(\frac{n}{n+2}\right)^2\sum_{\lambda,\mu,\nu}[2(a_\lambda\cdot a_\mu)^2a_\nu^2+4(a_\lambda\cdot a_\mu)(a_\mu\cdot a_\nu)(a_\nu\cdot a_\lambda)]$$

$$\times\sum_{i,j}\psi_\lambda(i)\psi_\mu(i)\psi_\nu(i)g(i,j)\psi_\lambda(j)\psi_\mu(j)\psi_\nu(j). \qquad (4.2.18)$$

The second and third sums in (4.2.18) consitute the part of H_0 that is a homogeneous function of fourth order in a_λ (referred to below as $H^{(4)}$). $H^{(4)}\{a_\lambda\}$ can be rewritten in terms of the scalar variables a_λ^2 and quadrupoles $Q_\lambda^{\alpha\beta}=a_\lambda^\alpha\alpha_\lambda^\beta-a_\lambda^2\delta_{\alpha\beta}/n$:

$$\left.\begin{aligned}
&H^{(4)}=H_{sc}^{(4)}+H_{qu}^{(4)};\\
&H_{sc}^{(4)}=\frac{1}{2}\tau\sum_{\lambda,\mu}a_\lambda^2a_\mu^2\left(1-\frac{2}{3}\delta_{\lambda\mu}\right)\sum_i\psi_\lambda^2(i)\psi_\mu^2(i),\\
&H_{qu}^{(4)}=\frac{n}{2(n+2)}\sum_{\lambda,\mu}Q_\lambda^{\alpha\beta}Q_\mu^{\alpha\beta}\left(1-\frac{2}{3}\delta_{\lambda\mu}\right)\sum_i\psi_\lambda^2(i)\psi_\mu^2(i).
\end{aligned}\right\} \qquad (4.2.19)$$

(α, β here are spin-vector indices — they are summed over when repeated.) The scalar part $H_{sc}^{(4)}$ coincides with the corresponding part of the Hamiltonian (4.2.6) of the Ising case, whereas $H_{qu}^{(4)}$ is specific to the isotropic vector model. The quadrupole–quadrupole interaction $H_{qu}^{(4)}$ is repulsive; it is similar to the antiferromagnetic interaction and results in a zero mean value of the quadrupolar order parameter $Q^{\alpha\beta}=\sum_\lambda Q_\lambda^{\alpha\beta}$ (in full analogy with the infinite-range case). We assume that the qualitative picture of mode condensation that was found above for the Ising case holds for vector models as well. That is, the modes of greater and greater spatial extent condense progressively as the temperature decreases. Then at $-\tau\gg\tau_0$ the effective number of "neighbours" in the Hamiltonian $H^{(4)}$ is large; therefore the quadrupolar antiferromagnetic interaction $H_{qu}^{(4)}$ is strongly frustrated. This interaction should be contrasted with the ferromagnetic one: long-range ferromagnetic interaction suppresses fluctuations, whereas long-range antiferro-

magnetic interaction enhances fluctuations. It can be shown that the interaction $H_{qu}^{(4)}$ does not result in freezing in the considered temperature range, but it does ensure the following:

(i) The relevant spin configurations are nearly isotropic:

$$B^{\alpha\beta} = \sum_{\lambda} a_\lambda^\alpha a_\lambda^\beta \psi_\lambda^2(i) \approx B\delta_{\alpha\beta}; \tag{4.2.20}$$

(ii) the coefficient of the self-interaction term $(a_\lambda^2)\sum_i \psi_\lambda^4(i)$ in the effective Hamiltonian is large ($O(1)$, whereas in the case of Ising spins it is $O(\tau)$).

Naively, one would expect from the inspection of diagonal ($\lambda = \mu$) terms of $H^{(4)}$ that the self-interaction is given by the sum

$$W = g_0 \sum_{\lambda} (a_\lambda^2)^2 \sum_i \psi_\lambda^4(i), \quad g_0 = \frac{n-1}{6(n+2)}. \tag{4.2.21}$$

In fact, at low temperatures the intermode interaction can result in the renormalization of g_0, but it still remains of order unity, so that the naive guess (4.2.21) is at least qualitatively correct. Thus a_λ^2 can be determined from the equation

$$\frac{\partial H}{\partial a_\lambda^2} = [(\tau + B)^2 - \epsilon_\lambda] + g a_\lambda^2 \sum_i \psi_\lambda^4(i) = 0, \quad g = O(1), \tag{4.2.22}$$

which yields

$$a_\lambda^2 = g^{-1}(\epsilon_\lambda - \xi)\Theta(\epsilon_\lambda - \xi) V_\lambda. \tag{4.2.23}$$

Proceeding analogously to the Ising case, we get the equation for the boundary ξ:

$$\frac{|\tau|}{\tau_0^2} \approx \zeta^{2-\theta}, \quad \zeta = \frac{\xi - \epsilon_c}{\epsilon_0}. \tag{4.2.24}$$

From (4.2.24) we see that at $\tau \approx -\tau_0$, ξ is small (in contrast with the Ising case), whereas at $\tau \approx +\tau_0$, $\xi = O(1)$, i.e. the simple paramagnetic behaviour at $\tau \gtrsim +\tau_0$ and the superparamagnetic behaviour at $\tau \lesssim -\tau_0$ do not match each other smoothly as they do in the Ising case. This means that there is a peculiar crossover region at $|\tau| \sim \tau_0$. We do not dwell upon the system behaviour in this temperature range, but only

state that the thermal fluctuations of the amplitudes are large and simple formulae like (4.2.22) cannot be applied here (more details can be found in [3]).

Thus we conclude that in the temperature range $\tau_0 \ll -\tau \ll \tau_1$ the vector spin glass forms a superparamagnet with the interaction between vector "superspins" being small, so that they fluctuate freely. In Section 4.3 we discuss the interaction of these superspins and their freezing at $-\tau \sim \tau_1 \gg \tau_0$.

4.3 *Effective Superspin Interaction and Hierarchy of Superparamagnets*

4.3.1 Effective interaction We have learned that the superspins $\sigma_\lambda = a_\lambda / a_\lambda$ constitute a set of spin-glass slow variables at low temperatures $-\tau \gtrsim \tau_0$. The absolute values $|a_\lambda| = (a_\lambda^2)^{1/2}$ are given by (4.2.10) and (4.2.23) for the Ising and vector cases respectively. The interaction between σ_λ is due to the terms like (4.2.5) that we have neglected so far.

At lower temperatures (i.e. at larger $-\tau$) the boundary separating condensed and uncondensed modes moves to the mobility edge ϵ_c:

$$(-\tau)^a = r(\xi) \approx \epsilon_0 \left(\frac{\epsilon_0}{\xi - \epsilon_c} \right)^{\theta - 2} = \epsilon_0 \xi^{2-\theta}, \tag{4.3.1}$$

where $a = 1, 2$ for the vector and Ising cases respectively and we introduce the function $r(\xi)$:

$$r(\xi) = \sum_\lambda (\epsilon_\lambda - \xi) \left[\sum_i \psi_\lambda^4(i) \right]^{-i} \theta(\epsilon_\lambda - \xi).$$

The size of the condensed localized modes and their coordination number increase with decreasing temperature, so that at some temperature $-\tau \approx \tau_1$ the interaction between superspins becomes relevant.

We turn now to the study of this interaction. The simplest possible form of the effective interaction is

$$H_1\{\sigma_\lambda\} = -\frac{1}{2} \sum_{\lambda,\mu} I_{\lambda\mu} \sigma_\lambda \cdot \sigma_\mu. \tag{4.3.2}$$

To find the constants $I_{\lambda\mu}$, we differentiate the Hamiltonian (4.1.18) with respect to a_λ and a_μ and average over thermodynamic fluctuations

of a_λ weighted with the Hamiltonian $H_0\{a_\lambda^2\}$. At leading order in τ we get:*

$$I_{\lambda\mu} = |a_\lambda|\,|a_\mu| \sum_i \psi_\lambda(i)\psi_\mu(i)\,\delta B_i \tag{4.3.3}$$

where $\delta B_i \equiv B_i - B$ (cf. (4.2.7) and (4.2.8)). Note that the term with $B = B_i$ cancels in (4.3.3) owing to the orthogonality of different eigenfunctions $\psi_\lambda(i)$. The couplings $I_{\lambda\mu}$ are random and weakly (at most) correlated owing to the random character of the eigenfunctions $\psi_\lambda(i)$ and the "background" field δB_i. We therefore arrive at a problem formally equivalent to the initial one (cf. (4.1.1)). The effective strength of the σ_λ interaction is characterized by the parameter

$$I = \frac{1}{\mathcal{N}} \sum_{\lambda,\mu} I_{\lambda\mu}^2 \tag{4.3.4}$$

where $\mathcal{N}$ is the total number of "spins" σ_λ. The main contribution to the sum (4.3.4) comes from the largest-scale modes with $\epsilon_\lambda - \xi \approx \xi - \epsilon_c = \zeta\epsilon_0$. The corresponding eigenfunctions $\psi_\lambda(i)$ overlap each other strongly, with mean coordination number $\bar{Z} \sim \zeta^{1-\theta} \gg 1$ (cf. (4.2.14)). To estimate the matrix elements $I_{\lambda\mu}$, we need to know the correlation properties of $\psi_\lambda(i)$ and δB_i. In the simplest approximation, with all correlations neglected, we obtain

$$(\delta B_i)^2 = \frac{1}{\mathcal{N}} \sum_{i,\lambda} \langle (a_\lambda^2)^2 \rangle \psi_\lambda^4(i) \approx \begin{cases} \dfrac{\tau_0^3}{|\tau|} & \text{(Ising)}, \\ \tau_0^3 & \text{(vector)} \end{cases} \tag{4.3.5}$$

(where the main contribution to δB_i^2 comes from the modes with $\epsilon_\lambda - \xi \approx \epsilon_0$, whose $\langle (a_\lambda^2)^2 \rangle$ values are determined by thermal fluctuations), and then

$$I(\zeta) \approx \begin{cases} \tau_0 \zeta^{-\theta/2} & \text{(Ising)}, \\ \tau_0^4 \zeta^{3-2\theta} & \text{(vector)}, \end{cases} \tag{4.3.6}$$

where we have used (4.2.10), (4.2.23) and expressed all τ-dependent factors in terms of ζ. Clearly, the intensity $I(\zeta)$ of the $\sigma_\lambda$interaction does

* An extra factor $|\tau|$ in the expression for $I_{\lambda\mu}$ was erroneously written in our previous papers [3, 7].

grow as the temperature (i.e. ξ) decreases, and becomes strong at some value of τ, which can be estimated from (4.3.1) and (4.3.6).

Unfortunately, at present we can neither justify nor invalidate this simplest approximation. The trouble is that the scaling properties of eigenfunctions near the mobility edge are rather poorly understood in the absence of a quantitative theory of three-dimensional localization. At present the greatest proportion of the relevant information comes from computer simulations (see e.g. [13]), which point at rather rich scaling behaviour characterized by a multitude of different independent exponents. We have therefore undertaken numerical computation of $I(\zeta)$ (defined by (4.3.3) and (4.3.4)) behaviour using the exact eigenfunctions of the nearest-neighbour J_{ij} matrix (see the Appendix). It appears that $I(\zeta)$ does grow as ζ decreases, and appears to be of order unity at positive ζ, i.e. in the region of localized eigenfunctions.

Therefore below, instead of (4.3.6), we consider a more general scaling equation

$$I(\zeta) = \begin{cases} \tau_0 \zeta^{-\phi_I} & \text{(Ising)}, \\ \tau_0^4 \zeta^{-\phi_V} & \text{(vector)}. \end{cases} \tag{4.3.7}$$

Presumably $\phi_{I,V}$ are close to their naive estimates (4.3.6), but below we discuss various scenarios that are possible for general values of the exponents ϕ_I and ϕ_V.

The correlations between superspin σ_λ become strong at $I(\zeta) \approx 1$, i.e. at

$$\zeta_I \approx \tau_0^{1/\phi_I}, \quad \zeta_V \approx \tau_0^{4/\phi_V}. \tag{4.3.8}$$

The corresponding reduced temperatures $-\tau$ are

$$\tau_1^{(I,V)} \approx \tau_0^{\tilde{p}_{I,V}} \approx Z^{-p_{I,V}}, \quad p_{I,V} = \frac{2}{3}\tilde{p}_{I,V} \tag{4.3.9}$$

$$\tilde{p}_I = 1 - \frac{\theta - 2}{2\phi_I}, \quad \tilde{p}_V = 2 - 4\frac{\theta - 2}{\phi_V}. \tag{4.3.10}$$

We recall that a superparamagnetic state exists at $\tau_0 \ll -\tau \ll 1$; therefore, the estimates (4.3.9) can be applied only if $0 < \tilde{p}_{I,V} < 1$. This inequality is certainly satisfied for Ising spins, whereas the inequality $\tilde{p}_V < 1$ is more doubtful, but numerical estimates indicate that it is probably valid also.

At the temperature $-\tau \approx \tau_1$ we have $I = 1$ and the Hamiltonian $H_1\{\sigma_\lambda\}$ is near its critical point. In other words, we have made a discrete renormalization-group transformation from the initial spin-glass Hamiltonian (4.1.1) to the effective Hamiltonian (4.3.2). The main parameter characterizing the Hamiltonian (4.1.1) is the effective number of interacting neighbours (or the coordination number) Z, so to complete our RG transformation we just lack an estimate of the effective coordination number Z_1 for the Hamiltonian (4.3.2). Using (4.3.1), (4.3.10) and (4.3.11), we obtain

$$Z_1 = \tilde{Z}[\zeta(\tau_1)] \sim Z^q \tag{4.3.11}$$

where $q_I = \frac{2}{3}(\theta - 1)/\phi_I$, $q_V = \frac{8}{3}(\theta - 1)/\phi_V$ for the Ising and vector models respectively. The key point is the sign of $q - 1$. At $q > 1$ the effective coordination number increases under RG transformation, the Z^{-1} approximation that is employed improves and all the above derivation can be repeated again, and so on. In contrast, if $q < 1$ then the coordination number decreases under RG transformation and the considered model appears to be in the same universality class as the usual short-range model with $Z \sim 1$, which is still beyond any analytical theory. For the vector model, the condition $q_V > 1$ is certainly fulfilled, and the first possibility is realized. The situation with the Ising model is more subtle: the inequality $q_I > 1$ is equivalent to

$$3\phi_I < 2\theta - 2. \tag{4.3.12}$$

To clarify this point, we have studied numerically the effective interaction matrix $I_{\lambda\mu}(\zeta)$ constructed from the exact eigenfunctions of the random matrix J_{ij} with short-range interaction (see the Appendix). We estimate the effective coordination number of the interaction matrix $I_{\lambda\mu}(\zeta)$ and find that it is large in all reasonable ranges of ζ where we can expect freezing of superspins to be possible, so that we believe that it grows in the case of the long-range J_{ij} matrix also.

Now, before we proceed to discussion of the consequences of the constructed discrete critical hierarchy, we should justify the disregard of types of superspin interaction other than (4.3.2) (e.g. four-spin). The four-spin interaction term follows directly from (4.1.8):

$$\left.\begin{aligned} H_4\{\sigma_\lambda\} &= \frac{n}{4(n+2)} \sum_{\lambda,\mu,\nu,\eta} I_{\lambda\mu\eta\nu}(\sigma_\lambda \cdot \sigma_\mu)(\sigma_\eta \cdot \sigma_\nu), \\ I_{\lambda\mu\nu\eta} &= |a_\lambda|\,|a_\mu|\,|a_\nu|\,|a_\eta| \sum_i \psi_\lambda(i)\psi_\mu(i)\psi_\nu(i)\psi_\eta(i) \end{aligned}\right\}. \tag{4.3.13}$$

The effective strength of this interaction is described by the parameter

$$I_4 = \frac{1}{\mathcal{N}} \sum_{\lambda,\mu,\nu,\eta} I^2_{\lambda\mu\nu\eta}. \tag{4.3.14}$$

The mean-field theory [15, 16] of spin glasses with p-spin interaction shows that these spin glasses belong to a different universality class than the SK model. The phase transitions in these spin glasses are first-order transitions and the eigenmode analysis is not applicable. As far as we know, models with both types of interaction have never been studied, but a simple estimate shows that the interaction (4.3.13) is irrelevant at $I_4 \ll I$.

To compare I_4 and I, we again use the results of numerical simulations. To simplify computational problems, we compare not I_4 and I, but rather I_4 and $\tilde{I}$, where $\tilde{I}$ is defined by the same equations (4.3.3) and (4.3.4), but all amplitudes $|a_\lambda|$ are determined from (4.2.10) (or (4.2.23) in the vector case). In other words, in the definition of $\tilde{I}$ we do not take into account the thermal fluctuations that enhance the amplitudes of modes far from the mobility edge. (These modes make a negligible contribution to I_4 since they are strongly localized and slightly overlap each other, but it is these modes that determine the space variation δB of the B field, (4.3.3), (4.3.4).) Evidently, $\tilde{I} < I$. The ratio $R = I_4/\tilde{I}$ can be expressed in terms of the eigenfunctions of the J_{ij}:

$$R = \frac{\sum_{\lambda,\mu,\eta,\nu} (I'_{\lambda\mu\eta\nu})^2}{\sum_{\lambda,\mu} (I'_{\lambda\mu})^2}, \tag{4.3.15}$$

where

$$I'_{\lambda\mu} = \tilde{a}_\lambda \tilde{a}_\mu \sum_{i,\rho} \psi_\lambda(i)\psi_\mu(i) a_\rho^2 \psi_\rho^2(i),$$

$$I'_{\lambda\mu\eta\nu} = \tilde{a}_\lambda \tilde{a}_\mu \tilde{a}_\eta \tilde{a}_\nu \sum_i \psi_\lambda(i)\psi_\mu(i)\psi_\eta(i)\psi_\nu(i),$$

with $\tilde{a}_\lambda = (\epsilon_\lambda - \xi)\Theta(\epsilon_\lambda - \xi) V_\lambda$. We have computed the ratio R using two sets of eigenfunctions for two samples of different size: 10^3 and 12^3 (Figure 13). From inspection of the dependence $R(\xi)$, we conclude that it shows a rather weak singularity (if any) at the mobility edge ($E_c \approx 4.45$) and falls rapidly in the localized region ($E > E_c$), so that

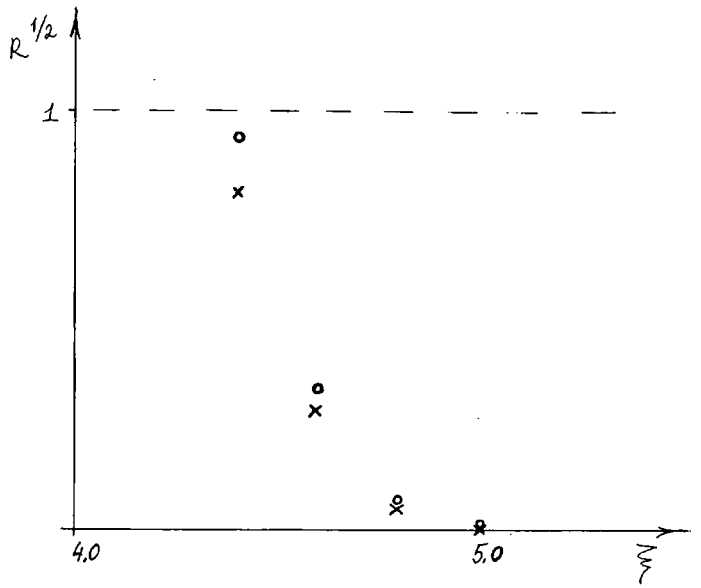

Figure 13 The ratio $R^{1/2}(\xi)$, (4.3.15), describing the influence of four-spin interactions.

four-spin interactions are relatively small and can hardly change the qualitative scenario described above.

4.3.2 Superparamagnet hierarchy and discrete RG transformation In the preceding section we showed that at temperature $T_1 = T_0(1-\tau_1)$ (with τ_1 given by (4.3.9)) the spin glass of "superspins" is near its freezing point. The effective coordination number $Z_1 \gg 1$ for this spin glass is given by (4.3.11). We can therefore repeat the above arguments and get a new set of spin variables (super-superspins) that constitute the new spin glass that is near its freezing point at T_2. To estimate T_2, we note that the effective temperature $T/I(\zeta(\tau))$ of the first-level spin glass of superspins varies on the scale of $|\tau| = (T_0 - T)/T_0 \sim \tau_1$. Therefore the effective reduced temperature of the second-level spin glass is $\tau^{(1)} = (\tau+\tau_1)/\tau_1$, and its critical value is $-\tau^{(1)} = \tau_1^{(1)} \sim Z_1^{-p}$ (cf. (4.3.9)), which corresponds to the following physical reduced temperature τ:

$$\left.\begin{aligned} -\tau = \tau_2 = \tau_1(1+\tau_1^{(1)}), \quad T = T_2 = T_1(1-\tau_1^{(1)}\tau_1) \\ Z_2 \sim Z_1^q. \end{aligned}\right\} \tag{4.3.16}$$

The properties of the RG transformation depend on the relationship between q and 1. First we consider the more interesting and more likely case of $q > 1$. Then the estimates (4.3.16) can be generalized easily for the case of the N-level hierarchy:

$$\frac{T_N - T_{N+1}}{T_N} = \tau_1 \tau_1^{(1)} \ldots \tau_1^{(N)}, \tag{4.3.17}$$

where

$$\tau_1^{(N)} \sim Z_N^{-p}, \quad Z_N \sim Z_{N-1}^q.$$

At temperature T_N superspins of the Nth level of the hierarchy become strongly correlated and "new" superspins controlling these "old' superspins appear. In other words, in the temperature range $T_N \lesssim T \lesssim T_{N-1}$ the system behaves as a superparamagnet with its spin being the superspins of the Nth level. Note that the crossover temperatures T_N can be defined only approximately, with inaccuracy $\tau_0^{(N)} \sim Z_N^{-2/3}$, but the difference $T_{N+1} - T_N \sim \tau_1^{(N)} \sim Z_N^{-p}$ is always larger than this inaccuracy.

The sequence of crossover points T_N converges rapidly to some temperature T_f at which an infinite hierarchy of localized modes appears. It is tempting to identify T_f with the transition temperature — indeed, we prove this below, showing that thermodynamic quantities (specifically the nonlinear susceptibility) have singularities at T_f. This scenario for the phase transition is an unexpected alternative to the usual one [14]. The latter implies condensation into one delocalized mode, while the alternative described above combines the ideology of the renormalization group with the general concept of hierarchicity in glasses that is so popular at present. However, the usual concept of a hierarchy based on the SK model implies (Section 2 and [17]) that at lower temperatures the hierarchy grows downwards ("ancestors" split into "descendants"), whereas in the scenario described above the hierarchy grows upwards, with new levels appearing on the tops of others.

To study the critical behaviour of physical properties, it is convenient to employ, as usual, the renormalization-group technique. However, the structure of the renormalization group in this case is very unusual,

so we shall discuss it in detail. First of all, the RG transformations are not continuous but discrete, since they transform one level of hierarchy into another. We note that in this respect this RG transformation resembles the phenomenological theory [18] of glass dynamics. Discrete sequences appear naturally in our scenario. For instance, we can define the sequence $\{T_N\}$ of temperatures T_N at which the Nth level of superspins appears or the sequence $\{T_N^*\}$ of temperatures T_N^* at which superspins of the Nth level become correlated. Estimation of T^* shows that

$$(T_N^* - T_N) \approx \tfrac{1}{2}(T_{N-1} - T_N), \tag{4.3.18}$$

(e.g. $T_0^* - T_0 \approx \frac{1}{2}T_0$, $T_1^* - T_1 \approx \frac{1}{2}\tau_1$). The critical behaviour of any observable $\mathscr{O}$ ($\mathscr{O}_N = \mathscr{O}(T_N)$) can be obtained from its transformation properties under RG transformation: $\mathscr{O}_N \to \mathscr{O}_{N+1} = \mathscr{T}(\mathscr{O}_N)$. However, these transformation properties can be different for observables for the temperature sequences $\{T_N\}$ and $\{T_N^*\}$ (and certainly for any other temperature sequence). In the absence of a continuous RG, there is no reason to expect that these RG transformations coincide. Therefore the critical behaviour can be more complicated than the usual scaling power law. Indeed, we show below that the nonlinear susceptibility χ_3 can be characterized by a continuous set of critical exponents in the interval (γ_-, γ_+), with each γ corresponding to some choice of the sequence $\{T_N'\}$. A similar (and presumably related) phenomenon has recently been discussed in a study [19] of multifractal objects.

To study critical behaviour, it is more convenient to rewrite (4.3.17) and (4.3.18) as

$$\left.\begin{aligned} \ln Z_N &\approx q^N \ln Z, \\ -\ln \frac{T_N - T_f}{T_f} &= \frac{p}{q-1}(q^{N+1} - 1) \ln Z, \\ -\ln \frac{T_N^* - T_f}{T_f} &= \frac{p}{q-1}(q^N - 1) \ln Z, \end{aligned}\right\} \tag{4.3.19}$$

where we have used the fact that $\tau_1^{(N+1)} \ll \tau_1^{(N)}$.

4.3.3 Nonlinear susceptibility The simplest quantity that exhibits a critical singularity in spin glasses is the nonlinear susceptibility $\chi_3 = -\partial^3 M/\partial h^3$ (we recall that the susceptibility $\chi = \partial^3 M/\partial h$ has no divergence in spin glasses). It is usually described by the power law

$$\chi_3(T) \sim (T - T_f)^{-\gamma}, \tag{4.3.20}$$

where experimental values of γ usually lie in the range 2.5–3.8 (the accuracy of individual measurements is better, but different materials and experimental techniques result in a large data scatter), whereas mean-field theory predicts $\gamma = 1$ [1–3]. The discrete RG results in a more complex behaviour than the power law (4.3.20). To obtain this, we start from the exact expression for χ_3:

$$\chi_3 = \frac{1}{N}\frac{6}{n^2}\sum_{\lambda,\mu}\langle \boldsymbol{a}_\lambda \cdot \boldsymbol{a}_\mu \rangle^2. \tag{4.3.21}$$

This expression can be simplified in the region $T \geqslant T_1^*$, where correlations $\langle \boldsymbol{a}_\lambda \cdot \boldsymbol{a}_\mu \rangle$, $\lambda \neq \mu$, are weak:

$$\chi_3 = \frac{6}{n^2}\frac{1}{N}\sum_{\lambda}\langle a_\lambda^2 \rangle^2 = \frac{6}{n^2}\int \rho(\epsilon)\langle a^2(\epsilon)\rangle^2 \, \mathrm{d}\epsilon. \tag{4.3.22}$$

Equation (4.3.22) gives the usual MFA result $\chi_3 \sim 1/\tau$ in the paramagnetic region $\tau = T - T_0 \geqslant \tau_0$. In the superparamagnetic region $\tau_0 \leqslant -\tau \leqslant \tau_1$ one can obtain (with (4.2.10), (4.2.23), (4.3.1) and (4.3.22))

$$\chi_3 \sim \frac{1}{\tau_0}\left(\frac{|\tau|}{\tau_0}\right)^{2(\theta-1)/(\theta-2)} \tag{4.3.23}$$

in the Ising case and

$$\chi_3 \sim \tau_0^{(1-\theta)/(\theta-2)}\left(\frac{|\tau|}{\tau_0}\right)^{(2\theta-3)/(\theta-2)} \tag{4.3.24}$$

in the vector case; note that in both cases the main contribution to χ_3 comes from the largest-scale condensed modes with $\epsilon_\lambda - \epsilon_c \approx \epsilon_0 \zeta$. The results (4.3.23) as well as (4.3.24) hold at $T \geqslant T_1^*$, i.e. at $(\tau + \tau_1)/\tau_1 \geqslant 1$. At the lower boundary of that region we put $|\tau| \sim \tau_1$ (cf. (4.3.9) and (4.3.10)) and get

$$\chi_3(T_1^*) \sim \tau_0^{-\tilde{S}} \sim Z^S, \quad S = \tfrac{2}{3}\tilde{S}, \tag{4.3.25}$$

and $\tilde{S}$ is given by

$$\tilde{S}_\mathrm{I} = 1 + \frac{\theta - 1}{\phi_\mathrm{I}}, \quad \tilde{S}_\mathrm{V} = -1 + \frac{4}{\phi_\mathrm{V}}(2\theta - 3) \tag{4.3.26}$$

for the Ising and vector models respectively.

At lower temperatures we enter the region $(\tau+\tau_1)/\tau_1 \ll 1$, which is the critical region for a first-level superparamagnet. We then repeat all of the above derivations once more, and so on. This results in a recurrence relation: $\chi_3(T^*_{n+1}) \sim Z_N^S \chi_3(T^*_N)$, i.e.

$$\ln \chi_3(T^*_N) \approx \frac{s}{q-1}(q^N-1)\ln Z. \tag{4.3.27}$$

On comparing (4.3.27) with (4.3.19), we obtain

$$\chi_3(T^*_N) \sim (T^*_N - T_f)^{-\gamma^*}, \tag{4.3.28}$$

where $\gamma^* = s/p$ is the critical exponent defined on the sequence $\{T^*_N\}$. One can also consider RG transformations defined on the sequence $\{T_N\}$ (cf. (4.3.17)) and obtain

$$\chi_3(T_N) \sim (T_N - T_f)^{-\gamma}, \quad \gamma = \frac{s + \frac{2}{3}(q-1)}{pq}. \tag{4.3.29}$$

It can easily be shown that $\gamma < \gamma^*$. However, γ does not coincide with the lower bound γ_-; the latter corresponds to the sequence $\{T^{**}_N\}$ of temperatures T^{**}_N defined by

$$T^{**}_N - T_N \approx T_N - T_{N+1} \tag{4.3.30}$$

(cf. (4.3.18)). The corresponding exponent is

$$\gamma_- = \frac{s + p(q-1)}{pq} = \frac{\gamma_+ - 1}{q} + 1. \tag{4.3.31}$$

The upper bound γ_+ coincides with γ^* and is given by

$$\gamma_+ \equiv \gamma^* = \frac{s}{p} = \begin{cases} \left(1 + \dfrac{\theta-1}{\phi_I}\right)\left(1 - \dfrac{\theta-2}{2\phi_I}\right)^{-1} & \text{(Ising)}, \quad (4.3.32a) \\ \left(-1 + \dfrac{4(2\theta-3)}{\phi_V}\right)\left(2 - \dfrac{4(\theta-2)}{\phi_V}\right)^{-1} & \text{(vector)}. \quad (4.3.32b) \end{cases}$$

We recall that all of these results hold under the conditions:

$$\left.\begin{array}{lll} \theta > 2, & \frac{1}{2}(\theta-2) < \phi_I < \frac{2}{3}(\theta-1) & \text{(Ising)}, \\ \theta > 2, & \phi_V < 4(\theta-2) & \text{(vector)} \end{array}\right\}. \tag{4.3.33}$$

To get a feeling for reasonable values of the exponents $\gamma_\pm$, we calculate them for the Ising model at reasonable values of the exponents θ and ϕ_I:

$$\theta = \frac{9}{4}\begin{cases} \phi_I = \frac{3}{4}: & \gamma_+ = 3.2, \quad \gamma_- = 2.98, \\ \phi_I = \frac{4}{5}: & \gamma_+ = 3.04, \quad \gamma_- = 2.96. \end{cases} \tag{4.3.34}$$

We see that $\gamma_+ - \gamma_- \ll \gamma_+$, so the $\chi_3(T)$ behaviour is hardly discernible from a simple power law; moreover, the critical exponents are in good agreement with experimental and simulation data [20, 21]. The situation with vector models is less certain owing to the much stronger dependence of γ on θ and ϕ_V; moreover, the difference $\gamma_+ - \gamma_-$ is much larger in this case.

To conclude this section, we emphasize once again its main qualitative result: the spin-glass phase transition is (at least for some spin glasses) a new type of phase transition, with critical behaviour characterized by a continuous set of exponents.

4.4 Critical Dynamics

Critical slowing down is undoubtedly the most spectacular manifestation of the spin-glass transition. "Slowing down" means critical growth of the upper boundary s_0 of the relaxation spectrum $g(s)$ defined by

$$q(t) = \overline{\langle S_i(0) S_i(t) \rangle} = \int_0^\infty \mathrm{d}s \; g(s) \mathrm{e}^{-t/s} \tag{4.4.1}$$

where $q(t)$ is the relaxation function. This growth results in the critical divergence of the average relaxation time $t_{\mathrm{av}} = \int_0^\infty sg(s)\,\mathrm{d}s$ and correlation time $t_0 = \int_0^\infty s^2 g(s)\,\mathrm{d}s$, but the bulk of the $g(s)$ spectrum remains intact as $T \to T_f$ (see Section 1.3).

In this section we show that this qualitative picture can be deduced from the theory of critical hierarchy [22].

For simplicity, we consider only the simplest microscopic model of the dynamics, i.e. purely relaxational dynamics, defined by the Langevin equations

$$\dot{S}_i^\alpha = -\Gamma_0 \frac{\partial H}{\partial S_i^\alpha} + \eta_i^\alpha(t), \tag{4.4.2}$$

where $\eta_i^\alpha(t)$ is thermal white noise $\langle \eta_i^\alpha(t) \eta_j^\beta(t') \rangle = 2T\Gamma_0 \delta_{ij} \delta_{\alpha\beta} \delta(t - t')$. Equation (4.4.2) describes the dynamics of vector spins: its Ising analogue is Glauber dynamics:

$$\frac{\partial}{\partial t} p\{S_i\} = \gamma_0 \sum_j \{-p\{S_1 \ldots S_j \ldots\} e^{-h_j(t)/T} + p\{S_1 \ldots -S_j \ldots\} e^{h_j(t)/T}\}, \tag{4.4.3}$$

where $p\{S_i\}$ is the probability of a spin configuration $\{S_i\}$ and $h_j = \Sigma_k J_{jk} S_k(t)$ is the instantaneous local field.

The dynamics of superspins controlling higher levels of hierarchy is also described by (4.4.2) and (4.4.3) but the parameter Γ_0 is renormalized. Clearly, our goal is to derive recursion relations between Γ_N and Γ_{N+1}.

In the mean-field critical region $\tau_0 \leqslant (T - T_0)/T_0 \ll 1$ the long-time dynamics can be described by time-dependent TAP equations

$$\frac{\partial m_i}{\partial t} = -\Gamma_0 \frac{\partial F_{\mathrm{TAP}}}{\partial m_i} + \eta_i(t), \tag{4.4.4}$$

where $F_{\mathrm{TAP}}\{m_i\}$ is given by (4.1.3) (we neglect small corrections to Γ_0). We can then use an eigenfunction representation and eliminate the "fast" modes a_α in a manner similar to that used in statics (see the discussion after (4.1.6)). The resulting equations in terms of the slow modes alone are

$$\frac{\partial a_\lambda}{\partial t} = -\Gamma_0 \frac{\partial H\{a_\lambda\}}{\partial a_\lambda} + \eta_\lambda(t), \tag{4.4.5}$$

where $H\{a_\lambda\}$ is defined in (4.1.18) and $\eta_\lambda(t)$ is white noise with correlations (4.4.2). In the temperature region $\tau_0 \leqslant (T_0 - T)/T_0 \leqslant \tau_1$ one can neglect the σ_λ-dependent part of the total Hamiltonian (4.1.18) and use the mean-field approximation for the "even" part of the Hamiltonian (that is, H_0 defined in (4.2.6) and (4.2.18)). Then the set of equations (4.4.5) splits into independent equations:

$$\frac{\partial a_\lambda}{\partial t} = -\Gamma_0 \frac{\partial H_0^{(\lambda)}}{\partial a_\lambda} + \eta_\lambda(t), \tag{4.4.6}$$

$$H_0^{(\lambda)} = \frac{1}{2} a_\lambda^2[(\tau + B)^2 - \epsilon_\lambda] + \frac{1}{4} g (a_\lambda^2)^2 \sum_i \psi_\lambda^4(i),$$

where $g \sim 1$ for $n \geqslant 2$ and $g \sim |\tau|$ for the Ising case; we suppose that the amplitude absolute values a_λ^2 relax much faster than the "spins" $\sigma_\lambda = a_\lambda / a_\lambda$. To find the relaxation rate Γ_1 for vector spins σ_λ, we put the a_λ equal to their equilibrium values $a_{\lambda 0}$ (cf. (4.2.23)) and replace a_λ in (4.4.6) by $\sigma_\lambda a_{\lambda 0}$. This results in the expression:

$$\Gamma_1^{(\lambda)} = \frac{\Gamma_0}{a_{\lambda 0}^2} \approx \frac{\Gamma_0 \sum_i \psi_\lambda^4(i)}{\epsilon_1^\lambda - \xi_\lambda(\tau)}, \tag{4.4.7}$$

so individual values $\Gamma_1^{(\lambda)}$ of the relaxation rates are λ-dependent. Below we consider "typical largest-scale" modes only; that is, the modes with $\epsilon_\lambda - \xi(\tau) \approx \epsilon_0 \xi(\tau)$ and $\sum_i \psi_\lambda^4(i) \approx Z^{-2}(\epsilon/\epsilon_c - 1)^\theta$ (cf. (4.1.12)). Then, using the "equation of state" (4.2.24), we obtain

$$\Gamma_1(\tau) \approx \Gamma_0 \tau_0^{2\theta-1} |\tau|^{1-\theta}. \tag{4.4.8}$$

The characteristic "bare" relaxation rate Γ_1 of the first hierarchy level is given by $\Gamma_1(|\tau| \sim \tau_1) \equiv \Gamma_1$ (recall that the σ_λ interaction strength becomes of order unity at $-\tau \sim \tau_1$). Thus we obtain with (4.3.9) and (4.3.10)

$$\Gamma_1 \approx \Gamma_0 \tau_0^{\tilde{y}_V} \approx \Gamma_0 Z^{-y_V}, \quad y_V = \frac{2}{3}\tilde{y}_V,$$
$$\tilde{y}_V = 1 + \frac{4(\theta-2)(\theta-1)}{\phi_V}. \tag{4.4.9}$$

This result can obviously be generalized to higher hierarchy levels:

$$\Gamma_{N+1} = \Gamma_N Z_N^{-y_V}. \tag{4.4.10}$$

At a given temperature T near T_f the slowest modes are those of the highest existing hierarchy level. In particular, at $T = T_N^*$ the "maximum"* relaxation time t_m can be estimated as $t_m \sim \Gamma_N^{-1}$. Then, similarly to the derivation of (4.3.28), we obtain

$$t_m(T_N^*) \sim (T_N^* - T_f)^{-z\nu}, \quad z\nu = \frac{y_V}{p_V}. \tag{4.4.11}$$

Obviously, we could also obtain a somewhat different value of $z\nu$, using another temperature sequence instead of $\{T_N^*\}$ (cf. Sections 4.3.2 and 4.3.3), but we shall not dwell upon this point. Another, even more interesting problem concerns the form of the function $q(t)$ at $\Gamma_0^{-1} \ll t \ll t_m$, but we leave this for the future.

We now turn to the case of an Ising spin glass. Here relaxation of

*In fact, there is no maximum relaxation time at $T \approx T_\rho$, as the spectrum $g(s)$ is unbounded from above (see Section 5); thus t_m is taken as the characteristic time such that $g(s)$ decreases rapidly at $s \gg t_m$.

"spins" $\sigma_\lambda = a_\lambda/a_{\lambda 0}$ can only proceed through thermally activated motion across the region $|a_\lambda| \ll a_{\lambda 0}$. The free-energy barrier ΔF_λ can be estimated using (4.4.6) as

$$\Delta F_\lambda \approx a_{\lambda 0}^2(\epsilon_\lambda - \xi) \approx \frac{(\epsilon_\lambda - \xi)^2}{|\tau|} \mathrm{V}_\lambda \tag{4.4.12}$$

(cf. (4.2.10)). Then the rate of $\sigma_\lambda \to -\sigma_\lambda$ flips can be obtained from the usual Kramers formula applied to the potential $H_0^{(\lambda)}$:

$$\begin{aligned} \Gamma_1^{(\lambda)} &\approx \left(\frac{\partial^2 H_0^{(\lambda)}}{\partial a_\lambda^2}\right)_{a_\lambda = a_{\lambda 0}} \exp\,(-\Delta F_\lambda) \\ &\approx (\epsilon_\lambda - \xi) \exp\left[-\frac{(\epsilon_\lambda - \xi)^2}{|\tau|} \mathrm{V}_\lambda\right]. \end{aligned} \tag{4.4.13}$$

We then obtain for "typical" modes with $\epsilon_\lambda - \xi \approx \epsilon_0 \zeta(\tau)$

$$\Gamma_1(\tau) \sim \Gamma_0 \epsilon_0 \zeta(\tau) \exp\left\{-\frac{\tau_0}{|\tau|}[\zeta(\tau)]^{2-\theta}\right\},$$

and, at $|\tau| \sim \tau_1$,

$$\begin{aligned} \Gamma_1 &\approx \Gamma_0 \tau_0^2 \left(\frac{\tau_1}{\tau_0}\right)^{2/(2-\theta)} \exp\left(-\frac{\tau_1}{\tau_0}\right) \\ &\approx \Gamma_0 Z^{-y_1} \exp\,(-Z^\omega), \end{aligned} \tag{4.4.14}$$

where

$$y_1 = \frac{2}{3}\left(2 + \frac{1}{\phi_1}\right), \quad \omega = \frac{\theta - 2}{3\phi_1}.$$

Recurrence relations (similar to that employed above) can be derived from (4.4.14) and lead to the following estimate for the critical behaviour of the "maximum" relaxation time t_m:

$$\ln t_m(T) \sim \frac{y_1}{p_1}\left|\ln\frac{T - T_f}{T_f}\right| + \frac{\omega(q_1 - 1)}{p_1}\frac{T_f}{T - T_f}. \tag{4.4.15}$$

This estimate is rather rough as it uses "characteristic" values of individual relaxation rates $\Gamma_1^{(\lambda)}$, with all fluctuations being neglected. Nevertheless, it seems to be instructive, as does (4.4.11), as they give the

only first-principles derivation of the critical slowing down in three-dimensional spin glasses. It is interesting that in the Ising case the $t_m(T)$ behaviour appears to be a combination of the usual power law $t_m \sim (T-T_f)^{-z\nu}$ and a generalized Vogel-Fulcher law $\ln t_m \sim (T-T_f)^{-\beta}$.

Note finally that the critical slowing down is due to the growth as $T \to T_f$ of new higher hierarchy levels, with the relaxation times of intermediate levels being slightly affected.

4.5 Vector Spin Glass with Weak Anisotropy

In previous sections we have considered the phase transition in basic spin-glass models: Ising and vector. However, the spin glasses that are most frequently encountered in experiments should be described neither by Ising nor by isotropic vector models but rather by a vector model with weak anisotropy.

There are a few physical mechanisms that are responsible for a weak anisotropy in vector magnetics. The first mechanism is spin–orbital interaction, which results in weak anisotropy of any real magnet. The second is coherent anisotropy, which is more important for some spin glasses (for example the easy-axis anisotropy that results in Ising behaviour or cubic anisotropy). The third mechanism (in some spin glasses this is responsible for the main part of the anisotropy) is Dzyaloshinsky–Moria interaction [23] or dipolar interaction, which both result in a random anisotropy term in the spin Hamiltonian:

$$H_A = \sum_{i,k} G_{ik}^{\alpha\beta} S_i^\alpha S_k^\beta, \tag{4.5.1}$$

where $G_{ik}^{\alpha\beta}$ is the anisotropic random interaction matrix:

$$\overline{G_{ik}^{\alpha\beta} G_{lm}^{\gamma\delta}} = G_0^2(\delta_{il}\delta_{km} + \delta_{im}\delta_{kl})(\delta_{\alpha\gamma}\delta_{\beta\delta} + \delta_{\alpha\delta}\delta_{\beta\gamma}). \tag{4.5.2}$$

The anisotropy parameter G_0 is usually relatively small, $G_0 \ll J$, but it always becomes relevant close to the freezing point. Indeed, the contribution of H_A to the Hamiltonian of the slow modes a_λ is

$$\begin{aligned} H_A\{a_\lambda\} &= \sum_{\lambda,\mu} \sigma_\lambda^\alpha \sigma_\mu^\beta |a_\lambda|\,|a_\mu| \sum_{i,k} G_{ik}^{\alpha\beta} \psi_\lambda(i)\psi_\mu(k) \\ &= \sum_{\lambda,\mu} \sigma_\lambda^\alpha \sigma_\mu^\beta \tilde{G}_{\lambda\mu}^{\alpha\beta}. \end{aligned} \tag{4.5.3}$$

The strength $\tilde{G}$ of the renormalized anisotropic interaction $\tilde{G}^{\alpha\beta}_{\lambda\mu}$ of condensed modes is estimated using (4.5.2):

$$\begin{aligned}\tilde{G}^2 &\sim G_0^2 a_\lambda^2 a_\mu^2 \sum_i \psi_\lambda^2(i)\psi_\mu^2(i) \\ &\sim G_0^2(\epsilon_\lambda - \xi)(\epsilon_\mu - \xi)\ \min\ (\nu_\lambda,\ \nu_\mu).\end{aligned} \tag{4.5.4}$$

Using (4.5.4) for "typical" condensed modes at $-\tau \approx \tau_1$, one obtains

$$G_1 = \tilde{G}(\tau_1) \sim G_0\left(\frac{\tau_1}{\tau_0}\right)^{1/2} \approx G_0 Z^{(1-\bar{p}_\nu)/3} \tag{4.5.5}$$

(cf. (4.3.10)). Thus the anisotropy strength parameter does grow under RG transformation. Then the RG machinery leads to the following temperature behaviour of the effective anisotropy strength:

$$G_N \equiv G(T = T_N^*) \sim G_0\left(\frac{T_N^* - T_f}{T_f}\right)^{-(1-\bar{p}_\nu)/2\bar{p}_\nu}. \tag{4.5.6}$$

Therefore in the vicinity of T_f the anisotropic part of the interaction appears to be of order unity, which leads to a Heisenberg–Ising crossover in the critical behaviour. Indeed, the eigenfunctions $\psi_\lambda^\alpha(i)$ of the total interaction matrix $J_{ij}^{(t)} = J_{ij}\delta_{\alpha\beta} + G_{ij}^{\alpha\beta}$ are nondegenerate and possess a nontrivial vector structure, whereas the amplitudes $a_\lambda \equiv \Sigma_i \tilde{m}_i^\alpha \psi_\lambda^\alpha(i)$ are scalars. Therefore the Hamiltonian governing the behaviour of $\sigma_\lambda = a_\lambda/|a_\lambda|$ is of the Ising type; at $G \gtrsim 1$ any possible correlations in this Hamiltonian are weak and can be neglected. It should be noted, to avoid confusion, that the Ising critical behaviour predicted in the random-anisotropy model does not mean any easy-axis anisotropy of the magnetic properties.

The same results were obtained in reference [24] in the framework of replica perturbation theory.

4.6 *Abelian Gauge Glass*

Granular superconductors in a strong external magnetic field are described by the Hamiltonian (Section 7)

$$H = \frac{1}{4}\sum_{i,j}[J_{ij}S_i^* S_j + \text{h.c.}], \tag{4.6.1}$$

where $S_i = e^{i\phi_i}$ and J_{ij} is a random Hamiltonian matrix described by the correlators

$$\overline{J_{ij}^2} = 0, \quad \overline{|J_{ij}|^2} = K(r_i - r_j). \tag{4.6.2}$$

At first sight, this model is a slight modification of an XY spin glass, but, as we show in this section, this modification is very important: it belongs to a different universality class. (In particular, it is possible that in one model the transition is absent and in the other it is present.) First, a historical remark is in order: the model (4.6.1), (4.6.2) was introduced some time ago [25, 26] and was studied phenomenologically in the framework of the gauge-invariant theory of the low-temperature spin-glass state [27, 28] (a brief review can be found in reference [29]).

As before, we start from the TAP Hamiltonian for the relevant modes (cf. (4.1.3)):

$$F_{\mathrm{TAP}}\{m_i\} = -\frac{1}{4}\sum_{i,j}(J_{ij}m_i^* m_j + \mathrm{h.c.}) - \frac{1}{8T}\sum_{i,j}|J_{ij}|^2(1-|m_i|^2) \times (1-|m_j|^2) + T\sum_i\left[|m_i|^2 + \frac{1}{4}|m_i|^4 + \frac{5}{36}|m_i|^6\right], \tag{4.6.3}$$

where the complex variables $m_i = \langle S_i \rangle_{\mathrm{fast}}$ describe the slow "magnetization" of each spin. We then expand m_i in terms of the eigenfunctions ψ_i of the matrix J_{ij}:

$$m_i = \sum_\lambda a_\lambda \psi_\lambda(i). \tag{4.6.4}$$

The difference between abelian gauge glass (AGG) and a spin glass now becomes evident: in the former the eigenfunctions are complex, whereas in the latter they can be chosen to be real. This difference has important consequences for the condensation process, namely in an XY spin glass condensation of a single mode is almost impossible (Section 4.2.3), whereas in an AGG condensation of a single mode is not hampered — just like the condensation in an Ising spin glass. This should be expected because a condensed mode in an AGG leads to an isotropic state, in contrast with a single condensed mode in the XY model. Formally repeating the derivation of the effective Hamiltonian of the a_λ^2 variables, we find that the coefficient of the a_λ^4 term is proportional to τ (recall that it was of order unity for the XY model and proportional to τ in the Ising case). The resulting equations for amplitudes a_λ^2 and reduced boundary ζ are:

$$\left.\begin{aligned} a_\lambda^2 &\approx \frac{\epsilon_\lambda - \xi}{\tau}\,\theta(\epsilon_\lambda - \xi)\mathrm{V}_\lambda, \\ \tau^2/\tau_0^2 &\approx \zeta^{2-\theta}(\tau) \end{aligned}\right\}. \tag{4.6.5}$$

As we should expect, these equations are identical with (4.2.10) and (4.2.13) for an Ising spin glass. Thus, the RG transformation of an AGG more closely resembles the RG transformation of an Ising spin glass than that of an XY spin glass. However, the critical exponents of the eigenfunctions near the mobility edge may differ for real and Hermitian J_{ij}, so the critical behaviour of Ising spin glasses and AGGs is also probably different. Moreover, the possibility that only one of them is described by the critical hierarchy scenario cannot be excluded. We emphasize once again that to clarify this point, a very accurate study of the exponent $2-\theta$ for real and Hermitian J_{ij} is necessary.

4.7 Concluding Remarks

We have described an analytic approach to the problem of the spin-glass phase transition in ordinary space. The heart of this approach is an explicit renormalization procedure that replaces the spins of the initial problem by superspins controlling a large number of initial spins. We have shown that for some spin glasses a completely new phase-transition scenario is possible (we call this a "critical hierarchy"), which cannot be described as macroscopic condensation into one (or a few) delocalized modes. Instead, a critical hierarchy can be described as a growth of the number of levels of controlling superspins, with this number diverging as $T \to T_f +$. In other words, the hierarchy pyramid is built upwards. This should be contrasted with the behaviour of the SK model below T_c, at which the number of hierarchy levels is already infinite and the hierarchy grows downwards with decreasing T (see Section 2).

From the other point of view, the "superspin" controlling the magnetization of a large number of initial spins can be regarded as a formal representation of the phenomenological theory of fractal clusters [30].

The discrete nature of the renormalization transformation is inevitable in this scenario and results in complicated critical behaviour of physical quantities (e.g. the nonlinear susceptibility), which presumably should be described using the concepts of multifractality [19].

The higher the level of controlling superspin, the slower is its relaxation. This simple statement leads to the critical slowing down of relaxation as $T \to T_f+$. At $T < T_f$ ergodicity is absent [31] and spin glasses display various ageing phenomena (Section 3). Indeed, at $\epsilon = (T_f - T)/T_f > 0$ the effective temperature of high hierarchy levels ($N > N(\epsilon) \sim \ln \epsilon^{-1}$) is very low, so that thermodynamic equilibrium is unattainable. Moreover, the higher the level, the stronger are non-equilibrium effects. This picture agrees qualitatively with experimental studies of ageing, which show the absence of an effective temperature describing the effects of ageing in spin glasses at $T < T_f$ (cf. [32]).

We find that all spin glasses belong to one of three universality classes: (i) Ising spin glasses; (ii) vector spin glasses, with the XY and Heisenberg models being in the same class; (iii) XY spin glasses with Hermitian interaction matrix J_{ij}. We cannot obtain reliable estimates of the critical exponents in these models since they depend (Sections 4.3.3 and 4.4) on the localization exponents θ and ϕ, which can be estimated only roughly for real matrices J_{ij} and are completely unknown for Hermitian ones. Moreover, we cannot prove unambiguously that the critical hierarchy scenario is realized in any of these models. To do this, more reliable results in the localization theory are necessary. Nevertheless, even the possibility of this scenario is very interesting, since other analytic microscopic approaches to real spin glasses have failed.

Direct numerical simulations of Ising spin glasses show [33] the existence of a genuine thermodynamic phase transition. The simulations of vector models are less convincing at present, but so far they point towards the absence of the transition [34]. (However, it should be remembered that all the models studied have nearest-neighbour interactions, and the possibility that these models and models with $Z \gg 1$ are in different universality classes always exists.) It would be very interesting to study experimentally spin glasses with large Z to fill the gap between the SK model and real spin glasses. Probably the rare-earth alloys $Y_{1-x}R_x$ (R = Er, Dy, Gd) are very well suited for this purpose (see [35] and Section 6.5).

Appendix to Section 4: Spectrum and Eigenfunctions of the Matrix J_{ij}

We describe properties of eigenfunctions and eigenvalues of the random matrices J_{ij} that we use in Section 4. We recall the definition of

the matrices studied. The elements of these matrices are random Gaussian variables described by correlators

$$\left.\begin{aligned} \overline{J_{ij}} = 0, \quad \overline{J_{ij}^2} = K(r_i - r_j), \quad \int K(r)\, \mathrm{d}^3 r = 1 \\ \int r^2 K(r)\, \mathrm{d}^3 r = \frac{6}{\kappa^2} \gg 1, \end{aligned}\right\} \tag{4.A.1}$$

and correlations between different matrix elements are absent.

In the infinite-range limit $Z \sim \kappa^{-3} \to \infty$ all eigenfunctions $\psi_\lambda(i)$ are delocalized and the density of states ρ obeys a semicircular law $\rho(E) = (2\pi)^{-1}\,(4 - E^2)^{1/2}$; all values of an eigenfunction $\psi_\lambda(i)$ are random Gaussian variables (see e.g. [8–10] and below). Different eigenfunctions are not correlated, but obey the orthonormalization condition

$$\sum_i \psi_\lambda(i)\psi_{\lambda'}(i) = \delta_{\lambda\lambda'}. \tag{4.A.2}$$

At finite $Z \gg 1$ the density of states is nonzero outside the interval $(-2, 2)$, but falls off rapidly at $|E_\lambda| > 2$. In the region where the density of states is small all states are localized, whereas deep inside the interval they remain delocalized and their properties differ slightly from the properties of eigenfunctions in the infinite-range limit. The localized and delocalized states are separated by the mobility edge $E_c = 2 + O(Z^{-1})$. The behaviour of the eigenfunctions close to the mobility edge is studied in the theory of Anderson localization [36, 37]. Unfortunately, this theory is still far from being complete: purely analytic results can be obtained only far from the mobility edge.

We start our discussion with these results that help us to estimate the width of the *"terra incognita"* near E_c and then employ the scaling hypothesis to describe the behaviour of the eigenfunctions near E_c. The scaling hypothesis implies that the behaviour in the vicinity of the transition point is universal, so to study it we can use the results of numerical simulations [13, 38] that we performed on a system with nearest-neighbour interaction J_{ij}.

To obtain analytic results, we use the replica trick, which allows us to represent the problem as a field theory. For instance, the density of states $\rho(E)$ is expressed as a field-correlation function [39]:

$$\left.\begin{aligned} \rho(E) &= \frac{-i}{\pi} \lim_{l\to 0} \int \mathscr{D}\varphi\ \varphi_i^{(1)}\varphi_i^{(2)} e^{iS\{\varphi\}}, \\ S\{\varphi\} &= \frac{1}{2}\sum_{i,\alpha}(\varphi_i^{\alpha})^2 + \frac{1}{4}\sum_{i,j,\alpha,\beta} K(r_i - r_j)\varphi_i^{\alpha}\varphi_i^{\beta}\varphi_j^{\alpha}\varphi_j^{\beta}, \end{aligned}\right\} \tag{4.A.3}$$

where l is the number of replicas: $\alpha = 1, \ldots, l$, $l \to 0$. Introducing the auxiliary matrix field $Q^{\alpha\beta}$ and performing the Gaussian integral over the field φ_i, we get

$$\left.\begin{aligned} \rho(E) &= -\frac{1}{\pi}\,\mathrm{Im}\lim_{l\to 0} \int \mathscr{D}Q^{\alpha\beta}[(E+i\delta)\delta_{\alpha\beta} + Q^{\alpha\beta})^{-1} e^{S\{Q\}}, \\ S\{Q\} &= -\frac{1}{4}\sum_{i,j,\alpha,\beta} Q_i^{\alpha\beta} K^{-1}(r_i - r_j) Q_j^{\alpha\beta} \\ &\quad -\frac{1}{2}\,\mathrm{Tr}\,\ln\,[(E+i\delta)\delta_{\alpha\beta} + Q_i^{\alpha\beta}]. \end{aligned}\right\} \tag{4.A.4}$$

The condition $Z \gg 1$ ensures that $Q_i^{\alpha\beta}$ varies smoothly in space, so that it can be replaced by a continuum field $Q^{\alpha\beta}(r)$ and $K^{-1}(r_i - r_j)$ can be replaced by

$$\left(1 - \frac{\nabla^2}{\kappa^2}\right)\delta(r_i - r_j).$$

Deep inside the interval $(-2, 2)$ the spatial variation of $\boldsymbol{Q}$ can be neglected completely, then the integral in (4.A.4) can be performed using the saddlepoint approximation, i.e. replacing $Q^{\alpha\beta}$ by its value at the saddlepoint, which is determined from the equation

$$\boldsymbol{Q} = -[\boldsymbol{Q} + \mathbf{1}(E+i\delta)]^{-1}. \tag{4.A.5}$$

The matrix equation (4.A.5) has only the diagonal solution: $Q^{\alpha\beta} = \delta^{\alpha\beta}Q_0$, with

$$Q_0 = \begin{cases} -\frac{1}{2}E + i(1 - \frac{1}{2}E^2)^{1/2} & (|E| \leqslant 2), \\ -\frac{1}{2}E + \mathrm{sgn}\,(E)\,(\frac{1}{4}E^2 - 1)^{1/2} & (|E| \geqslant 2). \end{cases} \tag{4.A.6}$$

Substituting (4.A.6) into (4.A.4), we get as a result the semicircular law for the density of states, which should be anticipated since so far we have taken into account only the terms of leading order in Z^{-1}. We now study the fluctuations of the matrix $\boldsymbol{Q}$ that develop on the background

of the solution (4.A.6): $\boldsymbol{Q} = Q_0\mathbf{1} + \tilde{\boldsymbol{Q}}$. These fluctuations are small so that in the action we need retain only terms of leading order in $\tilde{\boldsymbol{Q}}$ and get

$$S = \mathrm{Tr}\int \left\{\tilde{\boldsymbol{Q}}\left[\mathrm{i}(-\epsilon)^{1/2} - \frac{1}{2\kappa^2}\nabla^2\right]\tilde{\boldsymbol{Q}} + \frac{1}{6}\tilde{\boldsymbol{Q}}^3\right\} \mathrm{d}^3x, \quad (4.A.7)$$

where $\epsilon = |E| - 2$. The first correction to the correlation function of the fluctuations $G = \langle \tilde{\boldsymbol{Q}}\tilde{\boldsymbol{Q}} \rangle$ arises at the second order in the perturbation theory in $\mathrm{Tr}\,\tilde{\boldsymbol{Q}}^3$:

$$\delta G = G(\delta\Sigma)G, \quad \delta\Sigma = \frac{\kappa^3}{2\pi}\mathrm{e}^{\mathrm{i}\pi/4}(-4\epsilon)^{-1/3}. \quad (4.A.8)$$

Comparing (4.A.8) and the bare correlation function, we conclude that the corrections become important at

$$-\epsilon \lesssim \epsilon_0 = \frac{\kappa^4}{(4\pi)^{4/3}} \approx Z^{-4/3}. \quad (4.A.9)$$

A similar estimate [3] of the corrections to the density–density correlation function shows that they also become important in the region (4.A.9), so we conclude that $-\epsilon_0$ is the approximate boundary of the scaling region and the ordinary delocalized states. We now get an analogous estimate of the boundary between the scaling region and strongly localized states.

In the region $|E| > 2$ the density of states is zero at all orders of perturbation theory. To seek for exponentially small effects, we should take into account nontrivial saddlepoints of the action (4.A.7) [40]. The saddlepoint solution $\tilde{\boldsymbol{Q}}(\boldsymbol{r})$ can be parameterized by the ansatz $Q^{\alpha\beta}(\boldsymbol{r}) = -q(\boldsymbol{r})e^{\alpha}e^{\beta}$, where e^{α} is an arbitrary unit vector in replica space; therefore the saddlepoint equation for the function $q(\boldsymbol{r})$ becomes

$$\frac{1}{2\kappa^2}\nabla^2 q - \epsilon^{1/2}q + \frac{1}{2}q^2 = 0. \quad (4.A.10)$$

As was shown in [41], (4.A.10) has a nontrivial solution with finite action S_0. To find S_0, we rescale the variables and the function $q(\boldsymbol{r})$:

$$\left.\begin{aligned} q(\boldsymbol{r}) &= \epsilon^{1/2}f(\kappa\epsilon^{3/4}\boldsymbol{r}), \\ S_0 &= \frac{1}{3}\kappa^{-3}\epsilon^{3/4}\pi\int_0^{\infty} f^3(y)y^2\,\mathrm{d}y = c_1\kappa^{-3}\epsilon^{3/4}, \end{aligned}\right\} \quad (4.A.11)$$

where $f(y)$ obeys the dimensionless equation

$$f'' - \frac{2}{y} f' + 2f + f^2 = 0, \tag{4.A.12}$$

and the numerical constant c_1 can be obtained by numerical solution of (4.A.12). Therefore the density of states at $|E| > 2$ is given with exponential accuracy by

$$\rho(E) \sim \exp\left[-a_1(\epsilon/\epsilon_0)^{3/4}\right]. \tag{4.A.13}$$

From (4.A.13), we can see that the saddlepoint approximation is justified if $\epsilon/\epsilon_0 \gg 1$, so that the boundary between the scaling region and the localized states is also ϵ_0; thus the scaling region has a width ϵ_0 and is situated near $E_c \approx 2$. The density of states has no singularity at $E = E_c$ and varies smoothly in the scaling region, so we can use the semicircular law (which is correct at $2 - |E| \gg \epsilon_0$) to get an estimate in the scaling region:

$$\rho(E_c) \sim \epsilon_0 \sim Z^{-2/3}. \tag{A.4.14}$$

The spatial dimension of the localized states at $|E| - 2 \gg \epsilon_0$ can also be obtained using the saddlepoint approximation; it coincides with the spatial scale of the function $q(r)$, (4.A.11),

$$l(\epsilon) \sim \kappa^{-1}\epsilon^{-1/4} \quad (\epsilon_0 \ll \epsilon \ll 1). \tag{4.A.15}$$

To quantitatively characterize the size of the localized states, it is convenient to study the inverse participation ratio:

$$V_\lambda = \left[\frac{1}{3}\sum_i \psi_\lambda^4(i)\right]^{-1} = c_3(\kappa^3\epsilon^{3/4})^{-1}. \tag{4.A.16}$$

In the theory of spin glasses we also meet a slightly different quantity

$$\tilde{V}_\lambda = \left[\frac{1}{15}\sum_i \psi_\lambda^6(i)\right]^{-1/2} = \tilde{c}_3(\kappa^3\epsilon^{3/4})^{-1}, \tag{4.A.17}$$

which also describes the size of the localized states. In the region $|E| - 2 \gg \epsilon_0$ the saddlepoint approximation allows us to obtain the coefficients $\tilde{c}_3$ and c_3. In the framework of this approximation V_λ and $\tilde{V}_\lambda$ can be expressed in terms of integrals of the solution $q(r)$:

$$V^{-1} = \frac{1}{\Omega^2}\int q^2(r)\, \mathrm{d}^3r, \quad \tilde{V}^{-2} = \frac{1}{\Omega^3}\int q^3(r)\, \mathrm{d}^3r, \tag{4.A.18}$$

where $\Omega = \int q(r)\, d^3r$ is the normalization integral. The integrals over powers of q in (4.A.18) can be expressed through one numerical constant c_1 entering (4.A.11). To do this, we define a function of two variables $q(r, \lambda) = \lambda^{3/2} q(r\lambda)$ and consider the action (cf. [42])

$$S(\lambda) = S\{q(r, \lambda)\} = S_1(\lambda) + S_2(\lambda) + S_3(\lambda), \qquad (4.A.19)$$

$$S_1(\lambda) = \frac{1}{2}\epsilon^{1/2} \int q^2(r)\, d^3r, \quad S_2 = \frac{1}{4\kappa^2} \int (\nabla q)^2 d^3r,$$

$$S_3 = -\frac{1}{6} \int q^3(r)\, d^3r.$$

The saddlepoint equation implies that $(\partial S/\partial\lambda)_{\lambda=1} = 0$, i.e.

$$2S_2 + \frac{3}{2} S_3 = 0. \qquad (4.A.20)$$

Multiplying (4.A.10) by $q(r)$ and integrating it, we get another useful relation:

$$S_1 + S_2 + \frac{3}{2} S_3 = 0. \qquad (4.A.21)$$

Finally, integrating (4.A.10), we get

$$\Omega = \frac{1}{6} S_1. \qquad (4.A.22)$$

The three equations (4.A.20)–(4.A.22) allow us to obtain the coefficients c_3 and $\tilde{c}_3$:

$$c_3 = \frac{3}{4} c_1, \quad \tilde{c}_3 = \frac{3}{2^{1/2}4} c_1. \qquad (4.A.23)$$

(The analogous relations in the two-dimensional case are $c_3^{(2D)} = c_1^{(2D)}$, $\tilde{c}_3^{(2D)} = (\frac{2}{3})^{1/2} c_1^{(2D)}$.

The ratio $\Sigma_i \psi_\lambda^6 / (\Sigma_i \psi_\lambda^4)^2$ that we meet in the discussion of spin glasses is constant in the localized region and equal to $\frac{10}{3}$ (in the delocalized region it is equal to $\frac{5}{3}$).

The properties of the scaling region ($E - |E_c| \sim \epsilon_0$) cannot be obtained analytically. Following [37], we supppose that all correlators in the vicinity of E_c obey power laws. At the present time there is no reliable analytical theory that proves or disproves this hypothesis, to

say nothing of the analytic theory that yields the exponents. Thus we must use numerical simulations to obtain the properties of the scaling region. This is also not a simple problem because all correlators in this region fluctuate strongly; therefore, in order to get reliable results, enormous statistics on a large number of samples must be gathered — and this is beyond our present technical capabilities.

All the difficulties that we meet in numerical simulations are very well illustrated by our study of the participation ratio [13]. First of all, we observed that the inverse of the average participation ratio is not the same as the average of inverse participation ratio, and the difference between them is enhanced near the mobility edge. Moreover, owing to large data scatter, the critical exponents cannot be determined reliably even for the large systems studied ($20^3 = 8 \times 10^3$ atoms).

Specifically, we studied the eigenfunctions of a random Gaussian matrix that has nonzero elements J_{ij} only for ij nearest neighbours. The scaling hypothesis implies that the behaviour of correlators near the mobility edge for this matrix is the same as their behaviour in the narrow scaling region for a matrix with large coordination number. We obtain eigenfunctions of this matrix starting from the localized region employing the Lantsosh method. We studied samples of sizes L^3, with $L = 8$–20; the number of small samples was about 1000, but the number of the largest ($L = 20$) was only 6.

Perhaps the most important quantity for a full theory of spin glasses is the exponent θ of the inverse participation ratio (IPR) (4.2.12); however, the direct determination of this exponent is plagued by the uncertainty in the determination of the critical point E_c (for instance, from the simulations [13] we can only conclude that $\theta = 2.0 \pm 0.3$, which is clearly insufficient for our purpose).

Naively, one would expect that the IPR exponent can be deduced from the exponent of the localization length ν ($l \sim (\epsilon - \epsilon_c)^{-\nu}$): $\theta = 3\nu$. This is certainly not the case, since ψ_i^2 can by no means be approximated by a smooth function, but rather displays a complicated fractal behaviour, so that θ is related to the length exponent ν by $\theta = d_f \nu$, where d_f is the fractal dimension of ψ_i^2. The observed fact that the exponent θ depends on the way of averaging presumably means that different eigenfunctions have slightly different fractal dimensions, as they should in a multifractal system. However, the ratio $\sum_i [\psi_\lambda(i)]^{2+2n} [\sum_i \psi_i^4(i)]^{-n}$ behaves very smoothly in the vicinity of the mobility edge (we checked this for $n = 2$ and 3, our result for $n = 2$ is

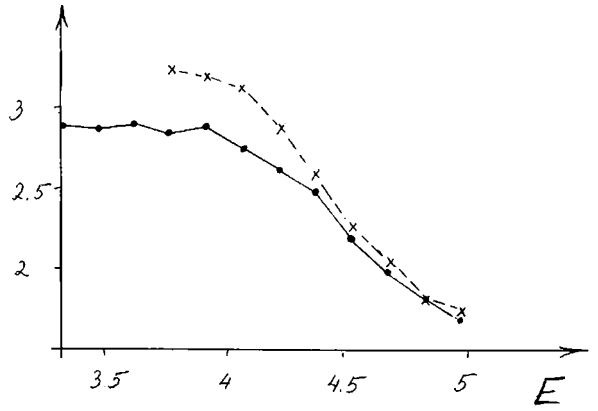

Figure 14 $\overline{\Sigma_i \psi_i^6/(\Sigma_i \psi_i^4)^2}$ versus energy E for three-dimensional systems of two sizes: $L = 20$ (6 samples, solid line), $L = 16$ (16 samples, dashed line).

plotted on Figure 14), which supports the idea that each eigenfunction is contained in a fractal volume and its amplitude ψ_i^2 fluctuates slightly within this volume. Since we know that there are no delocalized states in spaces of low dimension ($d \leqslant 2$), we conclude that $d_f > 2$. The analytic theory based on $2 + \epsilon$ expansion predicts $\nu = 1$, numerical simulations yield $\nu = 1.1 \pm 0.1$ (conductivity measurement [38]) and $\nu = 1.5 \pm 0.1$ (transfer-matrix technique [43]), so that one can hope that $\nu \geqslant 1$ more or less reliably. Thus, from these arguments, we conclude that $\theta > 2$.

To check this conclusion, we tested its consequences for a simplified model free energy

$$H = \sum_{\lambda} (\tau - \epsilon_\lambda) a_\lambda^2 + \frac{1}{2} \sum_{\lambda,\mu} a_\lambda^2 a_\mu^2 \sum_i \psi_\lambda^2(i) \psi_\mu^2(i) \qquad (4.A.24)$$

which describes Bose condensation in the disordered sample. Proceeding analogously to Section 4.2, we expect that for this model condensation results in the appearance of a molecular field

$$B_i = \sum_i \langle a_\lambda^2 \rangle \psi_\lambda^2(i), \qquad (4.A.25)$$

which can be replaced by its average at small τ: $B_i \approx B$. Then (for $\theta > 2$) at any τ the effective boundary $\xi = \tau + B$ is larger than ϵ_c, so that

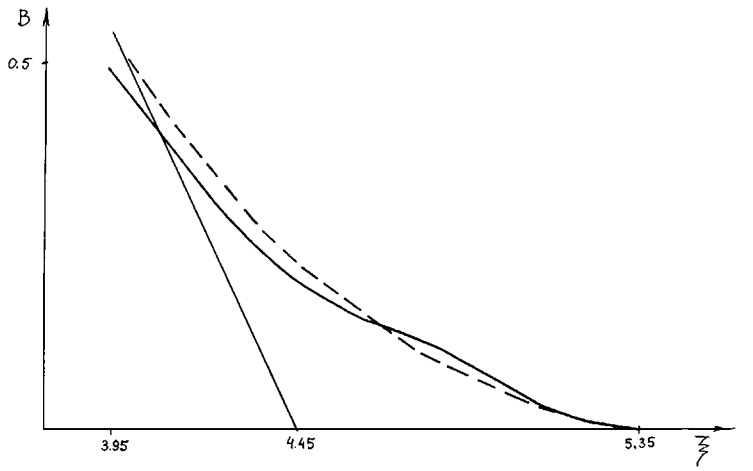

Figure 15 Average molecular field $\langle B_i \rangle$ (full line) and approximate solution B versus ξ for the simplified free energy (4.A.24).

condensation into the localized mode never occurs. This conclusion is based on two hypotheses: (i) fluctuations of B are small; (ii) $\theta > 2$. We have checked them both in numerical simulations using the exact eigenfunctions and eigenvalues of one sample of the maximum size (20^3). Our results are shown on Figure 15, where we plot the average $\langle B_i \rangle$ obtained from (4.A.25), with $\langle a_\lambda^2 \rangle$ corresponding to the minimum of the energy (4.A.24) obtained in the numerical solution and the result of the approximate procedure described in Section 4.2 that neglects the fluctuations of B_i. Surprisingly, these results are close despite the absence of a small parameter. To study condensation into the delocalized mode, we also plot $\tau - \epsilon_c$ (we choose $\epsilon_c = 4.45$, which is the upper boundary of possible ϵ_c), so that intersection of these lines corresponds to $\xi = \epsilon_c$, i.e. condensation into the delocalized mode in the infinite system. From Figure 15, we can see that this intersection happens at rather low τ and is presumably due to the finite size of the system studied.

Numerical simulations also help to study the properties of the interaction matrix $I_{\lambda\mu}$ of superspins (4.3.2), (4.3.3). We again use the exact eigenfunctions of the maximum available size (20^3) and the matrix $I'_{\lambda\mu}$ defined by:

$$I'_{\lambda\mu} = \tilde{a}_\lambda \tilde{a}_\mu \sum_{i,\rho} \psi_\lambda(i)\psi_\mu(i)\tilde{a}_\rho^2\psi_\rho^2(i), \qquad (4A.2.6)$$

with $\tilde{a}_\lambda = (\epsilon_\lambda - \xi)\Theta(\epsilon_\lambda - \xi)V_\lambda$. The matrix I' differs from I by a different definition of amplitudes $\tilde{a}_\lambda$ in which we neglect thermal fluctuations (which can be important for amplitudes $\tilde{a}_\rho^2$) and omit the factor $1/\tau$ that appears in the Ising case. As a result, the interaction (4.A.26) is weaker than the real interaction (4.3.2), (4.3.3), but we believe that its qualitative behaviour remains the same.

First of all, we consider the simplest problem: the behaviour of the effective interaction

$$\tilde{I}(\xi) = \frac{1}{\mathcal{N}} \sum_{\lambda,\mu} (I'_{\lambda\mu})^2, \qquad (4.A.27)$$

where $\mathcal{N}$ is the number of interacting "superspins". Our result is shown in Figure 16. We see that $I(\xi)$ grows very rapidly with decreasing ξ and becomes of order unity above the upper boundary of the mobility edge ($E_c = 4.5$). Since $\tilde{I}(\xi)$ is the lower boundary for the real effective interaction $I(\zeta)$, (4.3.4), we conclude that the effective freezing of superspins occurs before the mobility edge can be reached (if it can be reached at all).

The effective coordination number of the interaction (4.A.26) is a

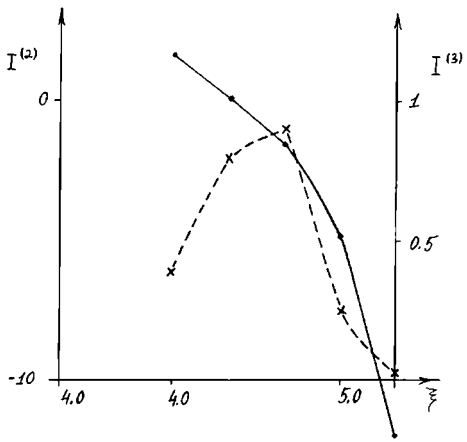

Figure 16 Constant of effective interaction $\tilde{I}(\xi)$ and correlator $I^{(3)}(\xi)$, (4.A.28).

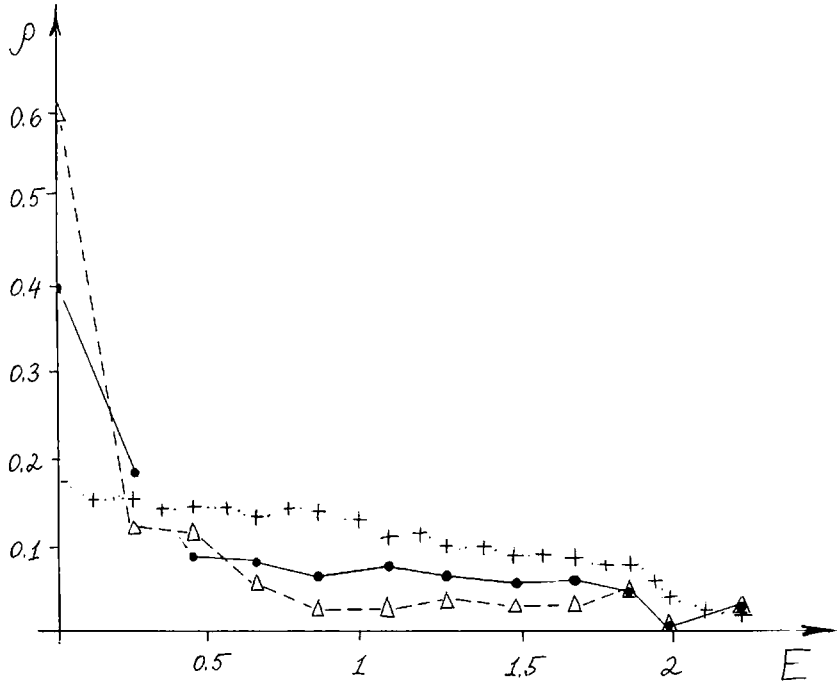

Figure 17 Density of states of the matrix $I'_{\lambda\mu}(\xi)$ for $\xi = 4.4$ (full line), $\xi = 4.7$ (dashed line) and nearest-neighbour interaction matrix J_{ij} (dotted line).

more difficult problem. Its density of states can easily be computed (Figure 17). It displays a rich behaviour, which resembles neither the semicircular law of the infinite-range J_{ij} nor the smooth density of states of the nearest-neighbour J_{ij} (which we also plot in Figure 5 for comparison). Presumably, this behaviour is due to correlations between elements of the matrix I (cf. Figure 2 in reference [44]). We check this hypothesis, computing the correlators

$$I^{(n)} = \frac{1}{\mathcal{N}} \frac{[\mathrm{Tr}\,(I')^n]}{[\tilde{I}(\xi)]^{n/2}}, \tag{4.A.28}$$

which measure the relative importance of higher-order correlations. We find (Figure 16) that all of these correlators are small at large $\xi > 5.0$ (far into the localized region), but they become of order unity

closer to the mobility edge, where, as we expect, freezing of superspins occurs and the density of states of I_{ij} displays a rich behaviour. Thus the peak in the density of states can be explained by the correlations (4.A.28). Then the sharp change of the behaviour of the density of states that happens at $\tilde{E} \approx 1.0$ (Figure 17) means that the effective coordination number of the matrix $I'_{\lambda\mu}$ is large. Since $I_{\lambda\mu}$ and $I'_{\lambda\mu}$ differ only by some factor, we believe that the coordination number of $I_{\lambda\mu}$ is also large in all reasonable regions of ξ. This in turn means that the effective coordination number increases at the next level of the hierarchy, even if we start from a nearest-neighbour interaction matrix. Naturally, we suppose that it also increases if it is initially large.

REFERENCES

[1] Thouless, D.J., Anderson, P.W. and Palmer, R.G. (1977) *Phil. Mag.* **35**, 593.
[2] Bray, A.J. and Moore, M.A. (1981) *J. Phys.* **C14**, 2629.
[3] Ioffe, L.B. and Feigel'man, M.V. (1985) *ZhETF* **89**, 654; (1985) *Sov. Phys. JETP* **62**, 376.
[4] Sompolinsky, H. (1981) *Phys. Rev.* **B23**, 1371.
[5] Dasgupta, C. and Somoplinsky, H. (1983) *Phys. Rev.* **B27**, 4511.
[6] Mezard, M. and Parisi, G. (1984) *J. Phys. (Paris) Lett.* **45**, L707.
[7] Feigel'man, M.V. and Ioffe, L.B. (1984) *J. Phys. (Paris) Lett.* **45**, L475.
[8] Metha, M.L. (1967) *Random Matrices and the Statistical Theory of Energy Levels*, p. 240. New York: Academic Press.
[9] Edwards, S.F. and Jones, R.C. (1976) *J. Phys.* **A9**, 1595.
[10] Ullah, N. (1964) *Nucl. Phys.* **58**, 65.
[11] Korenblit, I.Ya. and Shender, E.F. (1978) *Usp. Fiz. Nauk* **126**, 233.
[12] Ioffe, L.B. and Larkin, A.I. (1981) *ZhETF* **81**, 707.
[13] Ioffe, L.B. and Sagdeev, I.R. (1988) *Mod. Phys. Lett.* **B2**, 755.
[14] Anderson, P.W. (1970) *Mater. Res. Bull.* **5**, 549. Herte, J.A., Fleishman, L. and Anderson, P.W. (1979) *Phys. Rev. Lett.* **43**, 942. Hetz, J.A. (1983) *Phys. Rev. Lett.* **51**, 1880; NORDITA Preprint 1983/12.
[15] Gross, D.J. and Mezard, M. (1984) *Nucl. Phys.* **B240**, 431; Gardner, E. (1985) *Nucl. Phys.* **B297** [FS14], 74.
[16] Kirkpatrick, T.R. and Thirumalai, D. (1987) *Phys. Rev.* **B36**, 5388.
[17] Mezard, M. and Virasoro, M.A. (1985) *J. Phys. (Paris)* **46**, 1293. Rammal, R., Toulouse, G. and Virasoro, M.A. (1986) *Rev. Mod. Phys.* **58**, 765. Mezzard, M., Sourlas, N. and Toulouse, G. (1987) in *Proceedings of Colloquium on Glassy Dynamics*, p. 238. Lecture Notes in Physics, Vol. 275. Berlin: Springer-Verlag.
[18] Palmer, R.G., Stein, D.L., Abrahams, E. and Anderson, P.W. (1984) *Phys. Rev. Lett.* **53**, 958.
[19] Paladin, G. and Vulpiani, A. (1988) Anomalous scaling laws in multifractal objects. *Phys. Rep.* to be published.
[20] Binder, K. and Young, A.P. (1986) *Rev. Mod. Phys.* **58**, 801.
[21] (1987) *Proceedings of Heidelberg Colloquium on Glassy Dynamics*. Lecture Notes in Physics, Vol. 275. Berlin: Springer-Verlag.

[22] Feigel'man, M.V. and Ioffe, L.B. (1985) *J. Phys. (Paris) Lett.* **46**, L695.
[23] Levy, P.M. and Fert, A. (1981) *Phys. Rev.* **B23**, 4667.
[24] Bray, A.J. and Moore, M.A. (1982) *J. Phys.* **C15**, 3897.
[25] Fradkin, E., Huberman, B.A. and Shenker, S.H. (1978) *Phys. Rev.* **B18**, 4789.
[26] Hertz, J.A. (1978) *Phys. Rev.* **B18**, 4875.
[27] Dzyaloshinsky, I.E. and Volovik, B.E. (1978) *J. Phys. (Paris)* **39**, 693; (1978) *Sov. Phys. JETP* **48**, 555.
[28] Dzyaloshinsky, I.E. and Obukhov, S.P. (1982) *Sov. Phys. JETP* **56**, 456.
[29] Chowdhury, D. (1986) *Spin Glasses and Other Frustrated Systems*. Singapore: World Scientific.
[30] Confinentino, M. and Malozemoff, A.P. (1986) *Phys. Rev.* **B34**, 471. Confinentino, M.A. and de Oliveira, S.M. (1988) *Phys. Rev.* **B37**, 5877. Lundgren, L., Nordblad, P. and Svedlindh, P. (1986) *Phys. Rev.* **B34**, 8164.
[31] Palmo, R.G. (1977) in *Proceedings of Heidelberg Colloquium on Glassy Dynamics*, p. 275. Lecture Notes in Physics, Vol. 275. Berlin: Springer-Verlag.
[32] Refrigier, P., Vincent, E., Hammann, J. and Ocio, M. (1987) *J. Phys. (Paris)* **48**, 1533.
[33] Ogielski, A.T. (1985) *Phys. Rev.* B32, 7384.
[34] Morris, B.W., Colbourne, S.G., Moore, M.A., Bray, A.J. and Canisius, J. (1986) *J. Phys.* **C19**, 1157. Jain, S. and Young, A.P. (1986) *J. Phys.* **C19**, 3913. Olive, J.A., Young, A.P. and Sherrington, D. (1986) *Phys. Rev.* **B34**, 6341.
[35] Feigel'man, M.V. and Ioffe, L.B. (1987) *Phys. Rev. Lett.* **58**, 1157.
[36] Abrahams, E., Anderson, P.W., Licciardello, D.C. and Ramakrishnan, T.V. (1979) *Phys. Rev. Lett.* **42**, 673.
[37] Wegner, F. (1976) *Z. Phys.* **25**, 327; (1980) *ibid.* **36**, 209.
[38] Ioffe, L.B. and Sagdeev, I.R., *Mod. Phys. Lett.* B, to be published.
[39] Nitzan, A., Freed, K.H. and Cohen, M.H. (1977) *Phys. Rev.* **B15**, 4476.
[40] Cardy, J.L. (1978) *J. Phys.* **C11**, L321.
[41] Coleman, S., Glasser, V. and Martin, A. (1977) CERN Preprint NCN-2364.
[42] Kusmartzev, F.V. (1984) *Physica Scripta* **29**, 7; *ZhETF* **92**, 831.
[43] McKinnon, A. and Kramer, B. (1981) *Phys. Rev. Lett.* **47**, 1546; (1983) *Z. Phys.* **B53**, 1.
[44] Vinokur, V.M., Ioffe, L.B., Larkin, A.I. and Feigel'man, M.V. (1987) *ZhETF* **93**, 343.

5. NONEXPONENTIAL RELAXATION FAR ABOVE THE TRANSITION POINT

5.1 Disordered Ferromagnets

We begin with the well-known model of a three-dimensional disordered ferromagnet described by the Landau–Ginzburg Hamiltonian [1, 2]

$$H = \int d^3x [\tfrac{1}{2}(\nabla S)^2 + \tfrac{1}{2}\tau S^2 + \tfrac{1}{4}g(S^2)^2 + \tfrac{1}{2}V(x)S^2(x)] \quad (5.1.1)$$

with averaged transition temperature $T_c = 1$. Here $S(x)$ is an n-dimensional vector field and $V(x)$ is a random function with white-noise correlations:

$$\overline{V(x)\,V(x')} = \gamma\delta(x-x'). \tag{5.1.2}$$

The dynamics of the system is governed by a purely relaxational equation

$$\frac{\mathrm{d}}{\mathrm{d}t}S = -\frac{\delta H}{\delta S(x)} + \xi(x,\,t). \tag{5.1.3}$$

Here $\xi(x,\,t)$ is thermal white noise; the kinetic coefficient is taken equal to unity.

We consider systems with a small Ginzburg parameter Gi [1]:

$$Gi \approx g^2/2\pi \ll 1 \tag{5.1.4}$$

in the mean-field region $Gi \ll \tau \ll 1$. Our goal is to obtain the asymptotic behaviour of the (averaged) relaxation function $q(t) = \overline{\langle S(x,\,0)S(x,\,t)\rangle}$ at times t much larger than the characteristic timescale $t_0 = \tau^{-1}$. The weakness of thermal fluctuations makes it reasonable to use the representation of the $S(x)$ field in terms of normalized eigenfunctions $\psi_\lambda(x)$ of the operator $\hat{\mathrm{L}} = -\nabla^2 + \tau + V(x)$ determining the quadratic part of the Hamiltonian (5.1.1):

$$S(x) = \sum_\lambda a_\lambda\psi_\lambda(x), \quad \hat{\mathrm{L}}\psi_\lambda(x) = E_\lambda\psi_\lambda(x). \tag{5.1.5}$$

Since $\hat{\mathrm{L}}$ is random, it leads to the appearance of the well-known "Lifshitz tail" in the density of states $\rho(E)$ at $E_\lambda < \tau$, i.e. at positive $\epsilon = \tau - E$:

$$\rho(\epsilon) \sim \gamma^{-2}\epsilon^{3/2}\exp\left(-c_1\epsilon^{1/2}/\gamma\right), \quad \gamma^2 \ll \epsilon \ll \Lambda^2, \tag{5.1.6}$$

where Λ is an ultraviolet cut-off for the Hamiltonian (5.1.1) and $c_1 \approx 38$ (see e.g. [3]). Eigenfunctions $\psi_\lambda(x)$ in the region of the Lifshitz tail are localized with characteristic length

$$l(\epsilon) \sim \epsilon^{-1/2}. \tag{5.1.7}$$

Below we shall also need the "inverse participation ratio" (or "localization volume"):*

$$\mathscr{V}_\lambda = \left(\int \mathrm{d}^3x\,\psi_\lambda^4(x)\right)^{-1} = \frac{c_2}{\epsilon_\lambda^{3/2}} = \frac{c_1}{8\epsilon_\lambda^{3/2}} \approx \frac{5}{\epsilon_\lambda^{3/2}}. \tag{5.1.8}$$

* Note that we use a script letter $\mathscr{V}$ in Section 5.1 to avoid confusion with the potential V.

Note that the value of the ratio $c_1/c_2 = 8$ is exact; it can be obtained by the method employed in the Appendix to Section 4 for a similar problem.

We shall see now that it is these states in the "tail" that are responsible for the nonexponential behaviour of the relaxation function $q(t)$. Indeed, the "equation of motion" for the localized mode amplitude a_λ can be written as

$$\dot{a}_\lambda = (\epsilon_\lambda - \tau)a_\lambda + g\mathscr{V}_\lambda^{-1}a_\lambda a_\lambda^2 + \xi_\lambda(t), \tag{5.1.9}$$

where $\langle \xi_\lambda^\alpha(t)\xi_\mu^\beta(t')\rangle = 2\delta_{\lambda\mu}\delta^{\alpha\beta}\delta(t-t')$; we neglect the interaction of a_λ with other amplitudes a_μ.

The modes with $\epsilon > \tau$ are unstable in the linear approximation; a stable stationary solution of (5.1.9) yields

$$a_\lambda^2 = \frac{\epsilon_\lambda - \tau}{g}\mathscr{V}_\lambda. \tag{5.1.10}$$

Further analysis depends on the spin dimensionality n. We begin with the Ising ($n = 1$) case [4]. Then the modes with $\epsilon_\lambda > \tau$ can relax only as a result of a thermal activation process $a_\lambda \to -a_\lambda$. The free-energy barrier is

$$\Delta F_\lambda = \frac{(\epsilon_\lambda - \tau)^2}{4g}\mathscr{V}_\lambda = \frac{c_2}{4}\frac{(\epsilon_\lambda - \tau)^2}{g\epsilon_\lambda^{3/2}}. \tag{5.1.11}$$

Equations (5.1.9) and (5.1.11) are valid if $\Delta F_\lambda \gg 1$. These modes have very long relaxation times $t_\lambda \sim t_0 e^{\Delta F_\lambda}$ (here $t_0 = \tau^{-1}$) and determine the long-time asymptotic form of the $q(t)$ function:

$$q(t) = \sum_\lambda a_\lambda^2 e^{-t/t_\lambda} \sim \int d\epsilon\, \rho(\epsilon) \exp\left(-\frac{t}{t_0}e^{-\Delta F(\epsilon)}\right). \tag{5.1.12}$$

The main contribution to the integral (5.1.12) comes from the modes with $\Delta F(\epsilon) \approx \ln(t/t_0)$.

We obtain (using (5.1.6) and (5.1.11)) the following asymptotic form of $q(t)$ at $\ln t/t_0 \gg c_2\tau^{1/2}/4g$:

$$q(t) \underset{t\to\infty}{\sim} \left(\frac{t}{t_0}\right)^{-\alpha}, \quad \alpha = \frac{4c_1 g}{c_2\gamma} = \frac{32g}{\gamma} = \frac{g}{\tilde{\gamma}}. \tag{5.1.13}$$

This result is applicable when $q(t) \ll 1$, i.e. $\alpha \ln(t/t_0) \gg 1$. It is

interesting that a similar result holds for a two-dimensional version of the Hamiltonian (5.1.1) with $n = 1$:

$$q_{2D}^{(l)} \sim t^{-\alpha_2}, \quad \alpha_2 = \frac{4c_1^{(2)}g}{c_2^{(2)}\gamma} = \frac{8g}{\gamma}. \tag{5.1.13'}$$

Thus long-time relaxation in the disordered Ising model is governed by a power law even in the mean-field region $\tau \gg Gi$. The power-law exponent α is model-dependent; the most interesting case is $g \ll \tilde{\gamma}$, corresponding to $\alpha \ll 1$. That situation can be realized, for example, near the tricritical point of a disordered system (see e.g. [5]).

Let us now discuss the approximations used in the derivation of (5.1.13). Our most important assumption is that the mode–mode interaction can be neglected in (5.1.9). This assumption is justified by the fact that the interaction between well-localized modes is very weak because of the low probability of eigenfunction overlapping of these modes (corresponding corrections to $q(t)$ would be of order $q^2(t) \ll q(t)$). Furthermore, the fluctuation contribution made by the extended modes to the equation of motion for the localized modes can be neglected in the mean-field region.

An important problem is the crossover between the regime (5.1.13) and the ordinary short-term behaviour in the most interesting case $g \ll \tilde{\gamma}$, when there are two temperature regions: $Gi \ll \tau \ll Gi^{R}$ and $Gi^{R} \ll \tau \ll 1$. Here $Gi^{R} = (\gamma/c_1)^2 \approx \tilde{\gamma}^2$ denotes the "random" counterpart of the Ginzburg parameter. This parameter measures the range of τ where frozen disorder is relevant for thermodynamic properties.

In the first region the restriction $q(t) \ll 1$ (corresponding to $\ln (t/t_0) \gg \alpha^{-1}$) is the only condition for (5.1.13) to be valid. On smaller time-scales the relevant eigenmodes are essentially overlapping and their interaction must be taken into account.

Note that the continuum treatment employed is valid if the relevant value of ϵ in (5.1.12) satisfies the condition $\epsilon_\lambda \ll \Lambda$ (see (5.1.6)). Therefore the power law (5.1.13) holds in a wide interval

$$t_0 \exp\left(\frac{\tilde{\gamma}}{g}\right) \ll t \ll t_0 \exp\left(\frac{\Lambda c_2}{4g}\right). \tag{5.1.14}$$

At higher temperatures $t \gg Gi$, (5.1.13) holds for $\ln (t/t_0) \gg (\tau/Gi)^{1/2}$. In the opposite limit we obtain:

$$q(t) \sim \begin{cases} \exp\left[\left(\frac{\tau}{Gi^{R}}\right)^{1/2}\right] \exp\left[-\tau Gi\left(Gi^{R} \ln \frac{t}{t_0}\right)^{1/2}\right] & \left(\frac{t}{t_0} \gg \left(\frac{\tau}{Gi^{R}}\right)^{1/2}\right), \\ \exp\left(-\frac{t}{t_0}\right) & \left(1 \ll \frac{t}{t_0} \ll \left(\frac{\tau}{Gi^{R}}\right)^{1/2}\right), \end{cases} \tag{5.1.15}$$

where $t_0 = \tau^{-1}$.

Now consider the vector-spin case ($n \geqslant 2$). Slowly relaxing modes are rotations of $\sigma_\lambda = a_\lambda / |a_\lambda|$ at fixed values of a_λ^2 (given by (5.1.9)). The equation of motion is

$$\dot{\sigma}_\lambda = \xi_\lambda(t), \quad \langle \xi_\lambda^\alpha(t) \xi_\lambda^\beta(t') \rangle = \frac{2}{a_\lambda^2} (\delta^{\alpha\beta} - \sigma_\lambda^\alpha \sigma_\lambda^\beta) \delta(t - t'). \tag{5.1.16}$$

Thus the relaxation rate t_λ^{-1} associated with these rotations is

$$\Gamma(\epsilon_\lambda) = t_\lambda^{-1} = a_\lambda^{-2} = \frac{g \epsilon_\lambda^{3/2}}{c_2(\epsilon_\lambda - \tau)} \leqslant \epsilon_\lambda - \tau. \tag{5.1.17}$$

The inequality in (5.1.17) follows from the condition $\Delta F_\lambda \geqslant 1$. Then the saddlepoint integration in the eigenmode expansion

$$q(t) \sim \int \mathrm{d}\epsilon \, \rho(\epsilon) \exp\left[-t\Gamma(\epsilon_\lambda)\right] \tag{5.1.18}$$

yields the "stretched-exponential" result

$$q(t) \sim \exp\left(-\frac{c_1 \tau^{1/2}}{\gamma}\right) \exp\left[-\left(\frac{t}{t_{\mathrm{eff}}}\right)^{1/2}\right],$$

$$t_{\mathrm{eff}} = \frac{c_2}{2c_1} \frac{\gamma}{\tau g} \frac{2\tilde{\gamma}}{g\tau}, \tag{5.1.19}$$

which holds if the inequalities

$$q(t) \ll 1, \tag{5.1.20a}$$

$$t \ll t_{\mathrm{m}} = \frac{c_1 c_2}{2g\gamma} \approx \frac{3}{g\tilde{\gamma}} \tag{5.1.20b}$$

are fulfilled. At $t \gg t_m$ the saddlepoint value of ϵ in (5.1.18) is t-independent; therefore we have obtained $-\ln q(t) \sim t$. Actually, the situation at $t \geqslant t_m$ is more sophisticated and we shall discuss it later.

The inequalities (5.1.20a, b) are compatible with one another for $\tau \gg Gi^2 \approx \tilde{\gamma}^2$. Moreover, the condition $\tilde{\gamma} \gg g$ has to be fulfilled to get $t_{\text{eff}} \gg t_0 = \tau^{-1}$.

Now it would be useful to compare our approach with the one recently developed by Bray [6, 7], who has considered the model (5.1.1)–(5.1.3) as $n \to \infty$ and studied the eigenvalue density $\sigma(\mu)$ of the inverse susceptibility matrix $\chi^{-1}(x, x')$:

$$\chi(x, x') = T^{-1}\langle S(x) \cdot S(x') \rangle.$$

In the limit $n \to \infty$ it was also asserted that the dynamics of the model is reduced to its statics:

$$q(t) = \int d\mu \, \sigma(\mu) e^{-\mu t}, \tag{5.1.21}$$

so the long-time relaxation is determined by the form of the singularity of $\sigma(\mu)$ as $\mu \to 0$. To find $\sigma(\mu)$, we should study the entire nonlinear Hamiltonian (5.1.1). However, the problem is much simpler in the limit $n \to \infty$, where the "Hartree" approximation becomes exact [6]. Then the matrix $\hat{\chi}^{-1}$ reduces to the self-consistent Schrödinger operator

$$\hat{L} = \hat{L}_0 + g \sum_{\mu} \frac{\phi_\mu^2(x)}{\mu}, \tag{5.1.22}$$

where $\hat{L}_0 = -\nabla^2 + \tau + V(x)$ and $\phi_\mu(x)$ are eigenfunctions of the matrix $\hat{\chi}$. The spectrum density $\sigma(\mu)$ is then analyzed in terms of the Lifshitz-type arguments, with the result

$$\sigma(\mu) \underset{\mu \to 0}{\sim} \exp\left[-\left(\frac{A}{\mu}\right)^{1/2}\right], \quad A \sim \frac{\tau g}{\gamma}. \tag{5.1.23}$$

It follows from (5.1.21) that (5.1.23) leads precisely to the relaxation function (5.1.19). Thus the two approaches discussed produce the same result, and Bray's result is applicable for all $n \geqslant 2$ (but not for the Ising case!). Note, however, that (5.1.23) holds for any $\mu \to 0$, so that the restriction (5.1.20b) is absent in the Bray approach. We now return to the derivation of (5.1.19) and discuss the interval $t \geqslant t_m$.

The nonmonotonic behaviour of $\Gamma(\epsilon)$ in (5.1.17) results in the

appearance of t_m in our calculations: the minimum value of $\Gamma(\epsilon)$ corresponds to $\epsilon = 3\tau$ ($\Gamma_{\min} \sim g\tau^{1/2}/c_2$) and determines the edge of the relaxation-time spectrum at a given temperature. But, actually, only those fluctuations of the random potential $V(x)$ were taken into account that determine the density of states $\rho(\epsilon)$ of the linear problem. On the other hand, according to Bray's analysis, the essential fluctuations of $V(x)$ determining $\sigma(\mu)$ are different: in the large volume $\mathscr{V} \gg \Delta^{-3/2}$ these are fluctuations with $V(x) \approx \Delta$. The number of linear eigenstates, bounded states, generated by such potential fluctuations is large ($N \sim \mathscr{V}\Delta^{3/2} \gg 1$), with the lowest-level "energy" $\epsilon = \Delta$. Let us therefore estimate the contribution of these configurations to $q(t)$. The probability of finding a $V(x)$ fluctuation characterized by the quantities $\mathscr{V}$ and Δ is

$$\text{prob}\,(\mathscr{V}, \Delta) \sim \exp\left(-\frac{\Delta^2 \mathscr{V}}{2\gamma}\right). \tag{5.1.24}$$

The relaxation rate $\Gamma(\mathscr{V}, \Delta)$ associated with these fluctuations is (cf. (5.1.10), (5.1.17) with $\epsilon = \Delta$):

$$\Gamma(\mathscr{V}, \Delta) = a^2(N, \Delta) = \frac{g}{\mathscr{V}(\Delta - \tau)}. \tag{5.1.25}$$

Therefore we must minimize

$$q_{\mathscr{V},\Delta}(t) \sim \text{prob}\,(\mathscr{V}, \Delta)\, e^{-\Gamma(\mathscr{V},\Delta)t} \sim \exp\left[-\frac{\Delta^2 \mathscr{V}}{2\gamma} - \frac{gt}{\mathscr{V}(\Delta - \tau)}\right] \tag{5.1.26}$$

over $\mathscr{V}$ and Δ, which leads to

$$q(t) \sim \exp\left[-\left(\frac{8\tau g t}{\gamma}\right)^{1/2}\right] = \exp\left[-\left(\frac{t}{2t_{\text{eff}}}\right)^{1/2}\right], \tag{5.1.27}$$

with t_{eff} defined in (5.1.19). The extremum values of $\mathscr{V}$ and Δ are $\mathscr{V}_m = (g\gamma t/2\tau^3)^{1/2}$ and $\Delta_m = 2\tau$, so the inequality $\mathscr{V}_m \Delta_m^{3/2} \gg 1$ holds for $t \gg t_m$.

Thus the behaviour of $q(t)$ is essentially the same at $t \ll t_m$, (5.1.19), and $t \gg t_m$, despite the different nature of the respective $V(x)$ configurations. Note that the common feature inherent both in our approach and in Bray's is the absence of mode–mode interactions provided by the conditions $\tau \gg Gi$ and $n \gg 1$ respectively.

5.2 *Spin Glasses*

5.2.1 Large-Z Edwards–Anderson model [4, 8] The three-dimensional model with long-range (but finite) interaction is described by the Hamiltonian

$$H = -\frac{1}{2}\sum_{i,j} J_{ij} S_i \cdot S_j, \quad \overline{J_{ij}^2} = K(r_i - r_j), \tag{5.2.1}$$

where $\int d^3r\, K(r) = 1$ (this normalization provides a critical temperature $T_c = n^{-1}$, where n is the number of spin components) and

$$Z = \int d^3r\, r^2 K(r), \tag{5.2.2}$$

i.e. the number of interacting neighbours is large.

The critical behaviour of this model was considered in Section 4, and here the long-time relaxation in a high-temperature phase beyond the critical region $\tau \gg \tau_0 = Z^{-2/3}$ will be studied. The dynamics is supposed to be purely relaxational and can be expressed (at $\tau \ll 1$) as time-dependent TAP-like equations (see Section 4 for details):

$$\frac{\partial m_i}{\partial t} = -\frac{\delta H_{\mathrm{TAP}}}{\delta m_i} + \eta_i(t), \quad \langle \eta_i(t)\eta_j(t')\rangle = 2T\delta_{ij}\delta(t-t'), \tag{5.2.3}$$

with

$$H_{\mathrm{TAP}} = -\frac{1}{2}\sum J_{ij} m_i \cdot m_j + \frac{1}{4nT}\sum_{i,j} J_{ij}^2 (1-m_i^2)(1-m_j^2) + Tn\sum_i \left[\frac{m_i^2}{2} + \frac{n}{4(n+2)}(m_i^2)^2 + \frac{n^2(n+8)}{6(n+4)(n+2)^2}(m_i^2)^3\right]. \tag{5.2.4}$$

In the limit $\tau \gg \tau_0$, (5.2.3) can be decoupled in terms of eigenmodes of the matrix J_{ij} (cf. Section 4):

$$\frac{\partial a_\lambda}{\partial t} = (\epsilon_\lambda - \tau^2)a_\lambda - g_n\left[\frac{1}{3}\sum_i \psi_\lambda^4(i)\right] a_\lambda^2 a_\lambda - \left(\frac{1}{15}\sum_i \psi_\lambda^6(i)\right)(a_\lambda^2)^2 a_\lambda + \xi_\lambda(t), \tag{5.2.5}$$

where $\epsilon_\lambda = J_\lambda - 2$, $g_n = 2(n-1)/(n+2)$ for $n \geqslant 2$ and $g_1 = 2\tau$; for $n \geqslant 2$ the a^5 term can be neglected.

Extended eigenmodes with $\epsilon_\lambda < 0$ relax linearly with characteristic times $t_\lambda = (\epsilon_\lambda + \tau^2)^{-1}$, which results in the usual mean-field spin-glass relaxation law

$$q_0(t) \sim t^{-1/2} e^{-t/t_0}, \quad t_0 = \tau^{-2}. \tag{5.2.6}$$

We are interested in the "anomalous" part of the relaxation, which is due to nonlinear localized "condensed" modes with $\epsilon_\lambda > \tau^2$ whose density is exponentially low (see the Appendix to Section 4):

$$\rho(\epsilon) \sim \exp(-c_1 Z \epsilon^{3/4}), \quad c_1 = O(1) \tag{5.2.7}$$

In the Ising case the modes with $\epsilon_\lambda > \tau^2$ relax through a thermal-activation process by flipping over the free-energy barriers $\Delta F(\epsilon)$; therefore the long-time asymptotic form of the condensed-mode contribution to $q(t)$ is given by (cf. (5.1.12))

$$q_{\mathrm{an}}(t) \sim \int \mathrm{d}\epsilon \exp(-c_1 Z \epsilon^{3/4}) \exp\left\{ -\frac{t}{t_0} \exp[\Delta F(\epsilon)] \right\} \tag{5.2.8}$$

(remember that $T \approx T_c = 1$). The free-energy barriers $\Delta F(\epsilon_\lambda)$ are given by

$$\Delta F(\epsilon_\lambda) = \frac{1}{2}(\epsilon_\lambda - \tau^2) a_\lambda^2 - \frac{2\tau}{4} V_\lambda^{-1} a_\lambda^4 - \frac{1}{6} \tilde{V}_\lambda^{-2} a_\lambda^6, \tag{5.2.9}$$

where a_λ^2 obeys the minimization equation

$$\epsilon_\lambda - \tau^2 = 2\tau V_\lambda^{-1} a_\lambda^2 + \tilde{V}_\lambda^{-2} a_\lambda^4 \tag{5.2.10}$$

and we denote

$$V_\lambda = \left[\frac{1}{3} \sum_i \psi_\lambda^4(i) \right]^{-1} = \frac{c_2 Z}{\epsilon^{3/4}}, \quad c_2 = \frac{3}{4} c_1, \tag{5.2.11a}$$

$$\tilde{V}_\lambda = \left[\frac{1}{15} \sum_i \psi_\lambda^6(i) \right]^{-1/2} = \frac{c_3 Z}{\epsilon^{3/4}}, \quad c_3 = \frac{3}{2^{1/2} 4} c_1. \tag{5.2.11b}$$

V_λ as well as $\tilde{V}_\lambda$ measure the effective volume of the highly localized eigenfunction $\psi_\lambda(i)$ in the tail region $\epsilon \gg \epsilon_0$. The relations (5.2.11a, b) are derived in the Appendix to Section 4; note that the numerical coefficients $c_{2,3}$ are expressed exactly in terms of the coefficient c_1 entering

(5.2.7) for the density of states $\rho(\epsilon)$. Obviously, the general expression for $\Delta F(\epsilon)$ can be derived and used in (5.2.8), but we shall not write down these cumbersome formulae and will rather consider various asymptotic behaviours.

At $t \ll Z/\tau^{1/2}$ the anomalous contribution $q_{an}(t)$ is relatively small and the mean-field result (5.2.6) holds.

At longer times $q_{an}(t)$ is substantial; in the interval $Z/\tau^{1/2} \ll t \ll t_0 \exp(Z\tau^{3/2})$ the relevant values of ϵ in the integral (5.2.8) are in the range $\epsilon - \tau^2 \ll \tau^2$, so that the last terms in (5.2.9) and (5.2.10) can be neglected. The result is

$$\left.\begin{aligned} q(t) \sim \exp(-c_1 Z\tau^{3/2}) \exp\left[-\left(6c_1 Z\tau^{3/2} \ln\frac{t}{t_0}\right)^{1/2}\right], \\ \ln\frac{t}{t_0} \ll Z\tau^{3/2}. \end{aligned}\right\} \tag{5.2.12}$$

In the range $Z\tau^{3/2} \ll \ln(t/t_0) \ll Z$ the relevant values of ϵ obey the inequalities $\tau^2 \ll \epsilon \ll 1$ and the τ-containing terms in (5.2.9) and (5.2.10) can be neglected. Then we obtain $\Delta F(\epsilon) \sim \epsilon^{3/4}$, which leads to the power-law asymptotic behaviour

$$\left.\begin{aligned} q(t) \sim \left(\frac{t}{t_0}\right)^{-\alpha}, \quad \alpha_3 = 4 \times 2^{1/2} \approx 5.66, \\ Z\tau^{3/2} \ll \ln\frac{t}{t_0} \ll Z. \end{aligned}\right\} \tag{5.2.13}$$

The exponent in (5.2.13) is just the ratio $3c_1/c_3$; possible logarithmic factors are omitted.* A similar result can be obtained for the two-dimensional analogue of the considered system in the range $Z\tau^2 \ll \ln(t/t_0) \ll Z$:

$$q_{2D}(t) \sim \left(\frac{t}{t_0}\right)^{-\alpha_2}, \quad \alpha_2 = 3\left(\frac{3}{2}\right)^{1/2} \approx 3.67. \tag{5.2.13'}$$

The longest timescale $t \gg t_0 e^Z$, however, cannot be handled within the present approach, since the relevant eigenmodes would be in the range $\epsilon \geqslant 1$, where the results (5.2.7) and (5.2.11) are invalid. For $\epsilon \gg 1$ one could write an estimate:

*There was an error in [8], leading to the result $q \sim \exp[-(\ln t)^{3/5}]$ instead of Equation 5.2.13: the sixth-order term in the free-energy expansion $F(a_\lambda)$ was omitted.

$$\rho(J_\lambda = 2 + \epsilon_\lambda) \sim \exp\left(-\tfrac{1}{2} Z J_\lambda^2\right), \quad V_\lambda \simeq Z, \tag{5.2.14}$$

where $J_\lambda \ll Z^{1/2}$. Equations (5.2.14) describe Gaussian fluctuations of J_{ij}s localized in a volume $\sim Z$. Unfortunately, the contribution of these modes cannot be taken into account in the present approach since the continuum treatment of the dynamical TAP-like equations (5.2.3) and (5.2.4) appears to be inadequate. It seems probable that the longest-time asymptotics could be obtained through the original approach of reference [9] (see Section 1.5) to give $q(t) \sim \exp\left[-\text{const} \times \ln t\right)^{3/2}]$.

Turning to the vector-spin glass case ($n \geqslant 2$), it can be seen that the values of $\langle \boldsymbol{a}^2(\epsilon_\lambda)\rangle$ are strongly affected by thermal fluctuations, which is the result of larger values of the coupling constant: $g_n \sim 1$ for $n \geqslant 2$ (whereas $g_1 \sim \tau$, cf. (5.2.5)). It can be shown that the values of the relaxation rates $\Gamma(\epsilon_\lambda) \sim \langle \boldsymbol{a}^2(\epsilon_\lambda)\rangle$ (cf. (5.1.17)) increase with ϵ, so that there is no nontrivial saddlepoint in the integral $q(t) \sim \int d\epsilon\, \rho(\epsilon) e^{-\Gamma(\epsilon)t}$. It then appears that anomalous relaxation is absent for vector spin glasses. Actually, it is absent within the one-mode approximation considered above. The reason for this is the uniaxial nature of the magnetization associated with one mode $\boldsymbol{a}_\lambda \psi_\lambda(i)$, as opposed to the spherical isotropy of the magnetization field in the spin-glass state (cf. the discussion of this point in Section 4.2.3). A nontrivial contribution to long-time relaxation can be produced by "clusters" consisting of n modes $\boldsymbol{a}_{\lambda_p} \psi_{\lambda_p}(i)$, $p = 1, \ldots, n$, localized in the same volume with nearby eigenvalues $\epsilon_{\lambda_p} \approx \epsilon_\lambda$ and forming a nearly isotropic magnetization field

$$\boldsymbol{m}(i) = \sum_{p=1}^{n} \boldsymbol{a}_{\lambda_p} \psi_{\lambda_p}(i), \quad \boldsymbol{a}_{\lambda_p} = \frac{\boldsymbol{a}_\lambda}{n^{1/2}}\, \boldsymbol{e}_{\lambda_p},$$

where $\boldsymbol{e}_{\lambda_p}$ constitute an orthonormal basis. Then the dependence of the free energy on the common amplitude of the "cluster" $\boldsymbol{a}_\lambda$ is

$$F(\boldsymbol{a}_\lambda) \approx -\frac{1}{2}(\epsilon_\lambda - \tau^2)\boldsymbol{a}_\lambda^2 + \frac{\tau}{2}(\boldsymbol{a}_\lambda^2)^2 V_\lambda^{-1} + (\boldsymbol{a}_\lambda^2)^3 \tilde{V}_\lambda^{-2}, \tag{5.2.15}$$

where V_λ and $\tilde{V}_\lambda$ are defined similarly to (5.2.11); the effective coefficient in the "$\boldsymbol{a}_\lambda$" term is diminished to mode–mode interactions

(cf. Section 4.2.3). We can then make estimates similar to that employed in Section 5.1 for the vector ferromagnet case. We only present the results here: the anomalous contribution to $q(t)$ is the main one at $t \geqslant nZ/\tau^{1/2}$ and is given by the stretched exponential

$$-\ln q(t) \sim nZ\tau^{3/2} + \tilde{c}\left(\frac{t}{t_0}\right)^{1/2}, \quad t_0 \sim \frac{1}{\tau}, \quad \tau \sim 1, \tag{5.2.16}$$

whereas at shorter times (5.2.6) holds. Note that at $t \geqslant n^2Z^2\tau$ (when the second term in (5.2.16) is the main one) Bray's picture [6] is valid.

To conclude this section, we note that Bray's result [6] $-\ln q(t) \sim t^{1/2}$ appears to be universal for random vector systems with weak thermal fluctuations (in the sense of the Ginzburg criterion [1]).

5.2.2 Spin glasses with RKKY interactions [8] Consider the model of vector spins interacting via the RKKY potential:

$$J(r) = J_0 \frac{\cos p_0 r}{r^3} \tag{5.2.17}$$

(actually, the following analysis with some modifications can also be applied to other random power-law interactions). It is well known (see e.g. [10, 11]) that the transition temperature of such a system is proportional to the volume spin concentration c:

$$T_c = \theta c J_0 \ll T_0, \quad \theta \sim 1. \tag{5.2.18}$$

Here $T_0 = J_0/a^3$ is the interaction energy for the neighbouring spins and a is the lattice constant.

Note that the following analysis holds regardless of whether T_c is a point of true phase transition or just a point at which the relaxation regime is changing.

The qualitative arguments are as follows. Local spatial fluctuations of the concentration c result in fluctuations of the local transition temperature T_c. Therefore at any temperature in the wide interval

$$T_c < T < T_0 \tag{5.2.19}$$

there are regions of the systems that have local T_c higher than T. These regions contain clusters of $N \gg 1$ highly correlated spins, relaxing only

as a result of rotations of the clusters as a whole. The relaxation rate Γ_N of such a cluster containing N spins is

$$\Gamma_N = \Gamma_0 N^{-1}, \tag{5.2.20}$$

where Γ_0 is the rate of relaxation of a free spin.

The cluster could be considered as rigid only if its $\tilde{T}_c$ is much higher than T. On the other hand, if $\tilde{T}_c - T \ll \tilde{T}_c$ then Γ_N appears to be increasing:

$$\Gamma_N \sim \Gamma_0 N^{-1}[f(\tilde{\tau})]^{-1}, \tag{5.2.21}$$

where $\tilde{\tau}$ is the effective reduced temperature of the cluster: $\tilde{\tau} = 1 - T/\tilde{T}_c$ (cf. (5.2.14), where $\epsilon - \tau^2$ stands for $f(\tilde{\tau})$). In the framework of the scaling theory for the correlation volume $l^3(\tilde{\tau}) \sim \tilde{\tau}^{-3\nu} \ll V$ (V is the volume of the cluster) it is supposed that $f(\tilde{\tau}) \sim \tilde{\tau}^{\beta}$. It can be shown [8] that for $\tau = T/T_c - 1 \geqslant 1$ the main contribution to the relaxation function is due to the clusters with $\tilde{\tau} \sim 1$. For this reason the results are insensitive to the exact form of $f(\tau)$. What is important, however, is that at $\tau \sim 1$ both $f(\tau)$ and $f'(\tau)$ have to be 0(1). Of course, the critical region $\tau \ll 1$ cannot be treated in such simple terms.

Obviously, the probability of finding the cluster of N spins localized in the volume V ($N > cV$) is exponentially small:

$$P(N) \approx \exp\left[-V_c - N\left(\ln\frac{N}{cV} - 1\right)\right](2\pi N)^{-1/2}. \tag{5.2.22}$$

Its contribution to $q(t)$ is

$$q_N(t) = q_{EA}(\tilde{\tau}) N e^{-\Gamma_N t}, \tag{5.2.23}$$

where $q_{EA}(\tilde{\tau})$ is the Edwards–Anderson order parameter at the reduced temperature $\tilde{\tau}$. Note again that we must take $q_{EA}(\tau)$ to be its dynamic value at time $t \gg \Gamma_N^{-1}$, which is certainly nonzero at $T \ll \tilde{T}_c$, rather than the thermodynamic value. Thus for $q(t)$ at long times $t \gg \Gamma_0^{-1}$ we get

$$q(t) = \left\langle \int \frac{dN}{(2\pi)^{1/2}} q_{EA}(\tau) N^{1/2} \exp\left[-t\Gamma_N - Vc - N\left(\ln\frac{N}{cV} - 1\right)\right]\right\rangle_V. \tag{5.2.24}$$

The average here is over different volumes V restricted by the condition $N/cV > T/T_c$, which guarantees that $\tilde{T}_c > T$. The saddlepoint estimate yields

$$q(t) \sim \exp\left[-A\left(\Gamma_0 t \ln\frac{T}{T_c}\right)^{1/2}\right], \quad A \sim 1. \tag{5.2.25}$$

Of course, the logarithmic factor in (5.2.25) makes sense only for $T_c \ll T \ll T_0$.

The above arguments show that the relaxation of the RKKY system is of "stretched-exponential" type in the wide temperature interval far above T_c. This result is qualitatively in accord with neutron-spin-echo experiments [12], where nonexponential relaxation far above T_c was observed in diluted metallic spin glasses.

5.3 *A Sort of Conclusion: Diffusion over a Fractal Potential*

The systems considered in the previous sections were shown to exhibit two generic forms of nonexponential relaxation. For the Ising systems

$$q(t) \sim \exp\left[-\alpha(\ln t)^{\gamma}\right], \tag{5.3.1}$$

where $\gamma = \frac{1}{2}$ in the intermediate-time region and $\gamma = 1$ (i.e. power-law behaviour) at longer times. For vector-spin models the relaxation is stretched-exponential:

$$q(t) \sim \exp\left[-B(T)t^{\beta}\right] \tag{5.3.2}$$

where $\beta = \frac{1}{2}$. All of the systems considered above have a common feature: the interaction of thermal fluctuations is relatively weak (owing to the smallness of the coupling constant or the long range of the interaction). Obviously, most of the interesting systems do not possess this property; therefore, in the absence of a general theory, it seems useful to have some sort of phenomenological interpretation of the results (5.3.1) and (5.3.2). Obviously, a general reason for the anomalous relaxation in the Griffiths phase at $T > T_c$ (as well as in a spin-glass phase) is the existence of an infinite spectrum of relaxation times. In turn, it could be due to the presence of a large number of local minima of the free energy and a wide spectrum of potential barriers between them. Therefore in what follows a phenomenological approach is discussed in which the notions of a "large number of local minima" and of "large potential barriers" are elucidated in a more

explicit way. The approach [13] is based on the hypothesized fractal properties of the free-energy surface. As a result, some qualitative conclusions can be derived for the possible types of relaxation of the order parameter $q(t)$ and the nature of the Griffiths phase.

The relaxation process is treated here as an ordinary diffusion over the space of metastable states, which are local minima of the free-energy surface. It is assumed that the free-energy relief is a fractal potential relief, i.e. the number of local minima depends on the scale in the phase space. As the scale gets smaller, it is possible to distinguish a greater number of smaller minima inside any minimum of a larger scale (Figure 11), and the total number of distinguishable local minima grows indefinitely. As with other fractal-like structures [14], it is assumed that the total number of metastable states depends on the scale ξ as

$$K(\xi) \sim \xi^{-D}, \tag{5.3.3}$$

where D is the fractal dimension of the space of metastable states. An example of such a scaling relation is the result (3.2.13).

The scale in phase space could be defined in terms of the overlaps:

$$q^{\alpha\beta} = \frac{1}{N} \sum_i \langle S_i \rangle^{(\alpha)} \langle S_i \rangle^{(\beta)}, \tag{5.3.4}$$

where $\langle \ldots \rangle^{(\alpha)}$ denotes the average near the given minimum (α). The distance $\xi^{\alpha\beta}$ between the two states can then be defined as, for example,

$$\xi^{\alpha\beta} = \frac{1}{q^{\alpha\beta}} - 1. \tag{5.3.5}$$

The diffusion process can be considered as "hoppings" of a particle over local minima of the surface. Therefore the values of the barriers separating metastable states are crucial for the diffusion process. At the qualitative level it can be assumed that for a given scale ξ the barriers between the lowest-level minima have some characteristic value $U(\xi)$. The function $U(\xi)$ is some qualitative characteristic of the fractal-like potential relief.

Numerous recent studies of the low-temperature phase of spin glasses have revealed the existence of a hierarchically constrained dynamics of spin-glass degrees of freedom [15–19]; in other words, the relaxation of different degrees of freedom proceeds in sequence but not in parallel. Ultrametric organization of the metastable states in the low-

temperature phase of the SK model qualitatively supports such a picture. Numerous studies of relaxation in terms of diffusion over ultrametric spaces have given interesting results, which include power-law relaxation with a temperature-dependent exponent, and a dynamic phase transition from the ordinary diffusion law to an anomalously slow one [15, 17].

Of course, all of these studies were assumed to be appropriate first of all for slow relaxation in the low-temperature phase. However, the actual dynamic behaviour of the frozen spin-glass phase is obviously much more complicated and cannot be reduced simply to slow non-exponential relaxation (see Section 3). On the other hand, the ideas discussed above can be demonstrated to be successful also for phenomenological explanation of the nonexponential relaxation in the Griffiths phase above T_c.

While below T_c the free-energy barriers are expected to become infinite at some finite scale (which makes the system nonergodic), above T_c the barriers could remain finite for any finite scale. We shall consider the situation where the effective barriers grow monotonically as the scale ξ increases.

The diffusion process over such a potential relief can be described qualitatively by the equation

$$\frac{\mathrm{d}}{\mathrm{d}t}\langle \xi^2 \rangle = D(\xi), \tag{5.3.6}$$

where $\langle \xi^2 \rangle$ is the "Brownian" mean-square displacement and

$$D(\xi) = D_0 \mathrm{e}^{-U(\xi)/T} \tag{5.3.7}$$

is the scale-dependent diffusion constant. Equivalently, the system can be characterized by the continuous hierarchy of relaxation times:

$$\tau(\xi) \sim \tau_0 \mathrm{e}^{U(\xi)/T}. \tag{5.3.8}$$

Obviously, for a given temperature T there exists a characteristic scale $\xi(T)$,

$$U(\xi(T)) = T, \tag{5.3.9}$$

such that at scales $\xi \ll \xi(T)$ the barriers are effectively nonexistent and the diffusion is normal: $\langle \xi^2 \rangle \sim D_0 t$. The corresponding lower characteristic time is

$$\tau_0(T) \sim \xi_0^2(T)/D_0. \tag{5.3.10}$$

At times $t \gg \tau_0(T)$ the character of the diffusion and the form of $\langle \xi^2 \rangle(t)$ depend on the explicit form of $U(\xi)$ (see below).

The behaviour of the order parameter $q(t)$ in terms of this approach is given by

$$q(t) \sim q_0 \int_{\xi(T)}^{\infty} d\xi \; w(\xi) e^{-t/\tau(\xi)}, \tag{5.3.11}$$

which contains an additional weight function $w(\xi)$. Qualitatively, this function indicates what part of the degrees of freedom is involved in the excitation having the relaxation time $\tau(\xi)$. Treating these excitations of some intermediate scale as flippings of the spin clusters containing $N(\xi)$ spins (cf. Section 3.2), the weight function $w(\xi)$ can be defined as

$$w(\xi) = N(\xi)/N. \tag{5.3.12}$$

Therefore the relaxation of the order parameter $q(t)$ is controlled by two functions $w(\xi)$ and $U(\xi)$, which are supposed to be obtained from the microscopic theory (the explicit forms of $w(\xi)$ and $U(\xi)$ could be given, for example, by the RG theory described in Section 2.5). Since such a theory does not yet exist, we have reason for speculation.

We could consider the following simple functions:

$$w(\xi) \sim \xi^{-\gamma}, \tag{5.3.13a}$$

$$w(\xi) \sim e^{-\xi/\xi_0}, \tag{5.3.13b}$$

$$U(\xi) \sim J_0 \xi^{1/\alpha}, \tag{5.3.14a}$$

$$U(\xi) \sim U_0 \ln (\xi/\xi_1). \tag{5.3.14b}$$

The long-time-diffusion results corresponding to the functions (5.3.14a, b) are respectively (a) $\xi(t) \sim T \ln t$ and (b) $\xi(t) \sim t^{1/(2+U_0/T)}$.

Different combinations of the functions (5.3.13a, b) and (5.3.14a, b) give the following relaxation laws (the integral in (5.3.11) is estimated by the saddlepoint method):

(i) for (5.3.13b) and (5.3.14a)

$$q(t) \sim \exp\left[- A \left(\frac{T}{J_0} \ln \frac{t}{\tau_0} \right)^{\alpha} \right] \tag{5.3.15}$$

(the case $\alpha = 1$ corresponds to the model (a, d) in [16]);

(ii) for (5.3.13b) and (5.3.14b)

$$q(t) \sim \exp\left[-c\left(\frac{t}{\tau_0}\right)^{\beta}\right], \quad \beta = \frac{1}{1+U_0/T}; \tag{5.3.16}$$

(iii) for (5.3.13a) and (5.3.14b)

$$q(t) \sim \left(\frac{t}{\tau_0}\right)^{-\gamma T/U_0}; \tag{5.3.17}$$

(iv) the last combination of (5.3.13a) and (5.3.14a) gives $q(t) \sim [(T/U_0)\ln(t/\tau_0)]^{-\alpha\gamma}$, which obviously could correspond only to the low-temperature phase.

Therefore, depending on the form of the functions $U(\xi)$ (scale dependence of the potential barriers) and $w(\xi)$ (distribution of degrees of freedom), which should be obtained from the microscopic theory, the relaxation laws could have rather different asymptotics, including those of (5.3.1) and (5.3.2). Note, however, that the above consideration of relaxation in terms of potential barriers probably corresponds only to the Ising case, since in vector models there are essential barrier-free degrees of freedom.

In terms of the present speculative approach, the situation above T_c could be described as follows. It can be imagined that in the Griffiths phase below T_c the paramagnetic relaxation "shrinks down" and can be observed only at limited timescales. Namely, it can be assumed that the barriers of the fracal free energy are growing very slowly, i.e. the parameters α^{-1} and U_0 in the functions (5.3.14a, b) are small near T_0:

$$\alpha^{-1} \sim (1 - T/T_0)^{\delta} \tag{5.3.18a}$$

for $U(\xi) \sim J_0 \xi^{1/\alpha}$, or

$$U_0 \sim J_0(1 - T/T_0)^{\delta} \tag{5.3.18b}$$

for $U(\xi) \sim U_0 \ln \xi$. Then, in accordance with the diffusion picture described above, ordinary diffusion with $\langle \xi^2 \rangle \sim t/\tau_0$ will take place up to the scale given by (5.3.9):

$$\xi(T) \sim (T/U_0)^{\alpha} \tag{5.3.19a}$$

for $U(\xi) \sim U_0 \xi^{1/\alpha}$, or

$$\xi(T) \sim e^{-T/U_0} \tag{5.3.19b}$$

for $U(\xi) \sim U_0 \ln \xi$. In both cases it yields a characteristic time

$$\tau_g \sim \tau_0 \exp\left[\frac{\text{const}}{(1 - T/T_0)^{\delta}}\right], \tag{5.3.20}$$

such that ordinary paramagnetic relaxation takes place for times $t \ll \tau_g$,

$$q(t) \sim e^{-t/\tau_0}, \tag{5.3.21}$$

while for long times $t \gg \tau_g$ it becomes an anomalously slow relaxation (5.3.1) or (5.3.2).

The reason for the scaling form for the critical exponents (5.3.19a, b) is to ensure that above T_0 the relaxation is purely paramagnetic, but the explicit form of the temperature dependence of α or U_0 in the interval $T_c < T < T_0$ cannot be like (5.3.19a, b) at all.

Note in conclusion that in the Ising systems the relaxation process goes through thermally activated flipping of the compact spin clusters. It results in a power-law cluster-scale dependence of the potential barriers, which inevitably gives the relaxation law (5.3.1) for $q(t)$.

Therefore the Monte-Carlo results of Ogielski [20], giving the relaxation law (5.3.2) with $\beta = \beta(T)$ for Ising spin glasses, remain unexplained. Moreover, we believe that these results cannot be explained by treating critical relaxation as $T \to T_c$ and anomalous relaxation in the Griffiths phase separately. Indeed, for any temperature $T_c < T < T_0$, Ogielski observed the single scaling function

$$q(t) \sim t^{-x} \exp\left[-\left(\frac{t}{t_1}\right)^{\beta}\right] \tag{5.3.22}$$

for a whole range of times. Thus the obtained T-dependence of the exponent β with $\beta(T > T_0) = 1$ is just necessary in order to match (5.3.22) with the usual exponential relaxation at $T > T_0$.

Note that Bray's approach [6, 7] gives the coefficient $B(T)$ in (5.3.2) as tending to infinity as $T \to T_0 -$. It also makes it possible to match with the relaxation at $T > T_0$, although obviously the picture obtained is not compatible with the single scaling form for $q(t)$. Therefore it should again be recalled that a unified approach to critical relaxation and anomalous relaxation in the Griffiths phase is needed. The model of a disordered ferromagnet in the vicinity of the "impure" fixed point [21, 22] offers the possibility of developing such an approach. The suggested study of the susceptibility-matrix spectrum [6] would be very

interesting in this respect. Another interesting possibility is related to highly diluted infinite-range spin-glass models [23–25].

REFERENCES

[1] Patashinsky, A.Z. and Pokrovsky, V.L. (1978) *Fluctuation Theory of Phase Transition*. Oxford: Pergamon Press.
[2] Ma, S.-K. (1976) *Modern Theory of Critical Phenomena*. New York: W.A. Benjamin.
[3] Lifshitz, I.M., Gredeskul, S.A. and Pastur, L.A. (1982) *Vvedenie v teoriyu neuporjadochennih sistem*, p. 204. Moscow (in Russian).
[4] Feigel'man, M.V., "Power-low relaxation in the Griffiths phase", unpublished.
[5] Pentegov, V.I. and Feigel'man, M.V. (1988) *ZhETF* **94**, N.10, 345.
[6] Bray, A.J. (1987) *Phys. Rev. Lett.* 59, 586.
[7] Bray, A.J. (1988) *Phys. Rev. Lett.* **60**, 720.
[8] Feigel'man, M.V. and Ioffe, L.B. (1986) *J. Phys. (Paris)* **47**, 363.
[9] Randeria, M., Setha, J.P. and Palmer, R.G. (1985) *Phys. Rev. Lett.* **54**, 1321.
[10] Binder, K. and Young, A.P. (1986) *Rev. Mod. Phys.* **58**, 801.
[11] Larkin, A.I. and Khmelnitsky, D.E. (1970) *ZhETF* **58**, 1789.
[12] Mezei, F. (1982) *J. Appl. Phys.* **53**, 7654; (1983) *J. Magn. Magn. Mater.* **31–34**, 1327.
[13] Dotsenko, V.S. (1985) *J. Phys.* **C18**, 6023.
[14] Mandelbrot, B.B. (1982) *The Fractal Geometry of Nature*. San Francisco: Freeman.
[15] Ogielski, A.T. and Stein, D.L. (1985) *Phys. Rev. Lett.* **55**, 1634.
[16] Palmer, R.G., Stein, D.L., Abrahams, E. and Anderson, P.W. (1984) *Phys. Rev. Lett.* **53**, 958.
[17] Teitel, S. and Domary, E. (1985) *Phys. Rev. Lett.* **55**, 2176.
[18] Paladin, G., Mezard, M. and De Dominicis, C. (1985) *J. Phys. (Paris) Lett.* **46**, L985.
[19] De Dominicis, C. and Schreckenberg, M. (1987) in *Proceedings of Heidelberg Colloquium on Glassy Dynamics*, p. 255. Lecture Notes in Physics, Vol. 275. Berlin: Springer-Verlag, Eds. J.L. van Hemmen and I. Morgenstern.
[20] Ogielski, A.T. (1985) *Phys. Rev.* **B32**, 7384.
[21] Khmelsnitsky, D.E. (1975) *ZhETF* **68**, 1960.
[22] Lubensky, T.C. (1975) *Phys. Rev.* **B11**, 3573.
[23] Viana, L. and Bray, A.J. (1985) *J. Phys.* **C18**, 3037.
[24] Kanter, I. and Sompolinsky, H. (1987) *Phys. Rev. Lett.* **58**, 164.
[25] Rodgers, G.J. and Bray, A.J. (1988) *Phys. Rev.* **B37**, 3557.

6. SPIN GLASSES WITH HELICAL SHORT-RANGE ORDER

6.1 Mean-Field Theory

In this section we consider a model system of n-component classical spins σ_i ($n = 1, 2, 3$; $\sigma_i^2 = 1$) situated at random in a three-dimensional

matrix with concentration c, which interact with each other via a long-range pair potential $J(r)$. We choose [1, 2] the simplest form of this potential, which corresponds to a long-range oscillating interaction; its Fourier transform is

$$W(p) = W_0[1 + w(\hat{p})]\left[\frac{(p-p_0)^2}{\kappa^2} + 1\right]^{-1} \tag{6.1.1}$$

and consider only the case $\kappa \ll p_0$, $|w(\hat{p})| \ll 1$ ($\hat{p} \equiv p/p$), which corresponds to a long-range and nearly isotropic potential. Temporarily, we neglect $w(\hat{p})$, so that the interaction J acquires a simple form in the space representation also:

$$J_0(r) = W_0 \frac{\kappa p_0}{2\pi r} e^{-\kappa r} \sin p_0 r. \tag{6.1.2}$$

The considered model can be described by the Hamiltonian

$$H = -\frac{1}{2}\sum_{i,j} J(r_{ij})\sigma_i \cdot \sigma_j. \tag{6.1.3}$$

As usual, we can obtain quantitative results only if the concentration c is large so that the average coordination number

$$Z \approx c\kappa^{-3} \gg 1. \tag{6.1.4}$$

At first sight, the model (6.1.2), (6.1.3) looks like a slight modification of the Edwards–Anderson model. As we show below, this is just the case if the dimensionless parameter

$$\gamma = \kappa p_0^2/4\pi c \tag{6.1.5}$$

is large, whereas in the opposite case $\gamma \ll 1$ the properties of the model (6.1.2), (6.1.3) differ drastically from the properties of the EA model because in this case correlations between different J_{ij} become very important. These correlations can be described by a set of correlators K_m:

$$\begin{aligned} K_m &= \overline{J_{i_1 i_2} J_{i_2 i_3} \ldots J_{i_m i_1}} \\ &= c^{m-1} \int d^3 r_2 \ldots d^3 r_m \, J(r_1 - r_2) \ldots J(r_m - r_1) \\ &= c^{m-1} \int \frac{d^3 p}{(2\pi)^3} W^m(p). \end{aligned} \tag{6.1.6}$$

In the definition (6.1.6) each subscript is repeated twice, since the other correlators can be neglected if the condition (6.1.4) is ensured. Usually in spin-glass models it is supposed that J_{ij} are uncorrelated (i.e. K_m with $m > 2$ are neglected); in the model (6.1.2)–(6.1.3) this is justified only if γ, (6.1.5), is large.

First of all, we study the dependence of the critical temperature T_c on the parameter γ. As usual, to obtain the critical temperature for a system with a large coordination number, the mean-field approximation can be employed.

In the MFA the critical temperature is determined from the condition that the susceptibilty $\chi_{ij}(T) = \partial \boldsymbol{m}_i / \partial \boldsymbol{h}_j$ acquires a singularity at $T = T_c$. To derive the analytic expression for the critical temperature, we proceed further, in analogy with the calculations in Section 7.1 below and references [3, 4], where the same method is employed in different physical situations. Here we only briefly sketch the main points.

The summation of the series for the susceptibility χ_{ij} results in the equation

$$\frac{\partial \Sigma}{\partial \chi} \chi^2 = 1 \tag{6.1.7}$$

where $\chi = (hT_c)^{-1}$) is the exact one-point susceptibility of an n-component classical spin system in a paramagnetic state; $\hat{\Sigma}$ is the self-energy, which can be represented by a diagrammatic series (Figure 18), yielding

$$\hat{\Sigma} = \sum_{m=2}^{\infty} K_m \chi^{m-1}. \tag{6.1.8}$$

Figure 18 Sequence of diagrams contributing to the self-energy.

To calculate $\hat{\Sigma}$, we insert (6.1.6) into (6.1.8) and interchange the order of summation and integration, to get

$$\hat{\Sigma} = 2\gamma c W_0 [(1 - c\chi W_0)^{-1/2} - 1]. \tag{6.1.9}$$

Then inserting $\hat{\Sigma}$ from (6.1.9) into (6.1.7), we arrive at the equation for T_c:

$$\left.\begin{aligned} \gamma(cW_0)^2(1-c\chi W_0)^{-3/2}\chi^2 = 1, \\ \chi = (nT_c)^{-1}. \end{aligned}\right\} \tag{6.1.10}$$

At $\gamma \gg 1$ this is simplified to

$$(nT_c)^2 = \gamma(cW_0)^2 = K_2, \tag{6.1.11}$$

as for the Edwards–Anderson model, whereas in the opposite limit $\gamma \ll 1$ the singular terms in (6.1.10) become important and yield

$$nT_c \approx cW_0, \quad \tau_c \equiv 1 - \frac{cW_0}{nT_c} = \gamma^{2/3}. \tag{6.1.12}$$

The behaviour of nT_c/cW_0 in the general case is obtained by a qualitative solution of (6.1.10) (Figure 19).

Below we consider only the model in the range $\gamma \ll 1$. The mean-field theory of the low-temperature state of this model was developed in [1, 5], where it was shown that the spin-glass transition that occurs at T_c is followed by a second transition at $T = T_0$,

$$1 - \frac{cW_0}{nT_0} \equiv \tau_0 = -A\gamma^{2/3} \quad (A \sim 1), \tag{6.1.13}$$

into a state with long-range correlations, whereas in the intermediate state only short-range correlations are present as in an ordinary spin glass. This second transition is a first-order transition. In the framework of the MFA, genuine helical (or sinusoidal) long-range order is present in the low-temperature state. The whole phase diagram is depicted in Figure 19. Note the similarity between it and the phase diagram of the Hopfield model of associative memory (Section 8 below and reference [6]). This similarity is not a coincidence, but is due to the same form of the higher correlators K_m at low γ and low α in the Hopfield model.

So far we have neglected the anisotropy of the $W(p)$, i.e. we have put $w = 0$ in (6.1.1). Let the unit vector l_0 denote the l for which $w(l)$ is a maximum and consider the influence of the small parameter ϵ_A describing the anisotropy:

$$\epsilon_A = (\partial^2 w/\partial l^2)_{l=l_0}. \tag{6.1.14}$$

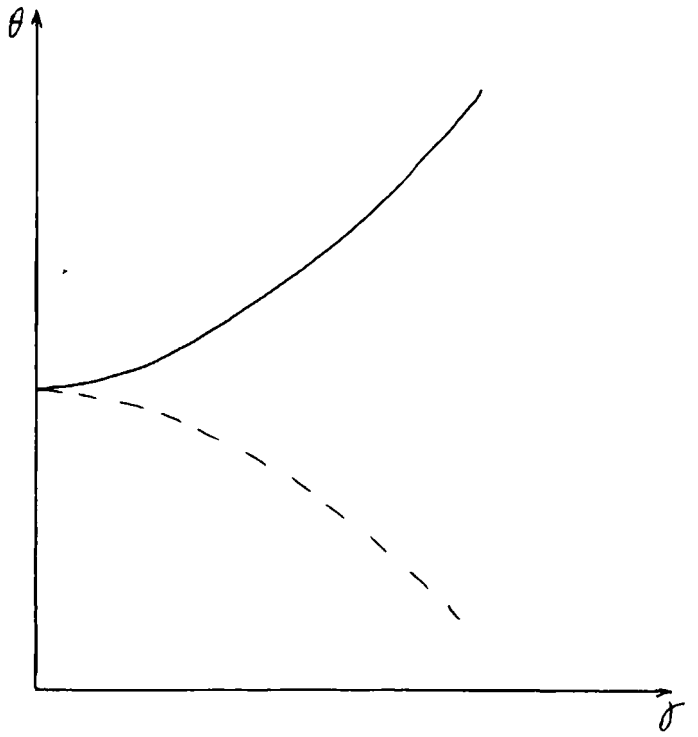

Figure 19 Phase diagram in the isotropic mean-field approximation. The qualitative solution of (6.1.10) for $\theta_c = nT_c/cW_0$ as a function of γ is represented by a full line; the qualitative behaviour of $\theta_0 = nT_0/cW$ is given by a broken line.

The equation for the self-energy becomes

$$\hat{\Sigma} = \gamma(cW_0)^2\chi \int_{-\pi}^{\pi} \frac{\sin\theta \, d\theta}{\zeta + w(0) - w(\theta) + [\zeta + w(0) - w(\theta)]^{1/2}}, \tag{6.1.15}$$

where $\zeta = 1 - cW_0\chi$; θ is the angle between l and l_0. From (6.1.15), we conclude that the new terms that it contains can be safely neglected if $\epsilon_A \ll \tau_c = \gamma^{2/3}$. In the opposite case $\epsilon_A \gg \tau_c = \gamma^{2/3}$ the singularity in $\hat{\Sigma}(\tau)$ is smoothed out and a unique second-order transition from the paramagnetic state to the low-temperature helical (or sinusoidal) state

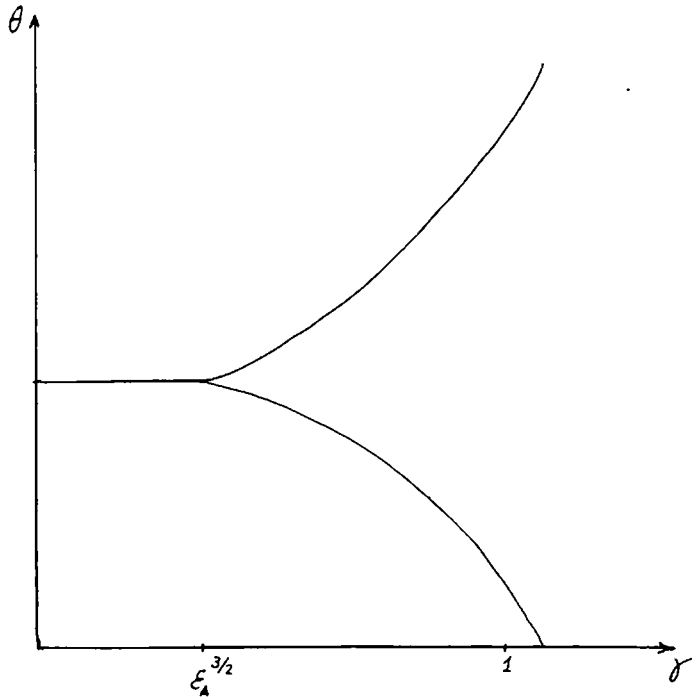

Figure 20 Qualitative phase diagram in the presence of anisotropy ($\epsilon_A \neq 0$).

occurs. This transition belongs to the "dirty XY" universality class [7] for $n = 2$ [7] and to the "random-axis XY" class for $n = 1$. The phase diagram for this case is shown as Figure 20. Below we consider the case $\epsilon_A \ll \gamma^{2/3}$ only, leaving aside the problem of the crossover region $\gamma^{2/3} \sim \epsilon_A$.

6.2 *Beyond MFA: The Role of Fluctuations and their Effective Action in the Helical State ($n = 3$)*

The helical low-temperature state is degenerate in energy (at $E_A = 0$) with respect to a rotation of wave vector $\boldsymbol{Q} = p_0 \boldsymbol{l}$. This degeneracy results in a very strong sensitivity of the long-range order in this state to thermal fluctuations and disorder — even at $\gamma \ll 1$. As usual, the most dangerous fluctuations are the long-wave ones, and to study their effect we need the effective action that governs them.

At first we study the simplified model with $\epsilon_A = 0$, leaving the discussion of the effect of finite ϵ_A to the end of Section 6.3. Moreover, we restrict ourselves to the study of the vicinity of T_0 because we believe that at low temperatures the large-scale fluctuations are not in thermal equilibrium, so that statistical considerations make no sense far below T_0.

To obtain the effective action, we rewrite the partition function of the model, introducing the auxiliary continuous field $S(r)$, which plays the role of a molecular field at the point r:

$$Z = \int \mathscr{D}S(r) \exp\left\{ -\frac{1}{2TW_0} \int \left[\left(\frac{\nabla^2 + p_0^2}{2p_0\kappa} S \right)^2 + S^2 \right] d^3r \right. \\ \left. - \sum_i \int \ln \left(\frac{T}{|S+h|} \sin \frac{|S+h|}{T} \right) \delta(r - r_i)\, d^3r \right\}, \tag{6.2.1}$$

where r_i are points of spin positions; $h = g_L \mu_B \mathscr{H}$, where $\mathscr{H}$ is the external magnet field and g_L and μ_B are the Landé factor and the Bohr magneton. Confining ourselves to the range of not too low temperatures and expanding the exponent in powers of S/T, we get (at $h = 0$)

$$Z = \int \mathscr{D}S(r)\, e^{-H[S]}$$

$$H[S] = \int \left\{ \frac{1}{2TW_0} \left[\frac{\nabla^2 + p_0^2}{2p_0\kappa} S(r) \right]^2 + \frac{1}{2TW_0} \left[1 - \frac{W_0}{3T} \sum_i \delta(r - r_i) \right] S^2 \right. \\ \left. + \frac{1}{180T^4} (S^2)^2 \sum_i \delta(r - r_i) \right\} d^3r. \tag{6.2.2}$$

It is possible to replace $\Sigma_i \delta(r - r_i)$ by c in the last term in (6.2.2). In the mean-field approximation at $T = T_0 \approx \frac{1}{3} c W_0$ (below we shall set $W_0 = 1$) there is a phase transition into an inhomogeneous state of helical type: $S = e_1 \cos Q \cdot r + e_2 \sin Q \cdot r$, where $e_1 \cdot e_2 = 0$. In the temperature range $\tau = 1 - c/3T \ll 1$ the Hamiltonian takes the form

$$H = \frac{1}{2T} \int \left\{ \left[\frac{\nabla^2 + p_0^2}{2p_0\kappa} S(r) \right]^2 + \tau S^2 + \frac{3}{10c^2} S^4 \right. \\ \left. + \left[1 - \frac{1}{c} \sum_i \delta(r - r_i) \right] S^2 \right\} d^3r. \tag{6.2.3}$$

We shall study the temperature range $|\tau| \gg \gamma^{2/3}$.

The last term in (6.2.3) leads to large-scale distortions of the helix. We derive an expression for the free energy of such deformations. We must take into account the influence of thermal fluctuations occurring on scales much smaller than the scales of distortions associated with random fields. Thus the last term in (6.2.3) can be neglected for the present.

S_α can be conveniently represented as

$$S_\alpha = a_\alpha(r)e^{i\theta} + a_\alpha^*(r)e^{-i\theta} + \varphi_\alpha(r), \tag{6.2.4}$$

where $\theta = p_0 \cdot r$, a_α is a complex vector, with a "slow" dependence on the coordinates, $a_\alpha^2 = 0$ (a can be represented as $a = e_1 + ie_2$), and φ_α are "fast" fluctuations with momenta $p \sim p_0$, $|p \pm p_0| \sim p_0$. The Green function of the fluctuations φ_α has been calculated in reference [9]:

$$\left.\begin{aligned} g_{\alpha\beta}(p) &= \langle \varphi_\alpha(p)\varphi_\beta(-p)\rangle = g_1(p)\rho_{\alpha\beta} + g_2(p)(\delta_{\alpha\beta} - \rho_{\alpha\beta}) \\ \rho_{\alpha\beta} &= \rho^{-1}(a_\alpha a_\beta^* + a_\beta a_\alpha^*), \quad \rho = |a_\alpha|^2 \\ g_1(p) &= \frac{T}{\left(\frac{p-p_0}{\kappa}\right)^2 + |\tau|}, \quad g_2(p) = \frac{T}{\left(\frac{p-p_0}{\kappa}\right)^2 + \left(\frac{6}{5}\gamma\right)^{2/3}} \end{aligned}\right\} \tag{6.2.5}$$

We clarify these formulae. The tensor $\rho_{\alpha\beta}$ chooses only fluctuations in the rotation plane of the formed helix; therefore g_1 corresponding to such longitudinal fluctuations has (at $|\tau| \gg \gamma^{2/3}$) a gap $|\tau|$. In the mean-field approximation the transverse fluctuations have no gap at all; however, when their interactions with each other are taken into account, it appears that they do acquire a gap.

Now consider slow deformation $a_\alpha(r)$ that leaves the amplitude $\rho = |a_\alpha|^2$ unchanged: $a_\alpha(r) = a_\alpha^{(0)} + \tilde{a}_\alpha(r)$. The vector a determines the plane where spins rotate: the normal to this plane is $n = i(a \times a^*)/\rho$. Let us represent the deformation $\tilde{a}$ as a sum $\tilde{a} = \tilde{a}_\perp + \tilde{a}_\parallel$ so that $\tilde{a}_\perp$ changes the direction n, and the deformation caused by $\tilde{a}_\parallel$ is equivalent to a slow variation of the angle $\theta(r)$ (see (6.2.4)), i.e. a shift of the helix without a change of the spin-rotation plane. Inserting (6.2.4) into (6.2.3), we obtain the part of the free energy that depends on the deformation $\tilde{a}_\parallel$ or, equivalently, on θ:

$$H_0[\theta] = \frac{\rho}{\kappa^2 T}\int \left\{ \left[\frac{(\nabla\theta)^2 - p_0^2}{2p_0}\right]^2 + \frac{(\nabla^2\theta)^2}{4p_0^2}\right\} d^3r, \qquad \rho = \frac{5}{6}|\tau|c^2. \tag{6.2.6}$$

It is possible to show the fluctuations $\phi_\alpha(r)$ do not lead to any substantial variation $H_0[\theta]$ at $|\tau| > \gamma^{2/3}$. It is quite different with the transverse deformation $\tilde{a}_\perp$: without $\phi_\alpha(r)$ fluctuations being taken into account, the part of the free energy dependent on $\tilde{a}_\perp$ is

$$H_0^{(0)}[\tilde{a}_\perp] = \frac{1}{8T\kappa^2 p_0^2}\int \{|\nabla^2 a|^2 + 4|p_0\cdot\nabla a_\alpha|^2 + 2i(p_0\cdot\nabla a_\alpha\ \nabla^2 a_\alpha - \text{h.c.})\}\, d^3r. \tag{6.2.7}$$

Hence it is clear that $H_0^{(0)}[\tilde{a}_\perp]$ becomes zero for all fluctuations with momenta p such that $p_0\cdot p + p^2 = 0$. Taking the thermal fluctuations into account leads to a nonzero energy for all deformations with nonzero momenta; therefore they affect $H_0[\tilde{a}_\perp]$.

This calculation leads [2] to the following long-wave Hamiltonian depending on the direction of the normal vector n to the spin rotation plane:

$$H_0[n] = \int \left\{ \frac{p_0^2}{12\pi\kappa}\left(\frac{6}{5}\gamma\right)^{-1/3}(\partial_\mu n)^2 + \frac{5}{8}\,\frac{|\tau|c}{\kappa^2}\left[\frac{(p_0\cdot\nabla)n}{p_0}\right]^2\right\} d^3r. \tag{6.2.8}$$

Thus the spectrum of the long-wave fluctuations of the normal direction n proves to be quadratic and strongly anisotropic: the ratio of the coefficients of the first and second terms of (6.2.8) is of order $\gamma^{2/3}/|\tau| \ll 1$. The peculiarity of $H_0[n]$ is that the fluctuation spectrum with momenta $q \perp p_0$ does not become more rigid at decreasing temperature and increasing $|\tau|$ (the increase in the amplitude of the structure is compensated by the weakening of the "fast" fluctuations $\varphi_\alpha(r)$, which led to the appearance of the first term in (6.2.8)).

We have shown that slow deformations of the helical structure in the Heisenberg magnet are described by the two vectors: $Q = \nabla\theta$ (helical wave vector) and n, the corresponding deformation energies being given by (6.2.6) and (6.2.8). These formulae are obtained if spatial

fluctuations of the concentration of spin position points are neglected. Taking account of these fluctuations (i.e. the last term in (6.2.3)) leads (in terms of the vectors $\boldsymbol{Q}$ and $\boldsymbol{n}$) to the appearance of terms of the random-anisotropy type. The general form of these terms can be found from symmetry considerations: the initial isotropy of the spin Hamiltonian (6.1.3) requires that the (unaveraged) effective Hamiltonian of the fields θ and $\boldsymbol{n}$ be invariant with respect to the shift $\theta \to \theta + \text{const}$ and the homogeneous rotation $\boldsymbol{n} \to \hat{\boldsymbol{O}}\boldsymbol{n}$ ($\hat{\boldsymbol{O}}$ is an orthogonal matrix). Expressions of lower order with respect to the derivatives satisfying these requirements are

$$\tilde{H}[\theta] = \int f_\mu(\boldsymbol{r})\partial_\mu\theta(\boldsymbol{r})\,\mathrm{d}^3\boldsymbol{r}, \tag{6.2.9}$$

$$\tilde{H}[\boldsymbol{n}] = \int g_{\mu\nu}(\boldsymbol{r})\partial_\mu\boldsymbol{n}\,\partial_\nu\boldsymbol{n}\,\mathrm{d}^3\boldsymbol{r}, \tag{6.2.10}$$

where $f_\mu(\boldsymbol{r})$ and $g_{\mu\nu}(\boldsymbol{r})$ are random functions with a small correlation radius. A simple scaling analysis reveals that the Hamiltonian $H_0[\boldsymbol{n}]$ is stable with respect to $\tilde{H}[\boldsymbol{n}]$ in the sense that small random fields $g_{\mu\nu}(\boldsymbol{r})$ do not destroy the long-range order of $\boldsymbol{n}$ (just the same as thermal fluctuations in ordinary three-dimensional systems). This situation is changed drastically in the presence of interactions with random anisotropy in the spin space, but we shall not dwell upon this.

A rather different situation occurs for the perturbation $\tilde{H}[\theta]$; the bare correlation function of the θ field is

$$G_0(\boldsymbol{q}) = \langle\delta\theta(\boldsymbol{q})\delta\theta(-\boldsymbol{q})\rangle = \frac{2Tp_0^2\kappa^2}{\rho[q^4 + 4(\boldsymbol{q}\cdot\boldsymbol{p}_0)^2]}. \tag{6.2.11}$$

Hence the thermal fluctuations $\langle(\delta\theta)^2\rangle = \int G_0(\boldsymbol{q})\,\mathrm{d}^3\boldsymbol{q}$ diverge logarithmically, whereas the deformations generated by a random field diverge following a power law:

$$\overline{\langle(\delta\theta)^2\rangle} = \int_{q_1} \overline{f_\mu^2(\boldsymbol{q})}q^2G_0^2(\boldsymbol{q})\frac{\mathrm{d}^3\boldsymbol{q}}{(2\pi)^3} = O(q_1^{-2}) \tag{6.2.12}$$

(we have supposed — and we prove it below — that $\overline{f_\mu^2(\boldsymbol{q})} \underset{q\to 0}{\to} \text{const}$). It follows from (6.2.12) that disorder-induced deformations of the helical structure are large and that they can destroy HLRO at sufficiently large scales.

The same holds for the case of XY spins ($n = 2$), where the vector $\boldsymbol{n}$ is

fixed so that smooth structure deformations are described by the Hamiltonian $H[\theta]$ alone.

We now need the exact form of $\tilde{H}[\theta]$, which was written speculatively in (6.2.9). It can be obtained by using the replica trick, and leads to the result [2]

$$\tilde{H}[\theta_a] = -\frac{25p_0^2\kappa^2|\tau|}{36\pi}\int d^3r \sum_{a,b=1}^{N} \frac{1}{|Q_a - Q_b|} \arctan \frac{|Q_a - Q_b|}{2\kappa|\tau|^{1/2}}. \tag{6.2.13}$$

Here a and b are replica indices, $N \to 0$, $Q_a = \nabla\theta_a(r)$ and it is assumed that $|Q_a - Q_b| \ll p_0$. All numerical coefficients here and below are written down for Heisenberg ($n = 3$) spins (the XY case differs slightly). Later, we shall only consider the principal term of (6.2.13) at $|Q_a - Q_b| \ll \kappa|\tau|^{1/2}$, so that the total effective long-wave Hamiltonian $H[\theta]$ is (see (6.2.6)):

$$H[\theta_a] = \int \left\{ \frac{5|\tau|c}{2\kappa^2} \sum_a \left[\frac{(\nabla\theta_a)^2 - p_0^2}{2p_0} \right]^2 - \frac{25}{432\pi\kappa|\tau|^{1/2}} \sum_{a,b} (\nabla\theta_a)\cdot(\nabla\theta_b) \right\} d^3r. \tag{6.2.14}$$

The second term of (6.2.14) is equivalent to the random Gaussian δ-correlated field $f_\mu(r)$ (see (6.2.9)). The dependence of $H[\theta_a]$ on the angle between Q_a and Q_b implies the emergence of locally specified directions $Q = \nabla\theta$ (owing to the disorder of the system). Note that terms of the type $(Q_a \cdot Q_b)^2$ occur in the description of ferromagnets with a random anisotropy axis of second order [8, 10]. However, in this case the vector Q_a is an independent variable and is not equal to $\nabla\theta_a$. In our case $\tilde{H}[\theta_a]$ can be represented as a series in even Legandre polynomials of $Q_a \cdot Q_b / Q_a Q_b$, i.e. anisotropies of all orders are present.

6.3 *The Destruction of Helical LRO*

6.3.1 Exact rotational degeneracy The Hamiltonian of long-wave fluctuations of type (6.2.14) was thoroughly studied in reference [5]. It was shown that the bare Green function of long-wave fluctuations $G_0(p) \sim [(p\cdot Q)^2 + p^4]^{-1}$ is renormalized owing to the presence of $\tilde{H}[\theta]$ and acquires the form $G(p) \sim p^{-7/2}$. Let us briefly

repeat this derivation. The change of variables $\boldsymbol{r} = \tilde{\boldsymbol{r}}/2p_0$, $\theta = \frac{1}{2}\tilde{\theta}$ brings $H[\theta_a]$ to the form

$$H[\tilde{\theta}_a] = \int \mathrm{d}^3\tilde{r}\left\{\frac{1}{2t}\sum_a \left\{\frac{1}{4}A[(\tilde{\nabla}\tilde{\theta}_a)^2 - 1]^2 + B(\tilde{\nabla}^2\tilde{\theta}_a)^2\right\}\right.$$

$$\left. - \frac{g}{t^2}\sum_{a,b}(\tilde{\nabla}\tilde{\theta}_a)\cdot(\tilde{\nabla}\tilde{\theta}_b)\right\}, \tag{6.3.1}$$

where $A = B = 1$ and

$$t = \frac{8\kappa^2 p_0}{5c|\tau|}, \quad g = \frac{\kappa^3 p_0^3}{54\pi c^2|\tau|^{5/2}}.$$

The bare Green function corresponding to (6.3.1) is ($N=0$)

$$G_{ab}^{(0)} = t\delta_{ab}G_0(\tilde{\boldsymbol{p}}) + gp^2G_0^2(\tilde{\boldsymbol{p}}), \tag{6.3.2}$$

where

$$G_0(\tilde{\boldsymbol{p}}) = [A(\tilde{\boldsymbol{Q}}\cdot\tilde{\boldsymbol{p}})^2 + B\tilde{p}^4]^{-1}. \tag{6.3.3}$$

$\tilde{\boldsymbol{Q}} = \tilde{\nabla}\tilde{\theta}$ is the bare helical wave vector, $\tilde{\boldsymbol{Q}}^2 = 1$. Note that fluctuations of the field $\theta(\boldsymbol{r})$ with momentum $\boldsymbol{p}$ correspond to fluctuations of the overall field $S(\boldsymbol{r})$ with the momenta $\boldsymbol{Q} + \boldsymbol{p}$. The formulae (6.3.1)–(6.3.3) for the Hamiltonian and Green functions are valid at sufficiently large scales where fluctuations of the amplitude of the order parameter can be neglected. These fluctuations are small (see (6.2.5)) at $|\boldsymbol{p} - \boldsymbol{p}_0| \ll \kappa|\tau|^{1/2}$, which in terms of the dimensionless variables used in (6.3.1)–(6.3.3), yields

$$\tilde{\boldsymbol{Q}}\cdot\tilde{\boldsymbol{p}},\ p^2 \ll \frac{\kappa|\tau|^{1/2}}{p_0} = q_0^2. \tag{6.3.4}$$

The first term of $G_{ab}(\boldsymbol{r})$ corresponds physically to the averaged irreducible correlation function $\langle\langle\theta(0)\theta(\boldsymbol{r})\rangle\rangle$ characterizing the thermodynamical properties of the system; the second term $\langle\theta(0)\rangle\langle\theta(\boldsymbol{r})\rangle$ describes the deformation of the "bare" structure with $\theta(\boldsymbol{r}) = \boldsymbol{p}_0\cdot\boldsymbol{r}$ caused by disorder. At $g = 0$ the theory (6.3.1) is logarithmically renormalizable [11]. The parameters A and B are renormalized as follows:

$$A(p) = \left(1 + \frac{5t}{64\pi}\xi\right)^{-4/5}, \quad B(p) = \left(1 + \frac{5t}{64\pi}\xi\right)^{2/5},$$

$$\xi = \ln\frac{q_0}{p}.$$

The renormalizations are caused by strong thermal fluctuations, characteristic of a three-dimensional system with one-dimensional periodicity. It is convenient to perform the calculation with the field $\tilde{\theta}(\tilde{r})$ represented as the sum of the "slow" part $\tilde{\theta}_0(\tilde{r})$ and a small "fast" part $\tilde{\theta}_1(\tilde{r})$ and to integrate the partition function over $\tilde{\theta}_1(\tilde{r})$. As a result, the coefficients A and B acquire additional terms proportional to

$$\sum_b \frac{1}{t} \int G_{ab}(\tilde{p}) G_{ba}(\tilde{p}) \tilde{p}^4 \frac{d^3\tilde{p}}{(2\pi)^3} \sim t\xi. \tag{6.3.5}$$

At $g \neq 0$ the first corrections to A and B are also of the form (6.3.5), but the most singular contribution comes from the cross-term resulting from the multiplication of the first term of (6.3.2) by the second term:

$$-\delta A^{(1)} = 6\,\delta B^{(1)} = g \int \tilde{p}^6 G_0^3(\tilde{p}) \frac{d^3\tilde{p}}{(2\pi)^3} = \frac{3}{64\pi} \frac{g}{q^2}. \tag{6.3.6}$$

The integral (6.3.6) diverges quadratically at small momenta; q is a cut-off. The corrections (6.3.6) result not from thermal fluctuations but rather from deformation of the one-dimensional periodic ground state due to disorder of the system. Summation of these strongly diverging corrections can conveniently be started with a formal study of the model of the type (6.3.1) in a space of dimension $5-\epsilon$ (at $d=5$ the integral (6.3.6) would diverge logarithmically). It was shown in [5] that at $d=5-\epsilon$ there is a stable fixed point where the parameters A and B behave in a power-law like fashion: $A(\tilde{p}) \sim (\tilde{p}\cdot\tilde{Q})^{6\epsilon/11}$, $B(\tilde{p}) \sim \tilde{p}^{-2\epsilon/11}$ (the exponents are given to first order in ϵ). This means that deformations of the structure due to disorder of the system bring about partial isotropization of the spectrum. It is natural that the exponent obtained at first order in ϵ-expansion cannot be used at $d=3$. In [5] arguments are given in favour of the following form of the three-dimensional Green functions at $\tilde{p} \ll q_1 \approx \frac{1}{8}g^{1/2}$:

$$\left.\begin{aligned} G^{ab}(\tilde{p}) &= tG(\tilde{p})\delta_{ab} + gp^2G^2(\tilde{p})), \\ G(\tilde{p}) &= [\overline{A}(\tilde{p}\cdot\tilde{Q})^{7/2} + \overline{B}\tilde{p}^{7/2}]^{-1}, \end{aligned}\right\} \tag{6.3.7}$$

where the coefficients $\overline{A} \approx q_1^{-3}$ and $B \approx q_1^{1/2}$ are determined (in order of magnitude) by the matching of (6.3.7) with (6.3.3) at $\tilde{p} \sim q_1$, $(\tilde{p}\cdot\tilde{Q}) \sim q_1^2$; $q_1 \approx \frac{1}{8}g^{1/2}$ is the scale where the correction to (6.3.6) becomes of order unity. The formula (6.3.7) yields a correlation function of small fluctuations with respect to the disorder-distorted ground state (note that the parameter g is not renormalized, so that (6.3.2) retains its validity if $G_0(\tilde{p})$ is replaced by $G(\tilde{p})$).

It follows from (6.3.7) that the mean-square deformation of the phase $\theta(\boldsymbol{r}) = \frac{1}{2}\tilde{\theta}(\tilde{r})$ grows rapidly with distance:

$$\overline{(\langle\theta(0)\rangle - \langle\theta(\tilde{r})\rangle)^2} = \frac{g}{2}\int \tilde{p}^2 G^2(\tilde{p})(1-\cos\tilde{p}\cdot\tilde{r})\,\frac{\mathrm{d}^3\tilde{p}}{(2\pi)^3} \sim \max\,(\tilde{r}_\perp^2 q_1^2,\ \tilde{r}_\parallel^2 q_1^4). \tag{6.3.8}$$

Here $\tilde{r}_{\perp,\parallel}$ are transverse and longitudinal (with respect to the direction of the vector $\tilde{\boldsymbol{Q}}$) components of $\tilde{r}$. Thus the parameter q_1 determines the range of correlations in the spin-glass state. These correlations appear to be strongly anisotropic, with longitudinal correlation length (in the initial dimentional units)

$$R_\parallel \approx \frac{1}{2p_0 q_1^2} \approx \kappa^{-1}(0.2\gamma)^{-2}|\tau|^{5/2} \tag{6.3.9a}$$

and much smaller transverse correlation length

$$R_\perp \approx \frac{1}{2p_0 q_1} \approx (\kappa p_0)^{-1/2}(0.2\gamma)^{-1}|\tau|^{5/4}. \tag{6.3.9b}$$

Let us now discuss the domain of applicability of these results. First of all, the characteristic scale q_1 must be smaller than the high-momentum cutoff q_0 defined in (6.3.4). This condition is fulfilled over the whole range of our theory $|\tau| \geqslant \gamma^{2/3}$, as can be shown immediately. Another and much stronger restriction comes from the physical requirement that the transverse correlation length $R_\perp$ be longer than the characteristic scale $\kappa^{-1}|\tau|^{-1/2}$ of the short-scale fluctuations (the corresponding inequality for $R_\parallel$ holds for $|\tau| \geqslant \gamma^{2/3}$) and is of the form

$$|\tau|^{7/2} \geqslant \frac{p_0}{\kappa}(0.2\gamma)^2. \tag{6.3.10}$$

Formally, this restriction originates from the approximation $|\boldsymbol{Q}_a - \boldsymbol{Q}_b| \ll \kappa|\tau|^{1/2}$ used in the derivation of the last term in the Hamiltonian (6.2.14). In the opposite case to (6.3.10) the whole Hamiltonian (6.2.13) has to be used — which, we believe, modifies the *quantitative* results but leaves the qualitative picture of broken HLRO unchanged.

Up to now we have discussed translational order in the helical state. Another relevant type of order is orientational order, which is measured by the correlation function of the helical wave vector $\boldsymbol{Q} = \nabla\theta$. This can be obtained in the form

$$C(r) = \overline{\langle Q(0)Q(r)\rangle} \sim r_\perp^{-\Delta}, \quad \Delta = 2.5q_1^2 \qquad (6.3.11)$$

(see equation (30) of reference [5] and the discussion after it). Therefore there is no specified direction of Q in the whole system, and the correlation function $G(p)$ at the smallest momenta must become completely isotropic ($G(p) \equiv G(p)$). We shall not, however, investigate this range of very large scales, but rather we shall confine ourselves to distances in the interval $q_1^{-1} \ll \tilde{r} \ll e^{1/\Delta}$, where the local direction is defined by Q and the correlation function has the form (6.3.7).

We now consider thermal fluctuations of the phase: $\delta\theta(r) = \theta(r) - \langle\theta(r)\rangle$. They are determined by the first term of (6.3.7) and prove to be strongly divergent:

$$\langle(\delta\theta)^2\rangle = \frac{1}{4}t\int G(\tilde{p})\frac{d^3\tilde{p}}{(2\pi)^3} \simeq 0.03t(q_1L)^{1/2}, \qquad (6.3.12)$$

where L is the scale of the long-wave cutoff (in the direction transverse to Q). Nevertheless, these fluctuations can be regarded as Gaussian; the point is that $A(p) \sim \bar{A}p^{3/2}$, and therefore the vertex of the fluctuation interaction Γ resulting from the term $A(\nabla\theta)^4$ contains a high power of the momentum, so the interaction of long-wave fluctuations is suppressed (see reference [12] for a detailed discussion of a similar situation). This means that averages of the type $\langle\cos\delta\theta\rangle$ can be calculated according to the formula $\langle\cos\delta\theta\rangle = \exp(-\frac{1}{2}\langle(\delta\theta)^2\rangle]$. The divergence $\langle(\delta\theta)^2\rangle$ (as $L \to \infty$) shows that the mean value of the molecular field $|\langle S(r_i)\rangle| = \langle\rho\cos\theta(r_i)\rangle$ and the Edwards–Anderson order parameter $\langle S_i\rangle^2 = q_{EA}$ are both zero. Thus we have the equilibrium low-temperature phase of the spin glass with $q_{EA} = 0$, and consequently with the paramagnetic linear susceptibility $\chi = c/3T$. It is pretty difficult to distinguish between such a spin glass and a paramagnet by equilibrium magnetic measurements, although formally the difference is ensured by the slowly decreasing correlation function (6.3.11). These conclusions are largely based on the absence of a long-wave fluctuation cutoff ($L = \infty$) in the isotropic Hamiltonian (6.1.2), (6.1.3).

6.3.2 The effects of weak degeneracy breaking There are two kinds of effects that can remove the degeneracy with respect to Q rotations and produce a finite cutoff L. The first is connected with the angular dependence of the original interaction (6.1.1), which is measured by the value of the parameter ϵ_A (see (6.1.13)). The energy of the helical state

grows, then $\boldsymbol{Q}$ deviates from the optimum direction $\boldsymbol{l}_0$. This leads [2] to the appearance of an additional term in the Hamiltonian (6.3.1):

$$H_{\mathrm{A}} = \frac{1}{2t} \int \mathrm{d}^3\tilde{r}\, \mu_{\mathrm{A}} \sum_a (\tilde{\nabla}\tilde{\theta}_a - \boldsymbol{l}_0)^2, \tag{6.3.13}$$

with $\mu_{\mathrm{A}} = \frac{1}{2}(\kappa/p_0)^2 \epsilon_{\mathrm{A}}$.

The second effect is operative in the case of XY spins and is connected with magnetic dipole–dipole interaction with energy

$$E_{\mathrm{d}} = \frac{1}{2} G_{\mathrm{d}} \sum_{i,j} \left[\frac{\sigma_i \cdot \sigma_j}{r_{ij}^3} - \frac{3(\sigma_i \cdot \boldsymbol{r}_{ij})(\sigma_j \cdot \boldsymbol{r}_{ij})}{r_{ij}^5} \right], \tag{6.3.14}$$

which forces the vectors $\boldsymbol{Q}$ and $\boldsymbol{n}$ to be colinear [2]. Then the direction of $\boldsymbol{n}$ is fixed by easy-plane anisotropy, and the effective Hamiltonian (6.3.1) acquires an additional term

$$H_{\mathrm{d}} = -\frac{\mu_{\mathrm{d}}}{2t} \int \mathrm{d}^3\tilde{r} \sum_a ((\tilde{\nabla}\tilde{\theta}_a)\cdot \boldsymbol{n})^2, \tag{6.3.15}$$

with

$$\mu_{\mathrm{d}} = \frac{18\pi G_d}{W_0} \left(\frac{\kappa}{p_0} \right)^2 = \frac{1}{2} \left(\frac{\kappa}{p_0} \right)^2 \epsilon_{\mathrm{d}}.$$

Generally the interactions (6.3.13) and (6.3.15) can compete if the vectors $\boldsymbol{n}$ and $\boldsymbol{l}_0$ are not colinear. Nevertheless, we shall not consider that situation: in yttrium-based alloys (which are the most probable candidates for the application of this theory) $\boldsymbol{l}_0$ as well as $\boldsymbol{n}$ are colinear with the hexagonal c-axis. Then the total bare Hamiltonian $H + H_{\mathrm{d}} + H_{\mathrm{A}}$ reaches a minimum at $\tilde{\nabla}\theta = Q\boldsymbol{l}_0$, $Q \approx 1 + \mu/A$. The bare Green function (6.3.3) acquires an additional term:

$$G_0(\tilde{p}) = [A(\tilde{\boldsymbol{Q}}\cdot\tilde{\boldsymbol{p}})^2 + B\tilde{p}^4 + \mu\tilde{p}^2]^{-1} \tag{6.3.16}$$

with $\mu = \mu_{\mathrm{A}}\,(n=3)$ or $\mu = \mu_{\mathrm{A}} + \mu_{\mathrm{d}}\,(n=2)$. Therefore fluctuations with the smallest momenta ($\tilde{p} \leqslant q_2$) are suppressed. We determine q_2, assuming that $q_2 \ll q_1$. In this case the Green function in the region $q_2 \ll \tilde{p} \ll q_1$ is (see (6.3.7))

$$\left.\begin{aligned} G^{ab}(\tilde{p}) &= t\delta^{ab} G(\tilde{p}) + g\tilde{p}^2 G^2(\tilde{p}), \\ G(\tilde{p}) &= [\bar{A}(\boldsymbol{n}\cdot\tilde{\boldsymbol{p}})^{7/2} + \bar{B}\tilde{p}^{7/2} + \mu\tilde{p}_\perp^2]^{-1} \end{aligned}\right\} \tag{6.3.17}$$

(it is possible to show that the parameter μ is not renormalized). Comparing the third term of $G^{-1}(p)$ with the second term, we get

$$q_2 \approx \mu^{2/3}\bar{B}^{-2/3} \approx \mu^{2/3}q_1^{-1/3}. \tag{6.3.18}$$

The quantity q_2^{-1} serves as the long-wave cutoff L in (6.3.12): calculating $\langle(\delta\tilde{\theta})^2\rangle$ by means of the correlation function (6.3.17), we get ($\theta = \frac{1}{2}\tilde{\theta}$)

$$\langle(\delta\theta)^2\rangle \approx 0.05tq_1^{2/3}\mu^{-1/3}. \tag{6.3.19}$$

Thus for the EA order parameter q_{EA} we obtain

$$q_{EA} = \overline{|\langle S_i\rangle|^2} = 2\rho\overline{\langle\cos\delta\theta\rangle^2} = c^2\frac{5}{3}|\tau| \exp(-\Pi|\tau|^{-11/6}), \tag{6.3.20}$$

where

$$\Pi \approx (0.4\gamma)^{5/3}\left(\frac{\kappa}{p_0}\right)^{2/3}\epsilon^{-1/3}, \tag{6.3.21}$$

with $\epsilon = \epsilon_A$ ($n=3$) or $\epsilon = \epsilon_A + \epsilon_d = \epsilon_A + 36\pi G_d/W_0$ ($n=2$). Formally, the value of Π at $\gamma \ll 1$ can be small as well as large, but the second possibility looks rather improbable, so we shall discuss the case $\Pi \ll 1$ only (the results for $\Pi \gg 1$ can be found in [2]).

The above results hold under the condition

$$\epsilon \ll \frac{p_0}{\kappa}(0.2\gamma)^2|\tau|^{-5/2}, \tag{6.3.22}$$

which is equivalent to the inequality $q_2 \ll q_1$. In the opposite case the direction of Q is fixed effectively and thermal fluctuations $\delta\theta$ are weak, so that we have a diluted helical antiferromagnet with HLRO, which belongs to the "dirty XY" universality class.

6.4 *Magnetic Response of a Helical Spin Glass*

6.4.1 Linear response The magnetic response of the helical state depends on the direction of the magnetic field with respect to the spin-rotation plane (which is determined by its normal n). The longitudinal (magnetic field in the spin-rotation plane) response depends on the phase variable $\theta(r)$ fluctuation strength, and therefore possesses a

complicated structure in rather weak fields; this response will be studied below. The transverse response does not have these properties; therefore we simply write down the result for the linear transverse susceptibility $\chi_\perp$ with respect to the field h (see (6.2.1)):

$$\chi_{\alpha\beta} = \frac{\partial \overline{\langle \sigma_\alpha \rangle}}{\partial h_\beta} = \chi_\perp(\delta_{\alpha\beta} - \rho_{\alpha\beta}) + \chi_\parallel \rho_{\alpha\beta}, \tag{6.4.1}$$

with $\rho_{\alpha\beta}$ defined in (6.2.5). The present definition of χ as an average susceptibility differs from that of Section 6.1 by a factor c (volume concentration of spins):

$$\chi_\perp = \frac{c}{3T}\left(1 - \frac{6}{5}\rho\right) = \frac{c}{3T_0}[1 + O(\tau^2)]. \tag{6.4.2}$$

For the longitudinal linear susceptibility $\chi_\parallel$, we obtain

$$\begin{aligned} \chi_\parallel &= \frac{c}{3T}\left(1 + \frac{3}{5}\rho - \frac{3}{2}q_{\mathrm{EA}}\right) \\ &= \frac{c}{3T_0}\left\{1 + \frac{3}{2}|\tau|\left[1 - \frac{5}{3}\exp(-\Pi|\tau|^{-11/6})\right]\right\}. \end{aligned} \tag{6.4.3}$$

Note that the average susceptibility $\chi = \frac{1}{3}(2\chi_\parallel + \chi_\perp)$ can be expressed (in contrast with $\chi_\parallel$ and $\chi_\perp$) in terms of the Edwards–Anderson parameter only:

$$\chi = \frac{c}{3T}(1 - q_{\mathrm{EA}}). \tag{6.4.4}$$

It can be seen that the $\chi_\parallel(T)$ behaviour (6.4.3) differs significantly from the paramagnetic case even in the strong-fluctuation region $q_{\mathrm{EA}} \ll \rho$. In that region the coefficient in the Curie law has the value characteristic for XY rather than Heisenberg spins. Thus the Heisenberg spin system acquires an effective easy-plane anisotropy because of helical-structure formation. The temperature behaviour of $\chi_\parallel$ depends strongly on the value of the parameter Π (see Figure 21). At $\Pi \ll \gamma^{11/9}$ the thermal fluctuations of the $\theta(r)$ phase are weak in the whole region $|\tau| \gg \gamma^{2/3}$. At $\Pi \gg \gamma^{11/9}$ $\chi_\parallel(T)$ has a smooth maximum at $\tau \sim \tau^* = \Pi^{6/11}$. The point τ^* corresponds to crossover between regions of strong and weak phase fluctuations.

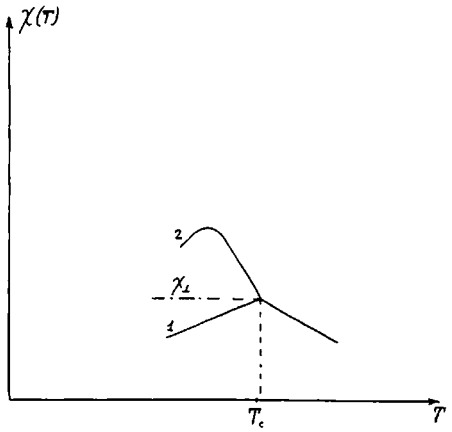

Figure 21 Qualititative T-dependence of the linear susceptibility. Line 1 corresponds to the longitudinal susceptibility $\chi_\parallel$ in the case $\Pi \ll \gamma^{11/9}$, whereas line 2 refers to $\gamma^{11/9} \ll \Pi \ll 1$. The transverse susceptibility $\chi_\perp$ is shown by a broken line.

6.4.2 Nonlinear susceptibility It is well known that the transition into the Edwards–Anderson spin-glass state is connected with the divergence of the nonlinear susceptibility $\chi_3 = -(\partial^2\chi/\partial h^2)_{h=0}$, Therefore such a divergence has to occur at the temperature T_c corresponding to the paramagnet → EA spin glass transition. More generally, it is tempting to connect the χ_3 divergence with the transition to a nonergodic state without long-range order. In this respect the helical-spin-glass state is of an intermediate nature, so it is interesting to study the behaviour of $\chi_{3,\parallel} = |\partial^2\chi/\partial h^2|$ in this state (we consider just the longitudinal response as that affected by soft thermal fluctuations).

A general expression for $\chi_{3,\parallel}$ in the region $\gamma^{2/3} \ll |\tau| \ll 1$ was obtained in reference [2]:

$$\chi_{3,\parallel} = \frac{25}{12}\,\frac{c\tau^2}{T_0^3}\int \mathrm{e}^{-tG(0)/2}\sinh^4\left[\frac{1}{8}\,tG(\tilde{r})\right]\mathrm{d}^3\tilde{r}, \qquad (6.4.5)$$

where $G(\tilde{r})$ is the inverse Fourier transform of $G(\tilde{p})$ from (6.3.17) and t is defined below (6.3.1). The most interesting case is $\gamma^{11/9} \ll \Pi \ll 1$, where the crossover between strong and weak phase fluctuations occurs. Then it can be shown that:

$$\chi_{3,\parallel} \approx 2\times 10^2 \frac{c\tau^2}{T_0^3}\left(\frac{p_0}{\kappa}\right)^2 \epsilon^{-2} f\left(\frac{|\tau|}{\tau^*}\right), \tag{6.4.6}$$

where $\tau^* = \Pi^{6/11}$ and the function $f(x)$ has the following asymptotic behaviour:

$$f(x) \sim \begin{cases} x^{11} & (x \ll 1), \\ x^{-22/3} & (x \gg 1) \end{cases} \tag{6.4.7}$$

(the complete form of the function $f(x)$ can be obtained by numerical integration in (6.4.5)). The large values of the exponents in (6.4.7) lead to a very sharp maximum of $\chi_{3,\parallel}$ at $\tau \approx \tau^*$, despite the absence of a true singularity.

6.4.3 Differential susceptibility in finite fields It was shown above (see (6.4.3)) that the linear susceptibility $\chi_\parallel(T)$ has a maximum at $|\tau| \approx \tau^* \gg \gamma^{2/3}$. The corresponding maximum in the finite-field differential susceptibility $\chi_\parallel(T, h)$ can be appreciably reduced and rounded by rather weak fields h owing to the large negative values of $\partial^2\chi_\parallel/\partial h^2 = -\chi_{3,\parallel}$ at $|\tau| \approx \tau^*$, (6.4.6); this effect is well-known in spin-glass physics [13].

We now discuss another aspect of the nonlinear response, which seems to be peculiar to the helical-spin-glass state. It appears that in the region $|\tau| \gg \tau^*$ an initial decrease of $\chi_\parallel(T, h)$ as a function of h is followed by an increase, which saturates at the "Curie-law" value determined by (6.4.3) and (6.4.4) at $q_{EA} = 0$. This phenomenon is a consequence of the obvious fact that the action of a uniform magnetic field on the diluted helical structure is similar to the action of a random field on an XY ferromagnet. The degree of disorder increases with h, which leads to a softening of the thermal-fluctuation spectrum and a decrease in q_{EA}. Obviously, this effect is relevant when thermal fluctuations at $h = 0$ are weak, i.e. $q_{EA} \approx 2\rho$.

It can be shown [2] that the main h-dependent term in the effective long-wave Hamiltonian $H[\tilde{\theta}_a]$ is of the form (cf. (6.3.1))

$$H_h[\tilde{\theta}_a] = \sum_{a,b} \int d^3\tilde{r} \left(-\frac{u}{t^2}\right)\tilde{\theta}_a\tilde{\theta}_b, \tag{6.4.8}$$

where

$$u = \frac{h^2\kappa^4}{30p_0cT_0^2}.$$

The replica Hamiltonian (6.4.8) corresponds physically to the presence of random fields coupled linearly with $\theta(r)$. Random fields of this type are the most relevant for large-scale structure deformation. In the region $u \ll g^2$ the Hamiltonian $H_h[\tilde{\theta}_a]$ is relevant on scales $L \gg q_1^{-1}$; therefore perturbative calculations have to be performed with respect to the "bare" spectrum (6.3.17). A calculation resembling that leading to (6.3.6) gives the following estimate for the characteristic value of the magnetic field h_0:

$$h_0 \approx 4\epsilon^{2/3} T_0 \left(\frac{c}{p_0^3}\right)^{1/6} \gamma^{1/3} |\tau|^{-1/3}. \tag{6.4.9}$$

At $h \gtrsim h_0$ the spectrum "stiffnesses" $\bar{A}$ and $\bar{B}$ (see (6.3.17)) decrease substantially. A quantitative description of the spectrum in this region appears to be too difficult at present. We believe that at $h \gtrsim h_0$ the intensity of phase fluctuations $\langle(\delta\theta)^2\rangle$ grows rapidly, so that q_{EA} decreases strongly. The qualitative behaviour of $\chi_\parallel(T, h)$ is depicted in Figure 22. Note that the field h_0 is much weaker than the characteristic internal fields ($\sim T_0$). The transverse susceptibility $\chi_\perp$ is insensitive to fields of order h_0.

All of the above discussion is relevant for the thermodynamic-equilibrium state. It is well known that variation of external fields in

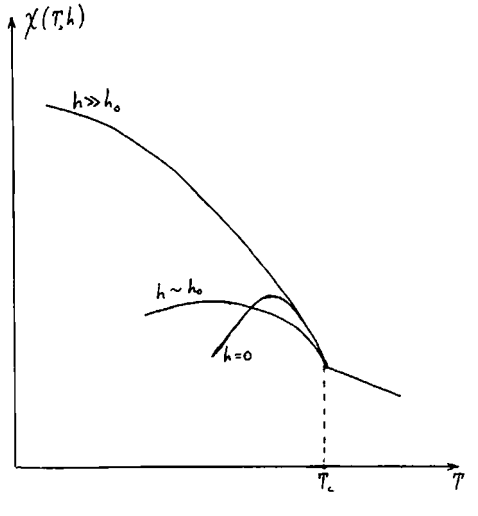

Figure 22 Differential longitudinal susceptibility $\chi_\parallel(T, h)$ at different magnetic fields h in the case $\gamma^{11/9} \ll \Pi \ll 1$.

spin-glass-like systems usually results in nonequilibrium states. Therefore our results for $\chi_{\parallel}(T, h)$ are relevant for field-cooled experiments, i.e. $\chi_{\parallel}(T, h) = \partial M_{FC}/\partial h_{\parallel}$.

6.5 *Application of The Theory: Y-based Alloys*

Recently Wenger and coworkers have reported [14, 15] the results of neutron-scattering experiments performed on diluted $Y_{1-x}Gd_x$ alloys ($x \geqslant 1.5 \times 10^{-2}$). They observed that at low temperatures short-range magnetic helical order appears. In these alloys the magnetic moments lie in the basal plane, whereas the wave vector of the helical structure is collinear with the hexagonal c-axis, with the wavelength being

$$\lambda = \frac{2\pi}{p_0} \approx 20 \text{ Å}. \tag{6.5.1}$$

The observed width of the scattering peaks is resolution limited if the transfer momentum is collinear with the c-axis, so that the corresponding longitudinal correlation length $R_{\parallel} > 600$ Å. This observation was interpreted by the authors as proof of the genuine helical antiferromagnetic long-range order in this state.

The thermodynamic properties of this state can be described [15] in terms of the theory of spin-density-wave stabilization developed by Overhauser [16] (see also the review [17]) who showed that the exchange of virtual paramagnons leads to a long-range oscillating interaction between localized Gd moments. Thus the effective interaction between Gd moments has the same form as the interaction between classical spins that we have considered in this section. Therefore we discuss here the application to YGd alloys of the theory developed in this section.

In this respect it is very important that the neutron magnetic scattering at the incommensurate wave vector p_0 persists up to rather high temperatures (25 K), with $T_0(x = 2.2\%)$ being only 6.64 K [14]. At these temperatures the scattering peak is broadened so that the corresponding longitudinal correlation length becomes 300 Å [14]. In this temperature range the intensity of the peak decreases with temperature roughly as T^{-1}. From these data, the key parameter of the theory, γ, can be determined [18]. Indeed, far above T_0, the correlation function $\langle S_i \cdot S_j \rangle$ is proportional to the interaction $J(r_i - r_j)$:

$$\langle S_i \cdot S_j \rangle \approx J(r_i - r_j)/T. \tag{6.5.2}$$

If the interaction $J(r_i - r_j)$ can be approximated by the form (6.1.1) then, from the experimental result that the correlation length is 300 Å at $T \approx 4T_0$, we conclude that the interaction length κ^{-1} is also

$$\kappa^{-1} \approx 300 \text{ Å} \tag{6.5.3}$$

in the Y-based alloys. Thus we are able to estimate γ. Using (6.5.3) and (6.5.1), we get

$$\gamma = \kappa p_0^2 / 4\pi c \approx 10^{-3} x^{-1}, \tag{6.5.4}$$

where $x = c/N_A$ is the atomic concentration of spins ($N_A = 3.0 \times 10^{22}$ at. cm^{-3} is the atomic density of Y). From the estimate (6.5.4), we conclude that the experiment was carried out in the range $\gamma \ll 1$, so that the existence of short-range helical order is only natural.

The problem of long-range order in this alloy deserves more careful consideration. As we have explained above, two situations are possible, with the choice between them being governed by the parameter ϵ_A. In the first one the anisotropy stabilizes the helical long-range order and the magnetic structure is antiferromagnetic, whereas in the second the long-wave fluctuations destroy the long-range order and result in spin-glass behaviour at large distances. The value of the parameter ϵ_A cannot be deduced from published experimental data; therefore we can only consider both situations separately, obtain properties of the system and compare them with experiment. (Note that ϵ_A can be deduced from data on the curvature of the diffraction peak in the direction transverse to p_0 at $T \gg T_0$.)

At $\epsilon_A \geqslant \gamma^{2/3} \approx 10^{-2} x^{-2/3}$ the degeneracy with respect to the rotation of the helix wave vector is unimportant, and a second order transition takes place at $T = T_c$, resulting in a helical antiferromagnet (Section 6.1). In the opposite case the anisotropy is small:

$$\epsilon_A \ll 10^{-2} x^{-2/3}, \tag{6.5.5}$$

so that degeneracy becomes important — at least at short scales. In this case two phase transitions occur (Section 6.1). There are no indications of two phase transitions in the experimental results [14, 15]; thus it is possible that $\epsilon_A \geqslant 0.15$. It would be very interesting to measure ϵ_A directly and compare the value with the above estimate. Anyway, the inequality (6.5.5) can be fulfilled in more-dilute alloys, and below we consider just this case. There are then two possibilities. The first is realized when the inequality opposite to (6.3.22) holds. In this case

large-scale fluctuations are suppressed and the low-temperature state possesses HLRO. More interesting is the opposite case, corresponding to the spin-glass state with HSRO; it should be realized under the condition (see (6.3.22))

$$\epsilon_A \ll 3 \times 10^{-3} x^{-2} |\tau|^{-5/2}. \tag{6.5.6}$$

Moreover, our quantitative results for the helical spin glass can be used if the inequality (6.3.10) holds, i.e.

$$|\tau|^{7/2} \geqslant 3 \times 10^{-3} x^{-2}. \tag{6.5.7}$$

In the parameter region defined by (6.5.6) and (6.5.7) the structure correlation lengths are (cf. (6.3.9))

$$R_\parallel \approx 10^2 x^2 |\tau|^{5/2} \text{ cm}, \quad R_\perp \approx 1.5 \times 10^{-3} x |\tau|^{5/4} \text{ cm}. \tag{6.5.8}$$

Let us consider, for example, an alloy with $x = 3 \times 10^{-3}$ at low temperature ($|\tau| \sim 1$). Then $\gamma \approx 0.3$, HSRO is realized at $\epsilon_A \leqslant 0.3$ (which looks very likely), and for the correlation lengths we have

$$R_\parallel \approx 10^5 \text{ Å}, \quad R_\perp \approx 500 \text{ Å}. \tag{6.5.9}$$

Thus we see that, even in this very dilute alloy, the longitudinal correlation length $R_\parallel$ appears to be practically infinite, whereas the transverse length $R_\perp$ is much smaller and can be obtained from the transverse width of the diffraction peak. It should be noted that just these measurements would be most informative in the phase-transition study.

All of the above estimates hold for $Y_{1-x}Dy_x$ and $Y_{1-x}Tb_x$ easy-plane alloys as well, but in this case ϵ_A should be replaced by $\epsilon = \epsilon_A + \epsilon_d$ (see Section 6.3); a rough estimate gives $\epsilon_d \approx 0.1$. It is possible, however, that strong spin–orbit coupling in these alloys can lead to some additional anisotropy within the easy plane and thus to stronger nonergodicity effects. Neutron-scattering (as well as synchrotron X-ray) experiments on these alloys at $x \approx (1+3) \times 10^{-3}$ would be very interesting.

Note finally that the spin-density-wave approach can probably be applied to some RKKY alloys also [17].

REFERENCES

[1] Feigel'man, M.V. (1983) *J. Phys.* **C16**, 6275.
[2] Ioffe, L.B. and Feigel'man, M.V. (1985) *ZhETF* **88**, 604.

[3] Vinokur, V.M., Ioffe, L.B., Larkin, A.I. and Feigel'man, M.V. (1987) *ZhETF* **93**, 343.
[4] Sompolinsky, H. (1987) in *Proceedings of Heidelberg Colloquium on Glassy Dynamics*, p. 485. Lecture Notes in Physics, Vol. 275. Berlin: Springer-Verlag. Eds. J.L. van Hemmen and I. Morganstern.
[5] Ioffe, L.B. and Feigel'man, M.V. (1983) *ZhETF* **85**, 1801.
[6] Amit, D.J., Gutfreund, H. and Sompolinsky, H. (1985) *Phys. Rev. Lett.* **55**, 1530; (1987) *Ann. Phys. (NY)* **173**, 30.
[7] Khmelnitsky, D.E. (1975) *ZhETF* **68**, 1960. Lubensky, T.C., (1975) *Phys. Rev.* **B11**, 3573.
[8] Dotsenko, V.S. and Feigel'man, M.V. (1983) *J. Phys.* **C16**, L803; (1984) *ZhETF* **86**, 1544.
[9] Brazovsky, S.A. (1975) *ZhETF* **68**, 175.
[10] Pelcovits, R.A., Pytte, E. and Rudnick, J. (1978) *Phys. Rev. Lett.* **40**, 476.
[11] Grinstein, G. and Pelcovits, R.A. (1981) *Phys. Rev.* **B26**, 915.
[12] Lubensky, T.C. and McKane, A. (1984) *Phys. Rev.* **B29**, 317.
[13] Binder, K. and Young, A.P. (1986) *Rev. Mod. Phys.* **58**, 801.
[14] Gotaas, J.A., Rhyne, J.J., Wenger, L.A. and Mydosh, J.A. (1986) *J. Magn. Magn. Mater.* **54–57**, 93.
[15] Wenger, L.E., Hunter, G.W., Mydosh, J.A., Gotaas, J.A. and Rhyne, J.J. (1986) *Phys. Rev. Lett.* **56**, 1090.
[16] Overhauser, A.W. (1959) *Phys. Rev. Lett.* **3**, 414; (1960) *J. Phys. Chem. Solids* **13**, 71.
[17] Mydosh, J.A. (1988) *J. Appl. Phys.* **63**, 4357.
[18] Feigel'man, M.V. and Ioffe, L.B. (1987) *Phys. Rev. Lett.* **58**, 1157.

7. SUPERCONDUCTING ANALOGUE OF SPIN GLASSES

7.1 Infinite-Range Model: Glass-Transition Temperature and Critical Dynamics

We consider a model [1, 2] consisting of two arrays of superconducting wires. Each array contains N parallel wires of equal length, and wires from different arrays are perpendicular to one another. The spacings between adjacent parallel wires are random, with average value l. Each wire from one array has a Josephson junction with each wire of the other array. In the presence of a magnetic field the phase of the order parameter varies along the wire; we denote the phase in the middle of the ith wire by φ_i (the wires are assumed to be thin so that the variation of phase across the wire can be ignored). Then the phase induced by the magnetic field is in the appropriate gauge, $\Phi_{ij} = x_i y_j l_H^{-2}$ and where $l_H = (hc/2eH)^{1/2}$ is the magnetic length, and x_i and y_i are the coordinates of the wires of the first and the second arrays (see Figure 23).

The Hamiltonian is of the form

$$\mathscr{H} = -\sum_{i,j} J_{ij}^{(0)} \cos(\varphi_i - \varphi_j - \Phi_{ij}) = -\operatorname{Re} \sum_{i,j} S_i^* J_{ij} S_j, \tag{7.1.1}$$

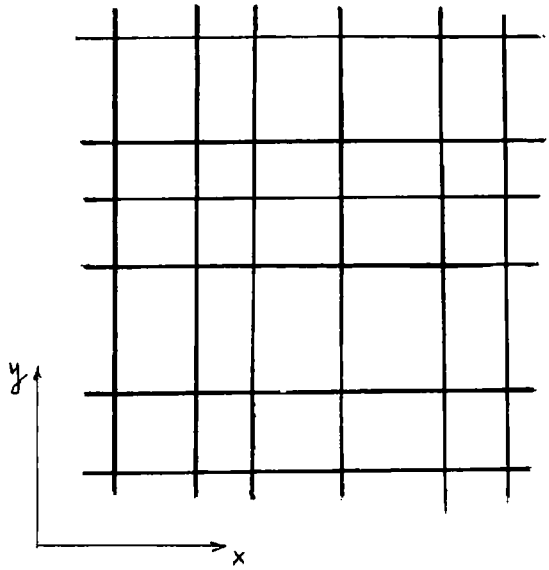

Figure 23 Random array of parallel superconducting wires.

with $S_i = e^{i\varphi_i}$ and $J_{ij} = J_{ij}^{(0)} e^{i\Phi_{ij}} = J \exp(ix_i y_j l_H^{-2})$. Here we neglect the fluctuations of the $J_{ij}^{(0)}$ values (and put $J_{ij}^{(0)} \equiv J$) since they are irrelevant in the infinite-range model. Below we shall suppose that $l_H \ll L = Nl$ (i.e. $H \gg H^* = \phi_0/L^2$, where ϕ_0 is the flux quantum) so that the phases Φ_{ij} are large. Thus the interactions J_{ij} are random, and their distribution can be described by a set of irreducible correlators:

$$K_{2m} = \overline{J_{i_1 j_1} J_{j_1 i_2} \ldots J_{j_m i_1}} = \left(\frac{2\pi l_H^2}{N^2 l^2}\right)^{m-1} J^{2m}. \tag{7.1.2}$$

Each subscript in the correlator (7.1.2) is repeated twice, but no summation is supposed. (Equation (7.1.2) is not valid in the case of a very weak magnetic field ($l_H \geq Nl$), which we do not consider here.)

It will be shown that the system properties depend on H, with characteristic scale H_0 given by

$$H_0 = \frac{\pi \hbar c}{Nl^2 e}. \tag{7.1.3}$$

At $H = H_0$ one flux quantum passes through the average area between adjacent wires. At $H \gg H_0$ the interaction (7.1.1) is completely random and corresponds to an XY spin glass. In the region $H^* \ll H \ll H_0$ the intervening behaviour of a "correlated spin glass" will be obtained.

We begin with the determination of the temperature $T_c(H)$ that corresponds to the transition from the high-T (*"paracoherent"*) state to the low-T glasslike state. An important difference between our problem and the usual case of an XY spin glass consists in the correlated nature of the interactions J_{ij}. Formally, a similar problem arises when one considers correlated spin glasses with helical correlations (see Section 6.1) or the Hopfield model of memory (see Section 8.1). Different (but equivalent) purely thermodynamic methods for the determination of T_c can be found in references [1] (generalized TAP [3] method) and [4] (replica method for the Hopfield model). Here we discuss a dynamic approach to T_c determination, which is most convenient for the present case. In this approach one calculates the average dynamic Green function $G(\omega, T)$ and defines T_c as the point of critical slowing down, i.e. the point of singularity of the effective kinetic coefficient:

$$\left.\frac{\partial G^{-1}(\omega, T_c)}{\partial \omega}\right|_{\omega \to 0} \to \infty. \tag{7.1.4}$$

We start from the expression for the total current I_{ij} through the junction (i, j) between the ith and jth wires:

$$I_{ij} = \frac{\hbar}{2eR}(\dot{\varphi}_i - \dot{\varphi}_j - \dot{\Phi}_{ij}) + \frac{2eJ}{\hbar} \sin(\varphi_i - \varphi_j - \Phi_{ij}) + \zeta_{ij}(t), \tag{7.1.5}$$

where the first term corresponds to the normal current (R is the junction resistance), the second to the superconducting current, while the last is the thermal noise (Nyquist) current distributed with correlation function $\langle \zeta_{ij}(t)\zeta_{kl}(t')\rangle = \zeta_{ik}\delta_{jl}(t-t')2T/R$. The equation of motion for the set of phases φ_i follows from (7.1.5) and current conservation (the Kirchhoff equations),

$$\sum_j I_{ij} = 0, \quad \sum_i I_{ij} = 0, \tag{7.1.6}$$

and can be rewritten in a more convenient form as

$$\dot{\varphi}_i = -\frac{1}{T}\,\mathrm{Im}\left(\sum_j S_i J_{ij} S_j^*\right) + \zeta_i(t),$$
$$\langle \zeta_i(t)\zeta_k(t')\rangle = 2\delta_{ik}\delta(t-t'). \tag{7.1.7}$$

In (7.1.7) and below the time is measured in the dimensionless units $t = \tilde{t}/t_r = \tilde{t}(4e^2RT/N\hbar^2)$. We shall use the method of the dynamic generating function [5, 6]:

$$\langle I_{ij}\rangle = \int I_{ij}(\varphi_i, \varphi_j)\exp\left(A[\psi, \varphi]\right)\mathscr{D}\varphi\,\mathscr{D}\psi, \tag{7.1.8}$$

where the angular brackets $\langle \ldots \rangle$ denote averaging over the thermal noise; $A[\psi, \varphi]$ is the effective action $A = A_0 + A_1$:

$$A_0 = \int \sum_i (\mathrm{i}\psi_i\dot{\varphi}_i - \psi_i^2)\,\mathrm{d}t,$$
$$A_1 = -\frac{1}{2T}\int \sum_{i,j}(\psi_i - \psi_j)J_{ij}S_iS_j^*\,\mathrm{d}t. \tag{7.1.9}$$

We begin with the calculation of the one-particle response and correlation functions:

$$\left.\begin{aligned} G_{ij}(t, t') &= -\langle S_i(t)\psi_j(t')S_j^*(t')\rangle, \\ C_{ij}(t, t') &= \langle S_i^*(t)S_j(t')\rangle. \end{aligned}\right\} \tag{7.1.10}$$

The response function G obeys the Dyson equation

$$G_{ij} = \delta_{ij}G' + G'\frac{J_{ik}}{2T}G_{kj}, \tag{7.1.11}$$

where G' is the sum of the one-particle irreducible diagrams (i.e. diagrams that cannot be disjointed by cutting one of the J-lines). In the leading-term approximation in J the function G' coincides with the bare (one-point) response function G_0. The higher-order terms in J lead to "reaction-field" corrections analogous to the TAP [3] term in the spin-glass static theory; thus we get $G' = (1 + \alpha - \mathrm{i}\omega)^{-1}$. Below we neglect the frequency dependence of α, which does not affect the low-frequency and static properties of the system. In the "thermodynamic" limit $N \to \infty$ the solution of (7.1.11) is given by the sum of diagrams that do not contain self-crossings (Figure 24):

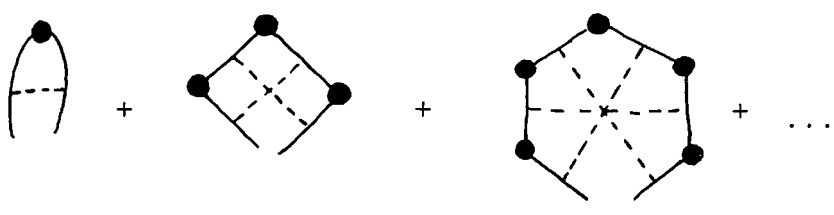

Figure 24 Diagram sequence for $\Sigma(\omega)$. Full dots are the Green functions $G(\omega)$; J_{ij} are shown as full lines and the averages of J_{ij} are shown as dashed lines.

$$\left.\begin{aligned} G_\omega &= G'_\omega(1+\Sigma_\omega G_\omega), \\ \Sigma_\omega &= \sum_m K_{2m}(NG_\omega)^{2m-1}. \end{aligned}\right\} \tag{7.1.12}$$

Insertion of K_{2m}, (7.1.2), into (7.1.12) and summation of the obtained series yields

$$(G'_\omega)^{-1} \equiv 1 + \alpha - i\omega = G_\omega^{-1} + \frac{J^2}{4T^2} G_\omega \left(1 - \frac{\pi l_H^2 J^2}{2T^2 l^2} G_\omega^2\right)^{-1}. \tag{7.1.13}$$

Above the transition point ($T > T_c$) the fluctuation–dissipation theorem (FDT) holds:

$$G(t) = -\theta(t)\frac{\partial}{\partial t} C(t), \tag{7.1.14}$$

which leads to the identity

$$G_{\omega=0} = \int G(t)\, dt = C(t=0) = \langle S_i(0) S_i^*(0)\rangle = 1. \tag{7.1.15}$$

We then differentiate (7.1.13) with respect to ω and take (7.1.4) and (7.1.15) into account. Finally, we obtain the transition temperature $T_c(H)$:

$$T_c(H) = \frac{J}{2}\left(\frac{N}{2}\right)^{1/2}\left[1 + \frac{2H_0}{H} + \left(1 + \frac{8H_0}{H}\right)^{1/2}\right]^{1/2}, \tag{7.1.16}$$

where H_0 is defined in (7.1.3). At $H \gg H_0$, (7.1.16) coincides with the well-known result for an XY spin glass [7]: $T_c = \frac{1}{2}JN^{1/2}$. The function $T_c(H)$ is presented graphically in Figure 25.

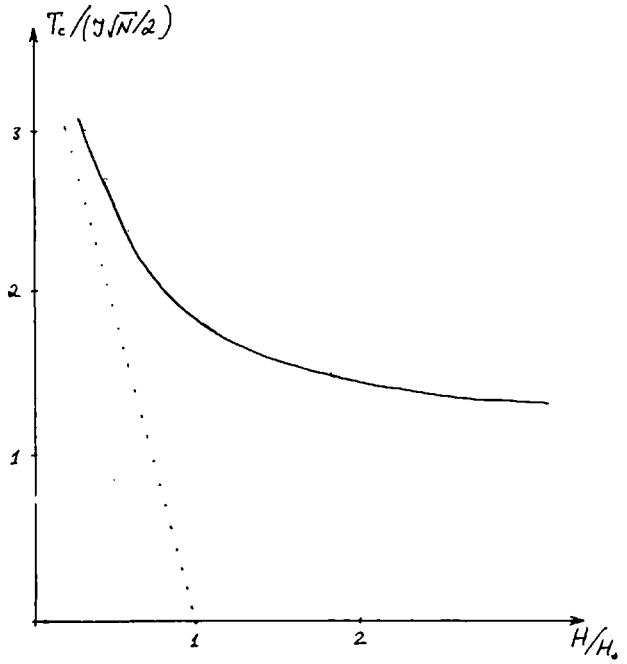

Figure 25 $T_c(H)$ behaviour at $H \gg H^*$; a possible first-order transition into the lowest-temperature phase is shown by a dotted line.

At small $\tau = T/T_c - 1$ and low frequency ω, (7.1.13) is simplified to

$$(G_\omega - 1)^2 + 2\tau(G_\omega + 1) + i\Gamma\omega = 0, \tag{7.1.17}$$

where Γ is the bare kinetic coefficient:

$$\Gamma = \frac{1-\kappa^2}{1+3\kappa}, \quad \kappa = \frac{J^2 N}{4T_c^2}\frac{H_0}{H}. \tag{7.1.18}$$

At $H \ll H_0$, $\Gamma \approx (H/2H_0)^{1/2}$; while in the opposite limit $H \gg H_0$, $\Gamma \to 1$. We then solve (7.1.17), Fourier-transform it and obtain

$$G(t) = \theta(t)\left(\frac{\Gamma}{4\pi}\right)^{1/2} t^{-3/2} e^{-t/t_0} \tag{7.1.19}$$

where $t_0 = \Gamma\tau^{-2}$. Then the FDT (7.1.14) yields the correlation function $C(t)$:

$$C(t) = \left(\frac{\Gamma}{\pi}\right)^{1/2}\left\{\frac{1}{t^{1/2}}\,\mathrm{e}^{-t/t_0} + \left(\frac{\pi}{t_0}\right)^{1/2}\left[\mathrm{erf}\left[\left(\frac{t}{t_0}\right)^{1/2}\right] - 1\right]\right\}. \tag{7.1.20}$$

These results ((7.1.19) and (7.1.20)) are valid near the transition point ($\tau \ll \Gamma$) and at large timescales $t \gg \Gamma^{-1}$.

We now consider the system response to a slow variation of the magnetic field $H(t)$. We study the total induced magnetic moment $M(t)$ of the system:

$$M = \frac{1}{c}\sum_{i,j} I_{ij x_i} y_j \tag{7.1.21}$$

$$= -\sum_{i,j} x_i y_j \left[\int \frac{2e}{\hbar c}\,\mathrm{Im}\,(J_{ij}S_iS_j^*)\mathrm{e}^{A_0[\psi,\varphi]+A_1[\psi,\varphi]}\,\mathscr{D}\psi\,\mathscr{D}\varphi - \frac{x_i y_j \dot{H}}{c^2 R t_\tau}\right].$$

We expand the exponential in (7.1.21) in powers of A_1, average all the terms over random J_{ij} (note that the dependence on time through $H(t)$ cannot be ignored here) and sum the resulting series in close analogy with the derivation of (7.1.12):

$$M(t) = -\left(\frac{N^3 l^2}{12}\right)^2 \frac{1}{c^2 R t_\tau}\left\{\frac{\mathrm{d}H}{\mathrm{d}t} + \frac{4}{1+\kappa}\int C(t,t')G(t,t')[H(t) - H(t')]\,\mathrm{d}t'\right\}. \tag{7.1.22}$$

(For the details of the derivation of (7.1.22) see [1].) To obtain the induced magnetic moment above the transition temperature, we insert (7.1.19) and (7.1.20) for G and C into (7.1.22):

$$M_\omega = \frac{\mathrm{i}\omega H_\omega}{c^2 R}\left(\frac{N^3 l^2}{12}\right)^2\left\{1 + \frac{2\Gamma}{\pi(1+\kappa)}\ln\frac{A\Gamma^2\tau^{-2}}{2-\mathrm{i}\omega t_1} + \frac{4}{\mathrm{i}\omega t_1}\left[(1-\mathrm{i}\omega t_1)^{1/2}\arctan\left[(1-\mathrm{i}\omega t_1)^{1/2}\right] - \tfrac{1}{4}\pi\right]\right\}, \tag{7.1.23}$$

where we have used physical time units: $\tilde{t} = t_\tau t$, $A \sim 1$, $t_1 = \Gamma\tau^{-2}(N\hbar^2/4e^2RT)$. The first term in the curly brackets in (7.1.23) corresponds to the normal current through the junctions while the second and the third are generated by superconducting fluctuations. Equation (7.1.23) implies that the effective conductivity of the network is

proportional to $\ln [\min (t_1, \omega^{-1})]$ and the effective inductance is proportional to $\min (t_1, \omega^{-1})$.

7.2 *Infinite-Range Model: Low-Temperature History-Dependent Behaviour*

The low-temperature phase of the system is characterized by the existence of a vast number of metastable states. The transition time t_{tr} between different metastable states is exponentially long in the thermodynamic limit $N \gg 1$. We consider the dynamics of the system on timescales shorter than t_{tr}, but longer than t_r: $t_r \ll t \ll t_{tr}$ (see Section 2.3 for a similar approach to the spin-glass SK model). On these timescales it is convenient to decompose the response and the correlation functions into fast and slow (anomalous) parts [6, 8]:

$$\begin{aligned} G(t, t') &= \tilde{G}(t, t') + \Delta(t, t'), \\ C(t, t') &= \tilde{C}(t, t') + q(t, t'), \end{aligned} \tag{7.2.1}$$

where the fast functions $\tilde{G}(t, t')$ and $\tilde{C}(t, t')$ decrease rapidly at $|t-t'| \gg t_r$, while the slow functions $\Delta(t, t')$ and $q(t, t')$ vary only on large timescales $t_{exp} \gg t_r$, which characterize the variation of the external parameter temperatures and the magnetic field. We emphasize once again that the final state of the system depends not only on the final values of the external parameters (T, H) but also on the path in the (T, H) plane that has led to these final values (however, the rate of motion along the path is not important). Here we shall obtain the equations that describe the final state of the system (and its history dependence) in the leading approximation over the reduced temperature $\tau = 1 - T/T_c$. We start from the dynamic generating functional (7.1.8). Averaging it over the randomness (cf. [1, 6]) yields the effective action $A = A_0 + A_{1eff}$:

$$\begin{aligned} A_{1eff} = \sum_i \iint [&- S_i(t) S_i^*(t') \psi_i(t) \psi_i(t') Q(t, t') \\ &+ (S_i(t) \psi_i(t) R^*(t, t') S_i(t') - \text{h.c.})] \, dt \, dt'. \end{aligned} \tag{7.2.2}$$

In the thermodynamic limit $N \gg 1$ both of the functions $Q(t, t')$ and $R(t, t')$ can be expressed through correlation and response functions $C(t, t')$ and $G(t, t')$ (this is due to the infinite-range interaction in the model under consideration). At small τ, $q(t, t') \sim \tau$, $\Delta(t, t') \sim \tau^2$;

therefore, keeping only the necessary terms (of the leading and the next order in τ), we get [1] at large timescales $|t-t'| \gg t_r$

$$R(t_1, t_2) = L(t_1, t_2)\Delta(t_1, t_2) + \eta \int \Delta(t_1, t)\Delta(t, t_2)\, dt, \tag{7.2.3}$$

$$Q(t_1, t_2) = L(t_1, t_2)q(t_1, t_2) + \eta \int [\Delta^*(t_1, t)q(t, t_2) + q(t_1, t)\Delta(t_2, t)]\, dt, \tag{7.2.4}$$

where we neglect the fast parts of G and C, which decay rapidly at $|t_1-t_2| \gg t_r$; $\eta = \kappa(3+\kappa)/(1-\kappa^2)$ and $L(t_1, t_2)$ is defined by

$$L(t_1, t_2) = \frac{J^2N}{4T_1T_2}\left\{1 - \frac{1}{2}\left[\frac{el^2N^2(H_1-H_2)}{6\hbar c}\right]^2 + \kappa g_1 g_2\right\} \times (1-\kappa g_1^2)^{-1}(1-\kappa g_2^2)^{-1}, \tag{7.2.5}$$

where

$$H_{1,2} \equiv H(t_{1,2}), \quad T_{1,2} \equiv T(t_{1,2}), \quad g_{1,2} \equiv g(t_{1,2}),$$

$$g(t) = \frac{T_c}{T(t)} \int G(t, t_1)\, dt_1 = \frac{T_c}{T(t)}\,[1-q(t, t)] \tag{7.2.6}$$

(the last equality in (7.2.6) is a consequence of the FDT, which holds for $\tilde{G}(t, t_1)$ and $\tilde{C}(t, t_1)$.

We now use the effective action (7.2.2) to determine the slow parts of the correlation and response functions, i.e. $q(t, t')$ and $\Delta(t, t')$, and obtain a closed system of equations for them. To average the correlation and response functions with the effective action (7.2.2), we introduce an additional slowly varying field $Z(t)$ with a Gaussian distribution:

$$[Z(t)Z(t')]_Z = Q(t, t'). \tag{7.2.7}$$

The averaging over thermodynamic ("fast") fluctuations of $S(t)$, which is subject to the effective field $h(t) = Z(t) + \int R(t, t')S(t')\, dt'$, can now be carried out, leaving only the averaging over $Z(t)$. Finally, averaging over $Z(t)$, keeping only the leading and the next orders in τ, yields

$$q(t, t') = Q(t, t')[1 - Q(t, t) - Q(t', t') + 2Q^2(t, t) + 2Q^2(t', t') + \tfrac{1}{2}|Q(t, t')|^2 + Q(t, t)Q(t', t')]$$

$$+ \int R^*(t, t'')Q(t'', t')\,dt'' + \int Q(t, t'')R(t', t'')\,dt'', \tag{7.2.8}$$

$$\Delta(t, t') = R(t, t')[1 - Q(t, t) - Q(t', t') + 2Q^2(t, t) + 2Q^2(t', t') + |Q(t, t')|^2 + Q(t, t)Q(t', t')] + \frac{1}{2}Q^2(t', t)R^*(t, t') + \int R(t, t'')\Delta(t'', t')\,dt''. \tag{7.2.9}$$

Equations (7.2.3), (7.2.4), (7.2.8) and (7.2.9) comprise a system of nonlinear integral equations that determine the functions $q(t, t')$ and $\Delta(t, t')$. These equations have a trivial solution $\Delta(t, t') = R(t, t') = 0$, which is analogous to the unstable replica-symmetric solution of the static model of an XY spin glass [7]. We seek another solution that violates the FDT and has $\Delta(t, t') \neq 0$. The functions $\Delta(t, t')$ and $R(t, t')$ are retarded, and this determines the limits of integration in (7.2.8) and (7.2.9). Using the condition $\Delta(t, t') \neq 0$ in the limit $t' \to t$, we get useful algebraic equations (for more details see [1]):

$$q(t, t) = \tau_t + \frac{3}{4(1+\eta)}\tau_t^2,$$

$$Q(t, t) = \tau_t + \left[2 + \frac{3}{4(1+\eta)}\right]\tau_t^2,$$

$$P \equiv \int [\Delta^*(t, t')q(t', t) + q(t, t')\Delta(t, t')]dt' = \frac{\tau_t^3}{1+\eta}, \tag{7.2.10}$$

where $\tau_\tau = \tau(t)$. The quantity $q(t, t)$ coincides with the Edwards–Anderson order parameter q_{EA} in the spin-glass theory. The dependence $q_{EA}(\tau)$ for XY spin glasses was studied in reference [9] within the framework of the Parisi replica-symmetry-breaking scheme [10, 11]. Our result (7.2.10) for $q(t, t)$ in strong fields $H \gg H_0$ coincides with $q_{EA}(\tau)$ obtained in [9].

Insertion of the expressions for $q(t, t)$ and $Q(t, t)$ into the system of equations (7.2.3), (7.2.8) and (7.2.9) gives a simplified final form:

$$\left[\frac{4}{3}|q(t_1, t_2)|^2 - \frac{1}{2}\left[\frac{el^2N^2(H_1 - H_2)}{6\hbar c}\right]^2 - (\tau_1^2 + \tau_2^2)\right]\bar{\Delta}(t_1, t_2) + \frac{2}{3}q^2(t_2, t_1)\bar{\Delta}^*(t_1, t_2)$$

$$+ \int \bar{\Delta}(t_1, t)\bar{\Delta}(t, t_2)\, dt = 0,$$

$$\left[\frac{2}{3}|q(t_1, t_2)|^2 - \frac{1}{2}\left[\frac{el^2N^2(H_1 - H_2)}{6\hbar c}\right]^2 - (\tau_1^2 + \tau_2^2)\right] q(t_1, t_2) + \int [\bar{\Delta}^*(t_1, t)q(t, t_2) + \bar{\Delta}(t_2, t)q^*(t, t_1)]\, dt = 0, \tag{7.2.11}$$

where $\tau_{1,2} = \tau(t_{1,2})$ and $\bar{\Delta} = \frac{4}{3}(1 + \eta)\Delta$. The system of equations (7.2.11) is invariant under reparametrization $t \to \tilde{t} = \tilde{t}(t)$, $\Delta(t, t') \to \Delta(\tilde{t}, \tilde{t}')\, d\tilde{t}'/dt$; therefore the solution is invariant under the same transformation, i.e. the final state of the system does not depend on the rate of motion along a given path in the (T, H) plane.

For the case of a constant magnetic field the system of equations (7.2.11) coincides (for real values of Δ) with the analogous system for an Ising spin glass in zero external field. Note an important property of these equations; the anomalous response function $\Delta(t, t')$ is equal to zero for all times t' such that $d\tau(t')/dt' \leqslant 0$ (see Section 2.3 for an extensive discussion).

We now study the magnetic moment M_S of the system below T_c, generated by superconducting currents induced by slow variation of the magnetic field $H(t)$ (cf. (7.1.22)):

$$M_S = -\left(\frac{N^3l^2}{12}\right)^2 \frac{e^2J}{c^2\hbar^2N^{1/2}} \frac{4}{(1+\kappa)^{1/2}(1-\kappa)} \int [q(t, t')\Delta(t, t') + q(t', t)\Delta^*(t, t')][H(t) - H(t')]\, dt'. \tag{7.2.12}$$

The value of M_S depends on the path in the (H, T) plane. For instance, $M_S = 0$ if the magnetic field was varied only at $T > T_c$, while variations of the magnetic field after cooling below T_c produce a diamagnetic response. Let us consider a common situation when the magnetic-field variation δH takes place after cooling at $t = t_f$ is complete. In the linear approximation in δH we can use $q(t, t')$ and $\Delta(t, t')$ calculated at $H =$ const; thus $\Delta(t, t') = 0$ at $t' > t_f$. Therefore the total contribution to the integral in (7.2.12) comes from the time domain $t' < t_f$, where $H(t) - H(t') = \delta H =$ const, so that the integral is proportional to the

quantity P calculated in (7.2.10). The final expression for the linear diamagnetic response is

$$M_S = -\left(\frac{N^3 l^2}{12}\right)^2 \frac{e^2}{\hbar c^2} \frac{J}{\hbar N^{1/2}} \frac{4(1+\kappa)^{1/2}}{1+3\kappa} \tau^3 \, \delta H \qquad (7.3.13)$$

(at $H \gg H_0$, $\kappa = 0$; while at $H \ll H_0$, $\kappa \to 1$ — see (7.1.18)).

The result (7.2.13) is valid for a sufficiently long timescale t_p of $H(t)$ variation:

$$\frac{1}{t_p} \ll \frac{e^2 R}{\hbar} \frac{J}{\hbar N^{1/2}} \tau^3; \qquad (7.2.14)$$

otherwise the fast part of the response must be taken into account.

The linear approximation (7.2.13) holds if the variation of the field is small so that the induced changes in $q(t, t')$ and $\Delta(t, t')$ are small: $\delta H \ll \delta H_m \approx 6\hbar\tau c/eN^2 l^2$. In the opposite case the integral (7.2.12) is no longer proportional to P and the whole system (7.2.11) has to be solved numerically in order to obtain M_S. A preliminary study [12] shows that at $\delta H \gg \delta H_{max}$ the induced magnetic moment is saturated at the maximum value M_{max}:

$$M_{max} \approx -\frac{(N^2 l)^2}{6} \frac{eJ}{\hbar c N^{1/2}} \frac{(1+\kappa)^{1/2}}{1+3\kappa} \tau^4. \qquad (7.2.15)$$

The derived equations (7.2.11) and the expression (7.2.12), in principle, offer the possibility of obtaining M_S for an arbitrary path in the (H, T) plane.

Note that (7.2.13) agrees with the result of reference [13] for the transverse stiffness ρ_S of a vector spin glass: $\rho_S \sim \tau^3$. The conclusion of John and Lubensky [14] regarding the zero value of ρ_S in the superconducting glass state is a consequence of the (unstable) replica-symmetric ansatz employed in [14].

Up to now, we have considered the spin-glass-like state of the Josephson network. It is rather clear that this is the only low-temperature state at $H \gtrsim H_0$, where J_{ij} correlations are irrelevant. However, at $H \ll H_0$ a different situation is possible. Indeed, it can be seen from (7.2.5) that at $H \ll H_0$ the leading-order expansion in q and τ that is employed is valid only in the region $\tau \lesssim \tau_H = (H/H_0)^{1/2}$. In similar problems for a helical spin glass (Section 6) and the Hopfield memory model (Section 8 below) the usual spin-glass state exists as an intermediate one; at lower

temperatures a first-order transition to a state with long-range order takes place. Such a transition at $\tau \sim \tau_H$ is also possible in the *Josephson network* (see the dotted line in Figure 25), but the nature of the supposed low-T state is unclear. Another possibility is a continuous crossover at $\tau \sim \tau_H$ to a state of the same symmetry, but different τ-dependences of the physical quantities.

It was tacitly assumed above that the temperature range under consideration is much lower than the transition temperature T_0 of each wire. If this is not the case then the T-dependence of J must be taken into account in all formula throughout the paper. In particular, (7.1.16) has to be considered as an equation for T_c (with J replaced by $J(T_c)$ in the right-hand side). The corresponding expression for τ at leading order in $T - T_c$ is then

$$\tau = (T - T_c)\left[\frac{1}{T_c} - \left(\frac{\partial \ln J}{\partial T}\right)_{T_c}\right]. \tag{7.2.16}$$

The temperature dependence of the Josephson-junction energy is given by

$$J_{ij}^{(0)} = \frac{\pi\hbar}{4e^2 R_{ij}} \Delta_{sc}(T) \tanh \frac{\Delta_{sc}(T)}{T} \underset{T \to T_0}{\sim} T_0 - T. \tag{7.2.17}$$

Thus we obtain (with (7.2.17)) the H-dependence of T_c in the field range $H^* \ll H \ll H_0$:

$$T_c(0) - T_c(H) \sim H^{1/2} \tag{7.2.18}$$

which holds if $T_0 - T_c(0) \ll T_c(0) - T_c(H)$.

7.3 *Finite-Range Systems*

7.3.1 Models and estimates We begin with a discussion of two previously studied models of superconducting glass (SCG). The first is a percolation network [14] consisting of superconducting granules situated at the lattice sites and coupled by Josephson junctions. The coupling $J_{ij}^{(0)}$ between two nearest-neighbour granules is either present and equal to J (with probability p) or absent. In the absence of a magnetic field this model is equivalent to an XY ferromagnetic spin model on the percolation network [15] (see (7.1.1) at $\Phi_{ij} \equiv 0$). A magnetic field induces nonzero phases:

$$\Phi_{ij} = \frac{1}{\phi_0} \int_{x_i}^{x_j} A(x) \cdot \mathrm{d}x, \tag{7.3.1}$$

so frustration of the interaction (7.1.1) appears. In (7.3.1) the integration is performed over the straight line between centres of granules x_i and x_j. The effect of frustration is strongest near the percolation threshold ($(p-p_c)/p_c \ll 1$), where the relevant lengthscale (i.e. the mean size of closed loops formed by interacting granules) is long: $\xi_p \sim (p-p_c)^{-\nu_p}$. John and Lubensky [14] obtained the mean-field phase diagram of this model at low T and small $p-p_c$. They showed the existence of three low-temperature states: the usual Meissner state, an Abrikosov vortex state and a spin-glass-like state. The last is the only low-temperature state that survives at "strong" magnetic fields $H \geqslant H_0 = \phi_0 \xi_p^{-2}$ corresponding to strong frustration of the interaction (7.1.1).

The second SCG model, studied by Shih, Ebner and Stroud [16], is constructed in close analogy with the real system of Pb granules immersed in a Zn matrix [17]. The intergranular interaction $J_{ij}^{(0)}$ in this system is due to the proximity effect:

$$J_{ij}^{(0)} = C\left(1 - \frac{T}{T_0}\right)^2 \exp\left[-\frac{r_{ij}}{\xi_n(T)}\right] f(r_{ij}/l_H), \tag{7.3.2}$$

where T_0 is the temperature of the superconducting transition within the granules (7.2 K for Pb), $\xi_n(T)$ is the coherence length of the normal metal, r_{ij} is the minimum distance between granules (i, j), and the function $f(x)$ (monotonically decreasing from 1 at $x = 0$ to zero as $x \to \infty$) describes the influence of the magnetic field on the electron wavefunctions in the normal metal. Under the experimental conditions [17] the granules used were of a size about the same as the interaction length $\xi_n(T) \approx 1.5$–2 μm, and the mean intergranular distance $\bar{r}_{ij} \approx 6$ μm, so that the system resembled a percolation network (see e.g. [18, 19]). A transition into a macroscopically coherent state at $H = 0$ was observed at $T_c \approx 4$ K, i.e. lower than T_0 but considerably higher than the superconducting-transition temperature of a Zn matrix (aprox. 0.8 K). Unfortunately, the effect of the magnetic field was not studied in reference [9]. This effect was investigated [16] by means of Monte-Carlo simulations on a model closely corresponding to the system described. The interaction energy was chosen in the form (7.1.1)

with $J_{ij}^{(0)}$ from (7.3.2) but without the factor $f(r/l_H)$; the phases Φ_{ij} are defined in (7.3.1). The results of reference [16] show the existence of a low-temperature state with finite superconducting density ρ_S at $T < T_c(H)$. The function $T_c(H)$ obtained in [16] decreases with increasing H and saturates at $H \gg H_0 \sim \phi_0 \bar{r}_{ij}^{-2}$ with $T_c(H \gg H_0) \approx 0.7 T_c(0)$. These results agree qualitatively with our result for the mean-field model (see (7.1.16) and Figure 25), although the simulation was performed for a system with short range interactions. Note, however, that the H-dependence of T_c in a real Pb–Zn composite system may differ from the dependence obtained in the simulations [16] because the latter did not take into account the dependence of the intergranular interaction strength $J_{ij}^{(0)}$ on the magnetic field (i.e. the factor $f(r_{ij}/l_H)$ in (7.3.2)), so that the gradual decrease of T_c in large magnetic fields is more plausible in real systems.

Both SCG models discussed above (as well as most of the granular [17, 20] and ceramic [21, 22] superconductors studied experimentally) are systems with short-range interaction. Unfortunately, the theory of short-range spin-glass systems is rather far from being properly developed at present. It is related in particular to vector spin glasses (and thus to SCG), where even the existence of a thermodynamic transition is a controversial subject (see Sections 4.3 and 4.6). Thus, in our opinion, the status of the mean field theories for these systems is unclear. To get a better understanding the results of these theories should be combined with extensive Monte-Carlo studies.

In order to fill the gap between the analytic theory for the infinite-range model and real systems, we now introduce [23] another class of SCG models with large but finite coordination number Z. These systems can probably be realized experimentally, but are of most relevance for theoretical study. We start from a two-dimensional version of the model and consider a system of superconducting wires (of lengths L and widths $d \ll L$) randomly situated in a plane with area density $\rho_2 \gg L^2$. Each intersection of two wires leads to a Josephson coupling of strength J. The average coordination number (i.e. the number of interacting neighbours) Z can be estimated as

$$Z_{2D} \approx \rho_2 L^2. \tag{7.3.3}$$

We now consider the correlation properties of the effective interaction J_{ij} in a magnetic field $H \gg H^* = \phi_0/L^2$ (cf. (7.1.2)). The main contribution to the correlator,

$$K_3 = \overline{J_{ij}J_{jk}J_{ki}} = J^3\,\overline{\exp\left(\Phi_{ij}+\Phi_{jk}+\Phi_{ki}\right)} = J^3\,\overline{\exp\left(\frac{iS_3}{l_H^2}\right)}, \tag{7.3.4}$$

stems from configurations of three wires (i, j, k) with the area of a small triangle $S_3 \leqslant l_H^2$ (see Figure 26). Therefore it is easy to see that $K_3 \sim J^3 l_H/L$. Similar considerations for higher values of m show that $(m \geqslant 2)$

$$K_m = \alpha_m J^m (l_H/L)^{m-2} \quad (\alpha_m \sim 1). \tag{7.3.5}$$

We now repeat the calculations of Section 7.1 and obtain the mean-field equations for the two-dimensional freezing temperature:

$$T_{2D}^{MF} \sim \begin{cases} J(T_{2D}^{MF}) L (\phi_0/H)^{1/2} \rho_2 & (H \ll H_0 = \rho_2 \phi_0), \\ J(T_{2D}^{MF}) \rho_2^{1/2} L & (H \gg H_0) \end{cases} \tag{7.3.6}$$

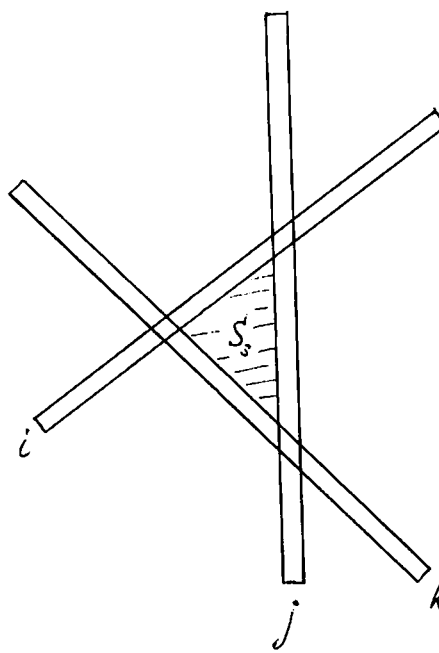

Figure 26 Three interacting superconducting wires.

(for the T-dependence of J, see (7.2.17)). It should be stressed that a real thermodynamic transition is undoubtedly absent in two-dimensional finite-range spin glasses [24]. Nevertheless, the value of T_{2D}^{MF} for a large-Z system is appropriate for showing the range of the dramatic slowing down of dynamical processes.

We now proceed to three-dimensional models. The first is a direct generalization of the above two-dimensional model to a multilayer structure without interlayer correlations in the wire positions. Then, for a large enough number N of layers, we obtain a three-dimensional (though anisotropic) system; all the estimates (7.3.4)–(7.3.6) hold for this case too. Obviously, the "true" critical behaviour of this system is two-dimensional in nature, but the corresponding temperature region (near T_c) can be made narrow for $N \gg 1$.

Another three-dimensional model consists of needle-like superconducting grains immersed randomly in a metallic or dielectric matrix ("a stack of hay"). In the first case the intergrain interaction is due to the proximity effect, and the effective thickness of the needles (i.e. the distance between two needles at which they interact strongly) can be estimated as $d_{\text{eff}} = \max(d, \xi_n(T))$; it is assumed that $d_{\text{eff}} \ll L$. In the second case the interaction is of Josephson type and $d_{\text{eff}} = d$. The average coordination number Z can be estimated as

$$Z \sim \rho L^2 d_{\text{eff}} \gg 1, \tag{7.3.7}$$

where ρ is the volume density of needles. The estimates of the J_{ij}-matrix correlations are performed analogously to the two-dimensional case, but with one important difference. Let us consider three needles in three dimensions; then the existence of interactions between the first and the third ones does not mean a high probability of third–first interaction. In fact, this probability is of order d_{eff}/L. The same factor appears (only once) for higher-order correlations; thus we obtain

$$K_2 = J^2(T), \quad K_m = \tilde{\alpha}_m J^m(T) \frac{d_{\text{eff}}}{L} \left(\frac{l_H}{L}\right)^{m-2} \quad (m \geqslant 3). \tag{7.3.8}$$

The asymptotic estimates of $T_c(H)$ following from (7.3.8) are similar to the previous one:

$$T_c \sim \begin{cases} J(T_c)(\rho d_{\text{eff}} L^2)^{1/2} \left(\dfrac{H_0}{H}\right)^{1/2} & \left(\dfrac{\phi_0}{L^2} = H^* \ll H \ll H_0\right), \quad (7.3.9) \\ J(T_c)(\rho d_{\text{eff}} L^2)^{1/2} & (H \gg H_0 \approx \rho d_{\text{eff}} \phi_0). \quad (7.3.10) \end{cases}$$

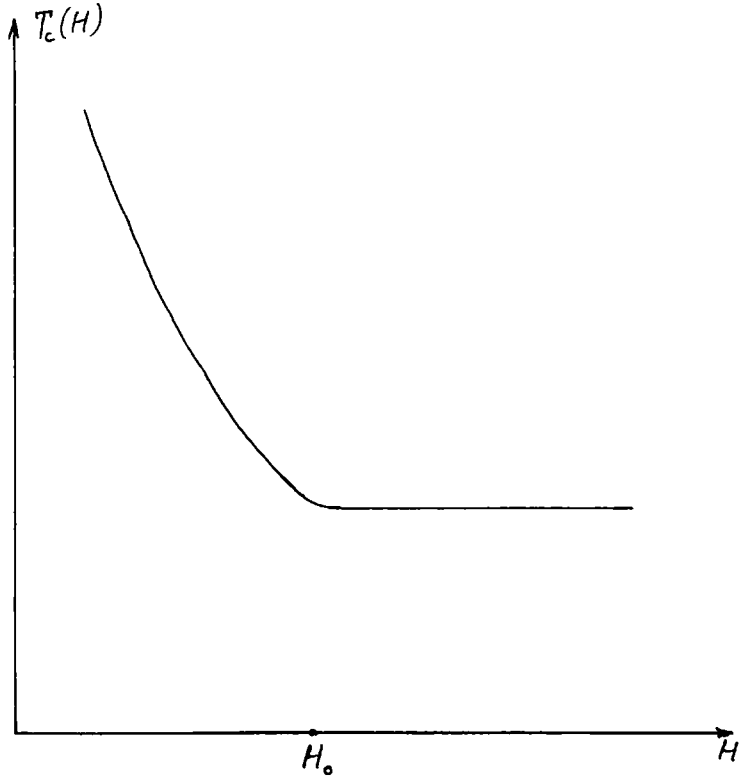

Figure 27 Qualitative dependence $T_c(H)$ for the "stack-of-hay" model.

Nevertheless, an important difference appears in the intermediate region $H \approx H_0$. It can be shown that (owing to the extra factor d_{eff}/L in (7.3.8)) the asymptotic dependences (7.3.9) and (7.3.10) do not merge smoothly as above, but nearly intersect so that the relative width of the crossover region is of order d_{eff}/L (see Figure 27). The T-dependence of J in (7.3.9) and (7.3.10) can be taken from (7.2.17) for the Josephson network or from (7.3.2) for the proximity network.

7.3.2 Critical dynamics of a superconducting glass Our main quantitative results for the infinite-range SCG model are (7.1.23) and (7.2.13) for the dynamic ($T > T_c$) and quasistatic ($T < T_c$) diamagnetic

responses respectively. It is of immediate interest to extend these results to the case of three-dimensional finite-range systems. The possibility of such an extension depends crucially on the existence of a thermodynamic phase transition in SCG systems, which are similar to XY spin glasses (see Section 4.6).

The problem of the existence of a phase transition in three-dimensional vector spin glasses is a controversial subject (see Sections 1.4 and 4.7). At present the common belief is (see e.g. [25]) that the phase transition, which is undoubtedly observed in real nearly isotropic spin glasses, is connected with the existence of a small but relevant anisotropy in the spin space. On the other hand, our analytic theory (Section 4) points at the possibility of a true phase transition — at least in models with large coordination number Z.

Superconducting glasses offer a unique possibility to look for three-dimensional critical behaviour in a truly isotropic system (any anisotropy in the order-parameter space being forbidden by the global gauge invariance). In spite of some subtle differences between SCG and XY spin glasses (see Section 4.6), the existence of a true phase transition in SCG systems would be very important for spin-glass theory in general (besides its obvious importance for the understanding of granular superconductivity).

Below we accept the hypothesis of an equilibrium phase transition in SCG and consider its implications for the diamagnetic response [23]. First, the general structure of (7.1.22) is retained for finite-range systems. Thus the frequency-dependent diamagnetic susceptibility can be expressed (with (7.1.14)) as $\chi(\omega) = i\omega\alpha(\omega)$, where

$$\alpha(\omega) = \alpha_0 \left[1 + \gamma \int_0^\infty C^2(t) e^{i\omega t} \, dt \right]. \tag{7.3.11}$$

Here $\gamma \sim 1$; α_0 is the high-temperature value produced by normal currents, whereas the second term is generated by superconducting fluctuations and is the main one in the critical region $\tau = (T - T_c)/T_c \ll 1$ (here and below we restrict the discussion to the case of strong frustration $H \geq H_0$).

The behaviour of $C(t)$ depends on the model considered. In models with large coordination number Z there exists a "mean-field critical" region (cf. Section 4) where the results (7.1.20) and (7.1.23) are applicable. Truly critical behaviour, which should reveal itself in the

vicinity of T_c, can be qualitatively expressed in the scaling form (we neglect here possible deviations from the usual scaling discussed in Section 4.3)

$$C(t) = \frac{1}{t^x} g\left(\frac{t}{t_1}\right), \tag{7.3.12}$$

with $t_1 \sim \tau^{-z\nu}$ being the characteristic relaxation time (in the infinite-range model $x = \frac{1}{2}$, $z\nu = 2$). The values of three-dimensional critical exponents are probably close to those of three-dimensional spin glasses, i.e. $x \ll 1$, $z\nu \gg 1$. These values can probably be calculated along the lines of the approach discussed in Section 4.6. Experimentally, the exponent x can be obtained by measuring the effective inductance $\mathscr{L}_{\text{eff}}$ at $\omega \gg t_1^{-1}$:

$$\mathscr{L}_{\text{eff}}(\omega) \sim \frac{\operatorname{Im} \alpha(\omega)}{\omega} \sim \omega^{-2+2x}, \tag{7.3.13}$$

whereas the exponent $z\nu$ can be found from the "phase angle" at $\omega \ll t_1^{-1}$:

$$\tan \theta = \frac{\operatorname{Im} \alpha(\omega)}{\operatorname{Re} \alpha(\omega)} \sim \omega t_1 \sim \omega \tau^{-z\nu}. \tag{7.3.14}$$

Moreover, the scaling function $g(t/t_1)$ can be obtained by means of the inverse Fourier transform of $\alpha(\omega)$:

$$\alpha(\omega) \sim \alpha_0 \int_0^\infty \frac{\mathrm{d}t}{t^{2x}} g^2\left(\frac{t}{t_1}\right) \mathrm{e}^{\mathrm{i}\omega t}. \tag{7.3.15}$$

The magnetic-response properties of short-range SCG systems can also be described by (7.3.12)–(7.3.15) if a finite-temperature transition exists in this case. Otherwise, a zero-temperature transition (similar to that of two-dimensional spin glasses [24]) can occur. In any case, drastic slowing down connected with the temperature decrease should reveal itself through the behaviour of the finite-frequency diamagnetic response (cf. (7.3.11)). Measurements on model systems with variable Z would be most useful in clearing up the phase-transition problem.

7.3.3 Low-temperature state: finite ρ_S and irreversibility We now proceed to discussion of the low-temperature properties of the SCG

state in finite-range systems. As a rigorous theory of this state is absent, we can only appeal to analogies with spin-glass phenomenology. Many features of the low-temperature behaviour of real spin glasses are described surprisingly well by the mean-field theory, whereas their behaviour at $T \geqslant T_c$ is in a very poor agreement with MFA predictions. In particular, the boundary of nonergodic behaviour (the de Almeida–Thouless line [26]) depends on the external magnetic field h in the same way in real spin glasses and the MFA theory. Moreover, similar "dynamic freezing" was obtained even in Monte-Carlo simulations [27] of a two-dimensional Ising spin glass despite the absence of a thermodynamic transition. The value of the exponent $(\frac{2}{3})$ in the de Almeida–Thouless law ($T_f(h) - T_f(0) \sim h^{2/3}$) is a direct consequence of the MFA relation $q(\tau) \sim |\tau|$ for the Edwards–Anderson order parameter measured on short timescales. Therefore the experimental corroboration of the exponent $\frac{2}{3}$ is an indication of the applicability of the MFA relation $q(\tau) \sim |\tau|$ to real spin glasses. Motivated by these arguments, we suppose that in the SCG state a dependence of the type (7.2.13) also holds for finite-range systems, since it follows from the general equation (7.2.12) and the relations $\Delta \sim q^2$, $q \sim |\tau|$, which are likey to be valid.

Thus we arrive at the following conclusion about the finite value of the superfluid density ρ_S (which is the equivalent of (7.2.13) for finite-range systems):

$$\rho_S = \text{const} \times |\tau|^3. \tag{7.3.16}$$

At the same time, we cannot rule out the possibility that (7.3.16) holds only in the nonequilibrium regime with the "constant" being a slow (say, logarithmic) function of time.

The concrete form of the history-dependent equations of state replacing the mean-field equations (7.2.11) is unclear. Nevertheless, it seems probable that some general properties of their solutions are retained (such as the vanishing of $\Delta(t, t')$ at t' corresponding to increasing temperature). At the same time, the independence of the physical properties on the rate of τ and H variations is a unique property of the infinite-range model. Moreover, in a real SCG system the irreversible behaviour is probably accompanied by the ageing phenomena common for spin glasses (see Section 1.3 for a discussion).

The quantity that is usually measured by experimentalists is the magnetic susceptibility χ. There are two types of contribution to χ,

namely χ_0, which is produced from individual granules, and χ_1, which results from intergranular supercurrents. In the SCG state χ_1 is completely irreversible (i.e. it contributes to diamagnetic shielding, but not to the Meissner effect), whereas χ_0 is reversible (in the low-field region $H \ll H_{c1}$, where the granules are in the Meissner state). Therefore the onset of magnetic irreversibility at some $T = T_f(H)$ in the field range $H_0 \gtrsim H \ll H_{c1}$ would be a manifestation of the SCG state. As follows from (7.3.16), in the vicinity of T_f the screening length $\lambda \sim \rho_S^{-1/2} \sim (T_f - T)^{-3/2}$ is very long and, in particular, can be larger than the sample size L. Indeed, it is known (see e.g. [28]) that in ceramic superconductors a broad temperature region exists that is characterized by weak diamagnetic shielding ($|4\pi\chi| \ll 1$). In that region the irreversible part of the susceptibility, χ_{irr}, should be proportional to ρ_S:

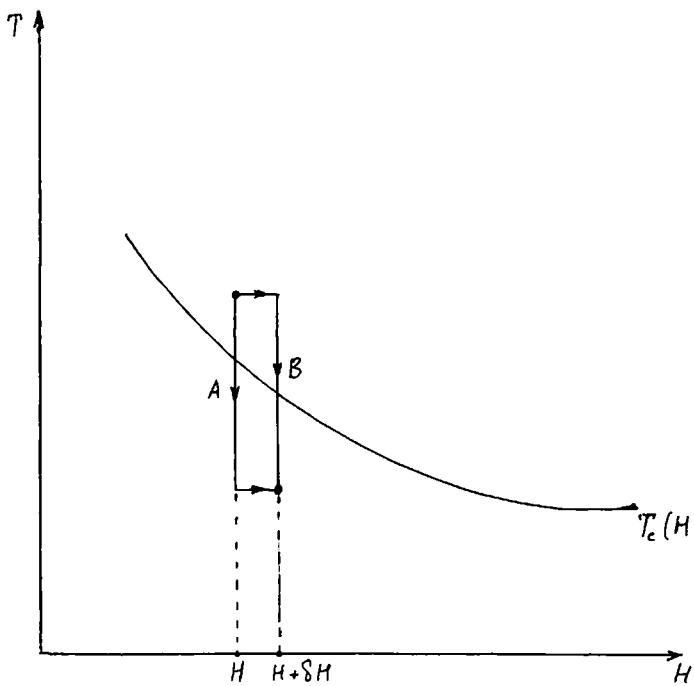

Figure 28 Thermal histories of samples used for determination of χ_{irr}.

$$\chi_{\rm irr} \sim [T_{\rm f}(H) - T]^3. \tag{7.3.17}$$

It should be emphasized that the result (7.3.17) is valid for the differential irreversible susceptibility, which can be measured by the following procedure: (i) the sample is cooled in the field H to the temperature $T < T_{\rm f}(H)$; (ii) the magnetic field is varied slightly, $H \to H + \delta H$, and the magnetization $M(H+\delta H, T)$ is measured (which corresponds to path A in Figure 28); (iii) the usual field-cooling magnetization $M_{\rm FC}(H+\delta H, T)$ (corresponding to path B in Figure 28) is measured; (iv) the irreversible susceptibility $\chi_{\rm irr}$ is calculated as

$$\chi_{\rm irr}(T) = \frac{M(H+\delta H, T) - M_{\rm FC}(H, T)}{\delta H}. \tag{7.3.18}$$

The temperature $T_{\rm f}(H)$ of the transition to the SCG state should be identified with the onset of nonzero $\chi_{\rm irr}$. Note that this criterion is somewhat different from that usually employed, which is the onset of the difference between the $M_{\rm FC}(T)$ and $M_{\rm ZFC}(T)$ curves. Physically, the point is that the zero-field-cooling magnetization $M_{\rm ZFC}$ is a strongly nonequilibrium quantity that should not be used in the determination of $T_{\rm f}(H)$. In practice, the difference between these two definitions of $T_{\rm f}(H)$ can be rather noticable, especially when the scaling behaviour of $\Delta T_{\rm f}(H)$ versus H is studied.

7.4 Conclusions

Granular superconductors with Josephson- or proximity-type couplings between granules can exhibit a superconducting-glass (SCG) state that is characterized by strong irreversibility and history-dependence of the diamagnetic response. The scale of the magnetic field H_0 that induces SCG behaviour is as estimated in Section 7.3.1 and can be rather low (approx. 1 Oe for ceramic materials). The SCG state is characterized (in contrast with the pinned Abrikosov vortex state) by

(i) strong critical enhancement of the dynamic diamagnetic response (Section 7.3.2), and
(ii) anomalous temperature dependence of the superfluid density and irreversible susceptibility: $\rho_{\rm S} \sim \chi_{\rm irr} \sim [T_{\rm f}(H) - T]^3$.

Recent experiments on high-$T_{\rm c}$ ceramics [22, 28, 29] show strong irreversibility effects and slow relaxation of the magnetic response. These

phenomena have been interpreted [29, 30] as evidence for the SCG state. However, at present these experiments cannot discriminate unambiguously [31] between the SCG and the Abrikosov state with vortex pinning. This can be done by a search for the above-mentioned peculiar properties of the SCG state. Some recent unusual results [32] concerning the temperature dependence of the magnetization relaxation rate at $T < T_f(H)$ should also be noted. It appears that the "logarithmic relaxation rate" $R = \partial \ln M / \partial \ln t$ is a nonmonotonic function of temperature that goes to zero at $T \to T_f(H)$. This type of behaviour has never been observed in spin glasses. Nevertheless, it seems at least compatible with the existence of an SCG state. The point is that there are two different sources of diamagnetic response in granular superconductors, the first being connected with the granules themselves, whereas the second is connected with weak intergranular currents. It is tempting to suppose that the logarithmic relaxation is produced mainly by the second source, while the total scale of the remanent magnetization can be determined by the first (it should be recalled that the irreversible magnetization produced by intergranular currents decreases very rapidly as $T \to T_f(H)$ (cf. (7.3.18)). It is therefore probable that the proper definition of the logarithmic relaxation rate should be $\tilde{R} = M_{irr}^{-1} \partial M / \partial \ln t$. It would be very interesting to find out whether the T-dependence of $\tilde{R}$ is of the usual spin-glass type.

Obviously, these arguments can be applied in the case of relatively weak external magnetic fields $H < H_{c1}$, in order to avoid strong irreversibility effects inside the grains. In the field range $H \gtrsim H_{c1}$ the usual vortex-creep picture [33] has been shown to be qualitatively acceptable [34].

Note finally that specially designed weak-link three-dimensional networks with controllable parameters (in particular, coordination number Z) would be very useful model systems for the study of the SCG state, similar to special-purpose Monte-Carlo computers for Ising-model studies.

REFERENCES

[1] Vinokur, V.M., Ioffe, L.B., Larkin, A.I. and Fiegel'man, M.V. (1987) *ZhETF* **93**, 343.

[2] Feigel'man, M.V., Ioffe, L.B., Larkin, A.I. and Vinokur, V.M. (1987) *Mod. Phys. Lett.* **B1**, 27.

[3] Thouless, D.J., Anderson, P.W. and Palmer, R.G. (1977) *Phil. Mag.* **35**, 593.
[4] Amit, D.J., Gutfreund, H. and Sompolinsky, H. (1985) *Phys. Rev. Lett.* **55**, 1530; (1987) *Ann. Phys. (NY)* **173**, 30.
[5] De Dominicis, C. and Peliti, L. (1978) *Phys. Rev.* **B18**, 353.
[6] Sompolinsky, H. and Zippelius, A. (1982) *Phys. Rev.* **B25**, 6860.
[7] Sherrington, D. and Kirkpatrick, S. (1978) *Phys. Rev.* **B17**, 4385.
[8] Sompolinsky, H. (1981) *Phys. Rev. Lett.* **47**, 935.
[9] Gabay, M., Garel, T. and De Dominicis, C. (1982) *J. Phys.* **C15**, 7165.
[10] Parisi, G. (1980) *J. Phys.* **A13**, 1101.
[11] Mezard, M., Parisi, G. and Virasoro, M.A. (1987) *Spin Glass Theory and Beyond.* Singapore: World Scientific.
[12] Ioffe, L.B., "Critical current in superconducting glass model", unpublished.
[13] Sompolinsky, H., Kotliar, G. and Zippelius, A. (1984) *Phys. Rev. Lett.* **52**, 392.
[14] John, S. and Lubensky, T.C. (1985) *Phys. Rev. Lett.* **55**, 1014; (1986) *Phys. Rev.* **B34**, 4815.
[15] Stephen, M.J. (1978) *Phys. Rev.* **B17**, 1444. Harris, A.B. and Lubensky, T.C. (1987) *Phys. Rev.* **B35**, 6964.
[16] Shih, W.Y., Ebner, C. and Stroud, D. (1984) *Phys. Rev.* **B30**, 134.
[17] Boysel, R.M., Caplin, A.D., Dalimin, M.N.B. and Guy, C.N. (1983) *Phys. Rev.* **B27**, 554.
[18] Ioffe, L.B. (1981) *ZhETF* **80**, 1199.
[19] Ioffe, L.B. and Larkin, A.I. (1981) *ZhETF* **81**, 707.
[20] Raboutou, A., Rosenblatt, J. and Peyral, P. (1980) *Phys. Rev. Lett.* **45**, 1035.
[21] Gaborich, A.M. and Moiseev, D.P. (1986) *Usp. Fiz. Nauk* **150**, 599.
[22] Müller, K.A., Takashige, M. and Bednorz, J.G. (1987) *Phys. Rev. Lett.* **58**, 1143. Klimenko, A.G., Blinov, A.G., Vesnin, Yu.I. and Starikov, M.A. (1987) *Pis'ma ZhETF Suppl.* **46**, 196. Mota, A.C., Pollini, A., Visani, P., Müller, K.A. and Bednorz, J.G. (1987) *Phys. Rev.* **B36**, 4011. Tuominen, T., Gordon, A.M. and Macartney, M.L. (1988) *Phys. Rev.* **B37**, 548. Giavanella, C., Chappert, C. and Beauvillain, P. (1988) *Europhys. Lett.* **5**, 535.
[23] Feigel'man, M.V., Ioffe, L.B., Larkin, A.I. and Vinokur, V.M. (1988) in *Progress in High-T_c Superconductors*, Vol. 4 (ed. A. Borone and A. Larkin), p. 340. Singapore: World Scientific.
[24] Young, A.P. (1984) *J. Phys.* **C17**, L517.
[25] Bray, A.J. and Moore, M.A. (1987) in *Proceedings of Heidelberg Colloquium on Glassy Dynamics*, p. 121. Lecture Notes in Physics, Vol. 275. Berlin: Springer-Verlag. Eds. J.L. van Hemmen and I. Morganstern.
[26] de Almeida, J.R.L. and Thouless, D.J. (1978) *J. Phys.* **A11**, 983; (1978) *ibid.* **C11**, L871.
[27] Kinzel, W. and Binder, K. (1983) *Phys. Rev. Lett.* **50**, 1509.
[28] Giovannella, C., Chappert, C. and Beavillain, P. (1988) *Europhys. Lett.* **5**, 535.
[29] Deutscher, G. and Müller, K.A. (1987) *Phys. Rev. Lett.* **59**, 1745.
[30] Morgenstern, I., Müller, K.A. and Bednorz, J.G. (1987) *Z. Phys.* **B69**, 33.
[31] Prejean, J.J. and Souletie, J. (1988) *Phys. Rev. Lett.* **60**, 1884.
[32] Tuominen, T., Gordon, A.M. and Macartney, M.L. (1988) *Phys. Rev.* **B37**, 548.
[33] Anderson, P.W. (1962) *Phys. Rev. Lett.* **9**, 309. Beasley, M.R., Labusch, R. and Webb, W.W. (1969) *Phys. Rev.* **181**, 682. Campbell, A.M. and Evetts, J.E. (1972) *Adv. Phys.* **21**, 199.
[34] Yeshurun, Y. and Malozemoff, A.P. (1988) *Phys. Rev. Lett.* **60**, 2202.

8. STATISTICAL MODELS OF NEURAL NETWORKS

8.1 The Hopfield Model

The first statistical model capable of performing the simplest actions of a content-addressable memory was introduced by Hopfield [1]. As we described in Section 1.8, its dynamics is governed by the Ising Hamiltonian

$$H = \sum_{i,j} J_{ij} S_i S_j, \tag{8.1.1}$$

where J_{ij} should be chosen according to the Hebb rule:

$$J_{ij} = -\frac{1}{N} \sum_{p=1}^{k} \xi_i^{(p)} \xi_j^{(p)}. \tag{8.1.2}$$

The patterns $\xi_i^{(p)}$ are random sets of Ising variables. We first discuss the retrieval properties of the model (8.1.1), (8.1.2), assuming patterns $\xi_i^{(p)}$ to be uncorrelated, but then in Section 8.2 we shall return to this point and study the retrieval of correlated patterns as well. The form (8.1.2) of the interaction matrix implies that interaction is of infinite range, which allows us to obtain analytical results in the thermodynamic limit $N \to \infty$.

It can be shown [2] that if k remains finite but $N \to \infty$ then at a critical temperature T_c the disordered paramagnetic state becomes unstable, and at lower temperatures $2k$ ordered states appear. Each of these states is correlated with one of the stored patterns $\xi_i^{(p)}$. To study these correlations, it is convenient to introduce "overlaps" m_μ of a given state with the pattern $\xi_i^{(\mu)}$, defined by

$$m_\mu = \frac{1}{N} \sum_i \langle \sigma_i \rangle \xi_i^{(\mu)}, \tag{8.1.3}$$

where $\langle \ldots \rangle$ denotes the thermal average. The local magnetization in the restored low-temperature state is proportional to $\xi_i^{(\mu)}$, with a coefficient m that can be found from the mean-field equations: $\langle \sigma_i \rangle = \xi_i^{(\mu)} m$, $m = \tanh \beta m$.

At lower temperatures new stable states appear, these states being mixtures of the initial patterns $\xi_i^{(\mu)}$. The number of "spurious" states increases with decreasing temperature and increasing k. All of these

states are separated by free-energy barriers of order N; thus they diminish the basins of attraction of the stored patterns and litter the memory. Moreover, at large k ($k \sim N/\ln N$) even the genuine restored states deviate from the stored patterns at a small number of sites (see Section 1.8).

Estimates show (see Section 1.8) that the maximum number of states that can be restored more or less satisfactorily is of order N. To clarify this question and obtain a more quantitative result, we consider the statistical properties of the Hopfield model in the thermodynamic limit $N \to \infty$ with $\alpha = k/N$ fixed. Note that the matrix J_{ij} defined by (8.1.2) is not a random matrix of the SK model since correlations between its elements are generally large and important; as usual, they are described by cyclic correlators (cf. [3])

$$K_m = \overline{J_{i_1 i_2} J_{i_2 i_3} \ldots J_{i_m i_1}} = \alpha N^{-(m-1)}, \tag{8.1.4}$$

which resemble the interaction matrices of a helical spin glass (Section 6.1) or a Josephson network in a magnetic field (Section 7.1). At high temperature fluctuations are strong and the system of spins is paramagnetic. With decreasing temperature, the system first undergoes a second-order transition into a spin-glass state. To obtain T_g, we proceed analogously to the derivation of Section 7.1 and get

$$T_g = 1 + \alpha^{1/2}, \tag{8.1.5}$$

which becomes the usual spin-glass result ($T_g = \alpha^{1/2}$) in the limit $\alpha \to \infty$.

In the study of memory networks we are interested not in the spin-glass phase but in the states that overlap strongly with stored patterns. The analytical approach to the study of these states was developed in reference [4]. It is based on the replica trick. As we shall see below, the replica-symmetry breaking can be ignored for almost all problems in the theory of networks — which simplifies calculations. The free energy f of such a state is

$$\begin{aligned} f = {} & \frac{1}{2} m^2 + \frac{1}{2} \alpha \left\{ \beta^{-1} \ln [1 - \beta(1-q)] \right. \\ & \left. + \frac{(1-\beta)(1-q)}{1-\beta(1-q)} + \beta r (1-q) \right\} \\ & - \beta^{-1} \overline{\langle \ln \{2 \cosh \{\beta [(\alpha r)^{1/2} x + m \cdot \xi]\}\} \rangle_x}, \end{aligned} \tag{8.1.6}$$

where the bar denotes the average over random $\xi_i^{(\mu)}$ and x denotes the average over the Gaussian variable x with zero mean and unit variance.

The free energy (8.1.6) depends on three order parameters: (i) the macroscopic overlaps m, (8.1.3); (ii) the mean-square overlap with other stored patterns

$$r = \alpha^{-1} \sum_{\mu > \mu_0}^{p} \overline{\langle m^\mu \rangle^2}; \tag{8.1.7}$$

and (iii) the Edwards–Anderson order parameter $q = \overline{\langle \sigma_i \rangle^2}$.

The equations for the order parameter (m, r, q) follow from the minimization conditions for the free-energy (8.1.6):

$$m = \overline{\langle \xi \tanh \{\beta[(\alpha r)^{1/2} x + \boldsymbol{m}\cdot\boldsymbol{\xi}]\} \rangle_x}, \tag{8.1.8a}$$

$$q = \overline{\langle \{\tanh \{\beta[(\alpha r)^{1/2} x + \boldsymbol{m}\cdot\boldsymbol{\xi}]\}\}^2 \rangle_x}, \tag{8.1.8b}$$

$$r = q[1-\beta(1-q)]^{-2}. \tag{8.1.8c}$$

Different states of a network obtained as solutions of (8.1.8a–c) as functions of the parameters α and T are illustrated by the phase diagram in Figure 29. For $\alpha > \alpha_c \approx 0.138$ there are no solutions with macroscopic overlaps, which means that in this parameter region the network cannot perform any functions of memory. At $\alpha < \alpha_c$ the states appear discontinuously if T is below the critical line $T_M(\alpha)$. In the vicinity of T_M the states are metastable, but below the second critical line $T_c(\alpha)$ they become global minima of the free energy. In the vicinity of the critical point ($T=1$, $\alpha=0$) the phase transitions become almost continuous, and the critical lines $T_M(\alpha)$ and $T_c(\alpha)$ run close to each other:

$$T_m(\alpha) = 1 - 1.95\ \alpha^{1/2}, \tag{8.1.9}$$

$$T_c(\alpha) = 1 - 2.6\ \alpha^{1/2}. \tag{8.1.10}$$

The quality of retrieval at $T=0$ is measured by the density of errors $\rho = \frac{1}{2}(1-m)$, where m can be found from a simplified (in the limit $T \to 0$) form of (8.1.8a) with $m^s = m\delta_{s1}$,

$$m = \operatorname{erf}[m/(2\alpha r)^{1/2}]. \tag{8.1.11}$$

The value of ρ is remarkably low even at the largest $\alpha = \alpha_c$: $\rho(\alpha_c) = 1.5 \times 10^{-2}$.

At very low temperatures $T \leqslant T_R(\alpha)$ the solution (8.1.8a–c) becomes

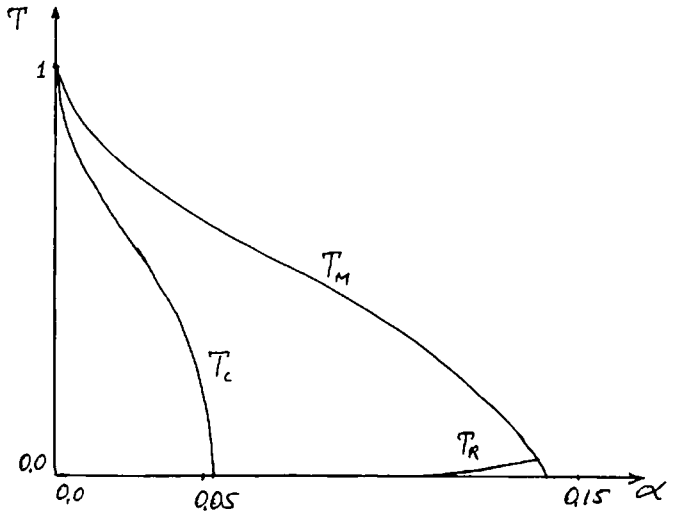

Figure 29 Phase diagram of the Hopfield model.

unstable with respect to replica-symmetry breaking (RSB), but these temperatures are so low — (even at $\alpha = \alpha_c$, $T_R = 0.07$) — that the effect of RSB is very small.

$$T_R(\alpha) = (8\alpha/9\pi)^{1/2} e^{-1/2\alpha} \tag{8.1.12}$$

Indeed, more detailed calculations [5] that take RSB into account result in $\alpha_c = 0.144$, which differs only slightly from the replica-symmetry result.

Perhaps more important are quantitatively small but qualitatively significant consequences of RSB, which means that every retrieval state is split into a multitude of close but distinct states. The number of these states is exponentially large $\mathcal{M} \sim e^{\kappa N}$ (however, the parameter κ is numerically small — representing the smallness of all RSB). Therefore the retrieval of a stored pattern starting from different patterns results in slightly different metastable states; thus the retrieval errors can hardly be established and corrected. In contrast, at $T > T_R(\alpha)$ there is a one-to-one correspondence between stored patterns and retrieval states.

The obvious drawback of the Hopfield model is its inability to store

and retrieve correlated patterns. A generalization of the matrix J_{ij} that allows storage and retrieval of *any* patterns was proposed in reference [6]. A study of it shows [7] that it works satisfactorily, but its learning rule is essentially nonlocal (in contrast with the local Hebb rule (8.1.2)) and so can hardly be of use in explaining the performance of biological systems or in technical applications. Thus we should look for other, less general, learning rules that can store and retrieve correlated patterns but are less costly. We begin with the scheme proposed in reference [8].

In this scheme a learning rule is proposed that allows the retrieval of correlated patterns that can be parametrized by a basic image ξ_i representing the class of objects:

$$\xi_i^{(\mu)} = \xi_i[1 - 2\eta_i^{(\mu)}]. \tag{8.1.13}$$

Here $\eta_i^{(\mu)}$ take the values 0 and 1, and Prob $(\eta_i^{(\mu)} = 1) = p \leqslant \frac{1}{2}$. At $p \ll 1$ all of the images $\xi_i^{(\mu)}$ differ slightly from the basic image ξ_i; at $p = \frac{1}{2}$ we return to the case of uncorrelated images. In the Hopfield construction (8.1.2) of the matrix J_{ij} the different images $\xi_i^{(\mu)}$ are indiscernible at $p \ll 1$; the stationary state of the system corresponds to the basic image ξ_i. To discern the "details" of the images, we choose the following form for J_{ij}:

$$\begin{aligned} J_{ij} &= \frac{1}{N}\xi_i\xi_j + \frac{1}{4\Delta N}\sum_{\mu=1}^{k}(\delta\xi_i^{(\mu)})(\delta\xi_j^{(\mu)}) \\ &= \frac{1}{N}\xi_i\xi_j\left[1 + \frac{1}{\Delta}\sum_{\mu=1}^{k}(\eta_i^{(\mu)} - p)(\eta_j^{(\mu)} - p)\right], \end{aligned} \tag{8.1.14}$$

where $\delta\xi_i^{(\mu)} = \xi_i^{(\mu)} - \overline{\xi_i^{(\mu)}} = \xi_i^{(\mu)} - (1-2p)\xi_i$ and Δ lies in the interval

$$p(1-p) = \Delta_0 \leqslant \Delta < \Delta_1 = 2\frac{p(1-p)^2}{1-2p}. \tag{8.1.15}$$

The simplest justification for our choice is the calculation of internal fields $h_i = \sum_j J_{ij}\sigma_j$ for one of the stored states ($\sigma_i = \xi_i^{(\lambda)}$):

$$\begin{aligned} h_i^{(\lambda)} &= \frac{1}{N}\sum_j \xi_i\xi_j\left[1 + \frac{1}{4\Delta}\sum_{\mu=1}^{k}(\delta\xi_i^{\mu})(\delta\xi_j^{\mu})\right]\xi_j^{(\lambda)} \\ &= \xi_i^{(\lambda)}\frac{\Delta_0}{\Delta} + \xi_i\left(1 - \frac{\Delta_0}{\Delta}\right)(1-2p) \\ &\quad + \frac{1}{4\Delta N}\sum_{\mu\neq\lambda}^{k}\sum_j (\delta\xi_i^{(\mu)})(\delta\xi_j^{(\mu)})\xi_j^{(\lambda)}. \end{aligned} \tag{8.1.16}$$

At $\Delta = \Delta_0$ the correlation between $h_i^{(\lambda)}$ and $\xi_i^{(\lambda)}$ is maximal; the last term in (8.1.16) represents a static "spin-glass" noise with variance $\sim (k/N)^{1/2} = \alpha^{1/2}$. Therefore the storage capacity of this system is of the same order of magnitude as the storage capacity of the Hopfield model.

We shall show here that this is indeed true. We have used a minor modification of the AGS method [4], the main difference being the existence of two types of linear order parameter:

$$m = \frac{1}{N} \sum_i \xi_i \langle \sigma_i \rangle, \tag{8.1.17}$$

$$u_\mu = \frac{1}{\Delta N} \sum_i \xi_i (p - \eta_i^{(\mu)}) \langle \sigma_i \rangle. \tag{8.1.18}$$

The retrieval state $\xi_i^{(\mu)}$ corresponds to the stationary state with both m and u_μ nonzero. If, on the other hand, in some state $m \neq 0$ but $u_h = 0$ for all η then this state corresponds to the basic image ξ. There are also two "spin-glass" order parameters q and r, which have the same meanings as above in (8.1.7) and (8.1.8). The equations for these order parameters can be derived in full analogy with reference [4]:

$$m = \overline{\xi_i \langle \tanh \{\beta [(\alpha r)^{1/2} x + h_i]\} \rangle_x}, \tag{8.1.19a}$$

$$u_\mu = \frac{1}{\Delta} \overline{\xi_i (c - \eta_i^{(\mu)}) \langle \tanh \{\beta [(\alpha r)^{1/2} x + h_i]\} \rangle_x}, \tag{8.1.19b}$$

$$q = \overline{\langle \tanh^2 \{\beta [(\alpha r)^{1/2} x + h_i]\} \rangle_x}, \tag{8.1.19c}$$

$$r = q \left(\frac{\Delta_0}{\Delta} \right)^2 \left[1 - (1-q) \beta \frac{\Delta_0}{\Delta} \right]^{-2}, \tag{8.1.19d}$$

where $h_i = \xi_i [m + u_\mu (p - \eta_i^{(\mu)})]$.

At $\Delta = \Delta_0$, (8.1.19a–d) possess a set of solutions with $m = (1-2p)\, m_0(T)$, $u_\mu = 2\delta_{\mu\mu_0} m_0(T)$ that corresponds to retrieval states $\xi_i^{(\mu)}$. Moreover, there is a solution with $u_\mu = 0$, $m = m_0(T)$ corresponding to the basic image ξ_i. For this set of solutions, (8.1.19a–d) coincide with the corresponding equations for the order parameters in the case of uncorrelated patterns. Thus we conclude that these solutions exist at $T < T_M(\alpha)$ with $T_M(0) = 1$ and $\alpha_c(T=0) \approx 0.14$. Note that the basic state ξ_i and its "satellites" $\xi_i^{(\mu)}$ are degenerate in energy.

At $\Delta_0 < \Delta < \Delta_1$ this degeneracy is broken and two phase transitions appear. The first one at $T = T_1(\alpha, \Delta)$ is due to the appearance of the basic retrieval state ξ_i. As the temperature decreases further, the second transition occurs at $T = T_2(\alpha, \Delta) < T_1(\alpha, \Delta)$. At $T < T_2(\alpha, \Delta)$ all of the satellite states can be retrieved. The functions $T_{1,2}(\alpha, \Delta)$ can be obtained numerically; here we present some analytical results. As $\alpha \to 0$, we obtain:

$$T_1(\alpha, \Delta) \to T_1(\Delta) = 1, \tag{8.1.20}$$

$$T_2(\alpha, \Delta) \to T_2(\Delta) \approx \begin{cases} 1 - 4\left(\dfrac{\Delta}{\Delta_0} - 1\right) & \left(\dfrac{\Delta}{\Delta_0} - 1 \ll 1\right), \\ \dfrac{4(1 - \Delta/\Delta_1)}{|\ln (1 - \Delta/\Delta_1)|} & \left(1 - \dfrac{\Delta}{\Delta_1} \ll 1\right). \end{cases} \tag{8.1.21}$$

In the limit $\alpha \to 0$ the first transition is of second order, as opposed to the second one, which is of first order and becomes of second order only as $\Delta \to \Delta_0$. Note that the temperatures $T_{1,2}(\alpha, \Delta)$ obtained above correspond to the appearance of metastable retrieval states (and are thus analogous to the line $T_M(\alpha)$ discussed above).

The storage capacity of the system at $T = 0$ is also determined by two characteristic values $\alpha_1(\Delta)$ and $\alpha_2(\Delta)$. At $\alpha < \alpha_1(\Delta)$ the basic image can be retrieved, and at $\alpha < \alpha_2(\Delta) < \alpha_1(\Delta)$ all of the satellites are discernible. The value of $\alpha_1(\Delta)$ is determined by the solvability condition for the equation

$$t\left[(2\alpha)^{1/2} + \frac{2}{\pi^{1/2}} e^{-t^2}\right] = \frac{\Delta}{\Delta_0} \operatorname{erf}(t). \tag{8.1.22}$$

The value of $\alpha_2(\Delta)$ is determined by the solvability of the system ($p \ll 1$)

$$\begin{aligned} \frac{(2\alpha)^{1/2}}{1 - B} t_1 &= \frac{\Delta}{\Delta_0} \operatorname{erf}(t_1), \\ \frac{(2\alpha)^{1/2}}{1 - B} t_2 &= \operatorname{erf}(t_2) - \left(\frac{\Delta}{\Delta_0} - 1\right) \operatorname{erf}(t_1), \\ B &= \left(\frac{2}{\pi\alpha}\right)^{1/2} [(1 - \Delta_0) \exp(t_1^2) + \Delta_0 \exp(-t_2^2)](1 - B). \end{aligned} \tag{8.1.23}$$

At $\Delta = \Delta_0$ both (8.1.22) and (8.1.23) reduce to a single equation coinciding with the corresponding equation in reference [4], so that $\alpha_1(\Delta_0) = \alpha_2(\Delta_0) = \alpha_c \approx 0.14$. The dependences $\alpha_1(\Delta)$ and $\alpha_2(\Delta)$ obtained numerically are shown in Figure 30. The corresponding values of t, t_1 and t_2 are shown in Figure 31. At $\Delta/\Delta_0 \leqslant \delta_1 \approx 1.16$, α_2 is equal to α_1, and both of them increase with Δ/Δ_0; at larger Δ/Δ_0, $\alpha_2 \neq \alpha_1$; and at still larger Δ/Δ_0, α_2 begins to decrease and tends to zero as $\Delta \to 2\Delta_0$. Its maximum value is

$$\alpha_{2\max} \approx 0.20, \tag{8.1.24}$$

which is attained at $\Delta/\Delta_0 \approx \delta_2 \approx 1.18$.

The effectiveness of the system can also be characterized by the value of the overlap $m^{(\mu)}$ between the stored patterns $\xi_i^{(\mu)}$ and the corresponding retrieved states (cf. (8.1.19)):

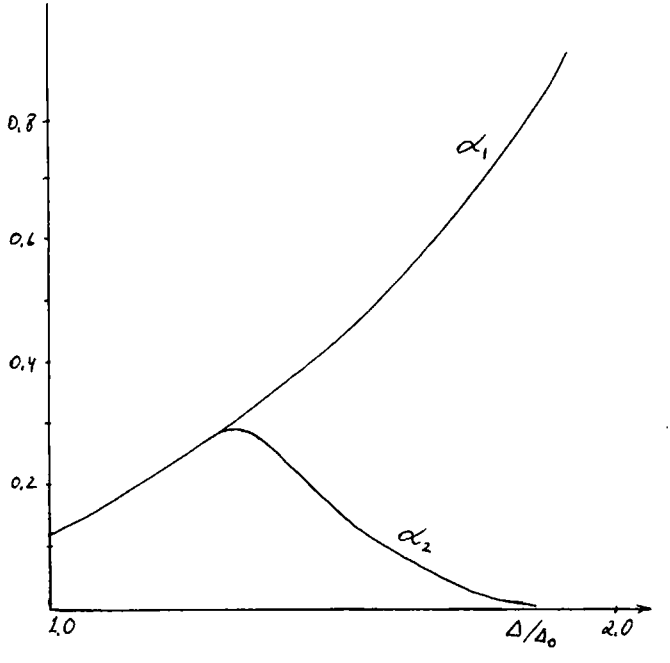

Figure 30 Storage capacity for correlated patterns.

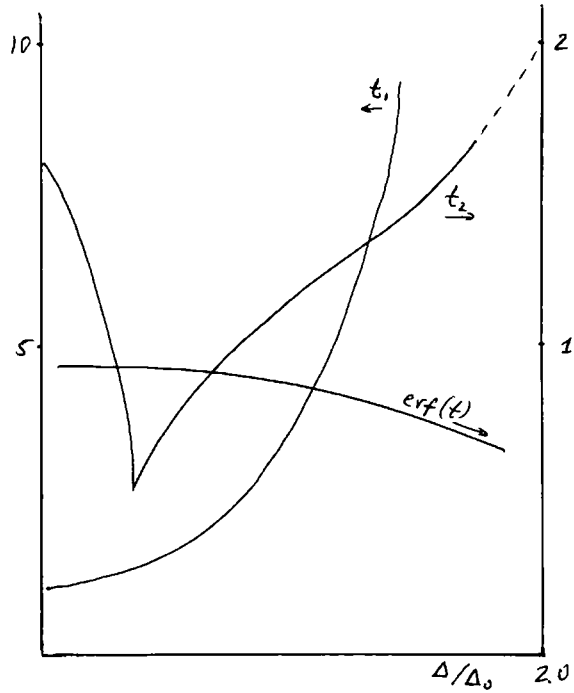

Figure 31 Quality of retrieval (see (8.1.22) and (8.1.23)) at $T = 0$ and at maximum stored states ($\alpha = \alpha_2, \alpha_1$).

$$m^{(\mu)} = \frac{1}{N}\sum_i \xi_i^{(\mu)} \langle \tanh\{\beta[(2\alpha r)^{1/2}x + h_i]\}\rangle_x$$
$$= (1-2p)m + 2\Delta u_\mu . \tag{8.1.25}$$

We calculate $m^{(\mu)}$ using (8.1.19) and obtain (at $p \ll 1$):

$$m^{(\mu)} = (1-2\Delta_0)\,\mathrm{erf}\,(t_1) + 2\Delta_0\,\mathrm{erf}\,(t_2), \tag{8.1.26}$$

where t_1, t_2 is the solution of (8.1.23). A similar overlap for the basic retrieval state is given by $m = \mathrm{erf}\,(t)$, where t is the solution of (8.1.22).

The storage prescription (8.1.14) is not unique. A different prescription was proposed in reference [9] in which the matrix J_{ij} was defined by (8.1.14) without the first term, but an additional term:

$$H_e = \frac{g}{2N}\left[\sum_i S_i - N(1-2p)\right]^2, \quad g \gg 1, \tag{8.1.27}$$

was added to the Hamiltonian to ensure the constraint $\langle S_i \rangle = 1-2p$. (The same constraint can also be ensured by imposing an appropriate threshold — which is more reasonable than the interaction (8.1.27) from a biological point of view.) If p is not very small then the performance of this storage prescription is similar to the performance of the algorithm studied in this section, but at very small p, $\alpha_0(p)$ decreases. However, both of these prescriptions are far from optimal because, as shown by Gardner [10], the maximum capacity $\alpha_{\max}$ is

$$\alpha_{\max} \approx \frac{1}{p\,|\ln p\,|} \tag{8.1.28}$$

at $p \ll 1$. The result was obtained [10] in a nonconstructive manner, so the explicit form of the matrix J_{ij} resulting in $\alpha_{\max}$ remained unknown, but it has recently been discovered [11] that the storage prescription resulting in $\alpha_{\max}$ is quite simple and J_{ij} can be constructed explicitly. This prescription acquires a simple form in the representation of the "V model", i.e. a model with dynamic variables $V_i = \frac{1}{2}(S_i+1) = 0, 1$. The Hamiltonian with these variables is

$$H = -\frac{1}{2}\sum_{i,j} T_{ij} V_i V_j + \theta \sum_i V_i \tag{8.1.29}$$

where

$$T_{ij} = (Np)^{-1} \sum_\mu (\eta_i^{(\mu)} - p)(\eta_j^{(\mu)} - p). \tag{8.1.30}$$

Here $\eta_i^{(\mu)}$ are patterns in the V representation, i.e. $\eta_i^{(\mu)} = \frac{1}{2}(\xi_i^{(\mu)}+1) = 0, 1$ and prob $(\eta_i^{(\mu)}=1) = p \ll 1$. We recall that these conditions are natural in biological systems, because the number of quiescent $(\eta_i^{(\mu)}=0)$ neurons is usually many times larger than the number of firing $(\eta_i^{(\mu)}=1)$ ones [12]. In fact, the model (8.1.29), (8.1.30) was introduced long ago, but when the Hopfield model became very popular it was abandoned. Amusingly, the theory of neural networks has come full circle, since we are now forced to study the original model and we conclude that it is far more convenient for biological applications.

Clearly, the model (8.1.29), (8.1.30) is equivalent to the Hopfield model with thresholds f_i correlated with the interaction matrix J_{ij}:

$$\left.\begin{aligned} H &= -\frac{1}{2}\sum_{i,j} J_{ij} S_i S_j + \sum_i f_i S_i \\ J_{ij} &= (4Np)^{-1} \sum_{\mu=1}^{k} (\beta_i^{(\mu)} - p)(\beta_j^{(\mu)} - p), \\ f_i &= \frac{1}{2}\theta - \sum_j J_{ij}, \quad \xi_i^{(\mu)} = 1 - 2\beta_i^{(\mu)} \end{aligned}\right\} \tag{8.1.31}$$

Before we study the statistical mechanics of the model (8.1.29), (8.1.30) analytically, let us make simple signal/noise estimates. The local field h_i acting upon the neuron at site i is

$$h_i = \sum_j T_{ij}\eta_j^{(1)} - \theta = \eta_i^{(1)} - p - \theta + \frac{1}{Np}\sum_{\mu=2}^{k} (\eta_i^{(\mu)} - p)(\eta_j^{(\mu)} - p)\eta_j^{(1)}. \tag{8.1.32}$$

The sum h_i^R on the right-hand side of (8.1.32) represents a random contribution from other patterns $\eta_i^{(\mu)}$ ($\mu \neq 1$), and its variance is $(pK/N)^{1/2}$. Comparing this "noise" term with other "signal" terms, we conclude that the pattern $\eta_i^{(1)}$ is stable if $1 - p - \theta \gg (pk/N)^{1/2}$ and $p + \theta \gg (pk/N)^{1/2}$. Thus we get

$$\alpha_c \leqslant p^{-1} \min\,[\theta^2, (1-\theta)^2] \quad \text{if } \theta, (1-\theta) \gg p.$$

The statistical mechanics of the V model is studied [11] analogously to the Hopfield model (we skip the details here) and results in the mean-field equations, which we write down in the limit $p \ll 1$:

$$\left.\begin{aligned} m_\mu &= \overline{(\eta_i^{(\mu)} - p)\langle F[\beta h_i + \beta(\alpha r)^{1/2}x]\rangle_x}, \\ q_0 &= \overline{\langle F[\beta h_i + \beta(\alpha r)^{1/2}x]\rangle_x}, \\ \frac{r}{p^2} &= \overline{\langle \{F[\beta h_i + \beta(\alpha r)^{1/2}x]\}^2\rangle_x}. \end{aligned}\right\} \tag{8.1.33}$$

Here $h_i = m(\eta_i^{(\mu)} - p) - \theta$ and $F(y) = (1 + e^{-y})^{-1}$. At zero temperature (8.1.33) are simplified:

$$\left.\begin{aligned} \frac{m}{p} &= \operatorname{erf}\left[\frac{\theta - m}{(2\alpha r)^{1/2}}\right] - \operatorname{erf}\left[\frac{\theta}{(2\alpha r)^{1/2}}\right], \\ \frac{r}{p^2} &= p \operatorname{erf}\left[\frac{\theta - m}{(2\alpha r)^{1/2}}\right] + \operatorname{erf}\left[\frac{\theta}{(2\alpha r)^{1/2}}\right], \end{aligned}\right\} \tag{8.1.34}$$

where we neglect the difference between q and r (i.e. the factor $C = \lim_{\beta\to\infty} \beta(q_0 - q)$) which is justified at $p \ll 1$ and $\alpha < \alpha_c(p)$. Finally, using the inequality $1-\theta \gg p$, we get the maximum storage capacity

$$\alpha_c \approx \begin{cases} \dfrac{\theta}{2p|\ln p|} & (1-\theta \geqslant |\ln p|^{-1/2}), \\ \dfrac{(1-\theta)^2}{2p|\ln (1-\theta)|} & (1-\theta \ll |\ln p|^{-1/2}). \end{cases} \tag{8.1.35}$$

Retrieval states are stable with respect to thermal fluctuations at $T < T_c(\alpha)$. The value of $T_c(0)$ is determined by the solvability condition for the equation ($\beta_0 = T_c^{-1}(0)$)

$$\frac{m}{1-p} = \{1 + \exp[\beta_0\theta - \beta_0 m(1-p)]\}^{-1} - [1 + \exp(\beta_0\theta + \beta_0 mp)]^{-1}. \tag{8.1.36}$$

This leads in the range $p \ll 1 - \theta \ll 1$ to the result

$$T_c(0) \approx \frac{1-\theta}{|\ln (1-\theta)|}, \tag{8.1.37}$$

which resembles the second line of (8.1.21). Note that the phase transition is of first order even as $\alpha \to 0$. The unusual feature of the model considered is that in the most interesting range $|\ln p|^{-1/2} \ll 1 - \theta \ll 1$ the storage capacity α_c increases with the threshold, whereas the transition temperature decreases. Thus the optimum choice of θ depends on the noise level presented in the system. The maximum storage capacity of that model appears to be about half of the supremum value (8.1.28).

All of the above discussion has been devoted to fully connected networks, which are rather unrealistic approximations for real neural networks. Thus one can wonder about the system's robustness with respect to the dilution of synapses. It was shown by Sompolinsky [13] that dilution does not qualitatively affect the network's performance if the number of bonds remains $O(N^2)$. In particular, 50% dilution in the Hopfield model leads to a decrease of α_c from 0.14 to 0.09; note that α_c is defined in the usual way as k/N so that the capacity per bond increases slightly with dilution. Strong dilution (leading to finite coordination number per neuron) results in more pronounced effects, which are discussed in references [14–16].

There is another feature of the Hopfield model that is highly questionable from a practical point of view, namely the continuous nature of the values of the synaptic efficiences J_{ij}. Actually, the Hopfield energy prescription implies $M = 2k + 1$ values allowed for each bond J_{ij}. Near to saturation of the memory, i.e. at finite $\alpha = k/N$, M should be $O(N)$, which is too large to be realized in a real system. However, it appears [13] that strong "clipping" of bonds $J_{ij} \to \text{sgn}\,(J_{ij})$ only slightly worsens the network's performance in the case of uncorrelated patterns: α_c decreases to 0.10. For the storage of correlated patterns, the effect of clipping would probably be more severe, but this problem has not so far been solved, or even addressed, to our knowledge.

8.2 Hierarchical Models of Memory

We discuss here networks that are capable of retrieving hierarchically organized patterns.

The idea of hierarchical organization arises naturally when one needs to store and retrieve a large number of correlated patterns where patterns can be grouped into classes, closely related classes into groups, and so on. This hierarchy is also well known in the theory of spin glasses; specifically, in the SK model all low-energy states are organized in a hierarchical tree [17] (see also Section 2).

We discuss two alternative approaches to the construction of hierarchical models of memory. In the first approach the whole network is inhomogeneous, with hierarchicity governed by the structure of the network ("rigid" models). In one of these models all spins are distributed between spin clusters, which in turn are gathered into superclusters, and so on. At each level of the hierarchy each cluster can be regarded as an independent Hopfield model storing a given part of all information [18]. In the other model the whole network is divided into layers [19], with the spins of each layer representing the magnetization signs of the clusters of the previous model. The layered structure permits us to see the spin configuration of each hierarchical level and also simplifies the learning algorithm. We discuss both these models in detail in Section 8.2.1.

In Section 8.2.2 we discuss the other approach [8] to hierarchical organization, in which the network is homogeneous, with the hierarchicity being governed by the choice of the matrix J_{ij}, i.e. a modification of the Hebb rule. Unfortunately, in the models studied so far the

maximum number of stored patterns remains $O(N)$, despite their hierarchical organization. We argue that this is an unavoidable consequence of homogeneity and interneuron pair interaction. In Section 8.2.3 we show that the storage capacity can be enhanced strongly by many-spin interaction [8].

8.2.1 Structured networks We divide a system of N Ising spins into a hierarchy of clusters $\{\Omega\}$, containing $|\Omega|$ spins, so that the cluster of the mth level contains k_0 subclusters of the $(m-1)$th level (in Figure 32, $k_0 = 4$):

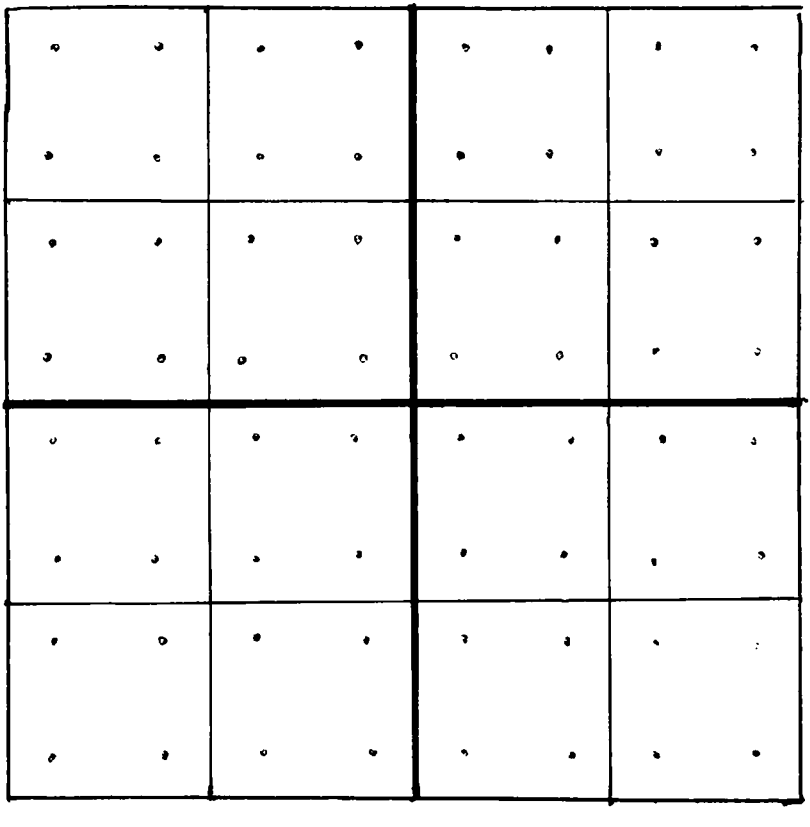

Figure 32 Ordered hierarchy of spin clusters.

$$|\Omega_m| = k_0|\Omega_{m-1}|, \quad |\Omega_m| = k_0^m. \tag{8.2.1}$$

In each lowest-level cluster there are k_0 spins and the number of hierarchical levels is

$$n = \ln N/\ln k_0. \tag{8.2.2}$$

The intermediate mth level is characterized by the family of clusters $\{\Omega_{a_1 a_2 \ldots a_n}\}$, where the subscript $a_p = 1, 2, \ldots, k_0$ ($p = 1, 2, \ldots, n$) enumerates the clusters of the pth level.

A given family of spin configurations will be assumed to belong to one common ancestor state in the next (second) hierarchical level if the magnetization $\{M_{a_1 \ldots a_n}\}$ of the first-level clusters $\{\Omega_{a_1 \ldots a_n}\}$ are the same for all of these configurations. Let each lowest-level cluster contain p_0 different patterns $\{\xi_i^{(\mu)}\}$ to be memorized. Then the above statement can be written as

$$\sum_{i \in \Omega_{a_1 \ldots a_n}} \xi_i^{(s)} = M_{a_1 \ldots a_n} \tag{8.2.3}$$

independent of $s = 1, 2, \ldots p_0$. In other words, without detailed information about the images on the level of distinct spins (roughened image), all patterns of this family give a fixed picture of magnetizations $\{M_{a_1 \ldots a_n}\}$ of the first-level clusters. Obviously, the number of these patterns is s_0^{N/k_0}.

The main point of the present hierarchical construction is that different states of the next (second) hierarchical level are composed of different configurations of the *signs* of the magnetizations $\{M_{a_1 \ldots a_n}\}$ with fixed modulus $|M_{a_1 \ldots a_n}|$. Each of these sign configurations has its own family of states of the previous level.

A given family of states of the second level (roughened images) will be assumed to belong to one common ancestor state in the next (third) hierarchical level if the magnetizations $\{M_{a_2 \ldots a_n}\}$ of the second-level clusters $\{\Omega_{a_2 \ldots a_n}\}$ are the same for all these states:

$$\sum_{a_1 \in \Omega_{a_2 \ldots a_n}} M^{(s_2)}_{a_1 \ldots a_n} = M_{a_2 \ldots a_n} \tag{8.2.4}$$

for all $s_2 = 1, 2, \ldots, p_0$. The number p_0 of course could be different in each level, but for simplicity we shall assume that it is a fixed parameter of the present construction.

In this way the whole hierarchical "tree" of states (Figure 6 —

Section 2) could be constructed. It is a discrete and simplified analogue of the spin-glass tree described by Virasoro and Mezard [20]. Obviously, the total number of spin patterns is

$$p_0^{Nk_0-1} p_0^{Nk_0-2} \ldots p_0^{Nk_0-n} e^{\lambda N/k_0}, \tag{8.2.5}$$

where

$$\lambda = \frac{1 - N^{-1}}{1 - k_0^{-1}} \ln p_0.$$

To memorize this tree of states, the following algorithm is proposed. In the first step the spin interactions $J_{ij}^{(1)}$ between spins inside the first-level clusters are defined as

$$J_{ij}^{(1)} = J \sum_{s_1=1}^{p_0} \xi_i^{(s_1)} \xi_j^{(s_1)}. \tag{8.2.6}$$

These interactions determine the ground-state spin configurations inside each cluster $\Omega_{a_1 \ldots a_n}$, but not their relative orientations since the interactions between spins of different clusters are so far absent.

In the next step the interactions between spins of the clusters $\Omega_{a_1 \ldots a_n}$ inside the second-level clusters $\Omega_{a_2 \ldots a_n}$ are defined as

$$J_{ij}^{(2)} = J \sum_{s_2=1}^{p_0} \frac{1}{k_0^2} M_{a_1 \ldots a_n}^{(s_2)} M_{b_1 a_2 \ldots a_n}^{(s_2)}, \tag{8.2.7}$$

with

$$i \in \Omega_{a_1 a_2 \ldots a_n}, \quad j \in \Omega_{b_1 a_2 \ldots a_n}, \quad (ij) \in \Omega_{a_2 \ldots a_n}.$$

The interactions $J_{ij}^{(2)}$ determine the ground-state spin configurations of the magnetizations $M_{a_1 \ldots a_n}$ inside the clusters of the second level $\Omega_{a_2 \ldots a_n}$, but not their relative orientations.

In the mth step the interactions between spins of the clusters $\Omega_{a_{m-1} a_m \ldots a_n}$ inside the clusters $\Omega_{a_m \ldots a_n}$ are defined as

$$J_{ij}^{(m)} = J \sum_{s_m=1}^{p_0} k_0^{-2(m-1)} M_{a_{m-1} a_m \ldots a_n} M_{b_{m-1} a_m \ldots a_n}, \tag{8.2.8}$$

with

$$i \in \Omega_{a_{m-1} a_m \ldots a_n}, \quad j \in \Omega_{b_{m-1} a_m \ldots a_n}, \quad (i, j) \in \Omega_{a_m \ldots a_n}.$$

The main problem with this construction is the danger of destroying the "internal" states of the given cluster by the "external" interactions with outer clusters. Assuming that the sign configurations inside clusters are random, the "internal" energy $E_{\text{int}}^{(m)}$ stabilizing some memorized configuration $\{M_{a_{m-1}\dots a_n}\}$ in the given cluster $\Omega_{a_m\dots a_n}$ can be estimated as

$$\begin{aligned} E_{\text{int}}^{(m)} &= -J \sum_{i,j\in\Omega_{a_m\dots a_n}} k_0^{-2(m-1)} M_{a_{m-1}\dots a_n} M_{b_{m-1}\dots a_n} \sigma_i \sigma_j \\ &\approx -J \frac{M_{m-1}^4}{k_0^{2(m-1)}} k_0^2 \approx -Jk_0^2, \end{aligned} \tag{8.2.9}$$

where the estimate $M_m^2 \sim |\Omega_m| = k_0^m$ is used. For the destablizing "external" energy of interaction of this cluster with some other cluster $\Omega_{b_m\dots a_n}$, we have

$$\begin{aligned} E_{\text{ext}}^{(m)} &= -J \sum_{\substack{i\in\Omega_{a_m\dots a_n} \\ j\in\Omega_{b_m\dots a_n}}} k_0^{-2m} M_{a_m\dots a_n} M_{b_m\dots a_n} \sigma_i \sigma_j \\ &\sim J \frac{M_m^2 M_{m-1}^2}{k_0^{2m}} k_0 \sim J. \end{aligned} \tag{8.2.10}$$

Owing to the "homogeneity" of the external interactions of the cluster $\Omega_{b_m\dots a_n}$ with another cluster $\Omega_{a_m\dots a_n}$, ferromagnetic ordering of the magnetizations $\{M_{a_{m-1}\dots a_n}\}$ can appear. Its energy can be estimated as

$$E_{\text{f}}^{(m)} \sim -J \frac{M_m^2 M_{m-1}^2}{k_0^{2m}} k_0^2 \sim -Jk_0. \tag{8.2.11}$$

Equations (8.2.9)–(8.2.11) show that for sufficiently large parameter k_0 the "internal" stabilizing energy will be the largest. One can also easily check that the energy of interaction with outer clusters of the $(m+k)$th level decreases as $k_0^{-k/2}$ and therefore is not dangerous either.

A characteristic feature of the present spin system is its finite-size scaling, described by the parameter k_0. At every scale the system is described by the effective new Ising variables $\tilde{\sigma}$, $M_{a_m\dots a_n} = |M_{a_m\dots a_n}| \tilde{\sigma}_{a_m\dots a_n}$, and although the spin–spin interactions decrease with scale: $J^{(m)} \sim k_0^{-m}$, the effective interactions of the variables $\hat{\sigma}$ are scale-invariant $\sim Jk_0$. The reason why the present memory machine is not "overloaded" (although it stores an exponential number of images) is that at every level of the hierarchy only subsystems of k_0 effective variables, each storing only p_0 memories, are active. Therefore below the critical

curve $T_c(p/k)$ in the (T, α) plane (e.g. for $p_0 \ll k_0$ and not very low temperatures) the model should work.

It is worth stressing that this memory model differs from that of Hopfield in some significant aspects. The Hopfield model can evoke a particular image among essentially different images, while our model can identify a particular image among many similar images. The essential point is that the images stored at every level of the hierarchy of our model must be composed of the same common block-elements. While the Hopfield model can simultaneously store the images of, for example, a cat and a car — and will identify every object with four legs and a tail as a cat — our model can store the images of, for example, only cat-like animals, but can identify not only cats among tigers and panthers but also the breed of a particular cat and finally a particular animal among $e^{\text{const}} \times N$ cats of that breed stored in its memory.

The degree of distinction of memorized images and the capacity of the memory is therefore controlled by the parameter k_0: the larger k_0 is, the smaller are the common elementary blocks of images on every level (and so the larger the degree of diversity of images) and the smaller the total number of memorized images.

Note finally that this memory model could of course be modified in many respects. In particular, the effective cluster interactions could be made scale-dependent so that the temperature could control the possible degree of distinction of roughened images on intermediate levels of the hierarchy. The parameters p_0 and k_0 could also be made scale-dependent.

Consider now a layered model of memory consisting of M layers, each having N_m Ising spins ($m = 1, 2, \ldots M$). Divide each layer into spin clusters $\{\Omega_{im}\}$ so that each cluster of the mth layer has Ω_m spins. Interactions of the layers are arranged in such a way that all spins of one cluster of the $(m-1)$th layer interact with one and only one spin of the next mth layer (Figure 33). For this reason, the number of spins in each subsequent layer decreases: $N_m/N_{m+1} = \Omega_m$. The interaction of the spin of the mth layer with the total magnetization of the spin cluster of the $(m-1)$th layer is ferromagnetic and fixes their signs as equal:

$$\operatorname{sign}\left(\sum_{i \in \Omega_{m-1}} \sigma_{i_{m-1}}\right) = \sigma_{i_m}. \tag{8.2.12}$$

Again the spin configurations to be memorized should be classified in the form of a hierarchical tree. A given family of spin configurations of the mth layer will be assumed to belong to one common ancestor state in

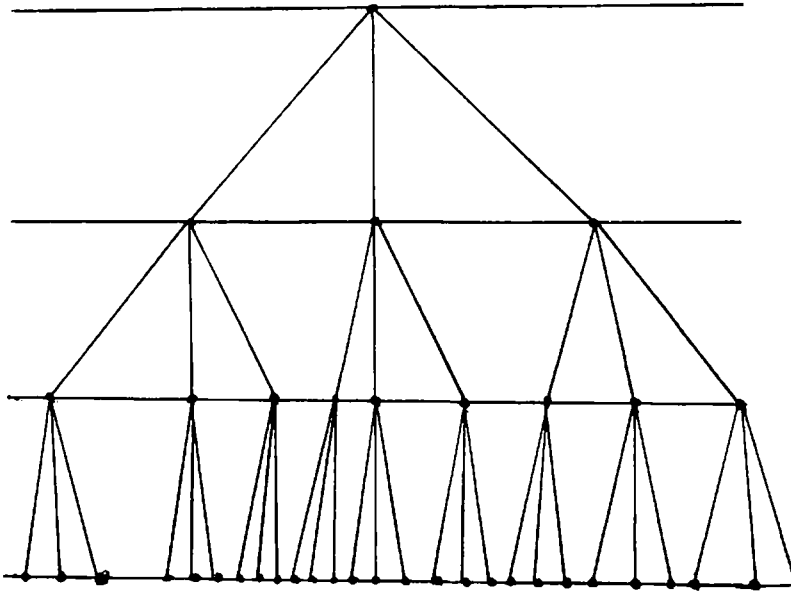

Figure 33 Layered hierarchy.

the next hierarchical level if the signs of magnetization of the spin clusters $\{\Omega_{i_m}\}$ in the mth layer are the same for all these configurations. Therefore the ancestor state of this family is given according to (8.2.12) by one spin configuration in the $(m+1)$th layer.

In this way, climbing from layer to layer, we can construct a whole hierarchical tree of states. The number of levels of the tree is equal to the number of layers of the spin system. The number of trees is equal to the number of spin configurations in the last Mth layer. The learning algorithm for all these spin states is as follows. Spin interactions in the layers are introduced according to the Hopfield model inside clusters only:

$$J_{ij} = \frac{1}{\Omega_m} J_0 \sum_{s=1}^{p_m} \xi_{i_m}^{(s)} \xi_{j_m}^{(s)}, \tag{8.2.13}$$

where $\xi_{i_m}^{(s)}$ $(s = 1, 2, \ldots, p_m)$ are cluster spin patterns composing the global spin configurations of the layer. Note that all spin con-

figurations memorized this way are "constructed" from some limited number of "blocks" — fixed spin states of the clusters. These "blocks" could of course be different in each cluster and in each layer. The number of "blocks" p_m in each cluster is limited by the critical curve $T_c(p_m/\Omega_m)$.

The total number of spin configurations in the family belonging to one ancestor state of the $(m+1)$th hierarchical level is obviously

$$(p_m)^{N_m/\Omega_m}.$$

As in the previous model, the total number of states of the whole tree is exponential.

Spin configurations of the upper layer where there are no clusters are memorized in the same way as in the Hopfield model.

The evocation process in the present memory model proceeds as follows. After the initial spin configuration is fixed in the first layer, it automatically fixes all spins in all other layers. Evocation begins in the upper layer where the most general information (the coarsest image) is stored. Here the correct tree is chosen. Then in each subsequent layer the corresponding branch of the tree is chosen. Finally, in the last layer the exact configuration is evoked.

Note that in an analogous way the hypothesized process of "learning" by this memory model could be imagined. After a new image to be learned is exposed to the first layer of the model, which already has a lot of "knowledge" in its memory, it will eventually enter into some family of coarse images at some hierarchical level. Then the spin interactions should be fixed only below this level, and this will create a new branch of a tree.

The model described above is of interest first of all in that it can be useful for recognizing and memorizing images as part of the hierarchical family of similar images.

Another important feature of the model is its scaling property. If there are two images of the same object but of different size, described by $\{\xi_i^{(1)}\}$ and $\{\xi_j^{(2)}\}$, then these two spin configurations are not close in the usual (spin-glass) sense (since the overlap $q^{12} = N^{-1}\sum_i \sigma_i^{(1)}\sigma_i^{(2)}$ could be close to zero). They are unavoidably different for the Hopfield model. The model presented here (with some modifications) can provide some sort of scale invariance to recognize the images as equivalent, although on different hierarchical levels.

It is noteworthy that similar hierarchical organization is a

characteristic property of the cortex of the brain — or at least of the visual cortex [21]. The visual cortex has six layers ($M=6$). Neurons of each subsequent layer receive and sum the signals from a group of neurons of the previous layer (as in Figure 33). In each subsequent layer, however, the image becomes not just coarser, but also there exists some sort of decomposition into components. For example, a particular neuron of the second layer receives information from such a "cluster" of neurons of the first layer that it can be excited only by the image of a line with definite size and definite direction. In the next layer neurons are excited by the same kind of line but without strictly determined position. The purpose of such an arrangement is at present not quite clear (it is probably a way of catching some general features of the image), but it can be simulated by the layered spin model described here.

8.2.2 Hierarchy of patterns in uniform networks A storage prescription that allows storage of a two-level pattern hierarchy can be obtained as a straightforward generalization of the prescription (8.1.14) discussed above. Consider a set of patterns $\{\xi_i^{(\lambda,\mu)}\}$ each enumerated by two indices (λ, μ). The first index shows the class of correlated patterns to which the pattern belongs, while the second refers to the pattern's number within the class. Individual patterns $\xi_i^{(\lambda,\mu)}$ appear as "satellites" of the basic patterns $\xi_i^{(\lambda)}$ defining the classes:

$$\xi_i^{(\lambda,\mu)} = \xi_i^{(\lambda)}[1-2\eta_i^{(\lambda,\mu)}], \tag{8.2.14}$$

where $\eta_i^{(\lambda,\mu)}$ take the values 0, 1 and prob $(\eta_i^{(\lambda,\mu)}=1)=p_\lambda<\frac{1}{2}$. Then this set of patterns can be stored if the interaction matrix J_{ij} is chosen in the form

$$\begin{aligned} NJ_{ij} &= \sum_{\lambda=1}^{l} \xi_i^{(\lambda)}\xi_j^{(\lambda)} + \frac{1}{4\Delta}\sum_{\lambda=1}^{l}\sum_{\mu=1}^{k_\lambda} \delta\xi_i^{(\lambda,\mu)}\,\delta\xi_j^{\lambda,\mu} \\ &= \sum_{\lambda=1}^{l} \xi_i^{(\lambda)}\xi_j^{(\lambda)}\left[1+\frac{1}{\Delta}\sum_{\mu=1}^{k_\lambda}(\eta_i^{(\lambda,\mu)}-p_\lambda)(\eta_j^{(\lambda,\mu)}-p_\lambda)\right], \end{aligned} \tag{8.2.15}$$

where

$$\begin{aligned} \delta\xi_i^{(\lambda,\mu)} &= \xi_i^{(\lambda,\mu)} - \tilde{\xi}_i^{(\lambda)} = \xi_i^{(\lambda,\mu)} - \frac{1}{k_\lambda}\sum_{\mu}\xi_i^{(\lambda,\mu)} \\ &= \xi_i^{(\lambda,\mu)} - (1-2c_\lambda)\xi_i^{(\lambda)} \end{aligned} \tag{8.2.16}$$

and Δ is about $\Delta_0 = p(1-p)$ (cf. (8.1.15)). Note that after the identification

$$\left.\begin{aligned} S_i^{\alpha\beta} &= \xi_i^{(\lambda,\mu)}, \quad S_i^{\alpha} = \tilde{\xi}_i^{(\lambda)} = (1-2p)\xi_i^{(\lambda)}, \\ q &= (1-2p)^2 = 1 - 4\Delta_0 = \frac{1}{N}\sum_i \xi_i^{(\lambda,\mu)}\xi_i^{(\lambda,\mu')} \end{aligned}\right\} \tag{8.2.17}$$

the expression (8.2.15) at $\Delta = \Delta_0$ takes the form

$$NJ_{ij} = \frac{1}{q}\sum_{\alpha} S_i^{\alpha}S_j^{\alpha} + \frac{1}{1-q}\sum_{\alpha,\beta}(S_i^{\alpha\beta} - S_i^{\alpha})(S_j^{\alpha\beta} - S_j^{\alpha}), \tag{8.2.18}$$

coinciding with the storage prescription for a two-level hierarchy proposed by Varga and Virasoro [22] heuristically, by analogy with the hierarchical organization of pure states in spin glasses [20]. Our present approach permits us to study this model quantitatively. We consider here the case $l \gg 1$, $k_\lambda \gg 1$ and put $p_\lambda = p$ for simplicity. Then it can be readily shown that the mean-field equations for the retrieval states coincide with (8.1.19) if the additional subscript λ is introduced ($m \to m_\lambda$, $u_\mu \to u_{\mu\lambda}$) and the parameter α is defined as

$$a = \sum_{\lambda=1}^{l} \alpha_\lambda = \frac{k}{N}, \tag{8.2.19}$$

where k is the total number of patterns. Thus all of the results following from (8.1.19) (which were derived for the case $l = 1$) are applicable to the two-level hierarchy. In the particular case $\Delta = \Delta_0$ (corresponding to the model of reference [22]) the system's properties coincide with those of the Hopfield model. All of the retrieval states are degenerate; they exist at $\alpha < \alpha_c(T)$, with $\alpha_c(0) \approx 0.14$. Thus we see that previously known limitation on the total number of stored patterns $k \leqslant 0.14N$ remains true despite their hierarchical organization.

Let us now consider a more general case $\Delta > \Delta_0$. The maximum storage capacity $\alpha_c^{\max} \approx 0.20$ is attained at $\Delta \approx 1.18\Delta_0$ (cf. (8.1.24)).

The degeneracy between the "basic" patterns $\xi_i^{(\lambda)}$ and their satellites $\xi_i^{(\lambda,p)}$ is lifted: the energy minima are deeper at the basic states; there are two critical temperatures $T_1(\alpha, \Delta)$ and $T_2(\alpha, \Delta)$ (see the preceding section). At $T_2(\alpha, \Delta) < T < T_1(\alpha, \Delta)$ the only retrieved states are the basic states $\xi_i^{(\lambda)}$; satellites $\xi_i^{(\lambda,\mu)}$ are undiscernible in this temperature interval. If the temperature decreases below $T_2(\alpha, \Delta)$, the whole set of

retrieved patterns $\{\xi_i^{(\lambda,\mu)}\}$ appears. This picture opens up the possibility of ordering the process of recognition in a hierarchical manner. Indeed, we can at first keep the temperature in the interval $T_2(\alpha, \Delta) < T < T_1(\alpha, \Delta)$ and rapidly recognize the class (defined by the basic image $\xi_i^{(\lambda)}$) to which the input pattern belongs. We then have to decrease the temperature below $T_2(\alpha, \Delta)$ so that detailed identification of the pattern can occur. Note here the interesting similarity between the above process and the method of optimization by simulated annealing [23].

We now discuss the quality of retrieval at $T = 0$. The relevant quantities are the average Hemming distances between stored patterns and retrieval states. For the basic states $\xi_i^{(\lambda)}$, these are $d_\lambda = 1 - m_\lambda$. For the satellite states $\xi_i^{(\lambda,m)}$ the corresponding quantities are $d_{\lambda,\mu} = 1 - m_{\lambda,\mu}$, with $m_{\lambda,\mu}$ being defined analogously to (8.1.25). However, it seems reasonable to define the relative distances

$$\tilde{d}_{\lambda,\mu} = \frac{1 - m_{\lambda,\mu}}{1 - q}, \tag{8.2.20}$$

with q being defined in (8.2.17), in order to characterize the quality of retrieval of detailed patterns. Thus we obtain with (8.2.26) and (8.1.27) (at $p \ll 1$)

$$\left.\begin{aligned} d_\lambda &= 1 - \operatorname{erf}(t), \\ \tilde{d}_{\lambda,\mu} &= \frac{1 - \operatorname{erf}(t_1)}{4\Delta_0} + \frac{1}{2}[\operatorname{erf}(t_1) - \operatorname{erf}(t_2)], \end{aligned}\right\} \tag{8.2.21}$$

where t and t_1, t_2 are the solutions of (8.1.22) and (8.1.23) respectively.

The above discussion can be generalized to a multilevel hierarchy of patterns along the lines of reference [22]. We define individual patterns $\xi_i^{(\lambda_1 \ldots \lambda_n)}$ recursively

$$\xi_i^{(\lambda_1 \ldots \lambda_n)} = (1 - 2\eta_i^{(\lambda_1 \ldots \lambda_n)})\xi_i^{(\lambda_1 \ldots \lambda_{n-1})}, \tag{8.2.22}$$

where $\eta_i^{(\lambda_1 \ldots \lambda_n)}$ takes the values 0, 1 with prob $(\eta_i^{(\lambda_1 \ldots \lambda_n)} = 1) = p_n$. Then the storage prescription for memorizing an n-level hierarchy is given by the recursion relation

$$NJ_{ij}^{(n)} = NJ_{ij}^{(n-1)} + \frac{1}{4\Delta} \sum_{\lambda_1 \ldots \lambda_n} (\xi_i^{(\lambda_1 \ldots \lambda_n)} - \xi_i^{(\lambda_1 \ldots \lambda_{n-1})})(\xi_j^{(\lambda_1 \ldots \lambda_n)} - \tilde{\xi}_j^{(\lambda_1 \ldots \lambda_{n-1})}), \tag{8.2.23}$$

with

$$\tilde{\xi}_i^{(\lambda_1 \ldots \lambda_{n-1})} = \sum_{\lambda_n} \xi_i^{(\lambda_1 \ldots \lambda_n)} \Big/ \sum_{l_n} 1 = (1-2p_n)\xi_i^{(\lambda_1 \ldots \lambda_{n-1})}.$$

If all $\Delta^{(n)} = p_0(1-p_n)$ then (8.2.23) is equivalent to the form proposed in reference [22]. Virtually the same result was obtained [25] by using the orthogonalization procedure [5] applied to the hierarchically ordered set of patterns.

The total number of patterns that can be simultaneously stored is restricted by $O(N)$, as can be shown similarly to the case of a two-level hierarchy. Apparently, this fact is in contradiction with the famous result of the exponential number of states in the spin-glass hierarchy (which was the initial ultimate goal of the storage prescription [22]).

To clarify this matter, we obtain rough estimates of the storage capacity from information-theory arguments. The maximum amount of information that can be stored by $\frac{1}{2}N(N-1)$ synapses J_{ij} is

$$I_{\max} \approx \tfrac{1}{2}N^2 \log_2 M, \tag{8.2.24}$$

where M is the number of discrete values allowed for each J_{ij}. The information contained in the two-level hierarchy of patterns $\xi_i^{(\lambda,\mu)}$ is

$$I = Nk\left[p \log_2 \left(\frac{1}{p}\right) + (1-p) \log_2 \left(\frac{1}{1-p}\right)\right]. \tag{8.2.25}$$

The estimate of k follows from the inequality $I < \mathrm{I}_{\max}$. In the Hopfield-model case $M = 2k+1$, so that we get $2k < N \log_2 N$, which is correct but a weak inequality. Our storage prescription (8.2.15) implies $M \approx k/p$; thus we get

$$k < \tfrac{1}{2}N \frac{\log_2 (N/p^2)}{p|\log_2 p|} \tag{8.2.26}$$

at $p \ll 1$. This estimate correlates well with the results (8.1.28) and (8.1.35) and estimates for the storage capacity for iterative algorithms (see [24] and the discussion at the end of this section). In order to store, say, $k = O(N^2)$ patterns we should need a storage prescription that can use effectively $M = \mathrm{e}^{cN}$ allowed values of each J_{ij}. Even if such a prescription exists, it is hardly believable that such very fine tuning can be realized in any biological or technical system. It should be noted in passing that the crucial role of the discreteness of J_{ij} was discovered in the recent studies of general bounds on the storage capacity [26].

A somewhat different network with hierarchical memory was proposed by Gutfreund [27]. It is a generalization of the previously studied model [9] for the storage of correlated patterns (see our brief discussion around (8.1.27)). In the case of a two-level hierarchy the model consists of two networks. The first network recognizes "classes" $\xi_i^{(\lambda)}$, whereas individual patterns $\xi_i^{(\lambda,\mu)}$ are stored in the second network using the learning rule

$$J_{ij}^{(G)} = \frac{1}{N} \sum_{\lambda,\mu} (\xi_i^{(\lambda,\mu)} - \tilde{\xi}_i^{(\lambda)})(\xi_j^{(\lambda,\mu)} - \tilde{\xi}_j^{(\lambda)}), \tag{8.2.27}$$

which is just the second term of (8.2.15). At the first step of retrieval the first network recognizes the class $\xi_i^{(\lambda)}$ to which the retrieved pattern belongs, and applies the staggered field $h\xi_i^{(\lambda)}$ acting in the second network. The second step is the retrieval of the individual pattern $\xi_i^{(\lambda,\mu)}$ in the second network with the Hamiltonian

$$H = -\frac{1}{2} \sum_{i,j} J_{ij}^{(G)} S_i S_j + h \sum_i S_i \xi_i^{(\lambda)}. \tag{8.2.28}$$

The performance of this model is generally similar to that of the model (8.2.15). Note finally that the limitation (inevitable in any real system) of the allowed values of J_{ij} for each bond is probably much more severe for the hierarchical organization of memory model than it is for the Hopfield model (see the end of Section 8.1).

8.2.3 Multineuron interactions and the enhancement of storage capacity We have shown in reference [8] that the total number of stored patterns is restricted by $O(N)$ in spite of the hierarchical organization of memory. This can be traced to the fact that information persists permanently about all the details of the patterns $\xi_i^{(\lambda,\mu)}$, leading to overloading of the system. It seems reasonable to construct the memory in such a way that the pertinent class of images (λ, say) is recognized when detailed information about other ($\lambda' \neq \lambda$) classes is "turned off". This can be done by the following modification of the matrix J_{ij} (8.2.15):

$$N\tilde{J}_{ij} = \sum_{\lambda=1}^{l} \xi_i^{(\lambda)} \xi_j^{(\lambda)} \left[1 + \frac{1}{\Delta} \tilde{P}_\lambda \sum_{p_\lambda=1}^{k_\lambda} (\eta_i^{(\lambda,\mu)} - 1)(\eta_i^{(\lambda,\mu)} - 1) \right]. \tag{8.2.29}$$

Each factor $\hat{P}_\lambda = N^{-1}\Sigma_m \xi_m^{(\lambda)} S_m$ serves as a projection operator that turns on the information about the detailed structure of the patterns $\xi_i^{(\lambda,\mu)}$ when the system is in the state $\{S_i\}$ with nonzero overlap with the basic state $\xi_i^{(\lambda)}$. Thus the interaction matrix $\tilde{J}_{ij}$ depends on the system state, which implies the appearance of a "triple" interaction in the energy functional:

$$H = -\frac{1}{2}\sum_{i,j} \tilde{J}_{ij} S_i S_j - \sum_\lambda \mathscr{A}_\lambda \sum_i \xi_i^{(\lambda)} S_i$$

$$= -\frac{1}{2N}\sum_{i,j}\sum_\lambda \xi_i^{(\lambda)}\xi_j^{(\lambda)} S_i S_j - \frac{1}{2N^2\Delta}\sum_{i,j,m}\sum_\lambda \xi_m^{(\lambda)}\xi_i^{(\lambda)}\xi_j^{(\lambda)}$$

$$\times \sum_{\mu=1}^{k_\lambda} (\eta_i^{(\lambda,\mu)} - p)(\eta_j^{(\lambda,\mu)} - p) S_i S_j S_m - \sum_i \sum_\lambda \xi_i^{(\lambda)} \mathscr{A}_\lambda S_i. \tag{8.2.30}$$

The last term in (8.2.30) corresponds to external fields conjugated with the basic patterns $\xi_i^{(\lambda)}$; its purpose will be seen below.

We shall not dwell here upon the interesting problem of the biological relevance of the model (see e.g. [28]), but rather shall proceed to study its statistical mechanics. This can be done by methods similar to that of AGS [4]; the main difference consists in a more complicated relation between the order parameters m_λ and $u_{\lambda\mu}$ and the molecular fields h_i. The mean-field equations are

$$m_\lambda = \overline{\xi_i^{(\lambda)} \langle \tanh\,[\beta(R^{1/2}x + h_i)]\rangle_x}, \tag{8.2.31a}$$

$$u_{\lambda\mu} = \Delta^{-1}\overline{\xi_i^{(\lambda)}(p - \eta_i^{(\lambda,\mu)})\langle \tanh\,[\beta(R^{1/2}x + h_i)]\rangle_x}, \tag{8.2.31b}$$

$$q = \overline{\langle \tanh^2\,[\beta(R^{1/2}x + h_i)]\rangle_x}, \tag{8.2.31c}$$

$$h_i = \sum_{\lambda=1}^{l} \xi_i^{(\lambda)}\left[\varphi_\lambda + \sum_{\mu=1}^{k_\lambda}(p - \eta_i^{(\lambda,\mu)})\psi_{\lambda,\mu}\right], \tag{8.2.31d}$$

$$\varphi_\lambda = m_\lambda + \frac{\Delta}{2}\sum_{\mu=1}^{k_\lambda} u_{\lambda,\mu}^2 + \frac{\alpha_\lambda^{(2)}\Delta_0}{2\Delta}\,\frac{1 - \beta(1-q)^2 m_\lambda \Delta_0/\Delta}{[1 - \beta m_\lambda(1-q)\Delta_0/\Delta]^2} + \mathscr{A}_\lambda, \tag{8.2.31e}$$

$$\psi_{\lambda,\mu} = m_\lambda u_{\lambda\mu}, \tag{8.2.31f}$$

$$R = \frac{\alpha^{(1)} q}{[1-\beta(1-q)]^2} + q \sum_{\lambda=1}^{l} \frac{\alpha_\lambda^{(2)} (\Delta_0/\Delta)^2}{[m_\lambda^{-1} - \beta(1-q)\Delta_0/\Delta]^2}. \quad (8.2.31g)$$

Here $\alpha^{(1)} = l/N$ is the relative number of basic patterns and $\alpha_\lambda^{(2)} = k_\lambda/N$ is the relative number of satellite patterns in the λ class.

We are primarily interested in the solutions of (8.2.31a–g) that correspond to retrieved states, i.e. the solutions with all but one m_λ equal to zero. In order to obtain these solutions, we must choose the staggered field $\mathscr{H}_\lambda$ in the form

$$\mathscr{H}_\lambda = -\frac{\alpha_\lambda^{(2)} \Delta_0}{\Delta}, \quad (8.2.32)$$

thus compensating (at $m_\lambda = 0$) for the third term in (8.2.31e). Then for the retrieved state $\xi_i^{(\lambda,\mu)}$, (8.2.31d–g) can be reduced by

$$h_i = \xi_i^{(\lambda)} [\varphi_\lambda + (p - \eta_i^{(\lambda,\mu)}) m_\lambda u_{\lambda\mu}], \quad (8.2.33a)$$

$$\varphi_\lambda = m_\lambda + \frac{\Delta}{2}\left(\frac{\Delta_0}{\Delta}\right) + \frac{\alpha_\lambda^{(2)}}{2}\left(\frac{\Delta_0}{\Delta}\right)^2 \frac{\beta m_\lambda (1-q)[1+q-\beta m_\lambda (1-q)\Delta_0/\Delta]}{[1-\beta m_\lambda (1-q)\Delta_0/\Delta]^2}, \quad (8.2.33b)$$

$$R = \frac{\alpha^{(1)} q}{[1-\beta(1-q)]^2} + \left(\frac{\Delta_0}{\Delta}\right)^2 \frac{q\alpha_\lambda^{(2)}}{(m_\lambda^{-1} - \beta(1-q)\Delta_0/\Delta)^2}. \quad (8.2.33c)$$

The total number of patterns $k_{\text{tot}} = \Sigma_\mu k_\mu$ does not enter the equations for the retrieved states $\xi_i^{(\lambda,\mu)}$, which depend on $\alpha^{(1)}$ and $\alpha_\lambda^{(2)}$ only. This means that all the values $\alpha^{(1)}$, $\alpha_\lambda^{(2)}$ ($\lambda = 1, \ldots, l$) can be $O(1)$, so that

$$k_{\text{tot}} = O(N^2). \quad (8.2.34)$$

Our construction can be generalized to an n-level hierarchy along the lines of the preceding subsection (cf. (8.2.23)):

$$NJ_{ij}^{(n)} = NJ_{ij}^{(n-1)} + \frac{1}{4\Delta^{(n)}} \sum_{\lambda_1 \ldots \lambda_n} \hat{P}_{\lambda_1 \ldots \lambda_{n-1}} (\xi_i^{(\lambda_1 \ldots \lambda_n)} - \tilde{\xi}_i^{(\lambda_1 \ldots \lambda_{n-1})}) \times (\xi_i^{\lambda_1 \ldots \lambda_n} - \tilde{\xi}_i^{(\lambda_1 \ldots \lambda_{n-1})}), \quad (8.2.35)$$

$$\hat{P}_{\lambda_1 \ldots \lambda_{n-1}} = \hat{P}_{\lambda_1 \ldots \lambda_{n-2}} N^{-1} \sum_i (\xi_i^{\lambda_1 \ldots \lambda_{n-1}} - \tilde{\xi}_i^{\lambda_1 \ldots \lambda_{n-2}}) S_i.$$

We can then store

$$k_{\text{tot}} = O(N^n) \tag{8.2.36}$$

patterns with the cost of introducing $(n+1)$-neuron interactions. The estimate (8.2.36) can be explained by the following argument: the amount of information stored in the k_{tot} patterns is $I = O(Nk_{\text{tot}})$; the maximum information that can be contained in $\mathcal{N} = O(N^{n+1})$ couplings $J_{i_1 \ldots i_{n+1}}$ is $I_{\max} \sim N^{n+1} \log_2 M$, where M is the number of the allowed values of each $J_{i_1 \ldots i_{n+1}}$. The inequality $I < I_{\max}$ yields roughly the estimate (8.2.36).

The general form of the phase diagram for the two-level model (8.2.29) resembles the phase diagram of the model (8.2.15) with $\Delta > \Delta_0$. If all $\alpha_\lambda^{(2)}$ are equal, $\alpha_\lambda^{(2)} = \alpha^{(2)}$, then there are two phase transitions; the high-temperature one is due to the appearance of the basic retrieved states corresponding to the classes of patterns; the second transition occurs at somewhat lower temperatures and the detailed form of the patterns can be discerned. The second transition is of first order even in the limit $\alpha^{(2)} \to 0$. Generally, at arbitrary $\alpha_\lambda^{(2)}$ these transitions split into two sequences of transitions at the temperatures $T_1^{(\lambda)} = T_1(\alpha^{(1)}, \alpha_\lambda^{(2)})$ and $T_2^{(\lambda)} = T_2(\alpha^{(1)}, \alpha_\lambda^{(2)})$.

It can be seen from (8.2.31g) that for mixed states with several non-zero m_λ (i.e. the states that mix classes) the intensity of the "spin-glass" noise R is larger than for retrieved states and states that mix only patterns from the same class. As has been shown in reference [4], the mixed states rapidly become unstable with increasing R. Therefore, with the proper choice of $\alpha^{(1)}$ and $\alpha_\lambda^{(2)}$, the class-mixing states ("spurious categories" in the terminology of reference [22]) can be eliminated. Thus a "hierarchy among errors" [22] appears.

The main drawback of the model considered is that it needs a large number of complicated units providing multiple interactions, for example $O(N^2)$ triple interactions for the two-level hierarchy. Probably, the situation can be improved by using the projection operators $\hat{P}_\lambda$ defined on a randomly diluted subset of lattice sites:

$$\hat{P}_\lambda = \frac{1}{Nw} \sum_m w_m \xi_m^{(\lambda)} S_m, \tag{8.2.37}$$

where $w_m = 1$ with the probability $w \ll 1$ and $w_m = 0$ otherwise. Note finally that the same idea that led us to the use of projection operators $\hat{P}_\lambda$ was exploited in a different manner by Guttfreund [27], who used

instead an additional network (see our discussion at the end of Section 8.2.2). Generally, this idea can be formulated as follows: in order to make a hierarchical memory efficient, its Hamiltonian (or dynamics rules) should evolve during the course of retrieval.

8.3 Asymmetric Synapses

As we explained in Section 1.8, the assumption of the symmetry of the interaction matrix J_{ij} is totally unrealistic for biological systems. In this subsection we lift this assumption and discuss a generalization of the Hopfield model with asymmetric interaction. The asymmetry of the J_{ij} implies that the network can be described only by dynamical equations because the concept of energy (or Hamiltonian) is inapplicable. The simplest form of dynamics that is compatible with the Hopfield model (8.1.1) is purely relaxational dynamics of "soft" Ising variables σ_i:

$$\left.\begin{aligned} &\frac{\partial \sigma_i}{\partial t} = -\frac{\delta H_t}{\delta \sigma_i} + f_i(t), \quad \langle f_i(t) f_j(t) \rangle = 2T\delta_{ij}\delta(t-t') \\ &H_t = H + H_0, \end{aligned}\right\} \tag{8.3.1}$$

where the additional intrasite energy $H_0 = \frac{1}{2}\lambda \sum_i (\sigma_i^2 - 1)^2$, $\lambda \gg 1$, ensures that a neuron is either quiescent ($\sigma_i = 1$) or silent ($\sigma_i = -1$) and transitions between these states are fast.

First we consider the simplest modification of (8.3.1) with an asymmetric J_{ij} [8]:

$$\begin{aligned} &\frac{\partial \sigma_i}{\partial t} = \frac{\partial H_0}{\partial \sigma_i} + \sum_j \tilde{J}_{ij}\sigma_j + f_i(t), \\ &\langle f_i(t) f_j(t') \rangle = 2T\delta_j \delta(t-t') \end{aligned} \tag{8.3.2}$$

and suppose that the matrix $\tilde{J}_{ij}$ is totally asymmetric, i.e. that all interneuron connections are unidirectional: if neuron i is connected with j ($\tilde{J}_{ij} \neq 0$) then the reverse connection is absent ($\tilde{J}_{ij} = 0$) and vice versa. To store patterns, we modify all existing connections in the Hebb manner:

$$\tilde{J}_{ij} = J_{ij} + \epsilon_{ij}, \tag{8.3.3}$$

where $\epsilon_{ij} = 0, 1$ governs the existence of the connection $i \to j$; the matrix J_{ij} is defined by (8.1.2). We suppose that ϵ_{ij} equals 0 or 1 with equal probability and is independent for different pairs (i, j).

To study the properties of the stationary solutions of the dynamic

equations (8.3.2), we exploit the method of the dynamic generating functional (see e.g. Section 2.3). The dynamic correlation function is then represented by a functional integral:

$$\langle \sigma_i(t)\sigma_i(t')\rangle = \int \sigma_i(t)\sigma_i(t') \exp\,[\mathrm{i}S\{\sigma_i(t), \psi_i(t)\}]\, \mathscr{D}\psi_i(t)\, \mathscr{D}\sigma_i(t), \tag{8.3.4a}$$

$$S\{\sigma_i(t), \psi_i(t)\} = \int \mathrm{d}t \sum_i \left\{ \psi_i(t) \left[\dot{\sigma}_i(t) + \frac{\partial H_0}{\partial \sigma_i} - \sum_j J_{ij}\sigma_j \right] + T\psi_i^2 - \frac{T}{2}\frac{\partial^2 H_0}{\partial \sigma_i^2} \right\}. \tag{8.3.4b}$$

The last term in S originates from the functional determinant that ensures the proper normalization of the integral (8.3.4a).

We restrict ourselves to the case $\alpha \ll 1$, $T \ll 1$. In order to study the behaviour of the system in the vicinity of one of the stored patterns $\xi_i^{(\lambda)}$ (e.g. $\xi_i^{(1)}$), it is convenient to make a transformation of variables $\sigma_i \to \sigma_i\xi_i^{(1)}$, $\psi_i \to \psi_i\xi_i^{(1)}$, $J_{ij}^{(0)} \to J_{ij}^{(0)}\xi_i^{(1)}\xi_j^{(1)}$, which does not change the form of (8.3.4), and then to separate two parts in $J_{ij}^{(0)}$:

$$J_{ij}^{(0)} = J_{ij}' + \frac{1}{N}, \quad J_{ij}' = \frac{1}{N}\sum_{\mu=2}^{k} \xi_i^{(1)}\xi_j^{(1)}\xi_i^{(\mu)}\xi_j^{(\mu)}. \tag{8.3.5}$$

The conditions $\alpha \ll 1$, $T \ll 1$ allow us to treat $\tilde{J}_{ij}$ as random independent Gaussian variables (this can be done only because we consider states lying in the vicinity of the given stored pattern). We then average the dynamic correlation function (8.3.4) over $\tilde{J}_{ij}$ and ϵ_{ij}, taking into account that the quantities $\tilde{J}_{ij}' = \tilde{J}_{ij}(1+\epsilon_{ij})$ are completely uncorrelated,

$$\overline{\tilde{J}_{ij}'\tilde{J}_{kl}'} = \frac{2}{N}\delta_{ik}\delta_{jl}, \tag{8.3.6}$$

and obtain the effective action

$$S_{\mathrm{eff}} = \sum_i \int \mathrm{d}t \left\{ \psi_i \left(\dot{\sigma}_i + \frac{\partial H_0}{\partial \sigma_i} - \frac{1}{N}\sum_j \sigma_j \right) + T\psi_i^2 - \frac{T}{2}\frac{\partial^2 H_0}{\partial \sigma_i^2} \right\} + \alpha q \sum_i \left[\int \psi_i(t)\, \mathrm{d}t \right]^2 + S_1, \tag{8.3.7}$$

$$S_1 = \alpha \sum_i \iint \mathrm{d}t\, \mathrm{d}t'\, \psi_i(t)\psi_i(t')D(t-t').$$

Here $D(t)$ is the irreducible correlation function and q is the Edwards–Anderson order parameter:

$$\frac{1}{N}\sum_i \langle \sigma_i(t)\sigma_i(t')\rangle = q + D(t-t'), \quad \lim_{t\to\infty} D(t) = 0. \tag{8.3.8}$$

Note that the Ising character of the σ_i variables leads to the identity

$$D(0) = \overline{\langle \sigma_i^2(t)\rangle} - q = 1 - q. \tag{8.3.9}$$

We recall here that in the symmetric case the term S_1 in (8.3.7) would be of the form

$$\tilde{S}_1 = \frac{\alpha}{2}\sum_i \iint \mathrm{d}t\,\mathrm{d}t'\,[\psi_i(t)\psi_i(t')D(t-t') + 2\psi_i(t)\sigma_i(t')G(t-t')]$$

where $G(t) = -\dot{D}(t)\beta\Theta(t)$ is the response function, ensuring the fluctuation–dissipation theorem (FDT). The absence of the "G term" in S_1 leads to violation of the FDT and signifies the existence of non-thermal Gaussian noise $\chi(t)$ with correlation function

$$\langle \eta(t)\eta(t')\rangle = 2\alpha D(t-t'). \tag{8.3.10}$$

We show below that the intensity of this noise is exponentially weak at α, $T \ll 1$; $D(0) \sim \mathrm{e}^{-1/2\alpha}$. If we completely neglect the S_1 term in the effective action S_{eff} then the remaining part of the action does not violate the FDT. In that case we readily obtain the static order parameter and the magnetization $m = N^{-1}\Sigma_i\langle\sigma_i\rangle$ (cf. Section 2.3):

$$m = \left\langle\!\!\left\langle \tanh\frac{h}{T}\right\rangle\!\!\right\rangle_h, \quad q = \left\langle\!\!\left\langle \tanh^2\frac{h}{T}\right\rangle\!\!\right\rangle_h, \tag{8.3.11}$$

where $\langle\!\langle\ \ \rangle\!\rangle_h$ denotes the average over the Gaussian distribution $P(h)$ of frozen local fields h that have mean value m and dispersion $2\alpha q$:

$$\langle\!\langle h\rangle\!\rangle_h = m, \quad \langle\!\langle (h-m)^2\rangle\!\rangle_h = 2\alpha q. \tag{8.3.12}$$

At $\alpha \ll 1$ and at low temperatures ($T \to 0$) we get

$$m = 1 - 2\sqrt{\frac{\alpha}{\pi}}\,\mathrm{e}^{-1/4\alpha}.$$

We now return to the full problem (8.3.4) with the total action S_{eff}, which is in fact the self-consistent equation for the correlation function

$D(t)$. We calculate $D(0) = 1 - q$ as $T \to 0$, whose nonzero value signifies incomplete freezing of spins at $T = 0$ due to the presence of the internal noise $\eta(t)$. In the presence of external noise $\eta(t)$ the equations (8.3.11) become more complicated:

$$\begin{aligned} m &= \langle\!\langle \langle\!\langle \mu(t) \rangle\!\rangle_\eta \rangle\!\rangle_h, \\ q(t) &= \langle\!\langle \langle\!\langle \mu(0) \rangle\!\rangle_\eta \langle\!\langle \mu(t) \rangle\!\rangle_\eta \rangle\!\rangle_h, \end{aligned} \tag{8.3.13}$$

where $\mu(t)$ is the magnetization averaged over the thermal noise, at a given configuration of the external noise $\eta(t)$; $\langle\!\langle \ \rangle\!\rangle_\eta$ denotes the average over $\eta(t)$ with the correlation function (8.3.10) and with (8.3.12). The dynamical equations for $\mu(t)$ follow from the Fokker–Planck equations for the probability of the states of a single spin in the external field $h + \eta(t)$:

$$\frac{\partial \mu}{\partial t} = \tanh\left[\frac{h + \eta(t)}{T}\right] - \mu. \tag{8.3.14}$$

We note here that the exact form of (8.3.14) is determined by the details of single-spin relaxation; for example, the right-hand side of (8.3.14) can be multiplied by any factor depending on T and h (the value of this factor is governed by the H_0 part of the effective action (8.3.4)). The form (8.3.14) is the most natural form of relaxation in computer simulations or in neural networks because its rate does not depend on the values of the temperature or field. Solution of (8.3.14) is straightforward:

$$\mu(t) = \int_{-\infty}^{t} \mathrm{d}t' \mathrm{e}^{-(t-t')} \tanh\left[\frac{h + \eta(t')}{T}\right].$$

Inserting this into (8.3.12), we get an equation for q:

$$\begin{aligned} q = \int \frac{\mathrm{d}h}{(4\pi\alpha q)^{1/2}} \exp\left[-\frac{(h-m)^2}{4\alpha q}\right] \\ \times \left\{\int \frac{\mathrm{d}\eta}{[4\pi\alpha D(0)]^{1/2}} \tanh\left(\frac{h+\eta}{T}\right) \exp\left[-\frac{\eta^2}{4\alpha D(0)}\right]\right\}^2 \end{aligned} \tag{8.3.15}$$

To solve (8.3.15) for $D(0)$ as $T \to 0$, it is sufficient to approximate q and m by 1 and $\tanh(\xi/T)$ by $\operatorname{sgn}(\xi/T)$:

$$D(0) = \int \frac{\mathrm{d}h}{(4\pi\alpha)^{1/2}} \exp\left[-\frac{(h-1)^2}{4\alpha}\right]$$

$$\times \iint \frac{\mathrm{d}\eta_1\,\mathrm{d}\eta_2}{4\pi\alpha D(0)} [1 - \operatorname{sgn}(h+\eta_1)\operatorname{sgn}(h+\eta_2)] \qquad (8.3.16)$$

$$\times \exp\left[-\frac{\eta_1^2 - \eta_2^2}{4\alpha D(0)}\right].$$

It is convenient to make a change of variables $\eta_{1,2} \to \tilde{\eta}_{1,2} - h$ and then perform the integration over h. Equation (8.3.16) then becomes

$$D(0) = \int \frac{\mathrm{d}x}{(\pi\alpha)^{1/2}} \exp\left[-\frac{(x-1)^2}{4\alpha}\right] \left\{1 - \operatorname{erf}\left[\frac{|x|}{[2\alpha D(0)^{1/2}]}\right]\right\}. \qquad (8.3.17)$$

Under the assumption (which will be confirmed immediately) $D(0) \ll \alpha$, (8.3.17) can be solved. The result is

$$D(0) = \frac{8}{\pi^2} \mathrm{e}^{-1/2\alpha}. \qquad (8.3.18)$$

The calculation of m from (8.3.13) leads to the same result $m = 1 - 2(\alpha/\pi)^{1/2}\mathrm{e}^{-1/4\alpha}$, so the internal noise does not change m.

Thus we have shown that the totally asymmetric modification of the Hopfield model possesses at $\alpha \ll 1$ retrieved states that are very similar to the stored patterns. This result is corroborated by computer simulations [1]. The small number of short cycles observed in them agrees with our prediction of the existence of weak additional noise. To obtain our results, we have used the Gaussian character of the distribution of the local fields h_i; in the symmetric Hopfield model the distribution of the local fields h_i becomes non-Gaussian at a low-enough temperature $T < T_R(\alpha) \sim \mathrm{e}^{-1/2\alpha}$, where replica-symmetry breaking occurs. In the dynamic functional-integral technique the replica-symmetry breaking corresponds to the appearance of an anomalous part of the response function in the effective action. We have seen that in the asymmetric model the response function does not appear in the effective action, so no spin-glass effects can occur in this model, even at the lowest temperatures.

More general models with an arbitrary level of asymmetry and finite α have not yet been solved. The most important qualitative question

that should be answered in these studies is whether in these models the coexistence of a spin-glass state and synapse asymmetry is possible or whether any weak asymmetry destroys the spin-glass state. The results obtained so far point towards the second alternative.

Historically, the first of these results was obtained in reference [29], where it was shown that for any weak asymmetry a second-order transition into a spin-glass phase is impossible. Specifically, in [29] the "soft" version of the dynamic SK model was studied by means of a diagram expansion for the response function and correlator. Inspection of the series, which become singular at the phase transition for the symmetric model, shows [29] that this singularity disappears if any weak asymmetry is present. Assuming that no other diagram series can result in a singularity at the spin-glass phase transition, it can be concluded that any weak asymmetry eliminates the second-order spin-glass transition.

The second result was obtained in reference [30], where a simplified spin-glass model was solved in which the spins were linear variables except for a global constraint imposed on the total level of their fluctuations. This model can be solved analytically for any temperature or degree of asymmetry. This solution shows [30] that the amplitude of excess noise does not vanish in the limit of extremely weak asymmetry, but does become very slow. Thus at low temperatures weak anisotropy destroys the spin-glass state, but does so very slowly.

Presumably, these results can be generalized to any spin-glass model with weak asymmetry. In this case at any low temperatures the relaxation is slow, with complete freezing being possible only for a purely symmetric model. For neural networks, this means that the system cannot become entangled in spurious spin-glass states, but rather drifts slowly across them until it comes into the region of attraction of one of the retrieval states (or — unfortunately — their mixtures). Thus it would be natural for the asymmetry to improve the network performance. This improvement has possibly been observed in numerical simulations [31].

Certainly, network models aimed at biological applications should not only be asymmetric but also dilute, since in a neural network the number of neuron connections is far less than the number of neurons. Interestingly, these dilute models are generally simpler than their nondilute counterparts (note, however, that only random dilution has been studied so far). In particular spin-glass effects are further suppressed in

them. Specifically, in references [32, 33] a network with matrix J_{ij} defined by

$$J_{ij} = c_{ij} \sum_{\mu=1}^{k} \xi_i^{(\mu)} \xi_j^{(\mu)} \tag{8.3.19}$$

was studied with $c_{ij} = 0, 1$:

$$p(c_{ij}) = \frac{c}{N} \delta(c_{ij} - 1) + \left(1 - \frac{c}{N}\right) \delta(c_{ij}).$$

In the limit of strong dilution ($c \ll \ln N$) this model can be solved analytically [32, 33]. The solution shows [32] that in this model also spurious spin-glass states are absent. This result can easily be explained qualitatively. Generally, spins connected by $c_{ij} = 1$ are uncorrelated in this model since the calculation of the spin $\sigma_i(t)$ involves a tree of ancestors that connects σ_i to the initial conditions $\sigma_k(0)$, and the trees for two spins σ_i and σ_j do not intersect each other in general (note the importance of dilution randomness at this point). Certainly, in the absence of any correlations, no spin-glass effects can be expected. The even more complicated problem of evolution of a spin configuration having finite overlap with one (or two) stored patterns can be solved [33] analytically in this model. This solution shows that in the stationary state the spin configuration has a large overlap with a stored pattern:

$$m^* = 1 - \left(\frac{2\alpha}{\pi}\right)^{1/2} e^{-1/2\alpha}, \quad \alpha = \frac{k-1}{c} \ll 1. \tag{8.3.20}$$

Study of the evolution of two patterns converging to the same stationary state (8.3.20) starting from different initial conditions shows that their overlap q is also incomplete:

$$q^* = 1 - \frac{8}{\pi^2} e^{-1/\alpha}. \tag{8.3.21}$$

These results mean that, even at zero temperature, nonequilibrium noise causes the spin state to drift chaotically in the vicinity of a stored pattern just as it does in the undiluted model discussed earlier in this section.

Interest in asymmetric network models has led to investigation of the properties of nonsymmetric modifications of the SK model. Such

models were studied in references [29, 34]; in the limit of complete asymmetry the dynamic equations of this model were solved exactly in [34]. (Spin-glass effects are certainly absent in this limit.)

Completely different asymmetric models were introduced in reference [35]. In these models both symmetric and asymmetric synapses are present, with the response of the asymmetric ones being very slow. With appropriate choice of symmetric and asymmetric parts of the matrix J_{ij}, the symmetric part $J_{ij}^{S} = \sum_{\lambda=1}^{k} \xi_i^{(\lambda)} \xi_j^{(\lambda)}$ results in attraction to a stored pattern, whereas the slowly increasing asymmetric part $J_{ij}^{a} = \sum_{\lambda=1}^{k} \xi_i^{(\lambda+1)} \xi_j^{(\lambda)}$ results eventually in a transition to the next pattern. Thus this network is capable of recalling time sequences and cycles of patterns. Perhaps this model can explain the long-standing biological problem of recalling with high accuracy a given sequence of movements. An analytical theory of these cycles has recently been developed [36].

8.4 Unlearning Algorithms

As we discussed in Section 1, desirable memory models should allow local storage prescriptions and iterative learning procedures, so that at each storage task the network is presented with a new pattern, with other patterns stored before being transformed into the corresponding matrix J_{ij}. These conditions are satisfied trivially with the Hebb storage prescription (8.1.2), since in this prescription the storage of a new pattern is achieved by a replacement

$$J_{ij}^{\text{new}} = \frac{1}{N} \xi_i \xi_j + J_{ij}^{\text{old}}. \tag{8.4.1}$$

However, as we know, the Hebb rule (8.4.1) fails if the network tries to retrieve the correlated patterns (Sections 8.1 and 8.2). Clearly, the storage prescription (e.g. (8.2.15)) for correlated patterns cannot be represented in such a simple form as (8.4.1), since storage of a new pattern $\xi_i^{(\lambda,\mu)}$ requires knowledge of its basic pattern $\xi_i^{(\lambda)}$. To resolve this difficulty in a realistic memory model, we need an iterative algorithm that converges to some interaction matrix J_{ij} that allows the retrieval of correlated patterns.

The first of these algorithms was introduced by Hopfield [37], who showed that it improves the performance of the retrieval properties of the Hebb rule (8.1.2) and named it the "unlearning" procedure. In this

procedure the starting point is the Hebb matrix J_{ij}, (8.1.2). At each interation step a new chaotic pattern $\sigma_i^{(0)}$ is generated, which then evolves according to dynamical equations specified for this J_{ij} (e.g. (8.3.1)). The final stationary state $\sigma_i^{(f)}$ is generally some "spurious" state (sometimes, however, it can be stored $\xi_i^{(\lambda)}$). At the final step of iteration procedure the J_{ij} matrix is slightly changed:

$$J_{ij}^{\text{new}} = J_{ij}^{\text{old}} - \epsilon \frac{1}{N} \sigma_i^{(f)} \sigma_j^{(f)}, \tag{8.4.2}$$

where ϵ is a small parameter. The idea of the modification (8.4.2) is that spurious states become less attractive than the stored patterns $\xi_i^{(\lambda)}$.

Interestingly, this simple algorithm allows retrieval even of correlated patterns. At present we are not aware of any analytical explanation of this effect, but numerical simulations [38] seem convincing. In these simulations a network with 100 neurons was simulated. The simulation starts from the Hopfield model (8.1.1) with Hebb matrix (8.1.2), applied to the retrieval of 10 correlated patterns $p_+ = 1 - p_- = 0.4$ (p_+ is the probability of $\xi_i^{(\lambda)} = 1$, p_- that of $\xi_i^{(\lambda)} = -1$). To study the quality of retrieval, the probability of the process starting from a state at Hemming distance r from a stored pattern and evolving to this stored pattern was measured. Before the unlearning procedure this probability was less than unity, even for a process starting from stored patterns (Figure 34), i.e. some stored patterns were unstable. However,

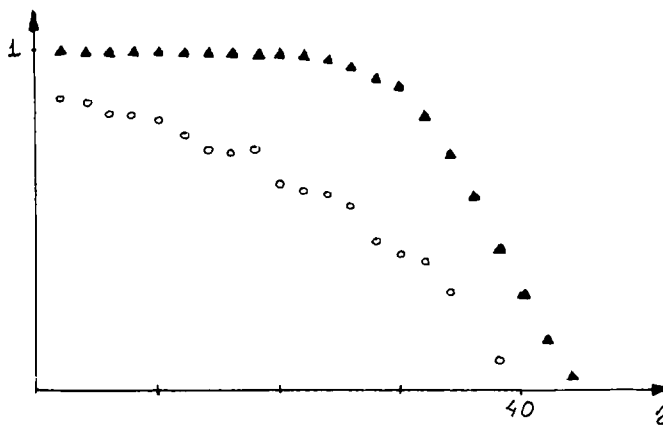

Figure 34 Probability of retrieval of the stored pattern, starting from a noisy configuration.

after the unlearning algorithm (8.4.2) was applied, the performance of the network improved dramatically (Figure 34) (to obtain this improvement, a total of 1000 iteration steps were necessary, but a similar improvement was obtained even after 200 iteration steps).

Why this unlearning algorithm works and the analytical form of the matrix J_{ij} that results from the iteration procedure are still unclear. However, it is possible to construct a more complicated unlearning algorithm that produces the form (8.2.15) of the matrix J_{ij} allowing retrieval of correlated patterns. In this algorithm the iteration procedure is used to store each new pattern. For instance, to store the kth satellite $\xi_i^{(\lambda,k)}$ of the basic pattern $\xi_i^{(\lambda)}$, we first add to J_{ij} a Hebb term,

$$J'_{ij} = J_{ij}^{\text{old}} + \frac{\Delta}{2N}\xi_i^{(\lambda,k)}\xi_j^{(\lambda,k)}, \tag{8.4.3}$$

just as in obtaining the Hebb rule. We then let the system of spins evolve according to their new dynamical equations starting from the configuration $\xi_i^{(\lambda,k)}$. The final stationary state $\sigma_i^{(f)}$ generally differs from $\xi_i^{(\lambda,k)}$ and presumably coincides with one of the satellites stored before. Thus, adding to the matrix J_{ij} a new term

$$J_{ij}^{\text{new}} = J'_{ij} + (\xi_i^{(\lambda,k)} - \sigma_i^{(f)})(\xi_j^{(\lambda,k)} - \sigma_j^{(f)}) \tag{8.4.4}$$

and repeating this procedure many times, we finally arrive at the matrix J_{ij} given by (8.2.15).

This iterative algorithm is not the only one that results in a matrix J_{ij} that can retrieve correlated patterns. The elegant algorithm proposed in reference [39] converges to a matrix J_{ij}^* that satisfies the strong condition

$$\sum_{i,j} \xi_i^{(\lambda)} J_{ij}^* \sigma_i^{(\lambda)} > \delta \left(\sum_{i,j} J_{ij}^2 \right)^{1/2}$$

($\delta > 0$) for each noisy pattern $\sigma_i^{(\lambda)}$ differing from $\xi_i^{(\lambda)}$ at a small fraction of sites. This condition means that dynamical evolution at zero temperature starting from $\sigma_i^{(\lambda)}$ leads after one iteration step to $\xi_i^{(\lambda)} = \text{sgn}\,[J_{ij}^*\sigma_j^{(\lambda)}]$, which is clearly the stationary solution. To construct such a matrix J_{ij}^* at each iteration step, some pattern $\xi_i^{(\lambda)}$ and its noisy analogue $\sigma_i^{(\lambda)}$ are considered. Then the error mask is defined by

$$\epsilon_i^{(\lambda)} = \frac{1}{2}\left[1 - \text{sgn}\left(\xi_i^{(\lambda)} \sum_j J_{ij} S_j^{(\lambda)}\right)\right], \tag{8.4.5}$$

which takes the values 0 (or 1) if site is correctly (or incorrectly) retrieved. Then the matrix J_{ij} is updated:

$$J_{ij}^{\text{new}} = J_{ij}^{\text{old}} + \epsilon_i^{(\lambda)}\xi_i^{(\lambda)}S_j^{(\lambda)} + \epsilon_j^{(\lambda)}\xi_j^{(\lambda)}S_i^{(\lambda)}. \qquad (8.4.6)$$

It can be shown [39] that if a J_{ij}^* satisfying this condition exists then the iteration procedure (8.4.6) converges to it. However, this iteration scheme requires a large number of sweeps over the whole set of patterns $\xi_i^{(\lambda)}$, and it thus implies that, in order to store the next pattern, we should know all patterns stored previously — which is certainly a big drawback.

In a slightly different algorithm [10, 40] the study of the noisy patterns ξ_i is replaced by a more stringent condition on the molecular fields at each site, which ensures that they are aligned with $\xi_i^{(\lambda)}$ and are not small. This algorithm is more economic in computer simulations, but it also requires a lot of sweeps over the whole set of patterns.

REFERENCES

[1] Hopfield, J.J., (1982) *Proc. Natl. Acad. Sci. USA* **79**, 2554; (1984) *ibid.* **81**, 3088.
[2] Amit, D.J., Gutfreund, H. and Sompolinsky, H. (1985) *Phys. Rev.* **A32**, 1007.
[3] Sompolinsky, H., (1987) in *Proceedings of Heidelberg Colloquium on Glassy Dynamics*, p. 485. Lecture Notes in Physics, Vol. 275. Berlin: Springer-Verlag.
[4] Amit, D.J., Gutfreund, H. and Sompolinsky, H. (1985) *Phys. Rev. Lett.* **55**, 1530; (1987) *Ann Phys. (NY)* **173**, 30.
[5] Crisanti, A., Amit, D.J. and Gutfreund, H. (1986) *Europhys. Lett.* **2**, 337.
[6] Personnaz, L., Guyon, I. and Dreyfus, G. (1985) *J. Phys. (Paris) Lett.* **46**, L359; (1986) *Phys. Rev.* **A34**, 4217.
[7] Kanter, I. and Sompolinsky, H. (1987) *Phys. Rev.* **A35**, 380.
[8] Feigel'man, M.V. and Ioffe, L.B. (1987) *Int. J. Mod. Phys.* **B1**, 51.
[9] Amit, D.J., Gutfreund, H. and Sompolinsky, H. (1987) *Phys. Rev.* **A35**, 2293.
[10] Gardner, E. (1987) *Europhys. Lett.* **4**, 481; (1988) *J. Phys.* **A21**, 257.
[11] Tsodyks, M.V. and Feigel'man, M.V. (1988) *Europhys. Lett.* **6**, 101.
[12] Abelles, M. (1982) in *Studies of Brain Function*. New York: Springer-Verlag.
[13] Sompolinsky, H. (1986) *Phys. Rev.* **A34**, 2571.
[14] Kanter, I. and Sompolinsky, H. (1987) *Phys. Rev. Lett.* **58**, 164.
[15] Parisi, G. and Mezard, M. (1987) *Europhys. Lett.* **3**, 1067.
[16] Kanter, I. (1988) *Phys. Rev. Lett.* **60**, 1891.
[17] Mezard, M., Parisi, G., Sourlas, N., Toulouse, G. and Virasoro, M. (1984) *Phys. Rev. Lett.* **52**, 1156; (1984) *J. Phys. (Paris)* **45**, 843.
[18] Dotsenko, V.S. (1985) *J. Phys.* **C18**, L1017.
[19] Dotsenko, V.S. (1986) *Physica* **140A**, 410.
[20] Mezard, M. and Virasoro, M.A. (1985) *J. Phys. (Paris)* **46**, 1293; Rammal, R., Toulouse, G. and Virasoro, M.A. (1986) *Rev. Mod. Phys.* **58**, 765. Mezard, M. Sourlas, N. and Toulouse, G. (1987) in *Proceedings of Heidelberg Colloquium on*

Glassy Dynamics, p. 238. Lecture Notes in Physics, Vol. 275. Berlin: Springer-Verlag. Eds. J.L. van Hemmen and I. Morgenstern.
[21] Hubel, D.H. and Wiesel, T.N. (1977) *Proc. R. Soc. Lond.* **B198**, 1.
[22] Parga, N. and Virasoro, M.A. (1986) *J. Phys. (Paris)* **47**, 1857.
[23] Kirkpatrick, S., Gelatt, C.D. and Vecchi, M.P. (1983) *Science* **220**, 671; Morgenstern, I. (1987) in *Proceedings of Heidelberg Colloquium on Glassy Dynamics*, p. 399. Lecture Notes in Physics, Vol. 275. Berlin: Springer-Verlag. Eds. J.L. van Hemmen and I. Morgenstern.
[24] Wallace, D.J. (1986) in *Lattice Gauge Theory — a Challenge in Large Scale Computing* (ed B. Bunk, K.H. Mutter and K. Schilling), p. 313. New York: Plenum.
[25] Cortes, G., Krogh, A. and Hertz, J.A. (1987) *J. Phys.* **A20**, 4449.
[26] Gardner, E. and Derrida, B. (1988) *J. Phys.* **A21**, 271.
[27] Gutfreund, H. (1988) *Phys. Rev.* **A37**, 570.
[28] Peretto, P. and Niez, I.I. (1986) *Biol. Cybern.* **54**, 53.
[29] Hertz, J.A., Grinstein, G. and Solla, S.A. (1987) in *Proceedings of Heidelberg Colloquium on Glassy Dynamics*, p. 538. Lecture Notes in Physics, Vol. 275. Berlin: Springer-Verlag. Eds. J.L. van Hemmen and I. Morgenstern.
[30] Crisanti, A. and Sompolinsky, H. (1987) *Phys. Rev.* **A36**, 4922.
[31] Parisi, G. (1986) *J. Phys.* **A19**, L675.
[32] Kree, R. and Zippelius, A. (1987) *Phys. Rev.* **A36**, 4421.
[33] Derrida, B., Gardner, E. and Zippelius, A. (1987) *Europhys. Lett.* **4**, 167.
[34] Rieger, H., Schreckenberg, M. and Zittarz, J. (1988) Preprint.
[35] Sompolinsky, H. and Kanter, I. (1986) *Phys. Rev. Lett.* **57**, 2861.
[36] Riedel, U., Kühn, R. and van Hemmen, J.L. (1987) in *Proceedings of Heidelberg Colloquium on Glassy Dynamics*, p. 437. Lecture Notes in Physics, Vol. 275. Berlin: Springer-Verlag. Eds. J.L. van Hemmen and I. Morgenstern.
[37] Hopfield, J.J., Feinstein, D.I. and Palmer, R.B. (1983) *Nature* **304**, 158.
[38] Ioffe, L.B. and Sagdeev, I.R., unpublished.
[39] Gardner, E., Stroud, N. and Wallace, D.J. (1987) Edinburgh Preprints 87/394; 87/410.
[40] Diederich, S. and Opper, M. (1987) *Phys. Rev. Lett.* **58**, 949. Krouth, W. and Mezard, M. (1987) *J. Phys.* **A20**, L745.